UNIVERSITÀ DEGLI STUDI DI UDINE
hic sunt futura

www.uniud.it

UNIVERSITY OF UDINE

Ph.D. Course in Biomedical Science and Biotechnology

XXXIV Cycle

Ph.D. Thesis

"ALTERNATIVE TARGETS IN ANTICANCER THERAPY: THE EMERGING ROLE OF PROTEOTOXIC STRESS"

Ph.D. Student:

Luca Iuliano

Supervior:

Prof. Claudio Bracolini

DISCUSSION YEAR 2022

INDEX

1 ABSTRACT

Chemotherapy failure is one of the most common and crucial problem in the treatment of tumors. Indeed, acquired mutations and alterations can lead to cell death resistance of the cancer cells. The small molecule G5 and its successor 2c are dienone derivatives with two sterically accessible electrophilic β-carbons, which can act as Michael acceptors to target nucleophiles, such as cysteines. G5 and 2c trigger multiple stresses, which converge in the activation of the proteotoxic stress. However, their peculiar cell death mechanism is not fully elucidated. A shRNA screening of glioblastoma cells was adopted in order to identify the key players involved in this cascade. GSK3β seems a promising target as a crucial interactor for G5, but the knockdown (using siRNA) and the knockout (generated by using CRISPR/Cas9 technique) of GSK3β have revealed that this kinase is only partially involved in this cascade. Instead, we show that GSK3β is crucial for the necroptotic cell death induced by the quinone DMNQ.

Leiomyosarcomas (LMS) are rare but aggressive smooth muscle tumors, characterized by complex karyotypes. Limited therapeutic options are available for LMS. Beside surgical resection, the treatment with the genotoxic compound Doxorubicin is commonly adopted to limit the dissemination and progression of the disease. However, the acquired resistance of LMS to Doxorubicin treatment, due to the accumulation of mutations, leads to relapse and correlates with a bad prognosis. Hence, new therapeutic strategies need to be found. A bioinformatic analysis of a signature of genes upregulated after 2c treatment, involving several elements of the proteotoxic response, correlates negatively with the survival of LMS patients. From this observation, we hypothesize that aggressive LMS coexist with high levels of proteotoxic stress, and they could be under crisis when challenged by further proteotoxic stress making them more vulnerable.

We show that 2c can induce proteotoxic stress in LMS cells before leading them to enter in cell death programs. Indeed, the chaperones *HSPA6* and *HSPA1A* show a dramatic increase in mRNA levels in these cells after treatment with 2c. Moreover, 2c triggers mitochondrial dysfunction and by STED technique microscopy, we unveil that this small molecule can reorganize the sub-mitochondrial clusters of DIABLO/SMAC.

In order to improve its efficiency *in vivo*, 2c was engineered through a conjugation with PEG and a small peptide, generating a pro-drug version of the compound called 2cPP. This new molecule can release 2c through the action of secreted proteases present in the tumor microenvironment. 2cPP induces similar levels of cell death in LMS cells as 2c, but unlike 2c, is unable to induce cell death in normal smooth muscle cells. When assessed for antitumoral activities *in vivo*, using different xenograft models of LMS, 2cPP showed a strong antitumoral effect.

The cell death mechanism induced by 2c and the genes involved in this process are still not clarified. To better understand and dissect this pathway, an RNA-Seq experiment was performed by comparing the results between tumoral cell lines and its normal counterpart treated with 2c. The results reveal that normal cells modulate more genes than the tumoral ones after 2c treatment, in both upregulation and downregulation. Furthermore, while tumoral cells generally upregulate pro-apoptotic genes and downregulate anti-apoptotic genes, normal cells could have a more balance response in order to keep the cells alive, demonstrating the fact that normal cells show less cell death than the tumoral ones after 2c treatment. Regarding proteotoxic stress, both the cells activate similar pathways when they are treated with 2c.

Cotreatments of LMS cells with 2c and other common small molecules reveal that two compounds can induce an additive effect of 2c in terms of cell death rate: MKC3946, an inhibitor of IRE1, and YKL-06-061, an inhibitor of SIKs. Despite the final role is to increase the cell death induced by 2c for both the inhibitors, we show that they can act in a different way to achieve this result. Indeed, MKC3946 augment the levels of cell death through blocking survival pathways induced by the activation of the UPR response, instead YKL-06-061 potentiate these pathways in an uncontrolled way leading to a switch from a pro-survival to a pro-death effect.

In conclusion, all our data seem promising for LMS treatment and highlight that proteotoxic stress may be an alternative strategy in anticancer therapy.

2 INTRODUCTION

2.1 THE IMPORTANCE OF PROTEOSTASIS AND ITS REGULATION

2.1.1 THE PROTEOSTASIS MEANING

Among the macromolecules present in all the organisms, the proteins are certainly the ones with a strong significance in terms of cellular mechanisms and signaling. Indeed, they play a plethora of roles that start from the gene expression to cell differentiation and protection [1]. To achieve their roles, the proteins need to assembly into three or sometimes four different type of structures that allow them the possibility to answer their functions. When the proteins reach their correct structure and conformation, they are folded, and the organisms live in a situation of protein homeostasis or proteostasis [2]. Because the proteins are involved in many critical processes, it is clear that the maintenance of the status of proteostasis is crucial for the cells fate. For this reason, the cells have developed some mechanisms in order to control and favor the correct folding of the proteins [2].

Regarding the folding process, most of the proteins typically adopt a three-dimensional structure that is thermodynamically stable [3]. However, proteins with huge complex domains can lead to the production of some intermediates, that can leave exposed their hydrophobic aminoacid residues. These residues are more prone to generate a misfolded condition with the production of aggregates [4].

To maintain the status of proteostasis the cells can take advantage of a system called Proteostasis Network (PN), which involves both chaperones and some proteolytic mechanisms. All the components of the PN collaborate to monitor and guarantee the proteostasis, through the control of the correct folding of the proteins or through their degradation if it is not possible to help reaching the precise structure. [5-7]. Proteostasis is fundamental in the survival of the cells, indeed dysfunctions of the PN can lead to the development of pathologies, typically age-related, such as neurodegenerative diseases

(Alzheimer's disease, Huntington's disease, Creutzfeldt–Jakob disease, Parkinson's disease) [8-10].

2.1.2 THE MOLECULAR CHAPERONES NETWORK

Regarding the monitor of the correct folding of the proteins, the main players that allow this function are the chaperones. Chaperones generally need ATP hydrolysis and high amount of energy cost to ensure their functions. Molecular chaperones constitute about the 10% of the proteome and they play crucial functions in proteostasis both in normal conditions and during cellular stress responses [11]. Among them, one of the most important family is the Heat Shock Proteins family (HSPs) that allow the correct folding of the proteins when there are critical conditions, like oxidative and heat stress or hypoxia, that can impair the proteostasis [1]. The name of these peculiar chaperones derived from the fact that their expression is drastically enhanced when the cells are challenged with stresses and in particular with high temperature. HSPs are about 330 and includes both chaperones and co-chaperones [12]. The chaperones can be divided based on their size and on the ATP dependency mechanisms of action in ATP-dependent (HSP70s, HSP90s and HSP60s (the latter ones called also chaperonins)) and ATP-independent (small HSPs or sHSPs) [12]. Among the ATP dependent are present also the HSP100s which are involved in the disruption of the aggregates. The co-chaperones, instead, are regulatory proteins that can help the chaperones in their duties, indeed, they can give more specificity and selectivity between the chaperones and their substrates. Among the co-chaperones it is possible to identify the HSP40s that are the regulator proteins of the HSP70s [12,13]. The classification of the chaperones is reported in Figure 2.1.

Chaperones are critical in order to maintain the proteostasis, through the monitoring of the correct folding of the proteins. In order to start this process, they recognize and bind the hydrophobic sequences that are not normally exposed during the folding [14]. They can assist the folding of unfolded proteins by three distinct actions. First, the majority of the chaperones, such as HSP70s, can keep the targets in an unfolded state until natural fold is realized [11,15,16]. Second, chaperones like HSP70s and HSP60s can use ATP energy in order to unfold stable unfolded proteins, obtaining in this way proteins that are

refoldable [17,18]. Third, HSP70s, in complex with the co-chaperones HSP40s and HSP110s, can use the energy of ATP hydrolysis to induce the unfold and solubilize the aggregates into proteins that are refoldable [19,20]. Thus, cycles of binding and release of the ATP to the proteins appear throughout the process of folding, thanks to the chaperones. When the correct structure of the proteins is reached these cycles end [2,16].

Chaperone Family	Topology of Binding	Co-chaperone	Known Function
Hsp100	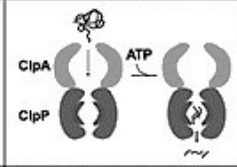	ClpP, SspB, Hsp70, Hsp40	• Works with DnaK in ATP-dependent disaggregation and proteolysis • Prevents aggregation, degradation and turnover of unassembled mitochondrial proteins • Reactivates heat-damaged proteins • Establishes and maintains prion phenotype in yeast
Hsp90	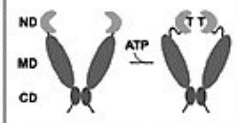	Hop, Hip, Hsp70, Immunophilins, Grp78	• Refolds proteins in stressed cells. Probable secretory chaperone in prokaryotes • Major cytosolic chaperone in eukaryotes. • Cytoprotection and intracellular signaling • In ER, controls protein homeostasis, folding and assembly of secretory proteins
Hsp70	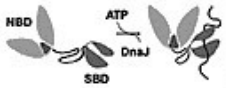	Hsp40, GrpE	• Ubiquitous Principal folding chaperone • Works with ClpB as disaggregase • Folding of newly synthesized proteins • Protein transport into ER and mitochondria
Hsp60 (Group I)	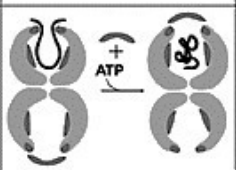	Hsp10	• Major chaperone for protein folding in prokaryotes • Stabilizes proteins during heat stress • Promotes folding of over-produced proteins • Major chaperone in mitochondria and chloroplast
Hsp60 (Group II)	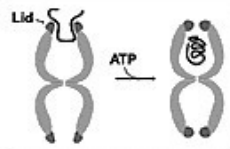	Prefoldin/GimC	• Promotes folding of a cytosolic proteins in eukaryotes • Refolding of unfolded polypeptides in vitro
sHsps		-	• Stabilizes unfolded polypeptides • Prevents aggregation • Works with Hsp70 in protein refolding • Structural protein of eye lens

Figure 2.1: Classification of the molecular chaperones [21].

HSP70s are cytosolic chaperones conserved during evolution and are the chaperones more present in the cells. HSP70s have many homologs located in several subcellular compartments, including for example the Heat shock cognate 70 (Hsc70) in the cytosol and BiP/GRP78, which is a crucial gene situated in the Endoplasmic Reticulum (ER). HSP70s can accomplish different activities such as folding newly synthesized polypeptides, refolding unfolded proteins, assist in the degradation of terminally unfolded

proteins, and directly destroy the already formed aggregates [11]. They can recognize different unfolded proteins through the interaction with four to five hydrophobic aminoacids exposed on the surface [15]. Fundamental for the chaperone activity of HSP70s is the switch between open and closed conformations of the Substrate Binding Domain (SBD) present in their structure. In the open conformation, the SBD has low affinity to the target proteins, instead, when is closed, though the ATP hydrolysis induced by co-chaperones, HSP70s can increase the affinity to the target proteins. This close conformation helps the target proteins in refolding by keeping them in an unfolded state until natural fold is reached. When the protein reaches the correct folding, it has no longer exposure of the hydrophobic residues and, thus, it is released from HSP70s [16].

HSP40s proteins, also called J-proteins, are a big co-chaperones family constituted by 49 members [22]. Among this, DNAJB6 and DNAJB8 are the most commonly known and can suppress the toxicity of polyglutamine aggregation in neurons [23]. HSP40s have an important role in regulate ATP hydrolysis of the HSP70s, indeed the 70-residue J domain of HSP40s can bind the unfolded proteins and can cooperate with the ATPase domain of HSP70s, inducing the ATP hydrolysis of itself. This phenomenon can approach the HSP40s-bound substrate to the SBD of HSP70s, which in turn can enhance the affinity of HSP70s to the substrate and induce the release of HSP40s from both the substrate and HSP70s [24]. Because of this allosteric conformational change, the substrate can be transferred from the bind with HSP40s to the bind with HSP70s. Apart from this conserved J domain, these co-chaperones have different domains, which are important for the regulation of several biological processes like intracellular localizations and target proteins binding for proteolysis [25].

HSP90s are chaperones, which are able to dimerize, localized in diverse distinct compartment of the cells (cytosol, nucleus, ER, and mitochondria) [26]. These chaperones are constitutively expressed in physiological conditions and their levels of expressions could highly increase if the cells are under a stress condition [27,28]. The activity of this family of chaperones can be modulated by the Heat Shock Factor 1 (HSF1), which is one of the main regulators of the Heat Shock Response (HSR) [29]. HSP90s proteins can bind diverse targets, such as kinases, nuclear receptors, transcription factors and cell surface receptors [11]. HSP90s present in their structure an N-terminal

ATP-binding domain (N-domain), a mid-domain which is important in the binding with the target (M-domain), and a C-terminal domain crucial for the dimerization (C-domain) [27,28]. ATP hydrolysis regulates the affinity between HSP90s and the substrates and induces, as well as HSP70s, a conformational change in HSP90s from an open conformation to a close conformation. In fact, in a free form, HSP90s can bind their substrates and the bind between the ATP and the N-domain leads to the conformation switch [30]. In the close conformation, the N-domains of two molecules of HSP90s dimerize each other. After the cycle of ATP hydrolysis, the substrate is release and again HSP90s are free in the open conformation. This switch can be regulated through several co-chaperones like Hop, p23/Sba1, and Cdc37 [27,28].

The mechanisms of action of HSP70s, HSP90s and their co-chaperones is illustrated in Figure 2.2.

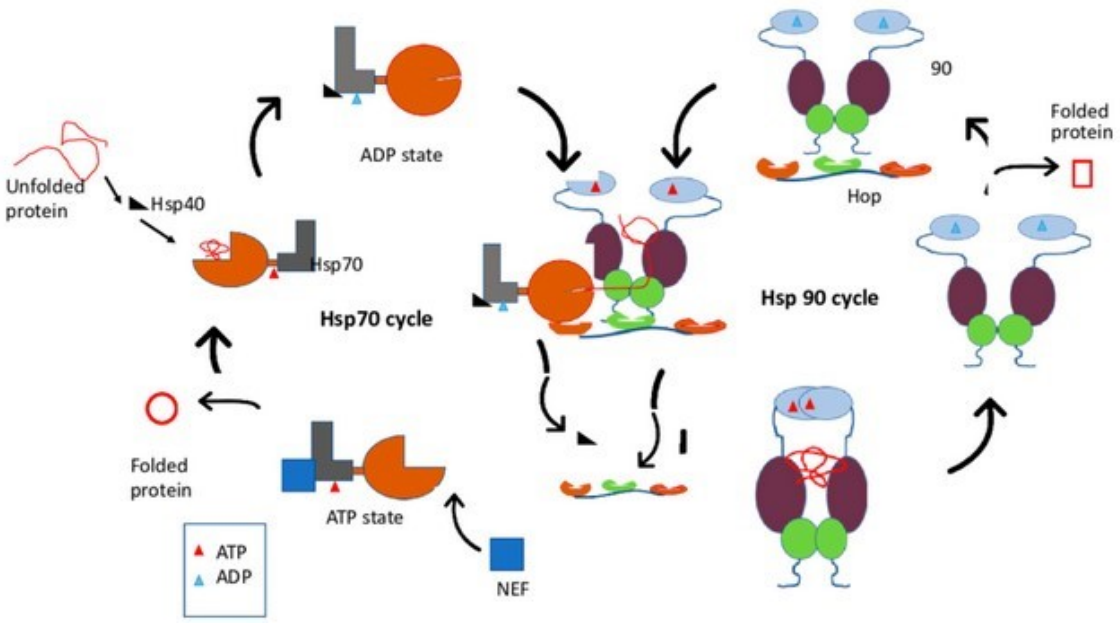

Figure 2.2: Mechanisms of action of HSP70s and HSP90s. Through the assistance of their co-chaperones, they can use cycles of ATP hydrolysis in order to help reaching the correct folding of the proteins [31].

HSP60s are a family of chaperones, called also chaperonins, of 60kDa present in the mitochondria [17,18]. One of the most known members is the bacterial chaperone GroEL. Under particular stresses, HSP60s can also move from the mitochondria to the cytosol [17,18]. HSP60s have a particular structure, in which they can create a double ring

complex of seven subunits for each ring. The substrates are kept in the center of this structure and here they can expose their hydrophobic residues leading to the refolding process [18]. The activity of HSP60s is regulated by the co-chaperone HSP10s present in the mitochondria, which can be seen as a lid for the HSP60s structure. After the ATP hydrolysis, HSP10s lid opens and, in this way, the folded protein can be release from HSP60s [18]. HSP60s and HSP70s can collaborate in the folding assistance process, and one example of this kind of collaboration is given by the HSP60s TCP-1 Ring Complex (TRiC), called also TCP1 complex (CCT) (TRiC/CCT). TRiC, through its activity and cooperation can help the protein to reach the correct folding without the creation of aggregates [2,32]. The catalytic cycle of HSP60s is illustrated in Figure 2.3.

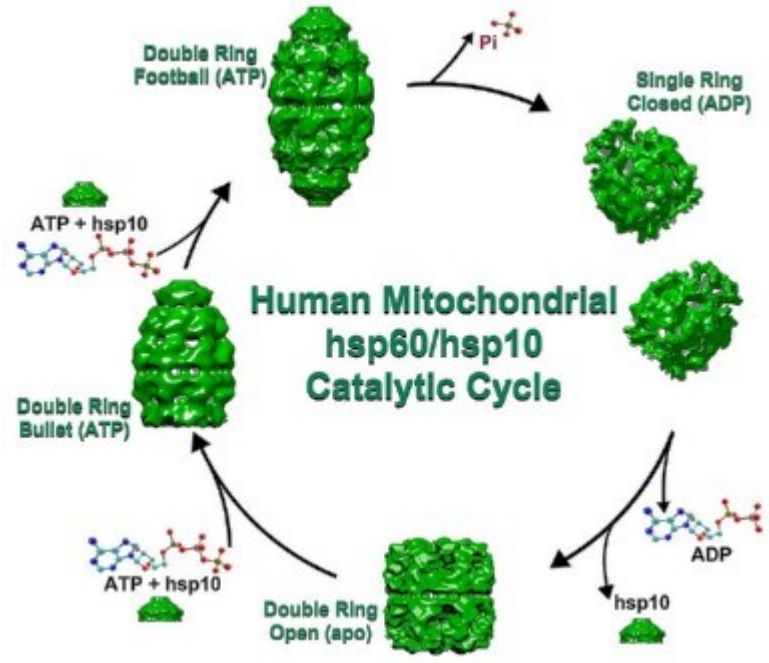

Figure 2.3: The catalytic cycle that leads to the folding of the target protein through HSP60s [33].

sHSPs differently from all the other HSPs work with a mechanism that is ATP independent. In humans are present 10 sHSPs, which present different size range from 12 to 42 kDa [34]. Under stress conditions, HSP27 and αB crystallin are the sHSPs, which are strongly induced [34]. In their structure, it is possible to identify a 100-residue α-crystallin domain with at the end some variable N-terminal and C-terminal portions. These portions are fundamental for the recognition of the target proteins and induce the creations of oligomers. The important role of the sHSPs is favoring the stable state of the

proteins during the folding, in order to avoid aggregates formation for other chaperones like HSP70s [35].

It is possible to divide the proteins into two groups: proteins that are able to fold quickly with the interaction with the chaperones that acts upstream (like HSP70s) and proteins that need more help during the whole process. Indeed, the proteins that are included in the first group just need the upstream chaperones and they do not need other downstream chaperones. Instead, the proteins that are included in the second group need more specialized chaperones (like HSP90s and the chaperonins) in order to obtain the correct folding [36]. The proteins of the second group are typically larger and they present a structure with several domains or some domains with a complex topology. Usually, they need a strong interaction with the chaperones, but they also need an interaction with the co-chaperones, in this way it is possible to define a big network called “chaperome” [37]. Furthermore, there are also some proteins that are unable to fold and they need the chaperones to fold like for example the actin of the cytoskeleton [38].

2.1.3 THE UBIQUITIN-PROTEASOME SYSTEM AND ITS COMPONENTS

In parallel to the folding assistance given by the chaperones, the cells have adopted some mechanisms of protein quality control that has the same aim of maintaining the proteostasis. In contrast with the chaperones, which can help the protein to reach the correct folding and continue living, these mechanisms lead to the degradation of the proteins that are misfolded. The major role in these types of systems is done by the Ubiquitin-Proteasome System (UPS) [39,40]. The UPS is crucial in the life of the cells because it controls the correct and physiological disruption of the proteins that is an important turn-over when these proteins are not correctly folded, too old or damaged [41].

This system take advantage from a signal that permits to select the proteins that need the degradation. This signal is a tag of ubiquitin, which can be conjugated to the target protein in a multistep process called ubiquitylation. The ubiquitin is a polypeptide of 76 aminoacids constituted by a fundamental glycine residue (G76) in the C-terminal, which is critical for its conjugation to specific target substrates. Moreover, the ubiquitin presents in its structure internal lysine residues that are significant in the creation of polyubiquitin chains [39,42]. This process needs the presence of three different classes of enzymes that divide it into three steps: E1 ubiquitin-activating enzymes, E2 ubiquitin-conjugation enzymes and E3 ubiquitin-ligases [43-45]. In the first step, E1 enzyme stimulates one molecule of ubiquitin by the development of a high energetic thiol ester bond between a cysteine residue present in the active catalytic site of E1 enzyme, and the critical G76 residue of ubiquitin, through a reaction, which requires the hydrolysis of ATP. Activated ubiquitin is transferred to the sulfhydryl group of one of the 30 to 40 ubiquitin carrier E2 enzymes existing in a eukaryotic cell. Later, the activated ubiquitin is transferred from one E2 enzyme to a specific E3 enzyme and in the ultimate step to the lysine of a specific target protein, thanks to the construction of an isopeptide covalent bond between the ubiquitin molecule and the target protein [46-48]. In the ubiquitylation process, the E3 ubiquitin-ligases are the enzymes that confer the major grade of specificity. For this reason, they constitute the largest family of enzymes involved in the process and they can be classified in three subfamilies (RING, HECT and RBR E3s) based on the diverse

enzymatic domains and on the mechanism by which the ubiquitin is transferred to the target protein [44,46,47].

The steps described above can be repeated many times, producing also tag of ubiquitin chains, as seen in Figure 2.4. The faith of the ubiquitin-tagged proteins is determined by the quantity of ubiquitin residues present on the protein, the lysine involved in the bond among the monomers, and the different pattern of the ramification of the poly-ubiquitin chains, making suitably a ubiquitin code [49]. In general, the classic signal for the protein degradation is given by a chain with at least four monomers of ubiquitin bond to each other through the lysine residue in position 48 (K48). Instead, if the proteins are tagged with a different polyubiquitin chain or with a single ubiquitin involving other lysine residues (as K6, K11, K27, K29, K33, K48 or K63), they act some non-degradational roles, in the context of DNA repair, DNA replication or signal transduction [50].

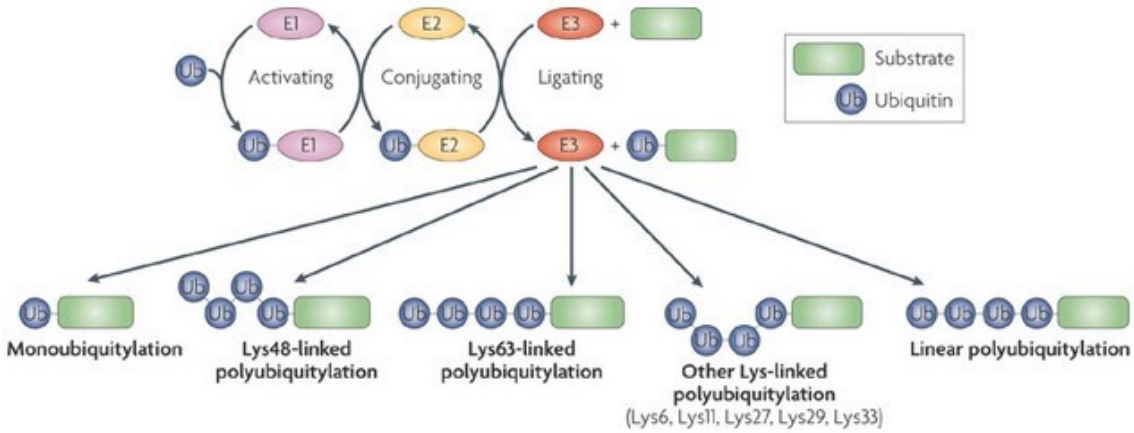

Figure 2.4: Ubiquitylation process with the action of the three class of enzymes involved and the possible ubiquitin chains ramifications [51].

At the end of the ubiquitylation, the target proteins, which are now tagged with the ubiquitin chain, are transported to the 26S proteasome. The 26S proteasome is an ATP-dependent complex that is present both in the cytosol and in the nucleus in all the eukaryotic cells and has about 50 subunits. In particular, among these subunits, two big subcomplexes can be distinguished: the 20S core and the 19S regulatory subunit [47,48,52]. The structure of the 26S proteosome and its components is represented in Figure 2.5.

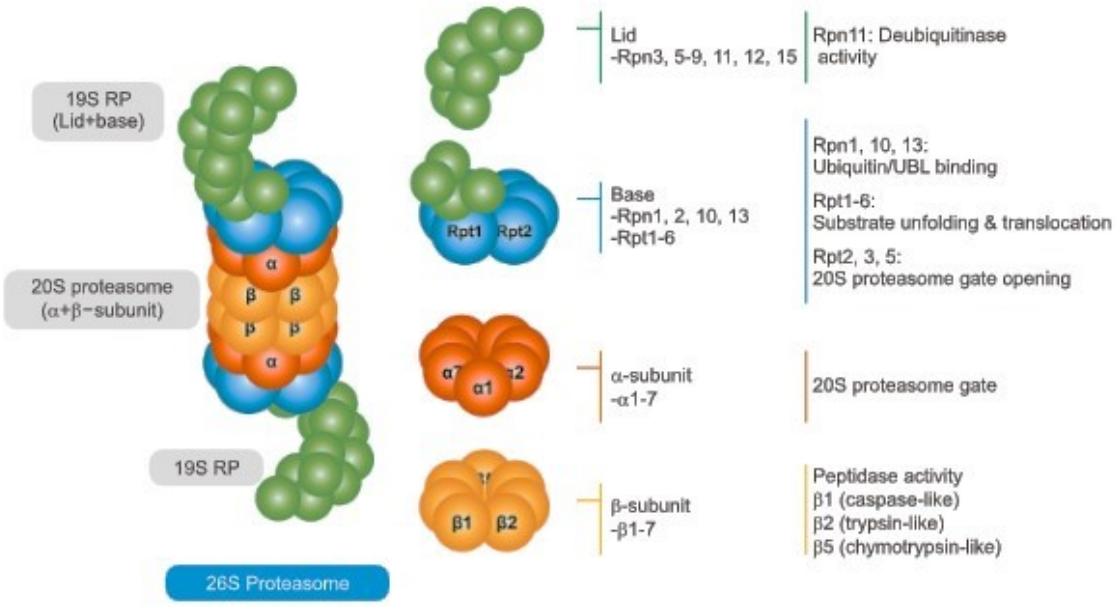

Figure 2.5: Schematic representation of the structure of the 26S proteasome through the definition of all of its components and functions [53].

The 20S core is a multimeric cylinder shape complex of 730 kDa that is the catalytic portion of the system and present two heptameric β-subunits, which have the catalytic role, and two heptameric α-subunits, which have the structural role. Among the β-subunits, it is possible to recognize three main activities between the different subunits: β1, which has a caspase-like activity, β2, which has a trypsin-like activity and β5, which has a chymotrypsin-like activity [54-56]. Thanks to the proteolytic activity of the catalytic chamber, the protein targets are degraded into oligopeptides (with a length between 3 to 15 amino acid residues). The oligopeptides are then hydrolyzed by cytosolic peptidases into free amino acids that are subsequently recognized by the Transporter associated with Antigen 1 (TAP1) complex and loaded into the class I major-histocompatibility complex (MHC-I) for their presentation to the immune system. Nevertheless, the 20S core alone is not able to proceed with the protein degradation, indeed, it is necessary that the 19S regulatory subunit bind the α-subunits of the 20S core for the assembly of the entire structure of the 26S proteasome [47,48,52,54,55].

In general, the proteasome is not able to degrade the proteins when they are in an aggregate form, and it is important that the protein target, which is the substrate of the proteasome, is unfolded before entering. Thus, before entering into the proteasome is

important that eventual aggregates are disrupted, and this is possible though the cooperation with the chaperones network. The process of unfolding the target proteins before translocating them in the 20S core is done through six ATPase subunits (Rpt1-6), which form a hetero-hexameric ring able to generate a mechanical force through the ATP hydrolysis. The mechanical force is employed to unfold the ubiquitylated proteins and to translocate them within the 20S core for the proteolytic degradation [57]. This AAA+ ATPases constitute one of the subunits of the 19S regulatory subunit that is a complex of about 930 kDa. The 19S regulatory subunit can be present on both the ends of the 20S core and, instead of the 20S core, do not have a catalytic role but it has a regulatory role [47,48,52].

Before entering into the 20S core, another essential step, in addition to the unfolding process, is the removal of the ubiquitin tag from the protein target because if not the proteins cannot enter into the 20S core. The 19S regulatory subunit can recognize the ubiquitin chain tagged to the protein target and remove from it through a class of enzymes called deubiquitinases (DUBs) which are able to hydrolyse the isopeptide bond between the ubiquitin and the protein target, previously formed by E3 ligases. The released monomers of ubiquitin are recycled by the cell for the ubiquitylation of the other intracellular proteins [39,48]. The DUBs are strongly regulated to avoid abnormal protein degradation, in fact, their activity is controlled at transcriptional and non-transcriptional level. For example, many cytokines can regulate the expression of the DUBs, inhibiting or enhancing their activity, or in some cases, the DUBs need to be in a complex to be activated. Additionally, the cellular microenvironment can influence this class of enzymes, as in the case of the Reactive Oxygen Species (ROS) generation which leads to the DUBs inhibition through the oxidation of their catalytic cysteine residues [52,58]. There are about 100 DUBs in one eukaryotic cell that can be divided in five classes, four of them are cysteine protease families: the Ubiquitin-Specific Processing proteases (USPs), the Ubiquitin C-terminal Hydrolases (UCHs), the Ovarian Tumour domain containing proteases (OTUs), and the Machado Joseph Disease (MJD)/Josephine domain DUBs. The last one is a zinc-metalloprotease family: the Jab1/Mpn/Mov34 (JAMM) [59].

The main DUBs that are linked with the 19S regulatory subunit are: RPN11/POH1, USP14 and UCH-L5 [60-62]. The action of these three DUBs is not independent of each

other and the timing of their respective functions is critical. In the specific, RPN11/POH1 is a metalloprotease (a JAMM member) and UCH-L5 and USP14 are both cysteine proteases, which catalytic enzymatic activity is stimulated upon the proteasome incorporation [52].

RPN11/POH1 is located at the entry of the 20S core canal and it acts directly on the protein targets. In fact, through the ATP hydrolysis, it is able to cleave the proximal end of the polyubiquitin chain from the protein target, releasing the entire ubiquitin chain. In this way, the target protein can enter in the proteolytic canal of the 20S core [52,63].

On the contrary, USP14 is important for the ubiquitin recycling. It is not a constitutive subunit of the proteasome, but it can reversibly associate with the RPN1 subunit on the 19S regulatory subunit [52]. In particular, USP14 seems to be able to promote the de-ubiquitination of those proteins characterized by multiple K48-linked polyubiquitin chains, by binding/disassociating cycles with the proteasome [62,64,65].

The other DUB, UCH-L5, is recruited to the proteasome by the RPN13 receptor present in the 19S regulatory subunit, and then its isopeptidase activity is increased. Indeed, it is shown *in vitro* that RPN13 can promote directly the activity of UCH-L5 on several ubiquitylated substrates. It can remove ubiquitin from the distal end of polyubiquitin chains, but unlike USP14, which releases di- and tri-ubiquitin from the chains, UCH-L5 produces only molecules of monoubiquitin. Furthermore, this DUB is able to cleave both K48- and K63-linked polyubiquitin chains [52,66,67].

2.1.4 PROTEOSTASIS NETWORK: COOPERATION BETWEEN CHAPERONES AND UPS

The PN is still not completely characterized in all of its components, however it is clear that an interconnection between chaperones and other machineries exists and the possible interactions between the systems are reported in Figure 2.6. It was revealed that some E3 ligases, involved in the degradation of unfolded proteins, can collaborate with some chaperones, such as UBR1, UBR2, San1, Hul5, E6-AP and Parkin. However, the most known E3 ligases interactor is the C-terminus of Hsc70-interacting protein (CHIP) [58-70].

CHIP is a protein of 35 kDa, which have a double function: can act as a co-chaperone of the HSP70s and HSP90s but can also act as an E3 ligase mediating the ubiquitylation process through its RING-like U-box domain [71,72]. The activity of CHIP as an E3 ligase need the presence of an E2 enzyme that in this case is UBCH5 [73]. CHIP, through the mediation of UBCH5, can interact with the substrates of HSP70s and HSP90s and lead to their ubiquitylation and subsequent proteasomal degradation [74]. In order to help and favor the transport of the target proteins to the 20S core, CHIP can interact with RPN10 (a subunit of the 19S regulatory subunit) [75]. In this mechanism, CHIP use its domain called Tetratricopeptide repeat (TPR) to interact with HSP70s and HSP90s and recognize the target proteins [76].

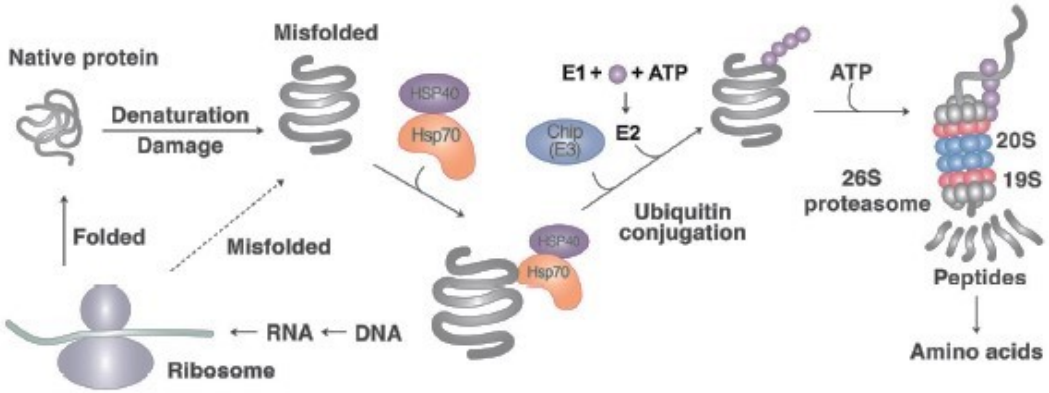

Figure 2.6: Cooperation between the molecular chaperones and the UPS degradation system in order to reach the proteostasis [77].

The co-chaperone BAG1 is also important in the degradation of the target proteins mediated by CHIP and HSP70s [78]. BAG1 can act as a nucleotide exchange factor (NEF) through its C-terminal region, indeed that region can interact with the ATPase domain of HSP70s, and this triggers the release of the protein targets from HSP70s [78]. Beside from this domain, BAG1 has an Ubiquitin-like (UBL) domain present in the N-terminal, which is important for its interaction with the 26S proteasome [79]. BAG-1 can also collaborate with CHIP in order to deliver the target proteins to the UPS. In addition, the sHSP HSP27 can regulate the ubiquitylation of the target proteins, by a direct interaction with the proteasome [80]. Indeed, this sHSP can interact with the chains of ubiquitin and can increase the disruption of the tagged proteins [80].

2.1.5 AGGREGATES DEGRADATION: THE ROLE OF AUTOPHAGY AND CHAPERONES

Although UPS can degrade the damaged and misfolded proteins, under stress condition the misfolding process can generate some insoluble aggregates that could not be destroyed through the proteasome catalytic core. To maintain the proteostasis, the cells have developed another system that can eradicate also these aggregates, using the lysosomal degradation [81]. This machinery involves the autophagy type of cell death, and all the system is called Autophagy Lysosomal Pathway (ALP). ALP is constituted of about 500 elements in which the core is represented by the ATGs products [82].

When there is the formation of the aggregates, these can be accumulated in a region of the cell that is positive for ubiquitin, and this can be a signal for the recruitment in this region of the autophagic machinery through the chaperones. This process is called Chaperone-Assisted Selective Autophagy (CASA) [83-85]. These aggregates are recognized by some autophagic adaptors like for example p62 [86]. p62 is generally inactive but can be activated when there is the binding with the argynilated N-terminal of the ER chaperone BiP/GRP78 [86]. In fact, if there is an accumulation of protein targets that cannot be degraded, BiP/GRP78 is argynilated on the N-terminal domain through the transferase ATE1. Subsequently. BiP/GRP78 translocates in the cytosol and can bind p62, triggering a conformational change of p62 and its interaction with LC3-II that is present on the autophagosomes [86]. In this way, the aggregates enter in the autophagosomes and later after the fusion with the lysosomes (with the formation of the autolysosomes), the cargo and p62 are degraded through the hydrolases present in the lysosomes [87,88].

However, in a normal and unstressed condition these aggregates can also be eliminated in a simpler system, which avoid the formation of the autophagosome, called Chaperone-Mediated Autophagy (CMA) [89]. In this process, the cytosolic proteins that need to be degraded are recognize through the presence of the pentapeptide KFERQ. The involvement of Hsc70 in the CMA is fundamental, in fact, it can favor the translocation of the substrate in the lysosome through a receptor present in the lysosome itself called LAMP2A (Lysosome-Associated Membrane Protein 2A) [89]. The activity of Hsc70 is

mediated by some co-chaperones like the HSP40s and BAG1 [90]. The interaction between Hsc70 and LAMP2A is possible when LAMP2A is stable and its stability is guaranteed by the lysosomal homolog of Hsc70 (Lys-Hsc70), which help LAMP2A to be available for another CMA [91].

UPS and ALP are alternative systems to eliminate the proteins that need to be degraded but with different substrates and pathway involved, which are reported in Figure 2.7. UPS degrades mainly short-lived proteins, instead autophagy is responsible for the degradation of long-lived proteins, which could become aggregates [92-94].

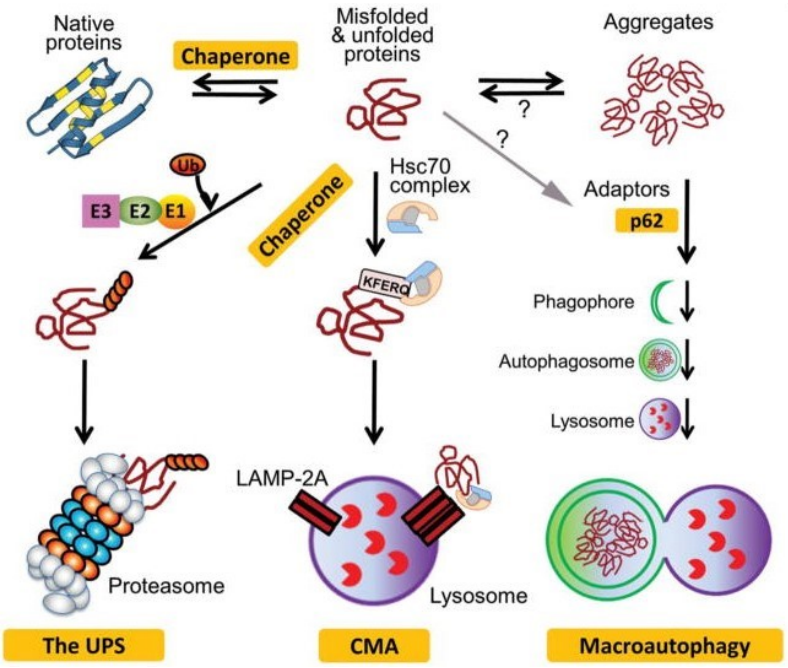

Figure 2.7: Differences in the pathways activated during UPS, autophagy and CMA [95].

However, these two mechanisms can also compensate each other if one is impaired. Indeed, UPS and ALP activation are not mutually exclusive and they can coexist in order to counteract the emergency of an unbalance level of proteostasis due to accumulation of unfolded proteins. In this condition, both UPS and autophagy system are upregulated through several mechanisms (such as ERAD or UPR, described in the next chapter) adopted by the ER, which is the key organelle for the maintaining of the proteostasis. This means that autophagy not only is fundamental in removing aggregates, but also can help in reducing the increasing burden of unfolded proteins in the UPS system [92-94].

It was shown that by inhibiting the 26S proteasome, the autophagy system resulted upregulated, with an augmented presence of LC3 positive vacuoles, probably through ER after the beginning of a proteotoxic stress situation [96]. Furthermore, a reduction of the expression of the Extracellular Mutant 29 (ECM29), which is a protein linked to the 26S proteasome, leads to increasing levels of LC3β and p62, defining that the impairment of UPS can stimulate autophagy [97]. The general mechanism that activates this pathway is not completely elucidated, however some points resulted clear. The impaired 26S proteasome leads to the accumulation of ubiquitylated proteins, generating aggregates. These aggregates form large inclusion bodies called aggresomes and they can be eliminated through the ALP activity. To facilitate ALP degradation, it was shown that the inhibition of the 26S proteasome induces the formation of an entrapment zone, which can help the lysosomes in reaching the correct position around the aggresome. In addition to this, ER resulted crucial in sustain the autophagy system when UPS is impaired, through enhancing the assembly of the pre-autophagosome, in the formation of the autophagosome and in its translocation to the vacuole [98].

p62 resulted to be a bridge between the inhibition of the 26S proteasome and the activation of autophagy. Indeed, the proteotoxic stress, induced by the inhibition of the 26S proteasome, triggers the phosphorylation of p62 at Ser403 and Ser409 through ULK1/ATG1. This phosphorylation status stabilizes the ubiquitylated proteins bound to p62, which leads to their correct degradation though the recruitment of the autophagic machinery [99].

ALP is also fundamental in the degradation of the 26S proteasome and the inhibition of this system can lead to an uncontrolled degradation by the UPS. This resulted in augmented proteasomal peptidases activities [100]. However, this point is controversial, in fact, other studies reported that the inhibition of autophagy does not have a direct impact on UPS and others that, in an autophagy-deficiency model, the resulting impairing in UPS derived by factors outside the proteasome [101,102].

Nevertheless, under severe stress conditions the accumulation of proteins that cannot be degraded occurs, generating insoluble aggregates, which are difficult to be eliminated

also with these machineries. In order to disaggregate these polypeptides, cells use the chaperones as disaggregases [103].

One example is the yeast chaperone HSP104 which is a member of the HSP100s family. Hsp104 is an AAA+ ATPase, which presents a structure with a hexameric ring and a central channel [104]. HSP70s, assisted by HSP40s, can deliver the aggregates to HSP104 and here they can be degraded and become new useful polypeptides [105,106].

In the humans, the disaggregation is made through the co-chaperone HSP110, another member of the HSP100s, after the interaction with HSP70s and HSP40s [107,108]. HSP110 has many similarities in both structure and function with the HSP70s and, as well as BAG1. Similarly, it can be a NEF for HSP70s. This NEF function can lead to the release from HSP70s of ADP [109]. The fundamental role of HSP110 in disaggregation has been shown in many models including amyloids, prefibrillar oligomers and reactivate proteins from aggregates [19].

2.2 PROTEOTOXIC STRESS: THE DARK SIDE OF THE PROTEOSTASIS FAILURE

2.2.1 AN INTRODUCTION TO PROTEOTOXIC STRESS AND THE ROLE OF THE ER

In addition to the systems described above related to the chaperones, the cells could adopt other mechanisms in order to maintain the proteostasis. These other mechanisms are needed because, despite the presence of the chaperones, some errors can occur during the folding caused by some stressors like heat, oxygen radicals, heavy metal ions and mutations. These mechanisms need the role of the ER and are shown in Figure 2.8. The presence of these errors can lead to the formation of aggregates, derived from misfolded or unfolded proteins, which are not functional and can trigger a status of pathological conditions [1,42,110].

The folding maturation process occurs into the ER but if the proteins are not able to fold properly, in the ER begins a process in order to restore the proteostasis called ER-Associated Degradation (ERAD). During the ERAD, the unfolded or misfolded proteins are constrained in the ER and later translocated to the proteasome for their degradation [111]. Critical for the ERAD is the presence of the cytosolic ATPase p97 (VCP/Cdc48), indeed, it can deliver the target proteins with ubiquitin tag from the ER to the proteasome by using the hydrolysis of ATP [112].

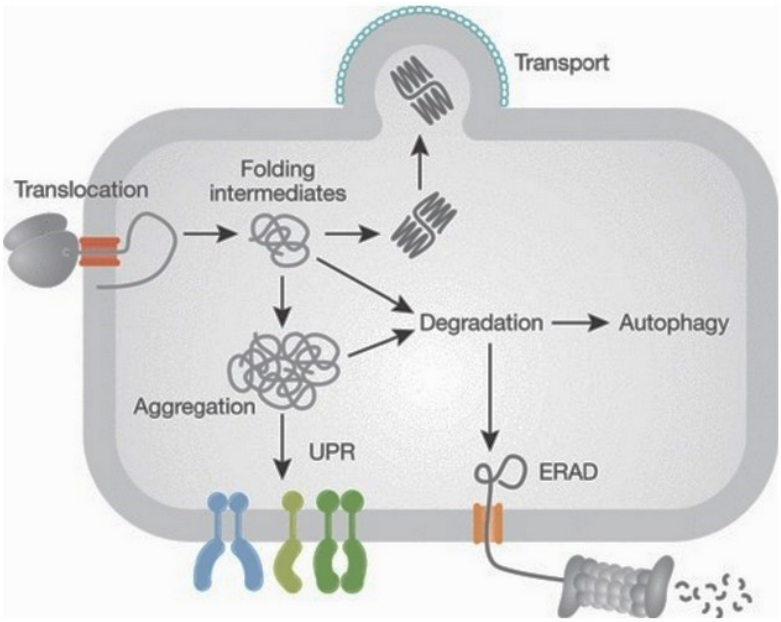

Figure 2.8: Functions of the ER in order to reduce the proteotoxic stress [113].

However, if it is impossible to restore the proteostasis due to a several accumulations of unfolded proteins in the ER, the system is overloaded, and it starts the ER dysfunction characterized by an unbalanced redox equilibrium. All of these events lead to a condition known as ER-stress [114,115]. ER-stress is a phenomenon that is deleterious for the cells, hence, to avoid this situation, the cells activate a pathway called Unfolded Protein Response (UPR) [116,117], which is a crucial response for the survival of the cells. Through UPR, the cells block the translation of new proteins, augment the activity of the chaperones and enhance the ERAD process. With these mechanisms, the accumulation of unfolded proteins is reduced and the status of proteostasis is reestablished [111,115-117]. The UPR pathway is controlled through three sensors: Protein kinase RNA-like ER Kinase (PERK), Inositol-Requiring Enzyme 1 (IRE1) and Activating Transcription Factor 6 (ATF6) [111,118,119]. The sensors work together in order to decrease the ER stress, activating different pathways. For example, when PERK and IRE1 are activated, they can decrease the synthesis of new proteins, in order to reduce the number of proteins that can enter through the ER, instead when ATF6 is activated, can upregulate the transcription of several chaperones in order to control if the folding of the protein is correct [111]. A crucial gene for the regulation of UPR activation in response to ER stress is BiP/GRP78, which is a chaperone of the HSP70s family. Indeed, BiP/GRP78 can

control the activation of the three main sensors of the UPR pathway (PERK, IRE1, and ATF6). When there is an increase in the amount of unfolded proteins, BiP/GRP78 can release the three sensors [120,121].

2.2.2 THE SENSORS OF THE UPR AND THE ATF NETWORK

The UPR response sensors can induce several different transduce mechanisms as reported in Figure 2.9.

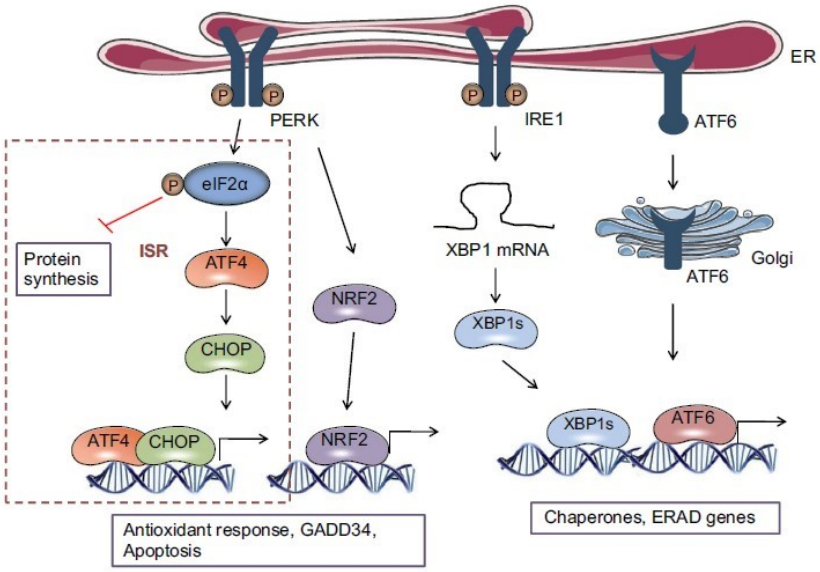

Figure 2.9: Cascade of signaling and downstream pathways induced by the three UPR response sensors [122].

The sensor PERK is a serine/threonine kinase, and it has various substrates. Among them, the most known is the eukaryotic translation Initiation Factor-2 alpha (eIF2α). When PERK is activated though the UPR, can phosphorylate eIF2α at residue Ser51 [115,116,123]. This phosphorylation leads to the block of the translation of the CAP-dependent proteins, which result in the reduction of the ER stress [111]. Another characterized substrate of PERK is the Nuclear factor erythroid-derived 2 (NRF2), which is known to be one of the master gene regulator in the homeostasis of the redox balance [124]. After its activation, PERK can phosphorylate NRF2 at the residue Thr80 that is located in the domain Neh2 [125]. This phosphorylation leads to the activation of NRF2, which determine its import in the nucleus. In the nucleus, NRF2 can induce the

transcription of the Antioxidant Response Elements (ARE), by the activation of the antioxidant response [126]. It is also defined that FOXO transcription factors [127,128] and the Diacyglycerol (DAG) [129,130] can be other substrates of PERK, and that their activation through phosphorylation can help in reducing the ER stress.

Beside PERK, in the cells exist also some PERK-related kinases, which are able to monitor several types of stresses. Some examples are: Protein kinase R (PKR) that control the antiviral response, General Control Nonderepressible 2 (GCN2) that control the aminoacid pool depletion and eukaryotic translation initiation factor-2 alpha kinase 1 (HRI) that control some stresses (heavy metals, heat shock, and proteasome inhibition) [131]. All of these kinases can phosphorylate eIF2α, leading to the block of the translation of new proteins with consequent reduction of the ER stress [132].

IRE1 is a protein that present multidomain and acts both as a kinase and as an endoribonuclease. Its RNAse function can lead to the RNA degradation in order to decrease the protein synthesis, a mechanism that is called Regulated IRE1-Dependent mRNA Decay (RIDD) [133]. Nevertheless, when there is a condition of low activation, IRE1 has a specific RNAse activity to some specific sequence, leading to the modulation of peculiar genes. The most crucial of these genes is X box-Binding Protein 1 (XBP1) which is fundamental for the survival of the cells. Generally, XBP1 is synthesized in an untranslated form, which result unspliced (uXBP1). However, IRE1, after its activation, can process and splice a 26-base intron of XBP1 resulting in the generation of a spliced form of XBP1 (sXBP1). The presence of sXBP1 can be seen as a general marker of the activation of UPR [134]. Furthermore, sXBP1 is also a crucial regulator in the UPR condition, because it can activate the transcription of several genes that are important for the resolving of the ER stress and the return to proteostasis [135].

ATF6 is a transmembrane protein that acts as a transcription factor only when is cleaved. In ER stress condition, it translocates from the ER to the Golgi apparatus in which is processed. The cleaved form of ATF6 can be import in the nucleus and here it can act as a transcription factor for genes that are related to the protein folding assistance (for example GRP78 and GRP94) [136].

Besides ATF6, other ATF genes are reported to be involved in the ER stress and UPR response, and one of the most crucial is ATF4 which is a transcription factor belonging to the cAMP Response Element-Binding protein (CREB)-2 family of proteins [137]. In fact, after the activation of PERK and the subsequent activation and phosphorylation of eIF2α, the latter one, besides blocking the translation of the CAP-dependent proteins, can induce the transcription of some critical mRNA including for example ATF4. ATF4 has a very short half-life and a low efficiency of translation, thus is difficult to detect it in normal conditions [138,139]. Indeed, after using proteasome inhibitors, its levels can dramatically increase through the UPR activation and the elimination of its suppressor [140]. The structure of ATF4 present several domains and among them there is a basic/leucine zipper domain (bZIP domain) which can directly bind the DNA, and for this reason can interact with many genes which can control its activities and its stability [137,138]. Among the several genes that can be controlled by ATF4, there are some of them related to the reduction of the proteotoxic stress and these genes can be directly transcribed by the activity of ATF4. One of the most important gene regulated through ATF4 is C/EBP Homologous Protein (CHOP), which is involved in the apoptotic pathway [141]. As well as ATF4, also the translation of CHOP is enhanced through the phosphorylation of eIF2α that avoid the problem of the short initiation sequence [142]. CHOP collaborates in reaching the proteostasis through the induction of the production of GADD34, which is a regulatory subunit of a specific complex phosphatase of eIF2α [143]. CHOP could regulate its own production and in the same way could also regulate the synthesis of ATF4. This system is important because the phosphorylation of eIF2α and the consequent induction of ATF4 and CHOP is triggered not only in the case of the presence of ER stressors, but also GCN2 and PKR can phosphorylate eIF2α [144].

2.2.3 CELL DEATH ACTIVATION THROUGH UPR RESPONSE

All of these mechanisms are fundamental in order to permit the surviving of the cells under stress condition. Nevertheless, if the proteostasis status is not restored, a continue activation of the UPR pathway can also trigger a switch to cell death pathways, as shows in Figure 2.10 [111,118].

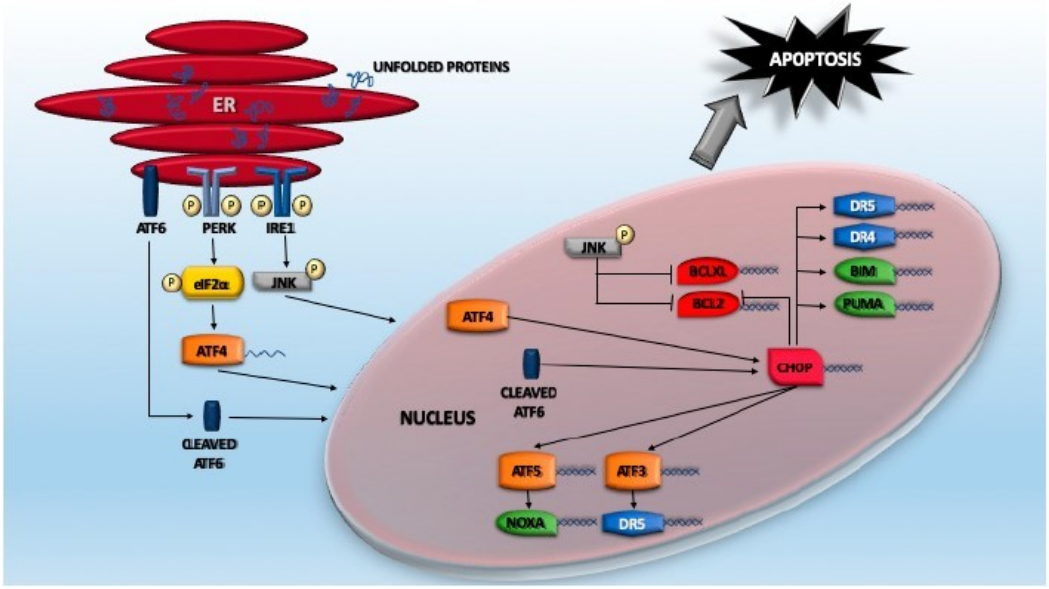

Figure 2.10: Cell death pathways induced by the ER stress through the stimulation of the UPR response stressors [145].

The axis PERK/ATF4/CHOP plays an important role in terms of cell death, indeed many models are studied for this pathway. For example, the loss of neurons after ischemia is regulated by CHOP [146] and also the loss of pancreatic cells in mouse model of diabetes [147]. Of mention, CHOP can also be involved in cell death mechanism without the presence of ATF4, indeed CHOP has also been transcribed by both ATF6 and XBP1 [148]. Regarding cell death, CHOP can induce the transcription of TNF-Related Apoptosis-Inducing Ligand (TRAIL) receptor 2 (TRAILR2) or called also Death Receptor 5 (DR5) [149,150]. In particular, in the 50-flanking region of the DR5 gene was found a CHOP-binding site [150]. Death Receptor 4 (DR4) could also have a role in the cell death induced through ER stress but with minor importance, indeed CHOP and ATF4 can promote its upregulation but with some differences between all the cellular models

considered and between the pathways activated [151,152]. Curiously, the signaling portion of CHOP seems to be involved also in ferroptosis in a GCN2 dependent and independent mechanism that result in a cysteine depletion [153,154]. However, the presence of only CHOP is not sufficient to induce cell death [155,156]. Instead, ATF4 is sufficient to induce cell death in Mouse Embryonic Fibroblasts (MEFs) and the presence of CHOP enhance the process. How the process works is not completely understood, but it is plausible that both the two genes collaborate in order to induce the UPR related genes and this can lead to the induction of cell death [155]. ATF4 is able also to induce cell death pathways in a CHOP independent manner, indeed, it can induce the downregulation of XIAP. XIAP is a member of the family of the Inhibitors of Apoptosis (IAP), which can bind and block the activity of the caspases and by a RING zinc finger domain linked to the E3 ligases can promote the ubiquitylation and the proteasomal degradation of their substrates like caspases [157].

For what concern the other ATFs it is shown that ATF3 and ATF5 could have a role in the cell death induced by the ER stress response. ATF3, which can favor an apoptotic type of cell death, was shown to have a role in the induction of DR5 through ER stress in p53-deficient colorectal cancer cells [158,159]. ATF5 is also controlled by the activity of CHOP and ATF4, indeed through a direct binding with the CAACTC Regulatory Elements (CARE) of the promoter of ATF5, its transcription is upregulated [123,131]. ATF5, similar to ATF4 and CHOP, is more translated after the phosphorylation of eIF2α, and it can induce the transcription of genes related to the apoptosis such as the BH3-only protein NOXA/PMAIP1 [160]. The downregulation of each ATF3, ATF4, ATF5 and CHOP can avoid the induction of NOXA after the induction of ER stress, and all of these genes can contribute to the feed-forward loop that can lead to the apoptosis [155,160,161].

IRE1 usually is identified as a protein related to the pro-survival feedback after ER stress, indeed after its activation it could induce the expression of several chaperones. Two isoforms are encoded for IRE1, which are IRE1α and IRE1β, but the most expressed and studied is IRE1α. As an anti-apoptotic role, through the RNAse activity, IRE1 can also lead to the degradation of several pro-apoptotic proteins such as DR5 [162]. It has been revealed that if IRE1α is continuously activated, its role become more pro-apoptotic. In fact, in that condition it can interact with TRAF2 that can activate Apoptosis Signal-

regulating Kinase 1 (ASK1) and also the downstream gene of ASK1 that is c-Jun N-terminal Kinase 1 (JNK) [163]. JNK can modulate and activate the whole apoptotic process but can also cooperate in the necrotic pathway after ER stress induction [164]. Thus, IRE1 demonstrates to have a dual role of both pro-survival and pro-death for the cells fate, and this can depend on the type and the intensity of the stress. Indeed, it was shown that in a high or chronic condition of ER stress, IRE1 through its RNAse activity can lead to the degradation of the anti-apoptotic proteins, favoring the appearance of the apoptosis [165]. For example, it was revealed that in a model of ER stress induced pancreatic cells, through the inhibition of IRE1, there is the promotion of cell survival [166].

2.2.4 APOPTOTIC CASCADE AND PROTEOTOXIC STRESS

It is well known that the proteotoxic stress can lead to apoptosis and in particular can trigger the activation of the mitochondrial or intrinsic apoptosis [122]. Instead, less is known about the role of extrinsic apoptosis, however it is clear that also this type of cell death can occur [167]. Indeed, it was shown that after the activation of PERK, there is an upregulation of the DR5 [167-171]. Recent studies also reveal that DR5 can be upregulated not only by the activation of the UPR pathway, but also the presence of unfolded proteins can directly interact with DR5 in the ER-Golgi Intermediate Compartment (ERGIC). In this way, DR5 can be assemble in complexes that can trigger the activation of caspase8, which is an activation different and independent from the classical one lead by its extracellular ligand (Apo2L/TRAIL), as reported in Figure 2.11 [172]. This mechanism of activation is still not known with some hypothesis that try to explain this, such as the increased levels of expression or the priming effect of misfolded proteins [172,173].

The ER stress can also induce an inflammatory response, which results in the upregulation of the receptors of TRAIL and subsequently the activation of NF-κB in a caspase8/FADD/RIPK1 dependent manner. This can also induce the production of cytokines in a ligand-independent manner, and this is seen in the protection observed in DR5-/- mice with inflammation induced by taxol [173]. All of these studies highlight that TRAIL can be engaged in different manners and can give rise to different cellular response depending on the context [174].

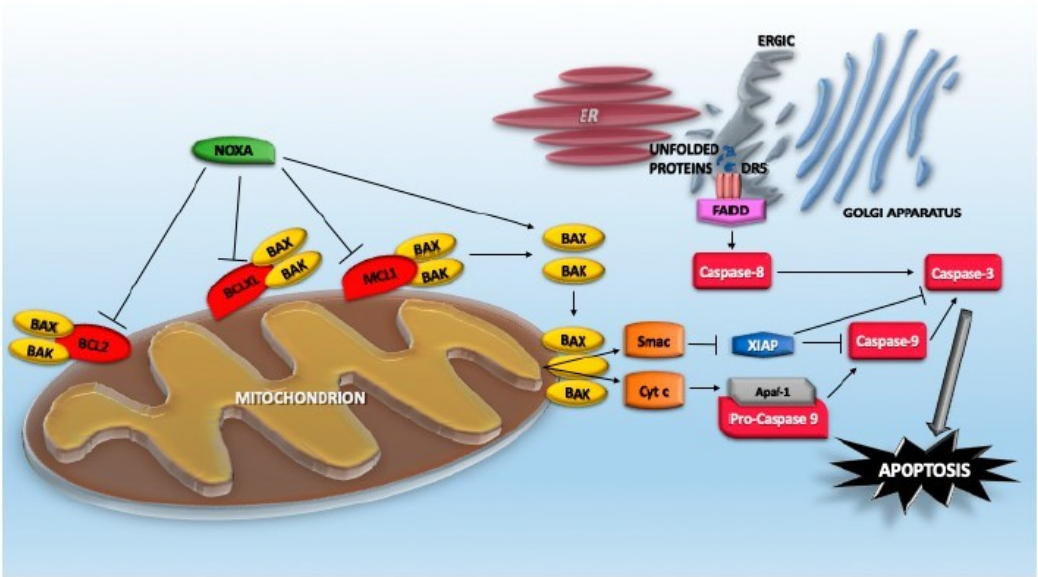

Figure 2.11: Apoptotic pathways, both extrinsic and intrinsic, activated during the UPR response [145].

Regarding the intrinsic apoptosis there is a group of proteins, called BCL2 family, which are fundamental in the induction of cell death and have different roles in the UPR response, as illustrated in Figure 2.11. BCL2 family members are a group of proteins that are directly involved in the apoptotic cascade, and they could have a pro-apoptotic or an anti-apoptotic role. All these types of proteins are present in the ER, and this could affect the Ca^{2+} concentration. [175]. Indeed, the anti-apoptotic ones can decrease the Ca^{2+} concentration, instead the pro-apoptotic like BAX and BAK can augment it [176,177]. In a situation of proteotoxic stress, the UPS through the accumulation of polyubiquitylated proteins become blocked. This leads to the expression of proteins that are not stable and some signaling pathways related to the cells fate are regulated. Two main UPS targets that control the cells fate are IkBα (the inhibitor of NF-kB) [178] and TP53 [179]. After UPS saturation, there are other apoptotic proteins that can accumulate both pro-apoptotic and anti-apoptotic (like NOXA, BIM and MCL1) [41,180,181].

MCL1 is a peculiar protein with a short half-life, and its role and stabilization are under study with different inhibitors. For example, the multiple kinase inhibitor erlotinib can increase the degradation through UPS of MCL1, furthermore can upregulate NOXA which can control the degradation of MCL1 assisted by Mitochondria-Associated

ubiquitin ligase MARCH5 [182,183]. MCL1 can be downregulated after the induction of the PERK pathway in response to an ER stressor like thapsigargin [184]. At a transcription level, the expression of MCL1 can be downregulated after the treatment with N-glycosylation 2-deoxyglucose, through ATF4 [185]. However, MCL1 was revealed to be upregulated in alive melanoma cells after treatment with an ER stressor and that MCL1 is the main responsible for their resistance to cell death [186].

Like MCL1, also the pro-survival proteins belong to the family of the IAPs (XIAP, cIAP1 and cIAP2 in mammals) can accumulate when there is UPS saturation derived from ER stress [187], in this way these proteins can try to maintain the cells alive in a stress situation. This switch between cell survival and cell death could be controlled through the regulation of the IAPs. In fact, a proteotoxic stress related gene, regulated through the master gene HSF1, called AIRAP, could control the levels of cIAP2 and the cell survival [188]. Another example is given by the fact that the two common ER stressor tunicamycin and thapsigargin can reduce the levels of XIAP. Furthermore, the translation of XIAP can be reduced through PERK and ATF4 can promote its degradation [157].

BCL2, another anti-apoptotic protein of the BCL2 family, can be downregulated by CHOP [156]. Furthermore, the activation of JNK by the IRE1 pathway induces the phosphorylation of BCL2 and of another anti-apoptotic protein that is BCLXL. When these two proteins are phosphorylated, they are inactive and this means that the apoptotic cascade, induced by the ER-stress, lead to the switch off of all the anti-apoptotic proteins, through different mechanisms [189,190].

One of the most important players in the apoptosis is the pro-apoptotic BCL-2 family member NOXA. NOXA, in particular, is one of the BH3-only proteins and among them is the smallest (only 54 residues), however its expression is dramatically increased in a condition of proteotoxic stress [191]. The first studies on this protein define it as a TP53 target gene [192]. Nevertheless, it was later seen that its transcription could be potentiate also in mechanisms that are p53 independent, for example in situation of stresses such as oncogenic transformation or proteotoxic stress. In fact, NOXA depletion can weakens apoptosis in the proteotoxic stress condition [193,194]. In the cell death cascade, NOXA can have a dual role of both sensitizer and activator through its BH3 domain present inside

the hydrophobic binding groove of both pro- and anti-apoptotic proteins. Regarding the sensitizer role, NOXA can interact with MCL1, BCLXL, and BCL2A1, leading to the release of some pro-apoptotic proteins like BAX and BAK, from the sequestration operated by these anti-apoptotic proteins. Instead, as an activator, NOXA can activate and promote the pro-death activity of BAX and BAK [195,196]. The expression of NOXA can be upregulated through ATF4 in cooperation with ATF3 [197]. This means that NOXA could be the mediator in the apoptotic cascade induced through the PERK/ATF4 axis like for example in the case of the cell starvation [185]. NOXA was also observed to regulate the apoptosis induced by ROS production in the ER compartment or by the classical ER stress inducer thapsigargin [198,199].

In order to activate the mitochondrial or intrinsic pathway of apoptosis, after proteotoxic stress, there are also other mechanisms, which involved other BCL2 proteins. For example, BIM/BCL2L11 and PUMA/BBC3 are other two BH3-only proteins that are reported to be upregulated during the ER stress and their abrogation can change the cell death response under proteotoxic stress [122,131,200]. While BIM was shown to be induced by CHOP transcriptionally [201], PUMA was shown to be induced in several cell lines when there is an ER stress stimulus [202].

Another important protein is BOK and its regulation relative to the proteotoxic stress condition. In general, BOK, which is a pro-apoptotic protein of the BCL2 family, is less expressed due to a short half-life of 15 minutes. However, during the ER stress condition, the E3 ligases that control the BOK degradation is saturated and, in this way, BOK can accumulate and induce the mitochondrial outer membrane permeabilization [203]. To escape this system, the cancer cells use the chaperone DNAJB12 (JB12), which is a member of the HSP40s, in order to control the degradation of BOK and maintain its low levels [204].

2.2.5 SUPPLEMENTARY CELL DEATH MECHANISMS INDUCED BY PROTEOTOXIC STRESS

Beside apoptosis, other cell death mechanisms could occur during ER stress, as shown in Figure 2.12.

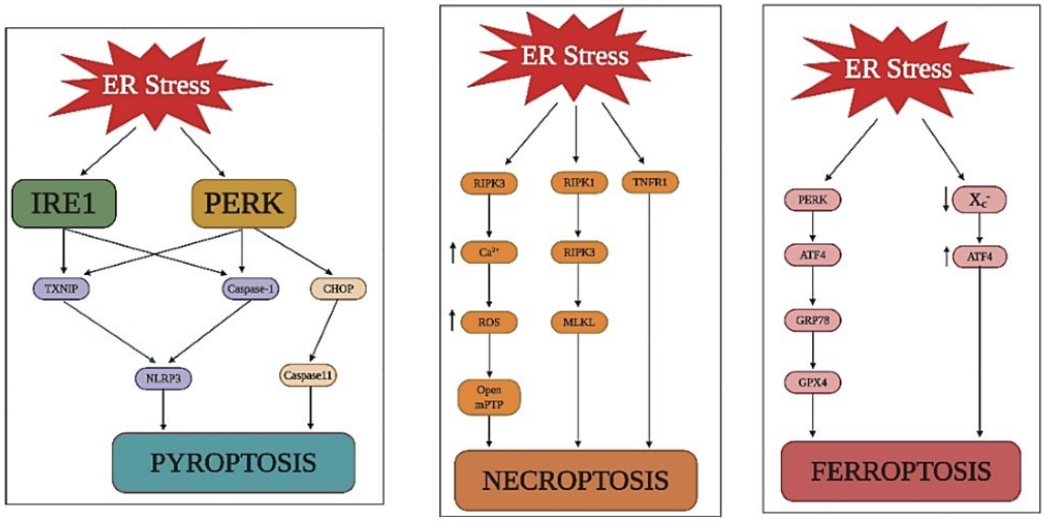

Figure 2.12: Additional cell death pathways induced during ER stress [205].

Proteotoxic stress can indirectly favor the accumulation of ROS and an unbalance homeostasis of the calcium. Both of these components lead to the dysfunction in the process of elimination of the damaged proteins act by UPS and autophagy, triggered by the presence of unfolded proteins and aggregates. This situation can directly alter ER and mitochondrial activities and, in this way, begin an alteration in the levels of ROS and calcium. The accumulation of these elements can be a signal for the cells to enter in cell death programs. However, it is still not clear how these events cooperate with the begins of the canonical apoptotic cascade. For example, it was shown that in some studies the accumulation of oxidative stress is seen in the initial part of the proteotoxic stress induced cell death [131,206]. What is clear is that the accumulation of these co-factors can induce different types of cell death after the triggering of proteotoxic stress [207]. Nevertheless, these different types of cell death induced by proteotoxic stress are still under investigation [208,209]. In this context, it was also reported that CHOP could lead to the induction of the transcription of Endoplasmic Reticulum Oxidoreductin 1 (ERO1α).

ERO1α can induce the hyper-oxidation of the ER environment, and it was shown that through a knockout of ERO1α in C. Elegans, the animal avoid the death induced by tunicamycin [143]. All of these types of cell death are more necrotic-like cell death than apoptotic ones, and in general they are an alternative response when the apoptotic pathway is impaired. For example, in a model of cell death induced by the mutant Huntingtin it was suggest a new model of switch from apoptosis to necrosis. Indeed, if the mutant protein is soluble, the cells have the potential of the membrane of the mitochondria hyperpolarized and the augmented levels of ROS induced apoptosis. Instead, if the mutant protein is in the form of aggregates, the cells have a high decrease in the potential of the mitochondria and go under quiescence with the result of the impair of the apoptotic pathway, leading to a slow cell death through necrosis [210]. This switch could be very interesting but needs to be verified with classical inducers of proteotoxic stress. The presence of NRF2 could also impair the necrotic death induced by proteotoxic stress, because it induces the creation of the autophagosomes in order to decrease the levels of protein aggregates [211]. In addition, NOXA could have a role in the necrotic type of cell death, as the mitochondrial targeting domains that are present in its structure can induce the mitochondrial fragmentation and cell death though necrosis occurs [212].

A peculiar form of necrotic cell death is necroptosis, which can be seen as a program type of necrotic cell death, and it is activated by the serine/threonine kinases Receptor Interacting Protein Kinase 1 and 3 (RIPK1 and RIPK3) with the assistance of the pseudokinase Mixed Lineage Kinase domain Like (MLKL) [213]. Small compound that induces necroptosis are able to trigger the UPR response, hence suggesting a possible correlation among necroptosis and proteotoxic stress [214]. Nevertheless, is not an easy task to understand if the UPR response could have a pro-survival effect or it directly act as a part of the cell death pathway. For example, it was revealed that, in a study about UPR in a canonical necroptotic model induced by the Tumor Necrosis Factor α (TNFα), the two classical PERK inhibitor (GSK2606414 and GSK2656157) can inhibit also RIPK1 [215]. RIPK1 has a plethora of functions and can also counteract the cell death induced by proteotoxic stress. Indeed, the overexpression of RIPK1 can trigger the autophagy cascade and can induce resistance from the cell death induced though ER stress in melanoma cells [216]. Instead, in a model of hypoxia with UPR activation and ER

stress condition, the role of necroptosis is not evident, while the role of pyroptosis through activation of NRL family Pyrin domain containing 3 (NLRP3) inflammasome is more evident with the action of Thioredoxin-Interacting Protein (TXNIP) [217].

Another particular type of cell death is an iron-dependent cell death called ferroptosis that leads to the accumulation of lipids peroxides after the failing of the glutathione-dependent antioxidant defenses [218,219]. However, there are not so many studies and evidences that linked ferroptosis and proteotoxic stress, but it is possible that an association could exist [220]. Indeed, several ferroptotic inducers can lead to the activation of the UPR response [220]. As mentioned before, in the initial stage, the role of UPR could be seen as a mechanism of pro-survival of the cells [221]. Nevertheless, the presence of ROS accumulation could connect the ferroptosis and the ER stress. Glutathione peroxidases, in fact, can mediate ferroptosis through the reduction of the presence of hydroperoxyl groups of complex lipids and can reduce the activity of lipoxygenases. Furthermore, they can also react with the protein isomerases in the process of oxidative protein folding control acts in the ER [222].

The response of the cells to the proteotoxic stress inside the cell population could vary between the cells, in fact, some cells could die, instead others could survive. The presence of the chaperones is crucial in order to define this switch from proteostasis to proteotoxicity, and the chaperone HSF1 resident in the ER can control it [223]. HSF1 is a master gene regulator for the expression of the chaperones after the induction of proteotoxic stress. Indeed, in this kind of stress condition, HSF1 is activated through phosphorylation and it trimerizes and can induce the transcription of several chaperones [224]. It was shown through a study that *foci* of HSF1 could be the ultimate decision between life and death. In fact, when there is a continue stress, these *foci* can change from fluid to a structure similar to a gel in which HSF1 is kept inside, in this way the chaperones could not be transcribed, and cell death occurs [225].

2.3 PROTEOTOXIC STRESS AS A TARGET IN THE ANTICANCER THERAPY

2.3.1 CANCER CELLS AND PROTEOTOXIC STRESS

In general, the protein synthesis process is prone to error, and it has been revealed that more than 30% of new synthesis protein are directly degraded into the proteasome in few minutes after their translation [226]. These proteins that are rapidly degraded are the Defective Ribosomal Proteins (DRiPs) or Rapidly Degraded Polypeptides (RDPs). It is fundamental to remove immediately the DRiPs, because the accumulation of these proteins can overload the proteasome and leads to proteotoxic stress [227]. The cancer cells generally synthesize a lot a new proteins, because they need them to survive and to escape from immunosurveillance, but for this reason the high rate of new synthesize proteins leads to an accumulation of DRiPs compared to the normal cells [228]. Cancer cell, for example, overactivate the mTORC1 pathway that promote high synthesis of new proteins, however this means that cancer cells have a strong dependence from the proteasome in order to avoid high proteotoxicity [60,229]. The cancer cells try to maintain the proteostasis, which is a fundamental status to stay alive, through the creation of immunoproteasomes, which can be seen as secondary elements in order to reduce the proteotoxic stress, and it was seen in cancer cells with mutation in RAS, PTEN, TSC1, or mTORC1 [230]. Beside from the newly synthesize proteins, cancer cells are also dependent from the environment, in fact in these cells, hypoxia, oxidative stress and starvation are more present than in the normal cells and all of these conditions can induce unfolded proteins and ER stress [122,131].

Proteotoxic stress could also be linked with the cellular metabolism, but this aspect needs further investigations [231]. For example, it was revealed that a switch from the oxidative metabolism to the glycolysis could generate cells resistant to the cell death induced by the UPS inhibitor bortezomib. The study of the regulation of the status of the mitochondria could be an alternative mechanism in response of proteotoxic stress and its regulation could be interesting for the anticancer therapy [232].

In parallel to the conditions related to the environment, in the cancer cells there is an accumulation of genetic alterations that can in turn induce proteotoxic stress. Some of these alterations are aneuploidy, copy number variations and point mutations [233,234]. Aneuploidy is generally associated with the presence of many stresses in the cancer cells such as metabolic and oxidative stress [235]. Regarding the proteotoxic stress, the aneuploidy can induce an unbalanced stoichiometry in the protein complex, causing protein aggregation and later proteotoxic stress. Indeed, the aggregate proteins are generated through an error in the expression of the subunits of the protein complexes due to a wrong number of chromosomes. For this reason, these excess subunits need to be degraded, however, in most of the cases, they aggregate generating ER stress, and on the other hand, in order to restore the normal amount of proteins, the cells aggregate other proteins to reduce the number of excess proteins [236]. Aneuploidy can also lead to reduce the expression of HSF1, causing a defect in the expression of the fundamental chaperones needed for the assistance in the protein folding. This reduces the expression of HSP90s with an accumulation of unfolded proteins and the generation of proteotoxic stress [237]. In addition, the overexpression of the genes can impair the normal proteostasis [238]. In fact, the generation of wrong variants of the proteins could also trigger the formation of unfolded proteins and aggregates [234].

Considering all these points, cancer cells need to upregulate all the mechanisms that can reduce the proteotoxic stress in order to maintain the proteostasis and, in this way, continue living, as also reported in the Figure 2.13 [239-241]. In fact, compared to the normal cells, cancer cells are more dependent on the expression of the HSPs and from the presence of UPS [242]. HSP90s and HSP70s are some HSPs fundamental for the cancer cells, because these chaperones can help the cells to escape from signals that are more related to the anti-proliferation, to the cell death and to the senescence. Furthermore, these chaperones are also related to drug resistance, angiogenesis and metastasis, which are all crucial stages for the survival of the cancer cells [243]. In a therapeutic perspective, try to use small molecules able to impair these survival mechanisms of the cancer cells can be a strategy in order to selectively kill these cells [244]. Many studies have reported the development of new therapeutic strategies involving the abrogation of these survival mechanisms, resulting in the unleash of high increase of proteotoxic stress [245,246].

However, in some cases it was observed that the presence of proteotoxic stress can confer a resistance in cells to other kind of small compound, for example in the case of HSF1 that confers resistance to lapatinib, which is an inhibitor of the Receptor Tyrosine Kinase (RTK), in breast cancer [247].

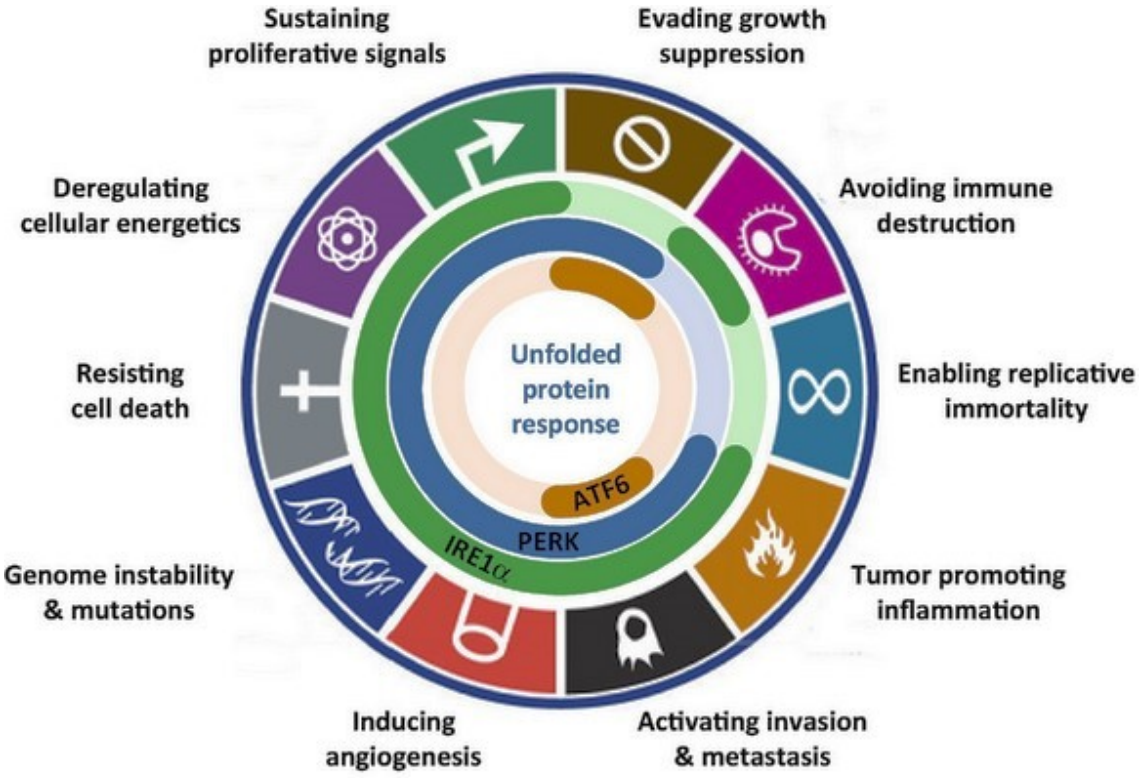

Figure 2.13: Different roles of the UPR for the survival of the cancer cells [248].

2.3.2 TARGETING PROTEOTOXIC STRESS: DISCOVERY OF UPS INHIBITORS

The dysregulation of every element of the UPS can be involved in many pathologies, as in the neurodegenerative diseases or cancer [249]. As mentioned before, cancer cells are characterized by high levels of the 26S proteasome activity that constitutes a critical advantage for cell survival. Indeed, in this way, they do not accumulate unfolded proteins and they can avoid cell death. Instead, if the 26S proteasome is inhibited, the protein disruption is stopped, and this results in the accumulation of polyubiquitylated proteins, which leads to cell death. Numerous studies have demonstrated that the cancer cells are more sensitive to the inhibition of the UPS compared to the normal cells [60,250]. For this reason, finding compounds able to block this system have rising the attention of the scientific community.

The first compound approved by the Food and Drug Administration (FDA) and by the European Medicine Evaluation Agency (EMEA) for the use in clinic is bortezomib, which is a reversible inhibitor of UPS [180,251]. Bortezomib is a dipeptidyl boronate, which can bind the β5 subunit of the 20S core of the 26S proteasome and can block its catalytic activity. This leads to the accumulation of polyubiquitylated proteins and the begin of the apoptotic cascade. However, this UPS inhibitor is not completely specific for the β5 subunit, in fact, it can inhibit also the β1 subunit and several other serine proteases with a lower affinity, such as cathepsin A and dipeptidyl peptidase II. Regarding its clinical use, it was approved for the treatment of relapsed or refractory multiple myeloma [252], and it has been also studied in different hematological malignancies and solid tumors, including non-Hodgkin's lymphoma, prostate, breast and non-small-cell lung cancers as single agent or in combinatory therapies [253].

Although bortezomib has shown promising results on diverse kind of cancers, the clinical trials reveal that some side effects could appear, such as thrombocytopenia, neuropathies and sometimes drug resistance. Indeed, possible mutations in the β5 subunit could impair the efficacy of this drug and was also shown that the appearance of high peripheral neuropathy, highlighted in the patients treated with bortezomib, can be due to the blocking of non-specific targets. Moreover, another negative characteristic related with the use of

bortezomib is the irreversibility of its binding to the β5 subunit of the 20S core, since it means that the patients need a frequent administration of the drug [180,250,251].

The finding of bortezomib begins to put the attention on the discovery of new UPS inhibitors, used as therapeutic agents, with the purpose to avoid the side effects generated with bortezomib treatment, and they are illustrated in Figure 2.14. MLN9708, also called ixazomib, is one of them and is the orally bioavailable analogue of bortezomib. It is still under studying for hematologic and solid tumor through the Phase I/II clinical trials. MLN9708 acts through a process mechanism in which, after its metabolization, it becomes the active form of the drug, called MLN2238. The active form works as a reversible inhibitor of the β5 subunit of the 20S core [250,251]. Another UPS inhibitor is marizomib, which differently from the other compound described, has a β-lactone-γ-lactam bicyclic ring in its structure without a linear peptide backbone. Like bortezomib is an inhibitor of the β5 subunit of the 20S core, but, as well as bortezomib, can bind other subunit of the 20S core (β1 and β2 subunits). Thus, also this compound shows neurotoxicity in treated patients, however it seems effective in the treatment of multiple myeloma and chronic lymphocytic leukemia [254].

Nevertheless, among all of these new proteasome inhibitors, up to now the best one appears to be carfilzomib: this compound is a tetrapeptide epoxy-ketone, which is able to bind and react with high selectivity with the β5 subunit of the 20S core, by an irreversible bound (on the opposite of the mechanism of bortezomib). In addition, carfilzomib demonstrates a reduced non-specific activity for the other β subunits of 20S core and for the other serine proteases. Regarding its use in clinical therapy, it has been approved as a single agent or in a combinatory strategy to treat the patients with relapsed and refractory multiple myeloma [255]. The preliminary data obtained from the treated patients highlight that, differently from bortezomib, carfilzomib does not show the presence of the peripheral neuropathy, and this result augments the attention on this drug in a therapeutic point of view for other types of cancer. Additionally, also for carfilzomib an orally bioavailable analogue was developed, and it is called oprozomib. Oprozomib again demonstrates promising results as antitumor agent in several kinds of cancer, such as multiple myeloma, squamous cell carcinoma of head and neck, non-Hodgkins lymphoma and colorectal cancer [256].

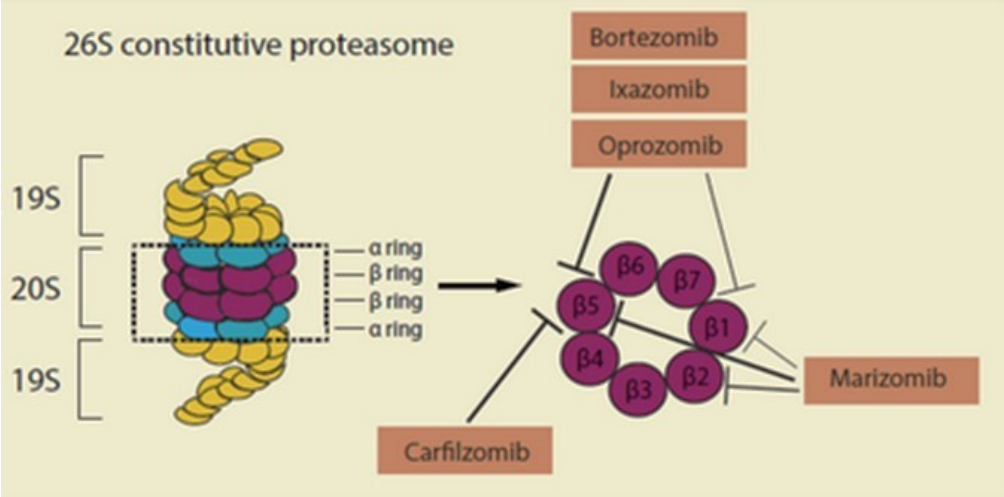

Figure 2.14: UPS inhibitors and their mechanisms of action; all the small molecules identified target subunits of the 20S core of the 26S proteasome [254].

2.3.3 G5: A PROMISING SMALL MOLECULE AS ANTICANCER AGENT

In addition to the opportunity to target the 20S core of the 26S proteasome, an increasing amount of discoveries are displaying the possibility of targeting the DUBs present in the 19S regulatory subunit as potential therapeutic strategy in the cancer treatment. The importance of the meaning of the role of the deubiquitylation process in a eukaryotic cell is established by the pathological resulting effect due to its blocking. For example, the chemical inhibition of the DUBs action induces the accumulation in the cytosol of polyubiquitylated proteins and afterward the beginning of the proteotoxic stress condition, which is lastly followed by the appearance of cell death [257]. For this reason, some DUBs inhibitors have been developed, and their capability to induce cell death through necrosis or apoptosis has been generally confirmed.

In particular, these inhibitors can be divided in two different groups: the selective inhibitors, which can act on a specific DUB or on a limited and selected number of DUBs, and the Non-Selective Isopeptidases Inhibitors (N-SIIs), which in contrast with the first ones can impair the capacity of various and numerous isopeptidases [168,258]. Among the N-SIIs, a new compound arises as a promising agent, which is called G5. G5 is a 4H-thiopyran-4-one, tetrahydro-3,5-bis[(4-nitrophenyl) methylene]-1,1-dioxide that in its structure present a cross-conjugated α, β unsaturated dienone and two electrophilic

sterically accessible carbons and its structure is represented in Figure 2.15. G5 can act as Michael acceptor and its carbons can interact with nucleophilic species, such as the catalytic cysteine of the proteins, among which there are the DUBs [259].

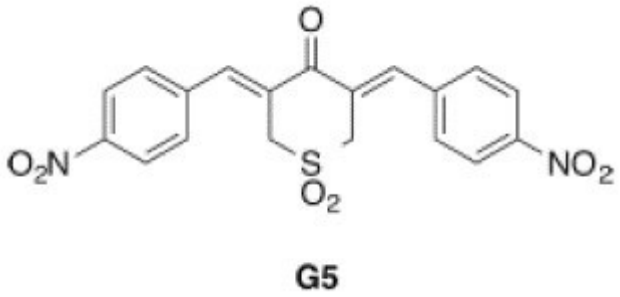

G5

Figure 2.15: Chemical structure of G5 [257].

Originally, it was verified that G5 can react with diverse DUBs as the proteasome-associated DUB UCH-L5 and the deISGylase USP18 with a strong affinity, while it can bind weakly UCH-L1 and USP2, through the inhibition of their deubiquitylating activity [168,257,259]. To better recognize *in vivo* the intracellular targets of this compound, was used a biotinylated version of G5, called 2c-biotin. The importance of find all targets is related to understand how it is thinkable to improve the drug characteristics and to predict the possibility of the appearance of possible side effects of the compound. This is an important part of a study when the aim is to use eventually a new unknown compound in clinic as a therapeutic agent. 2c-biotin was used in some experiments of biotin-pull down, which show that this compound has a higher affinity in binding USP33 and USP1, compared to the bind with USP14, USP18 and UCH-L5. Interestingly, this compound shows that it has the ability to bind some diverse targets that are totally not related to the isopeptidases, such as the serine/threonine kinase Akt, typically involved in the cell survival and growth regulation, and Cofilin-1, which is related to the process of the cytoskeleton actin disassembling. All of these evidences demonstrate that this class of inhibitors can cause extensive quantity of responses, since they can block various proteins in addition to the isopeptidases and this could elucidate the strong anticancer activity shown *in vivo* [260].

The N-SII G5 can induce different cellular processes in the treated cells: the cytosolic accumulation of polyubiquitylated proteins, the induction of the ER stress, the inhibition of NF- kB pathway [261], the p53 stabilization [169], and the activation of some death receptors and several pro-apoptotic proteins [168,245]. All these stresses let the cells start a cascade of cell death induced through a BCL2-dependent but apoptosome-independent pathway [41,168,209]. How this happens it still not perfectly clear, but it seems that some machineries of death receptor pathway normally degraded by the proteasome are involved, like DR4, DR5 and their specific ligands [262]. Their accumulation alongside with the decrease of anti-apoptotic c-FLIP expression levels, define a synergistic effect, which could explain the initiation of the cell death independently from the apoptosome [263]. In this context, it has been also demonstrated the influence given by the cytosolic accumulation of DIABLO/SMAC, which can reinforce the DR-induced cell death. In fact, DIABLO/SMAC can overcome the defense given by the anti-apoptotic BCL2 protein and can free the effector caspases from IAP inhibition also in the absence of the apoptosome formation [168].

Nevertheless, in contrast with bortezomib, the most fascinating feature of the N-SII G5 is its ability to activate an unusual necrotic pathway in an apoptosis-resistance condition [208]. This aspect has been shown in a study performed on glioblastoma cells, which have an intrinsic apoptosis resistance and the greatest sensitivity to die by necrosis [264]. Initially, it was shown that the glioblastoma cell line U87MG treated with a pan-caspase inhibitor in order to obtain cells resistant to the apoptosis, die in a caspase-independent manner after G5 treatment. Moreover, another study executed on murine embryonic fibroblasts derived from mice double-deficient for BAX and BAK support the previous evidence, because G5 can kill also those cells, which are apoptosis-resistant, through the triggering of a necrotic pathway [168,208].

Regarding the necrotic cell death pathway induced by G5, less is still known about the mechanisms and the possible interactors. A recent work published by our group, which is part of this PhD thesis, that take advantage of a library of shRNA infecting U87MG cells, was evaluated in order to better characterize this cascade, and one possible candidate obtained, as an interactor for G5, was the Glycogen Synthase Kinase 3 β (GSK3β). However, the knockout cells for GSK3β, obtained through the CRISPR-Cas9 technique,

show that those cells are still dying after G5 treatment, in a less way compared to the wild type cells, demonstrating that this protein has only a minor role in the necrotic cascade induced by G5 [206]. Up to now, it has been well described only the involvement of the Protein Phosphatase 2A (PP2A) in this cell death pathway. In particular, the catalytic activity of PP2A is augmented in response to the G5-treatment, resulting in an increased dephosphorylation of one of its specific targets: the Cofilin-1 [209]. Cofilin-1 is an actin-binding protein, characterized by a depolymerization activity controlled by the phosphorylation state of the serine in position 3 [265]. Thus, in the G5-treated cells, the N-SII, enhancing the activity of the phosphatase PP2A, induces the dephosphorylation and, subsequently, the activation of Cofilin-1, which stimulates the depolymerization of the actin filaments. This mechanism causes deep variations in the cytoskeleton and in the cellular morphology, causing the loss of the cellular adhesion and then the cell death [209].

2.3.4 THE BORN OF G5 DERIVATIVES: 2C, 2CPE AND 2CPP

The G5 induced cell death is still not clear, however this small compound seems promising for a therapeutical approach, but it has problems in the delivery *in vivo* (for example it is not soluble in aqueous systems), and for this reason many tentative were done in order to optimize this drug for an *in vivo* study. Hence, G5 was later modified through the vary of the positions of different atoms, thus obtaining G5 derivatives and the structure of the most relevant is reported in Figure 2.16 [257]. U87MG cell line was used in order to test all of these G5 variants, to better understand if they are able to induce necrosis or apoptosis depending on the chemical substituents. One of the variants raise the interest for its reactive -OH group and was called 2c. This -OH group is crucial because it permits an easy modification in order to improve the drug characteristics, like for example to improve the *in vivo* delivery [257]. Functional studies on 2c inhibitory activities revealed a less strong potential to inhibit DUBs such as UCHL1, UCHL5 and USP2, instead a stronger inhibiting effect on USP18 compared to G5. This functional aspect has an important meaning in terms of the resulting cell death effect of the two compounds, indeed, while G5 is more prone to induce necrosis, 2c seems to be more

prone to induce apoptosis, thus it is plausible that the two compounds can interact with different cysteine [257].

Despite the interesting differences between G5 and 2c, also 2c is not soluble in aqueous solutions, hence in order to have a compound useful for the anticancer therapy, it is important to modify 2c to improve the *in vivo* delivery. Firstly, 2c was conjugated with a molecule of Polyethylene Glycol (PEG), which is fundamental for the increasing in terms of solubility and bioavailability. 2c and PEG are conjugated through a sequence that can be recognized by some esterases and the resulting 2c derivative was called 2cPE, which represents the first N-SII pro-drug synthesized, and its structure is shown in Figure 2.16 [257]. By testing this compound on A549 lung carcinoma cell lines it was revealed that the compound was able to induce cell death and that the conversion from the pro-drug to the effective 2c is given by the esterase Phospholipase A2 Group 7 (PLA2G7) [258]. Considering the promising results, 2cPE was also tested in a xenograft model of A549 lung carcinoma in immunocompromised mice, demonstrating an anticancer activity without any significant side effects [257].

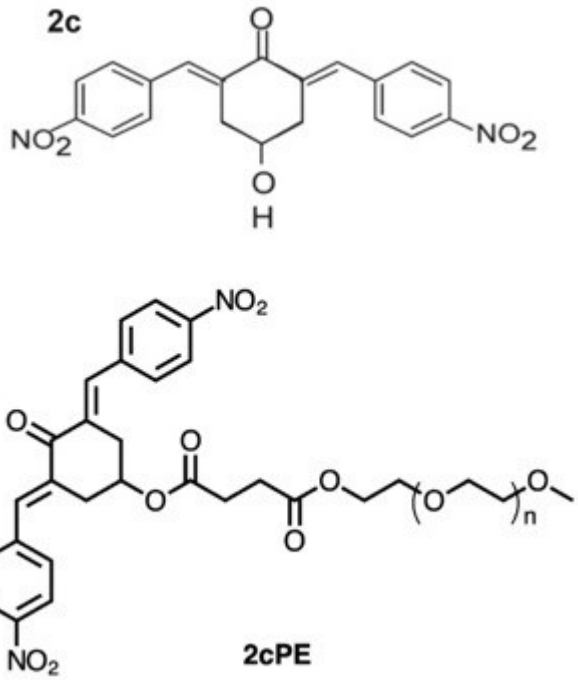

Figure 2.16: Chemical structure of 2c and 2cPE [257].

A recently published work on leiomyosarcoma (LMS) cell lines, which is part of this thesis, involve a new 2c derivate. In these cell lines 2cPE was incapable to induce cell death due to probably a less expression of PLA2G7 by these cells, and for this reason, another strategy was used. 2c was conjugated with PEG through a small peptide that could be processed in the tumor microenvironment by several proteases (including metalloproteinases and cathepsins). The generating pro-drug version of the compound was called 2cPP and its structure is shown in Figure 2.17 [266]. 2cPP demonstrates to be efficient in inducing cell death in both *in vitro* and *in vivo* models of LMS [266]. All of these compounds, G5, 2c and all its derivatives are the main characters of the study conducted in this thesis, because, despite their promising role as therapeutic agents, their mechanism of action need to be elucidated.

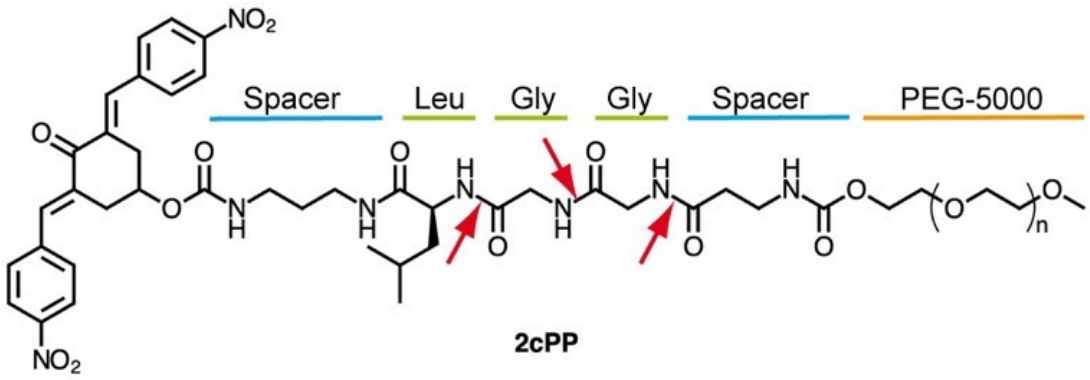

Figure 2.17: Chemical structure of 2cPP [266].

3 AIM

One of the most significant challenges in the anticancer therapy is the fighting against chemotherapy failure, in fact, cancer cells can acquire mutations and alterations, which lead to drug resistance in order to keep the cell alive. For this reason, the discovery of new therapeutic targets is critical to avoid tumor relapses and recurrence. UPS emerges as a possible new target in this context, indeed its inhibition leads to an accumulation of polyubiquitylated proteins that trigger cell death. The small molecule G5 is a N-SII, which acts as a Michael acceptor in order to bind nucleophiles like the cysteines of the DUBs. This compound can induce several stresses such as protein unfolding, glutathione depletion, ER stress, proteasomal impairments, and cytoskeletal stress in the cells, which lead to the activation of high rate of proteotoxic stress. This compound is able to trigger a necrotic-caspase independent cell death in glioblastoma cells, however less is known about its peculiar mechanism of action. Understanding the pathway by which this compound acts could be fundamental in a therapeutic point of view. Thus, the aim of this thesis was to better understand and clarify the pathways that are activated after the treatment with this compound and which are the key players involved. A subsequent step was the modification of this compound, which is not soluble in water, in order to have a more efficient compound useful for *in vivo* studies. To address these points, G5 and its derivatives were tested in glioblastoma cells, as they are reported to be more prone to die for necrosis instead of apoptosis and in leiomyosarcoma (LMS) cells, since this tumor is without therapeutic options. In particular, LMS is a tumor, which present a rare incidence but with an aggressive behavior determined by the presence of complex karyotypes. For this kind of tumors Doxorubicin treatments are the standard therapy, however, in many cases is not sufficient to eradicate the tumoral cells, thus the tumor can recur and metastasize. For this reason, new therapeutic options beside surgical resection need to be found for this kind of cancer.

3.1 SUMMARY OF THE PUBLISHED PAPERS

In order to better dissect the mechanism by which G5 can induce cell death, a shRNA-based viability screen was performed in glioblastoma cells after treatment with G5. Among all the possible candidates emerging from this screening, GSK3β seems to be a promising one. However, by testing G5 on glioblastoma cells knocked-out for GSK3β, cell death was still present, although at reduced levels, compared to the wild-type cells, defining that this kinase is partially involved in the G5 cascade. We demonstrated that GSK3β is a key element in the necrosis induced by the quinone DMNQ, a ROS generator. When wild-type cells are treated with DMNQ, the kinase is activated and Akt is inactivated. Furthermore, after the treatment, GSK3β is accumulated in the nucleus just before the collapsing of the potential of the mitochondrial membrane. The absence of GSK3β leads to a reduction of the accumulation of ROS after DMNQ treatment. We demonstrate that this is due to an overexpression of the genes related to the detoxification of the quinones (NQO1 and NQO2), probably through the activation of the Nrf2 pathway. It is possible that, in the case of G5, GSK3β is responsible for the cell death response due to redox unbalance.

G5 was subsequently modified to be more prone to be engineered in the new compound 2c, which shows a more apoptotic than necrotic type of cell death in glioblastoma cells. A bioinformatic analysis of a signature of genes, which are known to be upregulated after 2c treatment, including various players involved in the proteotoxic stress response, reveals a negative correlation between them and the survival of LMS patients. Starting from this observation, we want to understand if the aggressive LMS can coexist with high levels of proteotoxic stress or if they can reach a limit when they are challenged with an increasing further proteotoxic stress, generating tumoral cells that are more vulnerable and prone to cell death. We demonstrate that 2c can induce proteotoxic stress, cell death and mitochondrial dysfunction in LMS cells. Moreover, through STED confocal microscopy, we show that the treatment with 2c can lead to a peculiar re-organization of DIABLO/SMAC at sub-mitochondrial level. In order to enhance the selectivity and the efficacy for *in vivo* studies, 2c was later engineered to obtain 2cPP, a pro-drug of 2c and a PEG linked though an aminoacid chain that can be cleaved from proteases present only

in the tumor microenvironment. 2cPP seems promising, in fact, it can reduce the tumor volume of different LMS xenografts in mouse models.

All the data described in this section have been already published and are reported in this thesis in the section Publications. Thus, the subsequent Result section present in this thesis will be focused on the recently obtained and still unpublished results regarding the last months of the PhD working period.

4 RESULTS

4.1 RNA-SEQ ANALYSIS: A COMPARATIVE STUDY BETWEEN NORMAL AND TUMORAL CELLS IN RESPONSE TO 2C

2c is a small compound which, as well as its progenitor G5, is a N-SII that acts as a Michael acceptor for nucleophiles like cysteines [245]. As demonstrated in the recently published works, it is able to inhibit several DUBs leading to accumulation of polyubiquitylated proteins, triggering cell death. The effects of 2c are pleiotropic, including the induction of oxidative stress and in particular proteotoxic stress and ER stress [168,260]. LMS are rare and aggressive tumors that need new therapeutic strategies and we have previously shown that these tumors are prone to accumulate proteotoxic stress and are sensitive to cell death induced by 2c. For these reasons, LMS cell lines were used as cellular models for this thesis. However, the mechanism of cell death triggered by both G5 and 2c is not fully elucidated and new discoveries of these mechanisms could be fundamental in a clinical point of view. It seems, also, that this compound could be a promising therapeutic agent, indeed its derivative 2cPP can induce tumor volume reduction in LMS xenografts in mice [266]. Importantly, we show that 2c can induce cell death in HUtSMC (cell line which can be considered as the normal counterpart of LMS) but with lower rates compare to SK-UT-1 (LMS grade III cell line) [266]. For this reason, the study of the gene expression differences between normal and tumoral cells after 2c treatment is critical to unveil the diverse behavior of the cells treated with this compound, which converge in a different level of cell death induction.

In order to better understand and clarify which genes are involved in the cascade induced by 2c and to define the differences between normal and tumoral cells in terms of genes expression, an experiment of RNA-Seq was performed. SK-UT-1 and HUtSMC, immortalized with hTERT, cell lines were used in this experiment. The cells were treated with 2c for 3 h or 12 h and RNA of both treated and untreated cells were extracted and purify to be sequenced through RNA-Seq experiment. In order to confirm the efficiency

of the treatment, in particular for the immortalized HUtSMC cells, the cells were also treated for 24 h and cell death was assessed with TB (Figure 4.1A). The assay demonstrates that 2c is able to induce high levels of cell death and that HUtSMC immortalized with hTERT have lower cell death rate compared to SK-UT-1.

DEGs (differentially expressed genes) are divided between upregulated and downregulated based on their expression identified as log2 fold change compared to the untreated cells. Venn diagrams and the histogram representations show the different number of genes upregulated and downregulated between the two cell lines and in the two different time points (early gene at 3 h, late gene at 12 h) (Figure 4.1B-E). The number of late genes, both upregulated and downregulated, are more than the earlier ones in the two cell lines, probably due to an activation of several adaptive responses at later times. Furthermore, a number of genes resulted regulated at both time points in both the cell lines, which can be seen as maintained genes, demonstrating that there are genes modulated throughout all the cascade induced by 2c. Moreover, the number of upregulated genes is more of the downregulated ones, revealing that this compound can enhance and favor the expression of the genes instead of reducing it. The critical difference between the two cell lines is the fact that the number of genes, both upregulated and downregulated, is higher in the normal cells, indicating that the effect of this compound can induce the modulation of diverse genes in the normal cells, which can induce many pathways in order to keep the cells alive. Instead, tumoral cells, which are not able to counteract the effect of 2c, regulate less genes, suggesting that they directly undergo to cell death programs.

The histograms relative to the p-value of the RNA-Seq analysis, can better clarify which pathways are involved in the cell lines in the 2c response (Figure 4.1F-I). Considering the upregulated genes, in both the cells are present genes related to the adhesion and the component of the plasma membrane. However, only for HUtSMC can be found genes related to the apoptotic process and the regulation of cell death. This regulation is determine by the upregulation of the anti-apoptotic genes, instead the pro-apoptotic genes remain unaltered, demonstrating again that the normal cells regulate processes related to the cell death mechanisms to maintain the survival of the cells. Instead, SK-UT-1 regulate genes related to the epigenetic regulation, probably by activating cell death programs.

Interestingly in the maintained genes of both the cells are present genes upregulated in MERS-CoV infection, this could be due to the fact that it is reported that Coranavirus, during its replication, induces ER stress and activates UPR response [267]. Because it is known that this compound triggers ER stress it is possible that genes in common with the MERS-CoV infection resulted upregulated. Regarding the downregulated genes, in both the cells are present genes related to the cell division, cell cycle and cell metabolism. In fact, it has been reported that proteotoxic stress condition leads to promoting the cell cycle arrest [268]. The data obtained highlight that the compound regulates the normal activities of the cells related to the cell cycle by impairing them.

In the last Venn diagrams both the cell lines are put together and it is possible to identify that some genes upregulated or downregulated are shared between them (Figure 4.1J-K). However, the majority of the genes regulated after 2c treatment are not in common between the two cell lines, suggesting that by further studying these genes it could be possible to identify which are the critical genes that gave the strong different impact on the cell survival after the treatment with 2c. This could have a huge importance in terms of the selectivity of the compound between a tumoral cell and a normal one, and by defining these critical genes, new small compounds with this ability can be developed to be more precise in killing only the tumoral cells.

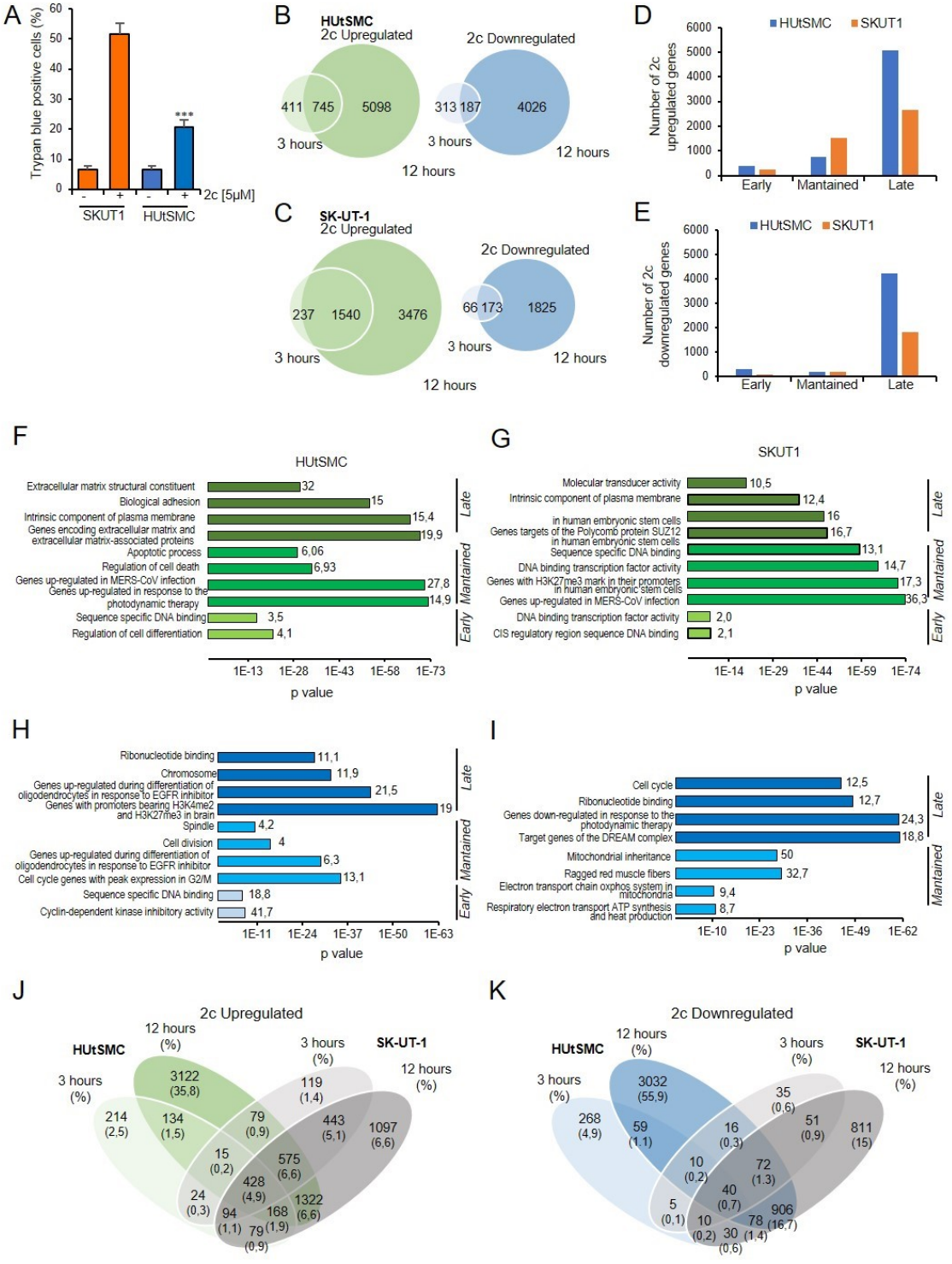
A
Trypan blue positive cells (%)
2c [5μM]
SKUT1
HUtSMC
B
HUtSMC
2c Upregulated
2c Downregulated
411 745 5098
313 187 4026
3 hours
12 hours
C
SK-UT-1
2c Upregulated
2c Downregulated
237 1540 3476
66 173 1825
D
HUtSMC SKUT1
Number of 2c upregulated genes
Early Mantained Late
E
Number of 2c downregulated genes
F
HUtSMC
Extracellular matrix structural constituent 32
Biological adhesion 15
Intrinsic component of plasma membrane 15,4
Genes encoding extracellular matrix and extracellular matrix-associated proteins 19,9
Apoptotic process 6,06
Regulation of cell death 6,93
Genes up-regulated in MERS-CoV infection 27,8
Genes up-regulated in response to the photodynamic therapy 14,9
Sequence specific DNA binding 3,5
Regulation of cell differentiation 4,1
Late
Mantained
Early
1E-13 1E-28 1E-43 1E-58 1E-73
p value
G
SKUT1
Molecular transducer activity 10,5
Intrinsic component of plasma membrane 12,4
in human embryonic stem cells 16
Genes targets of the Polycomb protein SUZ12 in human embryonic stem cells 16,7
Sequence specific DNA binding 13,1
DNA binding transcription factor activity 14,7
Genes with H3K27me3 mark in their promoters in human embryonic stem cells 17,3
Genes up-regulated in MERS-CoV infection 36,3
DNA binding transcription factor activity 2,0
CIS regulatory region sequence DNA binding 2,1
1E-14 1E-29 1E-44 1E-59 1E-74
p value
H
Ribonucleotide binding 11,1
Chromosome 11,9
Genes up-regulated during differentiation of oligodendrocytes in response to EGFR inhibitor 21,5
Genes with promoters bearing H3K4me2 and H3K27me3 in brain 19
Spindle 4,2
Cell division 4
Genes up-regulated during differentiation of oligodendrocytes in response to EGFR inhibitor 6,3
Cell cycle genes with peak expression in G2/M 13,1
Sequence specific DNA binding 18,8
Cyclin-dependent kinase inhibitory activity 41,7
1E-11 1E-24 1E-37 1E-50 1E-63
p value
I
Cell cycle 12,5
Ribonucleotide binding 12,7
Genes down-regulated in response to the photodynamic therapy 24,3
Target genes of the DREAM complex 18,8
Mitochondrial inheritance 50
Ragged red muscle fibers 32,7
Electron transport chain oxphos system in mitochondria 9,4
Respiratory electron transport ATP synthesis and heat production 8,7
1E-10 1E-23 1E-36 1E-49 1E-62
p value
J
2c Upregulated
HUtSMC
SK-UT-1
12 hours (%)
3 hours (%)
3122 (35,8)
214 (2,5)
134 (1,5)
79 (0,9)
119 (1,4)
443 (5,1)
1097 (6,6)
15 (0,2)
575 (6,6)
428 (4,9)
24 (0,3)
94 (1,1)
168 (1,9)
1322 (6,6)
79 (0,9)
K
2c Downregulated
3032 (55,9)
268 (4,9)
59 (1,1)
35 (0,6)
16 (0,3)
51 (0,9)
811 (15)
10 (0,2)
72 (1,3)
40 (0,7)
5 (0,1)
10 (0,2)
78 (1,4)
906 (16,7)
30 (0,6)

Figure 4.1: Number of genes regulated after 2c treatment in HUtSMC and SK-UT-1. A) Countings of the TB positivity expressing the percentage levels of cell death of SK-UT-1 and HUtSMC hTERT treated with 2c 2.5 μM for 24 h. Data were from 3 experiments. Columns mean loss of viability + SD. ***=p<0.005; B) and C) Venn diagrams representing the number of genes upregulated or downregulated after 2c treatment (5 μM) for 3 h or 12 h in HUtSMC hTERT (B) or in SK-UT-1 (C); D) and E) Histograms representing the number of genes upregulated (D) or downregulated (E) after 2c treatment (5 μM) in HUtSMC hTERT and SK-UT-1 for 3 h (early), 12 h (late) or in common between 3 h and 12 h (maintained); F) and G) Histograms representing the pathways and their corresponding p-value values resulting upregulated after 2c treatment (5 μM) in HUtSMC hTERT (F) or in SK-UT-1 (G) for 3 h (early), 12 h (late) or in common between 3 h and 12 h (maintained); H) and I) Histograms representing the pathways and their corresponding p-value values resulting downregulated after 2c treatment (5 μM) in HUtSMC hTERT (H) or in SK-UT-1 (I) for 3 h (early), 12 h (late) or in common between 3 h and 12 h (maintained); J) and K) Venn diagrams representing the number of genes upregulated (J) or downregulated (K) after 2c treatment (5 μM) for 3 h or 12 h in SK-UT-1 and HUtSMC hTERT.

4.2 DIFFERENTIAL GENES EXPRESSION BETWEEN NORMAL AND TUMORAL CELLS

As seen before, there is a difference in terms of the rate of cell death between the cell lines considered. For this reason, the expression value in log2 fold change of several critical elements involved in cell death pathways was analyzed in this experiment. The results presented in heatmap (Figure 4.2A) reveal that in SK-UT-1 the majority of the pro-apoptotic genes are upregulated, such as *PMAIP1*, *PUMA* and *BIM*, with an increase induction at 12 h, instead the majority of the anti-apoptotic genes are slightly downregulated or not regulated. In the case of HUtSMC, the analysis shows that at 3 h all the genes are only slightly regulated. At 12 h instead, *PMAIP1* is upregulated like SK-UT-1, but the majority of all the genes are downregulated, both pro-apoptotic, such as *BOK*, and anti-apoptotic, such as *BCL2L10*, demonstrating a balance between the different types of genes. Interestingly, the anti-apoptotic gene *BCL2A1* is strongly upregulated highlighting that the cell tries to activate all the pathways in order to survive and this is converted in the difference of the cell death rate between the cells.

LMSs have intrinsic high levels of proteotoxic stress and 2c is able to induce this type of stress in the cells, for this reason, genes involved in the UPR pathway and related to the ER stress were analyzed from the RNA-Seq data. The results in the heatmap (Figure 4.2B) show strong similarity among the two cell lines, with in general an upregulation of the most critical genes involved in this kind of pathway at 3 h, which is augmented at 12 h. Instead the less critical are not regulated or downregulated. In particular, the genes resulted upregulated are the ones related to the ATF network, such as *ATF3*, *ATF4*, *CHOP* (*DDIT3*) and *GADD34* (*PPP1R15A*), the UPR sensors, *IRE1* (*ERN1*) and *PERK* (*EIF2AK3*), several chaperones, such as *DNAJB9* and *HSPA5* and in general genes correlated with the UPR, such as *HERPUD1*, *FGF21* and *STC2*. The analysis confirms the sensibility of these cells to proteotoxic stress and that 2c enhance this stress conditions with no strong differences between SK-UT-1 and HUtSMC.

All the data collected from the RNA-Seq experiment reveal several pathways that can be modulated after the treatment with 2c and that the normal uterine cells have a different

response compared to the tumoral ones, with the regulation of many genes in order to keep the cells alive.

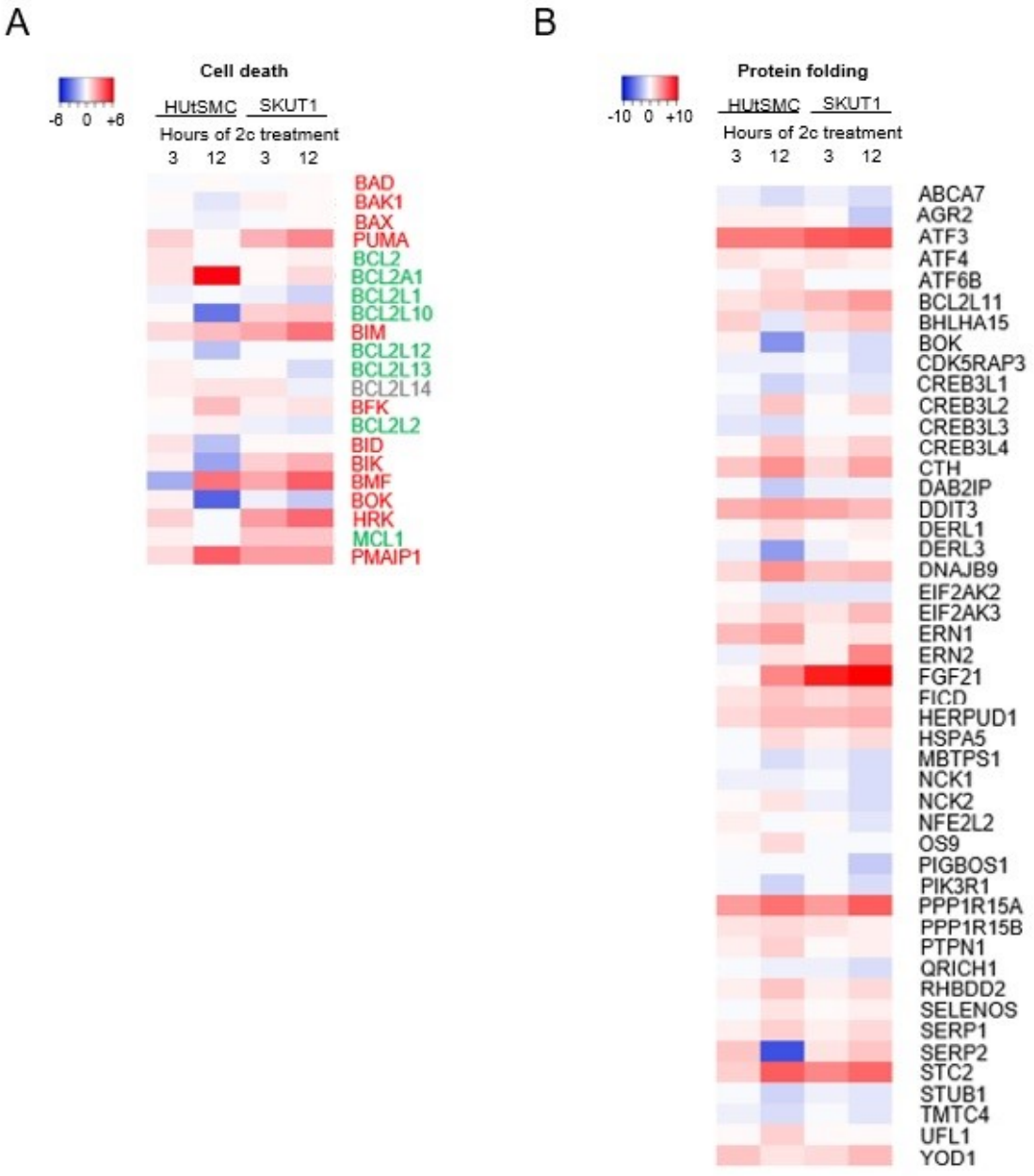

Figure 4.2: Expression levels of cell death and proteotoxic stress response genes in HUtSMC and SK-UT-1. A) Heatmap reporting the log2 fold change expression values of HUtSMC hTERT and SK-UT-1 after 2c treatment (5 µM) for 3 h or 12 h of genes related to cell death pathways (in green are reported the anti-apoptotic genes, in red are reported the pro-apopotic genes, in grey is reported a gene which could be both anti-apoptotic and pro-apoptotic); B) Heatmap reporting the log2 fold change expression values of HUtSMC hTERT and SK-UT-1 after 2c treatment (5 µM) for 3 h or 12 h of genes related to proteotoxic stress response.

4.3 COTREATMENT SCREENINGS TO IDENTIFY THE BEST PARTNER FOR 2C

The induction of cell death and proteotoxic stress by 2c in LMS, both in cell lines and animal models, was already demonstrated [266]. However, a small part of the cells could remain alive and maybe could become resistant to the treatment, in particular by using a low dosage which can be a good idea in a therapeutic point of view. Furthermore, the RNA-Seq analysis reveals that 2c can induce many different pathways and that this can help converging with the increasing of proteotoxic stress. For this reason, a good strategy could be to find another small compound, which acts as an inhibitor of a define protein or group of proteins or a pathway to put together in combination with 2c during the treatment.

As possible candidates for the combined treatment, several different kinds of small compounds were used which have diverse mechanisms of action or target. In particular, were chosen: genotoxic agents, which induce DNA damage, that are commonly used in the therapy of the LMS (Doxorubicin [269] and Gemcitabine [270]), general inhibitors of various signaling kinases (MK2206, inhibitor of Akt [271], XMD8-92, inhibitor of MAPK7 [272], Torin1, inhibitor of mTOR [273], YKL-06-061, inhibitor of Salt Inducible Kinases (SIKs) [274] and Selumetinib, inhibitor of MEK1/2 [275]), HDACs inhibitors commonly known or discovered in our lab (SAHA [276], TMP195 [277] and NKL54), well known autophagy inhibitors (Bafilomycin A1 and Chloroquine [278]), small compounds that inhibit the BCL2 family (ABT199 [279] and ABT263 [280]) and the IRE1 inhibitor MKC3946 [281].

In order to select the best candidates, a short screening was performed by cotreating LMS cell lines with 2c in combination with one of the compounds described above or each compound alone for 24 h. The experiment was made with three types of LMS cell lines: SK-UT-1, SK-LMS-1 (grade II LMS) and DMR (grade III metastatic LMS). The results were assessed through the quantification of the PI positivity of the cells in order to discriminate which cells are alive and which are dead (Figure 4.3A-C). The three cell lines show a similar behavior among all the cotreatment and single treatment, but with

different levels of positivity as expected from the previous results. In fact, the cell death rates are higher in SK-UT-1 and DMR, which are more aggressive, compared to SK-LMS-1. However, considering that the results are comparable in terms of trends, for the next experiments only SK-UT-1 were used.

This cell death screening reveals that the single cotreatment of all the small compounds is not able to induce high levels of cell death in 24 h, but when those inhibitors are used in combination with 2c, they can all increase the cell death rates of 2c alone (except for the case of Torin1 in SK-LMS-1). However, the additive effect is not the same for all the compounds. In fact, the majority of the inhibitors can increase the amount of cell death by 5 % that is very low and were excluded for the next experiments. Those excluded compounds are: the genotoxic agents, the HDACs inhibitors and some signaling kinases inhibitors. Only five compounds, which resulted with a strong statistical significance in increasing cell death in SK-UT-1, were considered as possible candidates, and they are: Torin1, YKL-06-061, Chloroquine, ABT263 and MKC3946.

The five candidates were used to understand if they could increase not only the amount of cell death, but also the amount of proteotoxic stress, as was previously demonstrated that high levels of proteotoxic stress can lead these cells to be more prone to cell death. In order to verify this point, an immunoblot was performed to see the levels of the phosphorylated form of eIF2α at residue Ser51, which means an activation of this protein due to the activation of PERK, after the induction of the UPR response to high levels of proteotoxic stress [123]. This was done by a single treatment or a cotreatment of the cells for 4 h, as we reported that the induction of proteotoxic stress in these cells after 2c treatment is early (Figure 4.3D). The results show that Torin1, ABT263 and MKC3946 are not able to activate eIF2α alone and they do not augment the levels of p-eIF2α induced by 2c. On the contrary, YKL-06-061 and Chloroquine can activate eIF2α and augment the levels of p-eIF2α induced by 2c. The results were also confirmed through densitometric analysis of the ratio between p-eIF2α and eIF2α (Figure 4.3E).

The screening regarding the proteotoxic stress reveals that YKL-06-061 and Chloroquine could be good candidates, but because the levels of cell death induced by Chloroquine alone are the highest compared to the other compounds, it was excluded in order to avoid

too much toxicity. However, because it induces the highest additive effect of cell death rate and due to its involving in ER stress, also MKC3946 was selected as a candidate.

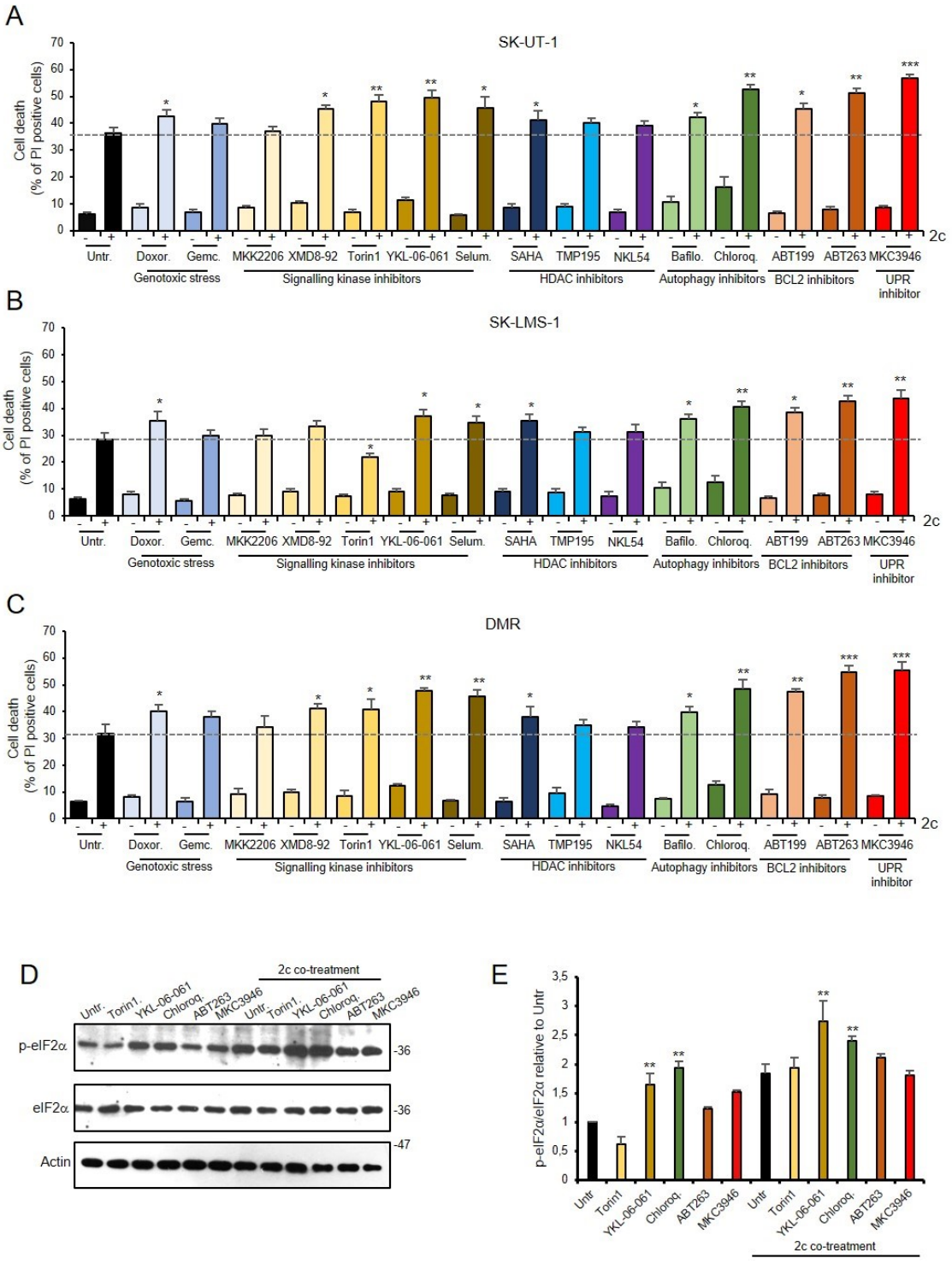

Figure 4.3: Results of the cotreatment screenings in order to define the best combination with 2c. A), B) and C) Countings of the PI positivity expressing the percentage levels of cell death of SK-UT-1 (A), SK-LMS-1 (B) and DMR (C) treated with 2c 2.5 µM alone or in combination with Doxorubicin 25 nM, Gemcitabine 10 nM, MK2206 10 µM, XMD8-92 1 µM, Torin1 100nM, YKL-06-061 1 µM, Selumetinib 1 µM, SAHA 2.5 µM, TMP195 20 µM, NKL54 5 µM, Bafilomycin A1 1 µM, Chloroquine 1 µM, ABT199 100nM, ABT263 100 nM, MKC3946 10 µM for 24 h. Data were from 3 experiments. Columns mean loss of viability + SD. *=p<0.05, **=p<0.01, ***=p<0.005; D) Immunoblot of eIF2α and p-eIF2α for SK-UT-1 treated with 2c 2.5 µM alone or in combination with Torin1 100nM, YKL-06-061 1 µM, Chloroquine 1 µM, ABT263 100 nM, MKC3946 10 µM for 4 h. Actin was used as loading control; E) Densitometric analysis of the immunoblot show in D). Columns mean ratio between optical density of p-eIF2α and eIF2α relative to untreated cells + SD. **=p<0.01.

4.4 THE PECULIAR EFFECTS ON PROTEOTOXIC STRESS OF MKC3946

In the 2c cotreatment screening, MKC3946 shows that it can increase the cell death rates of 2c, but it is not able to increase its induction of p-eIF2α, probably due to its ability inhibit the critical sensor IRE1. Regarding the data of cell death, in the screening this compound was the one that gives the highest additive effect in terms of cell death. For this reason, a new cell death assay assessed through TB positivity was performed with a dose dependent concentration of 2c in combination with MKC3946 (Figure 4.4A). The results highlighted that the most significant augment of the cell death rate compared to the single treatment is obtained with the lowest concentrations of 2c (0.5 μM, 1 μM and 2.5 μM).

In order to have another assay to verify the proteotoxic stress presence in the cells, the activation of IRE1 was assessed. IRE1, in fact, when is activated can process XBP1. This protein is generally unspliced (uXBP1), but when is processed by IRE1, a spliced form is generated (sXBP1) [134]. This processing can be visualized through an agarose gel, with EtBr, in which are loaded the PCR products, which amplify XBP1, derived from RT-PCR of the RNA extract from the cells [282]. Firstly, the processing was assessed by treating cells with only 2c in a time course (1 h, 2 h, 4 h ad 6 h) with two different concentrations (5 μM and 10 μM) (Figure 4.4B). The results reveal that 1 h is not enough to induce the processing (in case of 10 μM is slightly visible), instead from 2 h the presence of sXBP1 is clearer and is completely evident at 4 h. This result confirms the induction of proteotoxic stress by 2c with another assay and considering another UPR sensor.

MKC3946 is an inhibitor of IRE1 and with this assay it could be possible also to assess its efficiency to block the processing of XBP1. Only in this case was done a dose dependent treatment of MKC3946 (1 μM, 5 μM and 10 μM) alone or in combination with 2c (5 μM and 10 μM), all at 4 h when the eventual processing is clear (Figure 4.4C). The result shows that MKC3946 is not able to induce the processing of XBP1 alone and that only the concentration of 10 μM, which was the one used also in the screening, can inhibit

IRE1 resulting in the block of the processing of XBP1 after the 2c treatment. Indeed, only with that concentration sXBP1 is not appearing, and this concentration was used for all the other experiments.

The ability of MKC3946 to block the UPR response was subsequently assessed through the evaluation of the expression of two chaperones: *HSPA1A* and *HSPA6*. We previously demonstrated that after 2c treatment at early time points, the expression of these chaperones is dramatically augmented, due to the fact that the cells try to avoid the increasing of proteotoxic stress [266]. The expression of these genes was now assessed with the combination of 2c (5 μM and 10 μM) and MKC3946 at 4 h (Figure 4.4D-E). The results, as expected, show a strong increase of the mRNA levels of both the genes of both single 2c and combined treatment, however the levels are lower when 2c is in presence of MKC3946. Instead, MKC3946 alone is not able to induce the expression of the chaperones. Together all these data demonstrate that MKC3946 can reduce the UPR response also in the presence of a strong inducer of ER stress, such as 2c. In this way, the cells are highly dying not for a strong accumulation of proteotoxic stress, but due to the impossibility of the cells to activate a survival program.

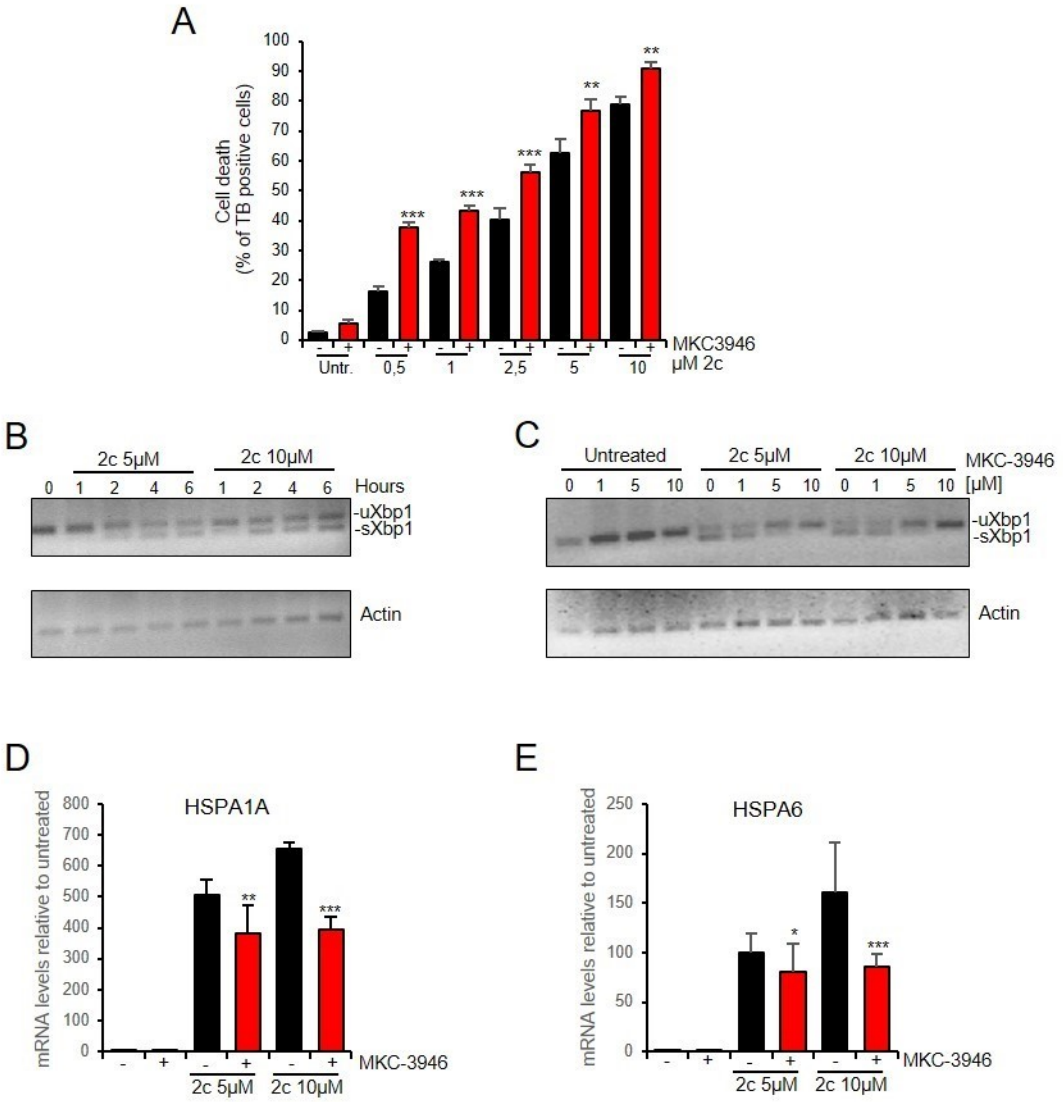

Figure 4.4: Characterization of the cell death pathway induced by the combination of 2c and MKC3946. A) Countings of the TB positivity expressing the percentage levels of cell death of SK-UT-1 treated with 2c (0.5 µM, 1 µM, 2.5 µM, 5 µM or 10 µM) alone or in combination with MKC3946 10 µM for 24 h. Data were from 3 experiments. Columns mean loss of viability + SD. **=p<0.01, ***=p<0.005; B) Visualization of the processing of XBP1 on agarose gel after PCR amplification. Samples derived from SK-UT-1 treated with 2c (5 µM or 10 µM) for several time points (1 h, 2 h, 4 h and 6 h). Actin was used as loading control; C) Visualization of the processing of XBP1 on agarose gel after PCR amplification. Samples derived from SK-UT-1 treated with 2c (5 µM or 10 µM) alone or in combination with MKC3946 10 µM for 4 h. Actin was used as loading control; D) and E) mRNA levels expression of *HSPA1A* (D) or *HSPA6* (E) of SK-UT-1 treated with 2c (5 µM or 10 µM) alone in combination with MKC3946 10 µM for 4 h. Data were from 3 experiments. Columns mean loss of viability + SD. *=p<0.05, **=p<0.01, ***=p<0.005.

4.5 CELL DEATH AND PROTEOTOXIC STRESS ACTIVATION: COMPARISON BETWEEN MKC3946 AND YKL-06-061 IN COMBINATION WITH 2C

SIKs, and in particular SIK2, are reported in many articles to be involved in the regulation of the ER stress. Indeed, these kinases can potentiate the activation of the UPR response in case of proteotoxic stress [274]. For this reason and for all the evidence seen before, the broad SIKs inhibitor YKL-06-061 was investigated, by comparing its effects with MKC3946 in terms of 2c additive effect.

Firstly, cell death rate was better investigated by performing a dose dependent treatment of 2c in combination with MKC3946 or YKL-06-061 for 24 h in both SK-UT-1 and the immortalized HUtSMC, in order to assess the toxicity in a more normal context. To be sure to not exclude candidates from the previous screening wrongly, one of the compounds that do not give a strong additive effect was assessed in the same experiment, which is ABT199 (Figure 4.5A-F). The results, by evaluating TB positivity, confirm that ABT199 is not able to potentiate in a strong way the cell death induced by 2c in both cell lines. Instead, both of the other two compounds can induce an additive effect in terms of cell death rate of 2c in SK-UT-1, in particular YKL-06-061 can lead to the strongest additive effect. However, the two compounds can also potentiate, in a lower way, the cell death induced by 2c in the immortalized HUtSMC, and also here in particular the effect is higher in the case of YKL-06-061. Interestingly, the dose in which the additive effect is more evident and significant is the lower ones, like for what was observed before for only MKC3946. Indeed, at higher concentrations, the effect of 2c is too strong also alone and the additive effect is less clear, especially in the case of MKC3946. For this reason, for the next experiments 2c was used with the concentration of 0.5 μM.

Proteotoxic stress induction was subsequently assessed through the evaluation of some markers, both in immunoblot and by PCR. A time course of 3 h and 12 h of the single treatment and the cotreatment of 2c with MKC3946 or YKL-06-061 was performed. As seen before, p-eIF2α is a marker of the activation of eIF2α, activated by PERK, one of

the main sensors of the UPR response. The immunoblot, presented in Figure 4.5G, shows that MKC3946 alone is not able to induce eIF2α phosphorylation. Furthermore, it seems not able to potentiate the phosphorylation also in the combination with 2c. Densitometric analysis (Figure 4.5H) reveals also that in the case of 3 h of cotreatment, the presence of MKC3946 slightly reduces the phosphorylation induced by 2c. On the contrary, YKL-06-061 can induce alone the activation of eIF2α, at both 3 h and 12 h, and the combination with 2c shows a strong activation of the protein, as also reported with densitometry (Figure 4.5G-H). Another method to assess the induction of ER stress condition is given by testing the activation of IRE1, another sensor of the UPR response. As shown before, this can be done by visualizing on an agarose gel the presence of sXBP1, a spliced form of XBP1 processed by IRE1 when it is activated under proteotoxic stress (Figure 4.5I). The result regarding MKC3946 confirms what was seen before: MKC3946 is not able to induce XBP1 processing, but it can avoid the processing effect induced by 2c by inhibiting IRE1. Instead, the presence of YKL-06-061 does not have an impact on the processing of XBP1. Indeed, this compound alone does not induce the processing of XBP1 and in the cotreatment it does not change the levels of the processing induced by 2c. All the results are the same in both the time points.

Beside the UPR response, the activation and the regulation of the chaperones is critical for the cell survival in a proteotoxic stress context. HSF1 is the master gene regulator that acts by controlling the expression of the HSPs in order to restore the proteostasis condition. Its activation can be observed through the levels of its phosphorylation of the residue Ser326 in immunoblot [224]. The results related to the evaluation of the levels of p-HSF1 in immunoblot, and with the relative densitometry (Figure 4.5G-H), are similar to what was observed for p-eIF2α. Indeed, the single compounds alone have different behavior on the activation of the protein at 3 h: MKC3946 does not activate, YKL-06-061 induce a low activation, 2c give the highest activation. At 12 h the results are the same but with lower levels of activation. Considering the combination of the compounds, the presence of MKC3946 slightly decrease the levels of phosphorylation induced by 2c alone at 3 h, instead at 12 h the combination promotes a bigger reduction of the levels of p-HSF1. YKL-06-061, instead, can highly increase the levels of phosphorylation of HSF1

compared to 2c alone at 3 h, however, this additive effect is reduced at 12 h observing similar levels with 2c alone.

Taken together, these data about the cotreatment demonstrate that the combination of 2c with these two small compounds highly augment its levels of cell death induction, however, regarding the activation of proteotoxic stress response programs the two compounds work by different mechanisms but generating the same result.

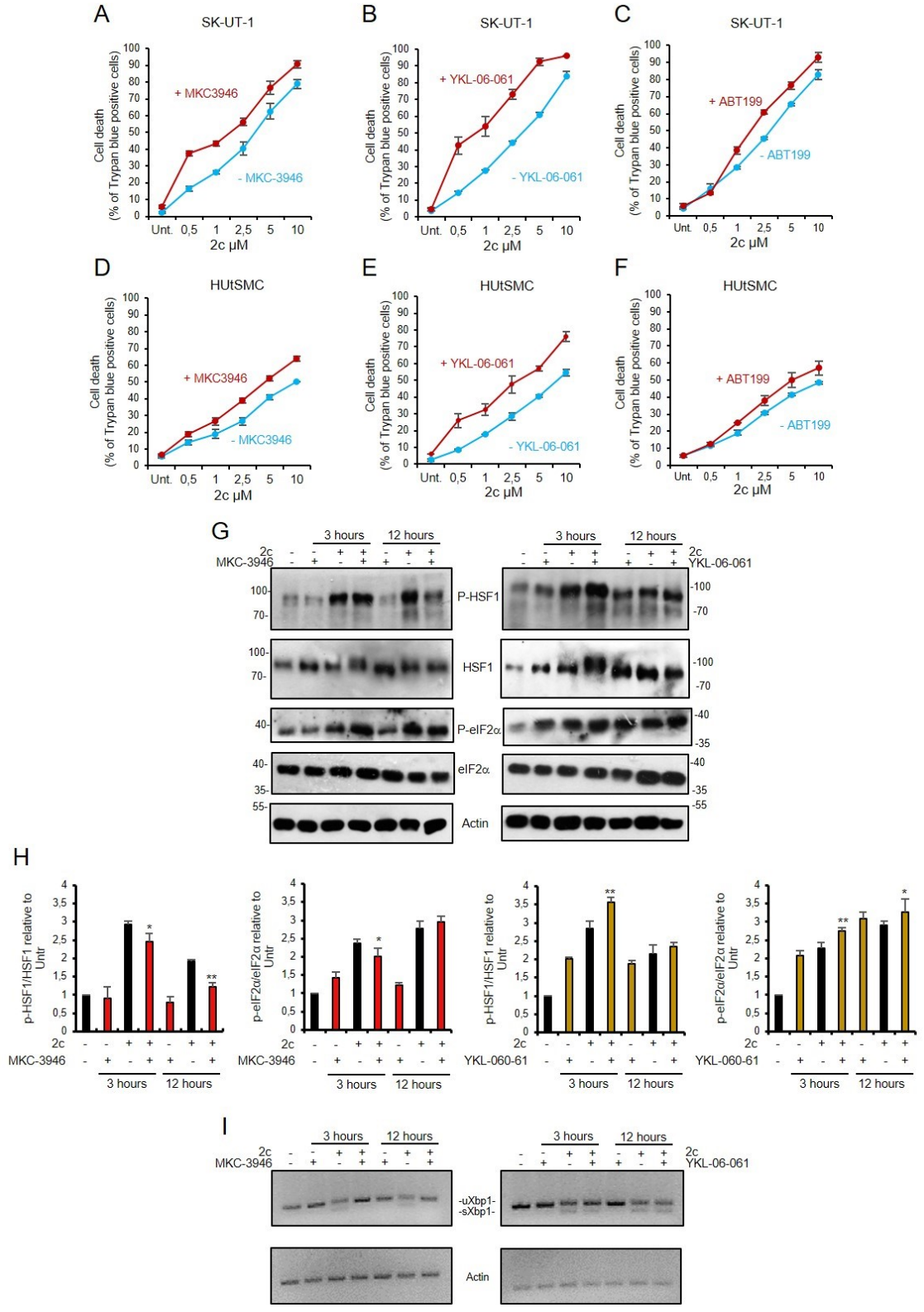
A
SK-UT-1
Cell death (% of Trypan blue positive cells)
+ MKC3946
- MKC-3946
Unt. 0,5 1 2,5 5 10
2c µM
B
SK-UT-1
+ YKL-06-061
- YKL-06-061
C
SK-UT-1
+ ABT199
- ABT199
D
HUtSMC
E
HUtSMC
F
HUtSMC
G
3 hours
12 hours
2c
MKC-3946
YKL-06-061
P-HSF1
HSF1
P-eIF2α
eIF2α
Actin
H
p-HSF1/HSF1 relative to Untr
p-eIF2α/eIF2α relative to Untr
YKL-060-61
I
-uXbp1-
-sXbp1-

Figure 4.5: Comparison of the effects on cell death and proteotoxic stress response between the combination of 2c with MKC3946 and with YKL-06-061. A), B) and C) Countings of the TB positivity expressing the percentage levels of cell death of SK-UT-1 treated with 2c (0.5 µM, 1 µM, 2.5 µM, 5 µM or 10 µM) alone or in combination with MKC3946 10 µM (A), YKL-06-061 1 µM (B) or ABT199 100 nM (C) for 24 h. Data were from 3 experiments. Columns mean loss of viability + SD; D), E) and F) Countings of the TB positivity expressing the percentage levels of cell death of HUtSMC hTERT treated with 2c (0.5 µM, 1 µM, 2.5 µM, 5 µM or 10 µM) alone or in combination with MKC3946 10 µM (D), YKL-06-061 1 µM (E) or ABT199 100 nM (F) for 24 h. Data were from 3 experiments. Columns mean loss of viability + SD; G) Immunoblot of eIF2α, p-eIF2α, HSF1 and p-HSF1 for SK-UT-1 treated with 2c 0.5 µM alone or in combination with MKC3946 10 µM (on the left) or with YKL-06-061 1 µM (on the right) for 3 h or 12 h. Actin was used as loading control; H) Densitometric analysis of the immunoblot show in G). Starting from the left, the first two histograms are related to the cotreatment between 2c and MKC3946, instead the other two are related to the cotreatment between 2c and YKL-06-061. Columns mean ratio between optical density of p-eIF2α and eIF2α or between optical density of p-HSF1 and HSF1 relative to untreated cells + SD. *=p<0.05, **=p<0.01; I) Visualization of the processing of XBP1 on agarose gel after PCR amplification. Samples derived from SK-UT-1 treated with 2c 0.5 µM alone or in combination with MKC3946 10 µM (on the left) or with YKL-06-061 1 µM (on the right) for 3 h or 12 h. Actin was used as loading control.

5 DISCUSSION

The discovery of new therapeutic targets is one of the most fundamental and critical aspect of anticancer research. Indeed, the frequency of the chemotherapy failure gives rise to the necessity to achieve this goal and new drugs need to be found. This problem is caused mainly by the appearance of mutations and alterations, which leads to the chemotherapy resistance, resulting in recurrence of the tumors [283].

Cancer cells are more prone to have high levels of proteotoxic stress due to the necessity of these cells to produce a huge number of proteins in less time, generating misfolded or unfolded proteins. These can lead to an accumulation of damaged proteins that triggers proteotoxic stress. For this reason, these cells are highly dependent from the mechanisms involved in the reduction of proteotoxic stress, such as chaperones, proteins related to the UPR response and UPS [242]. In fact, chaperones are fundamental in the drug resistance and metastasis to maintain the tumoral cells alive [243].

Using small molecules able to block these survival mechanisms could be a good strategy as promising therapeutic option. Most of these strategies lead to a further raising of the proteotoxic stress, which, in this way, could not be counteracted by the cancer cells, triggering the activation of cell death programs [246]. Nevertheless, the induction of proteotoxic stress could also lead to cell death resistance in some cases [247].

Among all the possible targets leading to the induction of proteotoxic stress, UPS arises as a promising one [200]. UPS is fundamental in the disruption of the unfolded proteins and is constituted by several elements critical for its correct work. Between all of its elements, DUBs are isopeptidases able to remove the ubiquitin chain from the damaged proteins, leading them to the translocation in the proteasome to be degraded. Their inhibition triggers the accumulation of polyubiquitylated proteins, generating proteotoxic stress and cell death [168].

2c is a small compound with a structure derivates from the diaryldienone, which can alkylate the nucleophiles like the cysteine. It can act as a N-SII by interacting with the cysteines of the DUBs [245]. However, due to its non-selective nature, it was observed

that could also bind other target not related to the UPS or the proteostasis control [260]. Because of this, 2c can induce many kinds of signaling pathways in the cells through the activation of different stresses, such as oxidative stress [206]. All of these dysfunctions lead to the incapability of the cells to counteract this situation and lead to cell death.

LMS was chosen as a model of study due to its high malignancy and by the fact that has few therapeutic options. Furthermore, we demonstrated that this kind of tumor have intrinsic high levels of proteotoxic stress, and that this scenario could lead to the incapability of these cells to handling increasing proteotoxic stress. We have also demonstrated that 2c can induce in LMS cell lines proteotoxic stress, cell death and mitochondrial dysfunction. Regarding this point, by STED confocal microscopy, we reveal that 2c can reorganize the subclusters of DIABLO/SMAC present in the mitochondria. We also demonstrate the efficacy of a 2c derivative (2cPP) *in vivo* in LMS xenograft mouse models by reducing their tumor volume [266].

Despite its promising activity, less is known about the cell death mechanism induced by 2c and also about which genes are modulated after the treatment with this small compound. For this reason, an RNA-Seq experiment was performed, in order to better describe which genes or pathways are regulated by 2c. The experiment was done at two different time points and comparing a tumoral LMS cell line and its normal counterpart. The result reveals similarities and differences between the two cell lines, explaining why the normal cells are more resistant to the cell death induced by this small molecule. In general, the normal cells modulate more genes, both upregulated and downregulated, compared to the tumoral ones, probably in order to find a correct program that help reaching the cell survival. In fact, it was reported that this tissue can activate anti-apoptotic pathways in order to keep itself alive [284,285].

This analysis reveals the different pathways activated by the two different cells in the case of the upregulated genes. Epigenetic genes seem more regulated by this compound for tumoral cells, instead the apoptotic cascade is regulated in the normal cells, suggesting a way to survive. Cell adhesion is also regulated by both the cells, and this could be related to the fact that the only known gene involved in the 2c cascade is Cofilin-1, a gene related to the activity of the actin microfilaments [209]. This differential response of the two cells

could be due to a diverse activation of the pathways, which leads to cell survival of the normal cells.

In relation to the cell death mechanism, the tumoral cells upregulate pro-apoptotic genes and downregulate anti-apoptotic genes, suggesting again the activation of cell death mechanism. The results are in line with previous evidences about the fact that LMS are more prone to die via apoptosis and that in this circumstance they can activate pro-apoptotic proteins [286]. Furthermore, it was already shown in the literature that the expression of the anti-apoptotic gene *BCL2*, is less compared to the ones present in other benign sarcoma tumors (leiomyoma) [287]. Instead, the normal cells have a broad diverse response: in fact, both pro-apoptotic and anti-apoptotic genes are downregulated suggesting the creation of an equilibrium, which confers to these cells a status of cell death but with lower rates compared to the tumoral ones. Moreover, the strong upregulation of the anti-apoptotic gene *BCL2A1* leaves the balance tending to cell survive.

As expected from the previous published results, the majority of the genes related to the proteotoxic stress result upregulated, and this upregulation is reported also in the normal cells, but with lower levels. Thus, confirms the fact that 2c can induce high levels of proteotoxic stress in these cells. However, despite both the cells can activate genes related to the reduction and control of the proteotoxic stress, the tumoral cells could not manage this huge amount of stress, instead the normal cells are able to reduce the proteotoxic stress generated by 2c, generating less amount of cell death.

A recent work regarding the gene expression of normal uterine smooth muscle cells and different types of leiomyosarcomas demonstrates that both genomic profiles of the two kinds of cells have similar gene expression but with critical differences, which can differentiate also LMS from other tumors [288]. Furthermore, a gene profiling analysis between normal myometrium and LMS shows that LMS present an overexpression of pathways related to cell cycle, DNA damage and genome integrity. In fact, cell cycle regulation is critical in the sarcomagenesis and the upregulation was reported for *CDC7*, *CDC20*, *GTSE1*, *CCNA2*, *CCNB1*, and *CCNB2* [289,290]. In addition, our data support

this evidence of the modulation of the cell cycle in this kind of tumors and further investigation are needed.

This preliminary analysis on the result of this RNA-Seq experiment confirms the involvement of proteotoxic stress in 2c cell death cascade and that those normal cells activates different pathways from the tumoral ones for the survival, with a huge number of genes modulated. Further studies will have the aim to better understand and dissect the entire cascade of pathways and genes activated during the treatment with 2c. Another crucial point will also be the study of the critical elements that permit the differences in cell death rate between normal and tumoral cells. However, the possible interaction with other pathways lead to think about a possible combination of treatment of 2c with other small compounds.

Cotreatment of cancer cells with a combination of small molecules was reported in many cases, in order to obtain an additive or a synergistic effect [291,292]. 2c can induce high levels of cell death in LMS, however, it needs high concentrations. Discovering a small compound, which can potentiate its activity when is used at low doses, could have a strong impact for the cancer treatment. The enhancing activity was assessed through the cell death levels and the induction of proteotoxic stress, as we demonstrated that these kinds of tumors are sensitive to the presence of strong proteotoxic stress.

To define the best small molecule to combine with 2c, a screening to assess the enhancing of cell death was performed, revealing that the common genotoxic agents used in the LMS therapy do not have an impact on cell death induced by 2c. Despite from RNA-Seq is clear that epigenetic regulation could be involved in this mechanism, the HDACs inhibitors used do not potentiate the cell death induced by 2c. The screening was focused also on inhibitors of signaling kinases, autophagy, BCL2 family and IRE1. After assessing the induction of cell death, the proteotoxic stress condition was evaluated through verifying the activation of eIF2α, a downstream protein of the UPR sensor PERK. This second screening permits to exclude the inhibitors of BCL2 family and the inhibitors of the signaling kinases (except for YKL-06-061), which are not able to augment the activation of this protein. In addition, the inhibitors of autophagy were excluded due to

the fact that they can induce cell death alone generating too much toxicity. In the end, the best candidates were YKL-06-061 and MKC3946.

MKC3946 is an inhibitor of IRE1, which is another UPR sensor, thus directly involved in the ER stress. It was proposed as a novel therapeutic approach for the treatment of multiple myeloma [282]. The combination of 2c with this inhibitor shows high additive effect in terms of cell death rates, in particular at low doses of 2c, thus suggesting a promising usage as combined therapy. However, it is not able alone to induce the activation of elements related to proteotoxic stress and also it does not potentiate their activity in combination with 2c. Indeed, we show that the activation of eIF2α and HSF1 is similar or slightly reduced comparing 2c alone and the combination with MKC3946, in particular, the activation of HSF1 resulted more reduced at 12 h in the case of the combination. Furthermore, the expression of the chaperones *HSPA1A* and *HSPA6* resulted reduced with this combination compared to 2c alone. Moreover, after assessing that 2c can induce the processing of XBP1 (downstream target of IRE1), we demonstrate that the presence of MKC3946 blocks this splicing phenomenon, confirming the ability of this small compound to inhibit IRE1. All our data are in line with previous evidences reported by Mimura et al. in a model of multiple myeloma, indeed, they show that MKC3946 can block the activation of IRE1. Moreover, it can affect also to the activation of all the UPR response and the expression of the chaperones. Additionally, they reported that MKC3946 can potentiate the activity of bortezomib, which is another UPS inhibitor, also at low doses, sustaining the promising effect of this compound [282]. The potential combination of MKC3946 and bortezomib was also seen in a model of Acute Myeloid Leukemia, confirming that targeting IRE1 could be a new therapeutic strategy [281]. This combination was also seen to be crucial in another context that is the bone formation [293].

YKL-06-061 is a broad inhibitor of SIKs (SIK1/2/3) and arises as a promising therapeutic agent. These kinases have different roles in the cellular context and among these, they can also contribute in the proteostasis [274]. In particular, SIKs can potentiate the activation of the UPR response pathway by favoring the activation of the sensors PERK and IRE1 [294]. SIKs have an important role in the tumoral context, in fact, they can help

sustaining the survival of the cancer cells and promoting the tumorigenesis [274]. Thus, their inhibition could represent a future target of clinical relevance. In our conditions what we observed is that YKL-06-061 can strongly potentiate the cell death induced by 2c, in particular at low doses, and also can promote the activation of eIF2α and HSF1, especially at 3 h, suggesting that the inhibition of these kinases leads the cells to highly activate the UPR response. Moreover, the presence of YKL-06-061 alone can slightly induce the activation of eIF2α and HSF1. Regarding the processing of XBP1 the presence of YKL-06-061 combined with 2c does not affect the appearance of the sXBP1. SIKs and in particular SIK2, can modulate and control CREB1 which is directly involved in ER stress [274]. Despite this role, it was observed from other authors that the knockdown of SIK2 induces the upregulation of several genes related to the ER stress and the UPR, such as critical chaperones [295]. Furthermore, the knockdown of endogenous SIK2 or the expression of its mutated form leads to an impairment of the degradation of the ERAD substrates, leading to the disruption of the ER homeostasis. In this way, the cells continue activating ERAD and UPR pathway in an uncontrolled way [296]. All these evidences support our data, which seem to be in line with what is reported in literature.

These experiments of cotreatment show that both the inhibitors can highly increase the cell death rates induced by 2c, also using low doses of 2c, suggesting that they could be promising candidates in a possible therapeutic view. However, both the inhibitors increase the levels of cell death induced by 2c in immortalized HUtSMC, a normal counterpart of the tumoral LMS cell line SK-UT-1. This result could be a limit for the usage in a therapeutic approach, nevertheless using the combination of these small compounds with the 2c derivative 2cPP could be a strategy in order to avoid that the drug directly impact on the normal cells. In fact, it was previously shown that 2cPP is not working in HUtSMC because the normal cells are not able to process this pro-drug version of 2c [266]. With this strategy it could be also possible, if the *in vitro* results would be promising, to design an *in vivo* experiment with the treatment of LMS xenograft in mouse models with 2c and the combination with these two inhibitors.

Considering the proteotoxic stress induced in LMS after 2c treatment, the two inhibitors work in a different modality. In fact, MKC3946 can reduce the activation of HSF1,

resulting in a reduction of the chaperones expressions, and block the UPR response by blocking IRE1. Moreover, it seems that also it can induce the reduction of the activation of eIF2α. On the contrary, YKL-06-061 promotes the activation of eIF2α and HSF1 and has no effect on IRE1. The final resulting proposed model is that MKC3946, besides inhibiting IRE1, can reduce the activation of alternative signaling pathways needed to reduce the proteotoxic stress induced by 2c. In this way, the cells cannot recover to proteostasis status and undergo to cell death. Instead, YKL-06-061 potentiate the activation of all the signaling pathways related to the UPR response, except for IRE1. However, the level of activation of these pathways is too high and this leads to a switch from a pro-survival mechanism to a pro-death mechanism. Further studies are fundamental to better dissect the mechanism induced by the combination of these compounds. For example, studying the implications of the ATF network, which could be seen as a link between cell death and proteotoxic stress, could give new insights also in a therapeutic point of view.

All the data collected in this PhD project defining 2c as a promising therapeutic agent for the treatment of LMS, despite its mechanism of action is still not completely defined. Although this study focuses the attention on LMS, it is possible that our findings could also be applied in other tumoral context in which proteotoxic stress is intrinsically elevated, leading to a strong challenge to the cancer cell survival.

6 MATERIALS AND METHODS

6.1 CELL CULTURE CONDITIONS AND CHEMICAL REAGENTS USED

For all the experiments were used leiomyosarcoma cell lines of different malignancy grade (SK-UT-1, SK-LMS-1 and DMR). As a normal control were used the primary Human Uterine Smooth Muscle Cell line (HUtSMC) obtained through ATCC, within eight passages. As packaging cells for the retroviral infection were used the Phoenix Amphotropic (AMPHO) cells. All the cell lines were maintained in culture in an incubator at 37 °C and with an atmosphere of 5 % CO_2. The medium used to cultivate all the cells is Dulbecco's Modified Eagle's Medium (DMEM; Euroclone) supplemented with 10% Fetal Bovine Serum (FBS; Euroclone), glutamine (2 mmol/l; Euroclone), penicillin (100 U/ml; Euroclone) and streptomycin (100 µg/ml; Euroclone). All the cells were frequently tested as mycoplasma negative using Hoechst 33258 (Sigma-Aldrich) staining under microscopic inspection. The chemical reagents used are: 2c [257], Doxorubicin (Sigma-Aldrich), Gemcitabine (CSN Scientific), MK2206 (Sigma-Aldrich), XMD8-92 (CSN Scientific), Torin1 (Sigma-Aldrich), YKL-06-061 (CSN Scientific), Selumetinib (MedChemExpress), SAHA (Cayman Chemicals), TMP195 (MedChemExpress), NKL54 (synthetized by SIA Chemspace, Riga, Latvia), Bafilomycin A1 (Sigma-Aldrich), Chloroquine (Sigma-Aldrich), ABT199 (CSN Scientific), ABT263 (Sigma-Aldrich), MKC3946 (MedChemExpress), Propidium Iodide (PI; Sigma-Aldrich), Trypan Blue (TB; Sigma-Aldrich), Ethidium Bromide (EtBr; Sigma-Aldrich), Dimethyl Sulfoxide (DMSO; Sigma-Aldrich).

6.2 RETROVIRUS INFECTION OF HUTSMC CELLS

Because HUtSMC is a primary cell line of normal cells, after several passages they undergo to natural cell death due to the achievement of the Hayflick limit. For this reason, it was decided to immortalize this cell line, by using the human hTERT telomerase and to obtain this result a retroviral infection of these cells was done. Firstly, AMPHO packaging cells were used in order to produce the virus and were transfected with a plasmid containing the human hTERT (pBABE-hTERT) or with the empty vector (pBABE-Neo) for the control, through the calcium phosphate method. The transfected cells were incubated for 48 h at 32 °C. Next, the viral particles present in the supernatant of the AMPHO cells were collected, diluted 1:1 with fresh medium, added with polybrene (8 μg/ml), filtered through 45 μm filters and used to infect HUtSMC cells, which were previously seeded at the concentration of 80000 cells/ml. After 24 h at 37 °C, the virus was removed by changing the medium and then, the infected cells were selected using the correct antibiotic (G418; Sigma-Aldrich).

6.3 DRUG TREATMENT OF THE CELLS

For the drug treatment, all the cells were seeded at the concentration of 80000 cells/ml (only for DMR 120000 cells/ml), and one day after seeding, were treated. The treatment was done with: 2c, another small compound or with the combination of 2c and that single small compound. DMSO was used in the untreated cells. Regarding 2c, its concentration was decided based on each experiment, with these different concentrations: 0.5 μM, 1 μM, 2.5 μM, 5 μM or 10 μM. For the other chemicals, one decided concentration was used for all the experiments: Doxorubicin 25 nM, Gemcitabine 10 nM, MK2206 10 μM, XMD8-92 1 μM, Torin1 100 nM, YKL-06-061 1 μM, Selumetinib 1 μM, SAHA 2.5 μM, TMP195 20 μM, NKL54 5 μM, Bafilomycin A1 1 μM, Chloroquine 1 μM, ABT199 100 nM, ABT263 100 nM, MKC3946 10 μM. The duration of every treatment varies based on each experiment. After the treatment, the cells were collected for cell death counting, to obtain a cell protein lysate or for RNA extraction.

6.4 CELL DEATH COUNTING

The cells were seeded and treated as written above, and the treatment was performed for 24 h. Cells were than trypsinized and centrifuged to obtain a pellet. After several washes with Phosphate Buffer Saline (PBS), the pellet of the cells was resuspended in 100 µl of PBS and incubated with PI 10 µg/ml or TB 0.1 % for 5 min at RT. The fluorescence intensity positivity of PI in the cells or the cell positivity to TB was determined through Countess II FL automated cell counter (Invitrogen).

6.5 PRODUCTION OF THE CELL PROTEIN LYSATES AND IMMUNOBLOT

The cells were seeded and treated as written above. After the treatment, the cells were lysed in order to purify its protein contents. The lysis was made through a denaturing lysis solution containing Sodium Dodecyl Sulfate (SDS), in which were added Phenylmethane Sulfonyl Fluoride (PMSF), as a protease inhibitor, and β-mercaptoethanol to destroy the disulfate bound. Cells were scraped with this solution and the collected protein lysates were sonicated for 5 min at 4 °C and next they were boiled for 5 min. Subsequently, the now denatured proteins were loaded in a polyacrylamide denaturing gel (containing SDS), in order to perform the electrophoresis (SDS-PAGE). After the electrophoretic run, the proteins present were transferred from the gel to a 0.2 µm-pore-sized nitrocellulose membrane, though a full wet transfer system. The obtained membrane was incubated in a solution of Tris HCl pH 7.5 1 M, NaCl 5 M and Tween-20 (Sigma-Aldrich) containing non-fat dry milk 5 % (Delikat Gramm) or, only for the phosphorylated antibodies, Bovine Serum Albumin 5 % (BSA; HyClone), for 1h at RT in order to block the aspecific sites. Later, after several washes in PBS with Tween-20, the membrane was incubated with the primary antibody diluted in the same solution described above (using non-fat dry milk 5 % for all the antibodies except for the phosphorylated ones where is used BSA 5 %) overnight at 4 °C. The primary antibody used are: anti-eIF2α (1:1000; Cell Signaling Technology), anti-p-eIF2α Ser51 (1:1000; Cell Signaling Technology), anti-HSF1

(1:1000; Cell Signaling Technology), anti-p-HSF1 Ser326 (1:5000; Abcam), anti-Actin (1:8000; Cell Signaling Technology). Then, after several washes in PBS with Tween-20, the membrane was incubated with the secondary antibody diluted in the same solution described above (using non-fat dry milk 5 % for all the antibodies) for 1 h at RT. The secondary antibody used is a goat anti-rabbit (1:4000; Sigma-Aldrich) conjugated with the horseradish peroxidase. Lastly, the blot derived from the membrane was developed by using Super Signal West Dura as recommended by the vendor (Pierce Waltham). The resulting signal was impressed, though chemiluminescence reaction on a photographic film. Densitometric analysis was performed using ImageJ to evaluate the ratio between the phosphorylated form of a single protein and the total form of the same protein.

6.6 RNA EXTRACTION AND QRT-PCR

The cells were seeded and treated as written above, and the treatment was performed for 4 h. TRIzol (Sigma-Aldrich) was used to lyse the cells in order to extract the RNA, and the resulting samples were collected. Then, chloroform was added to the samples, in this way, RNA can be separated from the other contaminants (DNA and proteins). The collected RNA was precipitated through using isopropanol and the obtained pellet was washed two times with ethanol 75 %. The RNA pellet was dried and resuspended with sterile nuclease-free water. 1 μg of extracted RNA was used in order to perform Retro-Transcription PCR (RT-PCR). RT-PCR was executed using a mixture of the RNA with several critical components for the reaction: 5x First Strand Buffer (Invitrogen), dithiotreitol (DTT; 0.1 M; Invitrogen), dNTPs Mix (2.5 mM; Thermo Scientific), oligo dT (20 μM; Eurofins Genomics), random primers (Invitrogen), RNase OUT Recombinant Ribonuclease inhibitor (30 U/μl; Invitrogen), and the reverse transcriptase enzyme, the Moloney Murine Leukemia Virus (M-MLV; 200 U/μl; Invitrogen). After RT-PCR, the obtained cDNA was assessed through quantitative Real Time PCR (qRT-PCR) using the SYBR Green (KAPA Biosystems) technology for the following genes: Glyceraldehyde 3-phosphate dehydrogenase (GAPDH), Hypoxanthine-guanine phosphoribosyltransferase (HPRT), Heat shock protein family A (HSP70) Member 1A (HSPA1A) and Heat shock protein family A (HSP70) Member 6 (HSPA6). The resulting

data were analyzed using the ΔΔCt method considering HPRT and GAPDH as normalizer genes. All the reactions were performed in triplicate.

6.7 RT-PCR AND EVALUATION OF THE XBP1 PROCESSING

The cells were seeded and treated as written above. After treatment, RNA was extracted from the cells as described above. 1.5 μg of extracted RNA was used in order to perform Retro-Transcription PCR (RT-PCR). RT-PCR was executed as described above, but without using oligo dT, replaced by the double amount of random primers. After RT-PCR, the obtained cDNA was used to perform a PCR using KAPA Biosystems Polymerase for the following primers: XBP1 Forward 5'-CCTGGTTGCTGAAGAGGAGG-3' and XBP1 Reverse 5'-CCA TGGGGAGATGTTCTGGAG-3', βActin Forward 5'-GGGTCAGAAGGATTCCTATG-3' and βActin Reverse 5'-GGTCTCAAACATGATCTGGG-3'. The thermal conditions for the PCR are: initial 5 min at 95° C, then 30 cycles of 30 sec at 95 °C, 30 sec at 60 °C and 30 sec at 72 °C and finally 7 min at 72 °C. To evaluate the XBP1 processing, the PCR products were load into a 2.5 % agarose gel and visualize through Gel Doc 2000 (Bio-Rad) using EtBr as DNA intercalant.

6.8 RNA EXTRACTION AND PURIFICATION FOR RNA-SEQ

The cells were seeded and treated as written above, and the treatment was performed for 3 h or 12 h. In order to extract and purify the RNA required for the RNA-Seq experiment, was used an RNA extraction kit called Quick-RNA MagBead kit (Zymo Research) following the manufacturer's instructions. Briefly, cells were lysed with a lysis buffer present in the kit and the lysates were collected through scrapers. Magnetic beads were added to the lysates and through isopropanol present in the kit buffers, the RNA was precipitated and bind to the magnetic beads and recovered by using a magnetic support. After several washes with the kit buffers and ethanol, DNaseI present in the kit was added to the samples in order to avoid DNA contamination. Finally, after other several washes

with the kit buffers and ethanol, RNA was eluted from the magnetic beads by resuspended it in sterile nuclease-free water. 3 μg of each extracted RNA was used for the RNA-Seq analysis.

6.9 RNA-SEQ ANALYSIS

RNA-Seq library preparation and sequencing were performed at Biodiversa s.r.l. (Rovereto (TN), Italy) following Illumina specifications. All the subsequent RNA-Seq analysis was performed by the Bioinformatic Unit of the Department of Medical Area of the University of Udine (Dott. Raffaella Picco and Dott. Emiliano Dalla) and by Prof. Claudio Brancolini. Data quality assessment was performed with fastqc and ShortRead library. Raw reads were clipped form their adapter sequences using the Trimmomatic software. Reads with an overall sequence mean Phred quality lower than 28 were discarded. The selected reads were mapped to the reference genome, downloaded from Ensembl (version 104) using STAR. Using the same tool, we checked whether RNA-Seq library are strand-specific or not. The resulting sam files were sorted and converted in bam files using samtools. Transcript assembly and quantification were done with StringTie. A Python script was used to extract all the read count information directly from the files generated by StringTie. Two CSV files containing the count matrices for genes and transcripts were obtained. Differential-expressed genes were identified using DESeq2 library in R. The thresholds applied were log2 fold change (|log2 FC|) >1 and FDR <0.05. Venn diagrams were created with VennDiagram (v1.6.20) or with the Venn diagram tool by the bioinformatics and evolutionary genomics group at VIB/Ghent University.

6.10 STATISTICS

All results are expressed as means ± standard deviations (SD) from at least three independent experiments. All the statistical analysis done was performed using a Student's t test on Excel software with p values represented as follows: *P<0.05; **P<0.01; ***P<0.005.

7 REFERENCES

1. Amm, I.; Sommer, T.;Wolf, D.H. *Protein quality control and elimination of protein waste: The role of the ubiquitin-proteasome system*. Biochim. Biophys. Acta 2014, 1843, 182–196.

2. Balchin, D.; Hayer-Hartl, M.; Hartl, F.U. *In vivo aspects of protein folding and quality control*. Science 2016,353, aac4354.

3. Anfinsen, C.B. *Principles that govern the folding of protein chains*. Science 1973, 181, 223–230.

4. Ellis, R.J.; Minton, A.P. *Protein aggregation in crowded environments*. Biol. Chem. 2006, 387, 485–497.

5. Morimoto, R.I. *Proteotoxic stress and inducible chaperone networks in neurodegenerative disease and aging*. Genes Dev. 2008, 22, 1427–1438.

6. Gokhale, S.; Nyayanit, D.; Gadgil, C. *A systems view of the protein expression process*. Syst. Synth. Biol. 2011, 5, 139–150.

7. Hipp, M.S.; Kasturi, P.; Hartl, F.U. *The proteostasis network and its decline in ageing*. Nat. Rev. Mol. Cell Biol. 2019, 20, 421–435.

8. Taylor, R.C.; Dillin, A. *Aging as an event of proteostasis collapse*. Cold Spring Harb. Perspect. Biol. 2011, 3, a004440.

9. Labbadia, J.; Morimoto, R.I. *The biology of proteostasis in aging and disease*. Annu. Rev. Biochem. 2015, 84, 435–464.

10. Higuchi-Sanabria, R.; Frankino, P.A.; Paul, J.W., III; Tronnes, S.U.; Dillin, A. *A futile battle? Protein quality control and the stress of aging*. Dev. Cell 2018, 44, 139–163.

11. Kastle, M.; Grune, T. *Interactions of the proteasomal system with chaperones: protein triage and protein quality control*. Prog. Mol. Biol. Transl. Sci. 2012, 109, 113–160. 10.1016/B978-0-12-397863-9.00004-3

12. Brehme, M.; Voisine, C.; Rolland, T.; Wachi, S.; Soper, J.H.; Zhu, Y.; Orton, K.; Villella, A.; Garza, D.; Vidal, M.; et al. *A chaperome subnetwork safeguards proteostasis in aging and neurodegenerative disease*. Cell Rep. 2014, 9, 1135–1150.

13. Bohush, A.; Bieganowski, P.; Filipek, A. *Hsp90 and its co-chaperones in neurodegenerative diseases*. Int. J. Mol. Sci. 2019, 20, 4976.

14. Buchner, J. *Supervising the fold: functional principles of molecular chaperones*. FASEB J. 1996, 10, 10–19.

15. Rudiger, S.; Germeroth, L.; Schneider-Mergener, J.; Bukau, B. *Substrate specificity of the DnaK chaperone determined by screening cellulose-bound peptide libraries*. EMBO J. 1997, 16, 1501–1507.

16. Hartl, F.U.; Bracher, A.; Hayer-Hartl, M. *Molecular chaperones in protein folding and proteostasis*. Nature 2011, 475, 324–332.

17. Itoh, H.; Komatsuda, A.; Ohtani, H.; Wakui, H.; Imai, H.; Sawada, K.; et al. *Mammalian HSP60 is quickly sorted into the mitochondria under conditions of dehydration*. Eur. J. Biochem. 2002, 269, 5931–5938.

18. Tutar, L.; Tutar, Y. *Heat shock proteins; an overview*. Curr. Pharm. Biotechnol. 2010, 11, 216–222.

19. Lo Bianco, C.; Shorter, J.; Regulier, E.; Lashuel, H.; Iwatsubo, T.; Lindquist, S.; et al. *Hsp104 antagonizes a-synuclein aggregation and reduces dopaminergic degeneration in a rat model of Parkinson disease*. J. Clin. Invest. 2008, 118, 3087–3097.

20. DeSantis, M.E.; Leung, E.H.; Sweeny, E.A.; Jackrel, M.E.; Cushman-Nick, M.; Neuhaus-Follini, A.; et al. *Operational plasticity enables hsp104 to disaggregate diverse amyloid and nonamyloid clients*. Cell 2012, 151, 778–793.

21. Kumar, C.M.S.; Mande, S.C.; Mahajan, G. *Multiple chaperonins in bacteria—novel functions and non-canonical behaviors*. Cell Stress Chaperones. 2015, Jul; 20(4): 555–574.

22. Odunuga, O.O.; Hornby, J.A.; Bies, C.; Zimmermann, R.; Pugh, D.J.; Blatch, G.L. *Tetratricopeptide repeat motif-mediated Hsc70-mSTI1 interaction. Molecular characterization of the critical contacts for successful binding and specificity*. J. Biol. Chem. 2003, 278, 6896–6904.

23. Hageman, J.; Rujano, M.A.; van Waarde, M.A.; Kakkar, V.; Dirks, R.P.; Govorukhina, N.; et al. *A DNAJB chaperone subfamily withHDAC-dependent activities suppresses toxic protein aggregation*. Mol. Cell 2010, 37, 355–369.

24. Summers, D.W.; Douglas, P.M.; Ramos, C.H.; Cyr, D.M. *Polypeptide transfer from Hsp40 to Hsp70 molecular chaperones*. Trends Biochem. Sci. 2009, 34, 230–233.

25. Kampinga, H.H.; Craig, E.A. *The HSP70 chaperone machinery: j proteins as drivers of functional specificity*. Nat. Rev.Mol. Cell Biol. 2010, 11, 579–592.

26. Lindquist, S. *Protein folding sculpting evolutionary change*. Cold Spring Harb. Symp. Quant. Biol. 2009, 74, 103–108.

27. Taipale, M.; Jarosz, D.F.; Lindquist, S. *HSP90 at the hub of protein homeostasis: emerging mechanistic insights*. Nat. Rev. Mol. Cell Biol. 2010, 11, 515–528.

28. Finka, A.; Goloubinoff, P. *Proteomic data from human cell cultures refine mechanisms of chaperone-mediated protein homeostasis*. Cell Stress Chaperones 2013, 18, 591–605.

29. Putcha, P.; Danzer, K.M.; Kranich, L.R.; Scott, A.; Silinski, M.; Mabbett, S.; et al. *Brain-permeable small-molecule inhibitors of Hsp90 prevent a-synuclein oligomer formation and rescue a-synuclein-induced toxicity*. J. Pharmacol. Exp. Ther. 2010, 332, 849–857.

30. Pearl, L.H.; Prodromou, C. *Structure and mechanism of the Hsp90 molecular chaperone machinery*. Annu. Rev. Biochem. 2006, 75, 271–294.

31. Zininga, T.; Shonhai, A. *Small Molecule Inhibitors Targeting the Heat Shock Protein System of Human Obligate Protozoan Parasites*. Int J Mol Sci. 2019, Nov 25;20(23):5930.

32. Hayer-Hartl, M.; Bracher, A.; Hartl, F.U. *The GroELGroES chaperonin machine: A nano-cage for protein folding*. Trends Biochem. Sci. 2016, 41, 62–76.

33. Wang, J.; Enriquez, A.S.; Li, J.; Rodriguez, A.; Holguin, B.; Von Salzen, D.; Bhatt J.M.; Bernal, R.A. *MitCHAP-60 and Hereditary Spastic Paraplegia SPG-13 Arise from an Inactive hsp60 Chaperonin that Fails to Fold the ATP Synthase β-Subunit*. Scientific Reports 2019, volume 9, Article number: 12300.

34. Quraishe, S.; Asuni, A.; Boelens, W.C.; O'Connor, V.; Wyttenbach, A. *Expression of the small heat shock protein family in the mouse CNS: differential anatomical and biochemical compartmentalization*. Neuroscience 2008, 153, 483–491.

35. Carra, S.; Alberti, S.; Arrigo, P.A.; Benesch, J.L.; Benjamin, I.J.; Boelens,W.; Bartelt-Kirbach, B.; Brundel, B.; Buchner, J.; Bukau, B.; et al. *The growing world of small heat shock proteins: From structure to functions*. Cell Stress Chaperones 2017, 22, 601–611.

36. Hartl, F.U. *Molecular chaperones in cellular protein folding*. Nature 1996, 381, 571–579.

37. Powers, E.T.; Balch, W.E. *Diversity in the origins of proteostasis networks—A driver for protein function in evolution*. Nat. Rev. Mol. Cell Biol. 2013, 14, 237–248.

38. Balchin, D.; Miliˇci´c, G.; Strauss, M.; Hayer-Hartl, M.; Hartl, F.U. *Pathway of actin folding directed by the eukaryotic chaperonin TRiC*. Cell 2018, 174, 1507–1521.

39. Hershko, A.; Ciechanover, A. *The ubiquitin system*. Annu. Rev. Biochem. 1998, 67, 425–479.

40. Ciechanover, A. *The ubiquitin proteolytic system: From a vague idea, through basic mechanisms, and onto human diseases and drug targeting*. Neurology 2006, 66, S7–S19.

41. Demarchi, F.; Brancolini, C. *Altering protein turnover in tumor cells: New opportunities for anti-cancer therapies*. Drug Resist. Updates 2005, 8, 359–368.

42. Pickart, C.M.; Eddins, M.J. *Ubiquitin: structures, functions, mechanisms*. Biochim Biophys Acta. 2004, Nov 29;1695(1-3):55-72.

43. Chowdhury, M.; Enenkel, C. *Intracellular dynamics of the Ubiquitin-Proteasome-System*. F1000Research 2015, 4, 367.

44. Morreale, F.E.;Walden, H. *Types of ubiquitin ligases*. Cell 2016, 165, 248.e1.

45. Buetow, L.; Huang, D.T. *Structural insights into the catalysis and regulation of E3 ubiquitin ligases*. Nat. Rev. Mol. Cell Biol. 2016, 17, 626–642.

46. Lecker, S.H.; Goldberg, A.L.; Mitch, W.E. *Protein degradation by the ubiquitin-proteasome pathway in normal and disease states*. J Am Soc Nephrol. 2006, Jul;17(7):1807-19.

47. Nandi, D.; Tahiliani, P.; Kumar, A.; Chandu, D. *The ubiquitin-proteasome system*. J BiosciMar 2006, 31(1):137-55.

48. Glickman, M.H.; Ciechanover, A. *The ubiquitin-proteasome proteolytic pathway: destruction for the sake of construction*. Physiol Rev 2002, Apr;82(2):373-428.

49. Suryadinata, R.; Roesley, S.N.A.; Yang, G.; Šarčević, B. *Mechanisms of Generating Polyubiquitin Chains of Different Topology*. Cells. 2014, Sep; 3(3): 674–689.

50. Thrower, J.S.; Hoffman, L.; Rechsteiner, M.; Pickart, C.M. *Recognition of the polyubiquitin proteolytic signal*. EMBO J. 2000, Jan 4;19(1):94-102.

51. Dikic, I.; Wakatsuki, S.; Walters, K.J. *Ubiquitin-binding domains — from structures to functions* Nature Reviews Molecular Cell Biology 2009, volume 10, pages 659–671.

52. D'Arcy, P.;Wang, X.; Linder, S. *Deubiquitinase inhibition as a cancer therapeutic strategy*. Pharmacol. Ther. 2015, 147, 32–54.

53. Jang, H.H. *Regulation of Protein Degradation by Proteasomes in Cancer*. J Cancer Prev. 2018, Dec;23(4):153-161.

54. Baumeister, W.; Walz, J.; Zühl, F.; Seemüller, E. *The proteasome: Paradigm of a self-compartmentalizing protease*. Cell 1998, 92, 367–380.

55. Voges, D.; Zwickl, P.; Baumeister, W. *The 26S proteasome: A molecular machine designed for controlled proteolysis*. Annu. Rev. Biochem. 1999, 68, 1015–1068.

56. Kisselev, A.F.; Akopian, T.N.; Castillo, V.; Goldberg, A.L. *Proteasome active sites allosterically regulate each other, suggesting a cyclical bite-chew mechanism for protein breakdown*. Mol. Cell 1999, 4, 395–402.

57. Tomita, T.; Matouschek, A. *Substrate selection by the proteasome through initiation regions*. Protein Sci. 2019, 28, 1222–1232.

58. Clague, M.J.; Barsukov, I.; Coulson, J.M.; Liu, H.; Rigden, D.J.; Urbé, S. *Deubiquitylases from genes to organism*. Physiol Rev. 2013, Jul;93(3):1289-315.

59. Amerik, A.Y.; Hochstrasser, M. *Mechanism and function of deubiquitinating enzymes*. Biochim Biophys Acta. 2004, Nov 29;1695(1-3):189-207.

60. Sgorbissa, A.; Potu, H.; Brancolini, C. *Isopeptidases in anticancer therapy: Looking for inhibitors*. Am. J. Transl. Res. 2010, 2, 235–247.

61. Rehman, S.A.A.; Kristariyanto, Y.A.; Choi, S.Y.; Labib, K.; Hofmann, K.; Kulathu, Y. *MINDY-1 is a member of an evolutionarily conserved and structurally distinct new family of deubiquitinating enzymes*. Molecular. Cell 2016, 63, 146–155.

62. Kuo, C.L.; Goldberg, A.L. *Ubiquitinated proteins promote the association of proteasomes with the deubiquitinating enzyme Usp14 and the ubiquitin ligase Ube3c*. Proc. Natl. Acad. Sci. USA 2017, 114, E3404–E3413.

63. Beck, F.; Unverdorben, P.; Bohn, S.; Schweitzer, A.; Pfeifer, G.; Sakata, E.; Nickell, S.; Plitzko, J.M.; Villa, E.; Baumeister, W.; Förster, F. *Near-atomic resolution structural model of the yeast 26S proteasome*. Proc Natl Acad Sci U S A. 2012, Sep 11;109(37):14870-5.

64. Peth, A.; Besche, H.C.; Goldberg, A.L. *Ubiquitinated proteins activate the proteasome by binding to usp14/ubp6 which causes 20s gate opening*. Mol Cell. Dec 2009, 11; 36(5): 794–804.

65. Hanna, J.; Hathaway, N.A.; Tone, Y.; Crosas, B.; Elsasser, S.; Kirkpatrick, D.S.; Leggett, D.S.; Gygi, S.P.; King, R.W.; Finley, D. *Deubiquitinating enzyme Ubp6 functions noncatalytically to delay proteasomal degradation*. Cell. 2006, Oct 6;127(1):99-111.

66. Hamazaki, J.; Iemura, S.; Natsume, T.; Yashiroda, H.; Tanaka, K.; Murata, S. *A novel proteasome interacting protein recruits the deubiquitinating enzyme UCH37 to 26S proteasomes*. EMBO J. 2006, Oct 4;25(19):4524-36.

67. Yao, T.; Song, L.; Xu, W.; DeMartino, G.N.; Florens, L.; Swanson, S.K.; Washburn, M.P.; Conaway, R.C.; Conaway, J.W.; Cohen, R.E. *Proteasome recruitment and activation of the Uch37 deubiquitinating enzyme by Adrm1*. Nat Cell Biol. 2006, Sep;8(9):994-1002.

68. Gardner, R.G.; Nelson, Z.W.; Gottschling, D.E. *Degradation mediated protein quality control in the nucleus*. Cell 2005, 120, 803–815.

69. Heck, J.W.; Cheung, S.K.; Hampton, R.Y. *Cytoplasmic protein quality control degradation mediated by parallel actions of the E3 ubiquitin ligases Ubr1 and San1*. Proc. Natl. Acad. Sci. U.S.A. 2010, 107, 1106–1111.

70. Kettern, N.; Dreiseidler, M.; Tawo, R.; Hohfeld, J. *Chaperone assisted degradation: multiple paths to destruction*. Biol. Chem. 2010, 391, 481–489.

71. Ballinger, C.A.; Connell, P.; Wu, Y.; Hu, Z.; Thompson, L.J.; Yin, L.Y.; et al. *Identification of CHIP, a novel tetratricopeptide repeat-containing protein that interacts with heat shock proteins and negatively regulates chaperone functions*. Mol. Cell. Biol. 1999, 19, 4535–4545.

72. McDonough, H.; Patterson, C. *CHIP: a link between the chaperone and proteasome systems*. Cell Stress Chaperones 2003, 8, 303–308.

73. Cyr, D.M.; Hohfeld, J.; Patterson, C. *Protein quality control: U-box containing E3 ubiquitin ligases join the fold*. Trends Biochem. Sci. 2002, 27, 368–375.

74. Demand, J.; Alberti, S.; Patterson, C.; Hohfeld, J. *Cooperation of a ubiquitin domain protein and an E3 ubiquitin ligase during chaperone/proteasome coupling*. Curr. Biol. 2001, 11, 1569–1577.

75. Connell, P.; Ballinger, C.A.; Jiang, J.; Wu, Y.; Thompson, L.J.; Hohfeld, J.; et al. *The co-chaperone CHIP regulates protein triage decisions mediated by heat-shock proteins*. Nat. Cell Biol. 2001, 3, 93–96.

76. Lanneau, D.; Wettstein, G.; Bonniaud, P.; Garrido, C. *Heat shock proteins: cell protection through protein triage*. ScientificWorldJournal 2010, 10, 1543–1552.

77. Ciechanover, A.; Kwon, Y.T. *Protein Quality Control by Molecular Chaperones in Neurodegeneration* Front Neurosci. 2017, Apr 6;11:185.

78. Takayama, S.; Bimston, D.N.; Matsuzawa, S.; Freeman, B.C.; Aime-Sempe, C.; Xie, Z.; et al. *BAG-1 modulates the chaperone activity of Hsp70/Hsc70*. EMBO J. 1997, 16, 4887–4896.

79. Alberti, S.; Esser, C.; Hohfeld, J. *BAG-1–a nucleotide exchange factor of Hsc70 with multiple cellular functions*. Cell Stress Chaperones 2003, 8, 225–231.

80. Garrido, C.; Brunet, M.; Didelot, C.; Zermati, Y.; Schmitt, E.; Kroemer, G. *Heat shock proteins 27 and 70: anti-apoptotic proteins with tumorigenic properties*. Cell Cycle 2006, 5, 2592–2601.

81. Galluzzi, L.; Baehrecke, E.H.; Ballabio, A.; Boya, P.; Bravo-San Pedro, J.M.; Cecconi, F.; Choi, A.M.; Chu, C.T.; Codogno, P.; Colombo, M.I.; et al. *Molecular definitions of autophagy and related processes*. EMBO J. 2017,36, 1811–1836.

82. García-Prat, L.; Martínez-Vicente, M.; Perdiguero, E.; Ortet, L.; Rodríguez-Ubreva, J.; Rebollo, E.; Ruiz-Bonilla, V.; Gutarra, S.; Ballestar, E.; Serrano, A.L.; et al. *Autophagy maintains stemness by preventing senescence*. Nature 2016, 529, 37–42.

83. Carra, S.; Seguin, S.J.; Lambert, H.; Landry, J. *HspB8 chaperone activity toward poly(Q)-containing proteins depends on its association with Bag3, a stimulator of macroautophagy*. J. Biol. Chem. 2008, 283, 1437–1444.

84. Gamerdinger, M.; Hajieva, P.; Kaya, A.M.; Wolfrum, U.; Hartl, F.U.; Behl, C. *Protein quality control during aging involves recruitment of the macroautophagy pathway by BAG3*. EMBO J. 2009, 28, 889–901.

85. Arndt, V.; Dick, N.; Tawo, R.; Dreiseidler, M.; Wenzel, D.; Hesse, M.; Fürst, D.O.; Saftig, P.; Saint, R.; Fleischmann, B.K.; et al. *Chaperone-assisted selective autophagy is essential for muscle maintenance*. Curr. Biol. 2010, 20, 143–148.

86. Cha-Molstad, H.; Sung, K.S.; Hwang, J.; Kim, K.A.; Yu, J.E.; Yoo, Y.D.; et al. *Amino-terminal arginylation targets endoplasmic reticulum chaperone BiP for autophagy through p62 binding*. Nat. Cell Biol. 2015, 17, 917–929.

87. Lamark, T.; Kirkin, V.; Dikic, I.; Johansen, T. *NBR1 and p62 as cargo receptors for selective autophagy of ubiquitinated targets*. Cell Cycle 2009, 8, 1986–1990.

88. Stolz, A.; Ernst, A.; Dikic, I. *Cargo recognition and trafficking in selective autophagy*. Nat. Cell Biol. 2014, 16, 495–501.

89. Kaushik, S.; Cuervo, A.M. *The coming of age of chaperone-mediated autophagy*. Nat. Rev. Mol. Cell Biol. 2018, 19, 365–381.

90. Agarraberes, F.A.; Dice, J.F. *A molecular chaperone complex at the lysosomal membrane is required for protein translocation*. J. Cell Sci. 2001, 114 (Pt 13), 2491–2499.

91. Bandyopadhyay, U.; Kaushik, S.; Varticovski, L.; Cuervo, A.M. *The chaperone-mediated autophagy receptor organizes in dynamic protein complexes at the lysosomal membrane*. Mol. Cell. Biol. 2008, 28, 5747–5763.

92. Zhang, T.; Shen, S.; Qu, J.; Ghaemmaghami, S. *Global analysis of cellular protein flux quantifies the selectivity of basal autophagy*. Cell Rep. 2016, 14, 2426–2439.

93. Dikic, I. *Proteasomal and autophagic degradation systems*. Annu. Rev. Biochem. 2017, 86, 193–224.

94. Li, J.; Zhang, D.; Wiersma, M.; Brundel, B.J.J.M. *Role of autophagy in proteostasis: Friend and foe in cardiac diseases*. Cells 2018, 7, 279.

95. Wang, C.; Wang, X. *The interplay between autophagy and the ubiquitin-proteasome system in cardiac proteotoxicity*. Biochim Biophys Acta 2015, 1852(2), 188–194.

96. Kyrychenko, V.O.; Nagibin, V.S.; Tumanovska, L.V.; Pashevin, D.O.; Gurianova, V.L,; Moibenko, A.A.; Dosenko, V.E.; Klionsky, D.J. *Knockdown of PSMB7 induces autophagy in cardiomyocyte cultures: possible role in endoplasmic reticulum stress*. Pathobiology: journal of immunopathology, molecular and cellular biology. 2014, 81, 8–14.

97. Gorbea, C.; Rechsteiner, M.; Vallejo, J.G.; Bowles, N.E. *Depletion of the 26S proteasome adaptor Ecm29 increases Toll-like receptor 3 signaling*. Sci Signal. 2013, 6, ra86.

98. Zaarur, N.; Meriin, A.B.; Bejarano, E.; Xu, X.; Gabai, V.L.; Cuervo, A.M.; Sherman, M.Y. *Proteasome Failure Promotes Positioning of Lysosomes around the Aggresome via Local Block of Microtubule-Dependent Transport*. Mol Cell Biol. 2014, 34, 1336–1348.

99. Matsumoto, G.; Wada, K.; Okuno, M.; Kurosawa, M.; Nukina, N. *Serine 403 phosphorylation of p62/SQSTM1 regulates selective autophagic clearance of ubiquitinated proteins*. Mol Cell. 2011, 4, 279–89.

100. Wang, X.J.; Yu, J.; Wong, S.H.; Cheng, A.S.; Chan, F.K.; Ng, S.S.; Cho, C.H.; Sung, J.J.; Wu, W.K. *A novel crosstalk between two major protein degradation systems: Regulation of proteasomal activity by autophagy*. Autophagy. 2013, 9, 1500–1508.

101. Korolchuk, V.I.; Mansilla, A.; Menzies, F.M.; Rubinsztein, D.C. *Autophagy inhibition compromises degradation of ubiquitin-proteasome pathway substrates*. Mol Cell. 2009, 33, 517–527.

102. Qiao, L.; Hamamichi, S.; Caldwell, K.A.; Caldwell, G,A.; Yacoubian, T.A.; Wilson, S.; Xie, Z.L.; Speake, L.D.; Parks, R.; Crabtree, D.; Liang, Q.; Crimmins, S.; Schneider, L.; Uchiyama, Y.; Iwatsubo, T.; Zhou, Y.; Peng, L.; Lu, Y.; Standaert, D.G.; Walls, K.C.; Shacka, J.J.; Roth, K.A.; Zhang, J. *Lysosomal enzyme cathepsin D protects against alpha-synuclein aggregation and toxicity*. Mol Brain. 2008, 1, 17.

103. Doyle, S.M.; Genest, O.; Wickner, S. *Protein rescue fromaggregates by powerful molecular chaperone machines*. Nat. Rev. Mol. Cell Biol. 2013, 14, 617–629.

104. Torrente, M. P.; Shorter, J. *The metazoan protein disaggregase and amyloid depolymerase system: Hsp110, Hsp70, Hsp40, and small heat shock proteins*. Prion 2013, 7, 457–463.

105. Lipinska, N.; Zietkiewicz, S.; Sobczak, A.; Jurczyk, A.; Potocki, W.; Morawiec, E.; et al. *Disruption of ionic interactions between the nucleotide binding domain 1 (NBD1) and middle (M) domain in Hsp100 disaggregase unleashes toxic hyperactivity and partial independence from Hsp70*. J. Biol. Chem. 2013, 288, 2857–2869.

106. Carroni, M.; Kummer, E.; Oguchi, Y.; Wendler, P.; Clare, D.K.; Sinning, I.; et al. *Head-to-tail interactions of the coiled-coil domains regulate ClpB activity and cooperation with Hsp70 in protein disaggregation*. Elife 2014, 3:e02481.

107. Gao, X.; Carroni, M.; Nussbaum-Krammer, C.; Mogk, A.; Nillegoda, N.B.; Szlachcic, A.; et al. *Human Hsp70 Disaggregase Reverses Parkinson's-Linked a-Synuclein Amyloid Fibrils*. Mol. Cell 2015, 59, 781–793.

108. Nillegoda, N.B.; Theodoraki, M.A.; Mandal, A.K.; Mayo, K.J.; Ren, H.Y.; Sultana, R.; et al. *Ubr1 and Ubr2 function in a quality control pathway for degradation of unfolded cytosolic proteins*. Mol. Biol. Cell 2010, 21, 2102–2116.

109. Rampelt, H.; Kirstein-Miles, J.; Nillegoda, N.B.; Chi, K.; Scholz, S.R.; Morimoto, R.I.; et al. *Metazoan Hsp70 machines use Hsp110 to power protein disaggregation*. EMBO J. 2012, 31, 4221–4235.

110. Peng, C.; Trojanowski, J.Q.; Lee, V.M. *Protein transmission in neurodegenerative disease*. Nat. Rev. Neurol. 2020, 16, 199–212.

111. Walter, P.; Ron, D. *The Unfolded Protein Response: From stress pathway to homeostatic regulation*. Science 2011, 334, 1081–1086.

112. Auner, H.W.; Moody, A.M.; Ward, T.H.; Kraus, M.; Milan, E.; May, P.; Chaidos, A.; Driessen, C.; Cenci, S.; Dazzi, F.; et al. *Combined inhibition of p97 and the proteasome causes lethal disruption of the secretory apparatus in multiple myeloma cells*. PLoS ONE 2013, 8, e74415.

113. Cyr, D.M.; Hebert, D.N. *Protein quality control—linking the unfolded protein response to disease*. EMBO Reports 2009, 10:1206-1210

114. Kannan, S.; Muthusamy, V.R.; Whitehead, K.J.; Wang, L.; Gomes, A.V.; Litwin, S.E.; Kensler, T.W.; Abel, E.D.; Hoidal, J.R.; Rajasekaran, N.S. *Nrf2 deficiency prevents reductive stress-induced hypertrophic cardiomyopathy*. Cardiovasc. Res. 2013, 100, 63–73.

115. Ri, M. *Endoplasmic-reticulum stress pathway-associated mechanisms of action of proteasome inhibitors in multiple myeloma*. Int. J. Hematol. 2016, 104, 273–280.

116. Lafont, E. *Stress management: Death receptor signalling and cross-talks with the unfolded protein response in cancer*. Cancers 2020, 12, 1113.

117. Hetz, C.; Zhang, K.; Kaufman, R.J. *Mechanisms, regulation and functions of the unfolded protein response*. Nat. Rev. Mol. Cell Biol. 2020.

118. Kaufman, R.J. *Orchestrating the unfolded protein response in health and disease*. J. Clin. Investig. 2002, 110, 1389–1398.

119. Harding, H.P.; Calfon, M.; Urano, F.; Novoa, I.; Ron, D. *Transcriptional and translational control in the mammalian unfolded protein response*. Annu. Rev. Cell Dev. Biol. 2002, 18, 575–599.

120. Wang, M.;Wey, S.; Zhang, Y.; Ye, R.; Lee, A.S. *Role of the unfolded protein response regulator GRP78/BiP indevelopment, cancer, and neurological disorders*. Antioxid. Redox Signal. 2009, 11, 2307–2316.

121. Couillault, C.; Fourquet, P.; Pophillat, M.; Ewbank, J.J. *A UPR-independent infection-specific role for a BiP/GRP78 protein in the control of antimicrobial peptide expression in C. elegans epidermis*. Virulence 2012, 3, 299–308.

122. Iurlaro, R.; Muñoz-Pinedo, C. *Cell death induced by endoplasmic reticulum stress*. FEBS J. 2016, Jul;283(14):2640-52.

123. Szegezdi, E.; Logue, S.E.; Gorman, A.M.; Samali, A. *Mediators of endoplasmic reticulum stress-induced apoptosis*. EMBO Rep. 2006, 7, 880–885.

124. Furukawa, M.; Xiong, Y. *BTB protein Keap1 targets antioxidant transcription factor Nrf2 for ubiquitination by the Cullin 3-Roc1 ligase*. Mol. Cell. Biol. 2005, 25, 162–171.

125. Bobrovnikova-Marjon, E.; Grigoriadou, C.; Pytel, D.; Zhang, F.; Ye, J.; Koumenis, C.; Cavener, D.; Diehl, J.A. *PERK promotes cancer cell proliferation and tumor growth by limiting oxidative DNA damage*. Oncogene 2010, 29, 3881–3895.

126. Harding, H.P.; Calfon, M.; Urano, F.; Novoa, I.; Ron, D. *Transcriptional and translational control in the mammalian unfolded protein response*. Annu. Rev. Cell Dev. Biol. 2002, 18, 575–599.

127. Zhang, W.; Hietakangas, V.; Wee, S.; Lim, S.C.; Gunaratne, J.; Cohen, S.M. *ER stress potentiates insulin resistance through PERK-mediated FOXO phosphorylation*. Genes Dev. 2013, 27, 441–449.

128. You, S.; Li, H.; Hu, Z.; Zhang,W. *eIF2 kinases PERK and GCN2 act on FOXO to potentiate FOXO activity*. Genes Cells 2018, 23, 786–793.

129. Bobrovnikova-Marjon, E.; Pytel, D.; Riese, M.J.; Vaites, L.P.; Singh, N.; Koretzky, G.A.; Witze, E.S.; Diehl, J.A. *PERK utilizes intrinsic lipid kinase activity to generate phosphatidic acid, mediate Akt activation, and promote adipocyte differentiation*. Mol. Cell. Biol. 2012, 32, 2268–2278.

130. Pytel, D.; Gao, Y.; Mackiewicz, K.; Katlinskaya, Y.V.; Staschke, K.A.; Paredes, M.C.G.; Yoshida, A.; Qie, S.; Zhang, G.; Chajewski, O.S.; et al. *PERK is a haploinsufficient tumor suppressor: Gene dose determines tumor-suppressive versus tumor promoting properties of PERK in melanoma.* PLoS Genet. 2016, 12, e1006518.

131. McConkey, D.J. *The integrated stress response and proteotoxicity in cancer therapy*. Biochem. Biophys. Res. Commun. 2017, 482, 450–453.

132. White, M.C.; Schroeder, M.D.; Zhu, K.; Xiong, K.; McConkey, D.J. *HRI-mediated translational repression reduces proteotoxicity and sensitivity to Bortezomib in human pancreatic cancer cells*. Oncogene 2018, 37, 4413–4427.

133. Hollien, J.; Weissman, J.S. *Decay of endoplasmic reticulum-localized mRNAs during the unfolded protein response*. Science 2006, 313, 104–107.

134. Cawley, K.; Deegan, S.; Samali, A.; Gupta, S. *Assays for detecting the unfolded protein response*. Methods Enzymol 2011, 490, 31–51.

135. Acosta-Alvear, D.; Zhou, Y.; Blais, A.; Tsikitis, M.; Lents, N.H.; Arias, C.; Lennon, C.J.; Kluger, Y.; Dynlacht, B.D. *XBP1 controls diverse cell type- and conditionspecific transcriptional regulatory networks*. Mol Cell 2007, 27, 53–66.

136. Hillary, R.F.; FitzGerald, U. *A lifetime of stress: ATF6 in development and homeostasis*. J. Biomed. Sci. 2018, 25, 48.

137. Pitale, P.M.; Gorbatyuk, O.; Gorbatyuk, M. *Neurodegeneration: Keeping ATF4 on a tight leash*. Front. Cell. Neurosci. 2017, 11, 410.

138. Rzymski, T.; Milani, M.; Singleton, D.C.; Harris, A.L. *Role of ATF4 in regulation of autophagy and resistance to drugs and hypoxia*. Cell Cycle 2009, 8, 3838–3847.

139. Lassot, I.; Ségéral, E.; Berlioz-Torrent, C.; Durand, H.; Groussin, L.; Hai, T.; Benarous, R.; Margottin-Goguet, F. *ATF4 degradation relies on a phosphorylation-dependent interaction with the SCF(betaTrCP) ubiquitin ligase*. Mol. Cell. Biol. 2001, 21, 2192–2202.

140. Wang, Q.; Mora-Jensen, H.;Weniger, M.A.; Perez-Galan, P.;Wolford, C.; Hai, T.; Ron, D.; Chen,W.; Trenkle,W.; Wiestner, A.; et al. *ERAD inhibitors integrate ER stress with an epigenetic mechanism to activate BH3-only protein NOXA in cancer cells*. Proc. Natl. Acad. Sci. USA 2009, 106, 2200–2205.

141. Cnop, M.; Toivonen, S.; Igoillo-Esteve, M.; Salpea, P. *Endoplasmic reticulum stress and eIF2 phosphorylation: The Achilles heel of pancreatic cells*. Mol. Metab. 2017, 6, 1024–1039.

142. Palam, L.R.; Baird, T.D.; Wek, R.C. *Phosphorylation of eIF2 facilitates ribosomal bypass of an inhibitory upstream ORF to enhance CHOP translation*. J. Biol. Chem. 2011, 286, 10939–10949.

143. Marciniak, S.J.; Yun, C.Y.; Oyadomari, S.; Novoa, I.; Zhang, Y.; Jungreis, R.; Nagata, K.; Harding, H.P.; Ron, D. *CHOP induces death by promoting protein synthesis and oxidation in the stressed endoplasmic reticulum*. Genes Dev 2004, 18, 3066–3077.

144. Donnelly, N.; Gorman, A.M.; Gupta, S.; Samali, A. *The eIF2alpha kinases: their structures and functions*. Cell Mol Life Sci 2013, 70, 3493–3511.

145. Brancolini, C.; Iuliano, L. *Proteotoxic Stress and Cell Death in Cancer Cells*. Cancers (Basel) 2020, Aug 23;12(9):2385.

146. Tajiri, S.; Oyadomari, S.; Yano, S.; Morioka, M.; Gotoh, T.; Hamada, J.I.; Ushio, Y.; Mori, M. *Ischemiainduced neuronal cell death is mediated by the endoplasmic reticulum stress pathway involving CHOP*. Cell Death Differ 2004, 11, 403–415.

147. Oyadomari, S.; Koizumi, A.; Takeda, K.; Gotoh, T.; Akira, S.; Araki, E.; Mori, M. *Targeted disruption of the Chop gene delays endoplasmic reticulum stressmediated diabetes*. J Clin Invest 2002, 109, 525–532.

148. Ron, D.; Walter, P. *Signal integration in the endoplasmic reticulum unfolded protein response*. Nat Rev Mol Cell Biol 2007, 8, 519–529.

149. Sullivan, G.P.; O'Connor, H.; Henry, C.M.; Davidovich, P.; Clancy, D.M.; Albert, M.L.; Cullen, S.P.; Martin, S.J. *TRAIL receptors serve as stress-associated molecular patterns to promote ER-stress-induced inflammation*. Dev. Cell 2020, 52, 714–730.e5.

150. Yamaguchi, H.; Wang, H.G. *CHOP is involved in endoplasmic reticulum stress-induced apoptosis by enhancing DR5 expression in human carcinoma cells*. J. Biol. Chem. 2004, 279, 45495–45502.

151. Li, T.; Su, L.; Lei, Y.; Liu, X.; Zhang, Y.; Liu, X. *DDIT3 and KAT2A regulate TNFRSF10A and TNFRSF10B expression in endoplasmic reticulum stress-mediated apoptosis in human lung cancer cells*. J. Biol. Chem. 2015, 290, 11108–11118.

152. Iurlaro, R.; Püschel, F.; León-Annicchiarico, C.L.; O'Connor, H.; Martin, S.J.; Palou-Gramón, D.; Lucendo, E.; Muñoz-Pinedo, C. *Glucose deprivation induces ATF4-mediated apoptosis through TRAIL death receptors*. Mol. Cell. Biol. 2017, 37, e00479-16.

153. Pathak, S.S.; Liu, D.; Li, T.; de Zavalia, N.; Zhu, L.; Li, J.; Karthikeyan, R.; Alain, T.; Liu, A.C.; Storch, K.F.; et al. *The eIF2 kinase GCN2 modulates period and rhythmicity of the circadian clock by translational control of Atf4*. Neuron 2019, 104, 724–735.e6.

154. Ratan, R.R. *The chemical biology of ferroptosis in the central nervous system*. Cell Chem. Biol. 2020, 27, 479–498.

155. Han, J.; Back, S.H.; Hur, J.; Lin, Y.H.; Gildersleeve, R.; Shan, J.; Yuan, C.L.; Krokowski, D.; Wang, S.; Hatzoglou, M.; et al. *ER-stress-induced transcriptional regulation increases protein synthesis leading to cell death*. Nat Cell Biol 2013, 15, 481–490.

156. McCullough, K.D.; Martindale, J.L.; Klotz, L.O.; Aw, T.Y.; Holbrook, N.J. *Gadd153 sensitizes cells to endoplasmic reticulum stress by down-regulating Bcl2 and perturbing the cellular redox state*. Mol Cell Biol 2001, 21, 1249–1259.

157. Hiramatsu, N.; Messah, C.; Han, J.; LaVail, M.M.; Kaufman, R.J.; Lin, J.H. *Translational and posttranslationalregulation of XIAP by eIF2alpha and ATF4 promotes ER stress-induced cell death during the unfolded protein response*. Mol. Biol. Cell 2014, 25, 1411–1420.

158. Hai, T.;Wolford, C.C.; Chang, Y.S. *ATF3, a Hub of the cellular adaptive-response network, in the pathogenesis of diseases: Is modulation of inflammation a unifying component?* Gene Expr. 2010, 15, 1–11.

159. Edagawa, M.; Kawauchi, J.; Hirata, M.; Goshima, H.; Inoue, M.; Okamoto, T.; Murakami, A.; Maehara, Y.; Kitajima, S. *Role of activating transcription factor 3 (ATF3) in endoplasmic reticulum (ER) Stress-induced sensitization of p53-deficient human colon cancer cells to tumor necrosis factor (TNF)-related apoptosis-inducing ligand (TRAIL)-mediated apoptosis through Up-regulation of death receptor 5 (DR5) by zerumbone and celecoxib*. J. Biol. Chem. 2014, 289, 21544–21561.

160. Teske, B.F.; Fusakio, M.E.; Zhou, D.; Shan, J.; McClintick, J.N.; Kilberg, M.S.; Wek, R.C. *CHOP induces activating transcription factor 5 (ATF5) to trigger apoptosis in response to perturbations in protein homeostasis*. Mol. Biol. Cell 2013, 24, 2477–2490.

161. Sharma, K.; Vu, T.T.; Cook, W.; Naseri, M.; Zhan, K.; Nakajima, W.; Harada, H. *p53-independent Noxa induction by cisplatin is regulated by ATF3/ATF4 in head and neck squamous cell carcinoma cells*. Mol. Oncol. 2018, 12, 788–798.

162. Lu, M.; Lawrence, D.A.; Marsters, S., Acosta-Alvear, D.; Kimmig, P.; Mendez, A.S.; Paton, A.W.; Paton, J.C.; Walter, P.; Ashkenazi, A. *Opposing unfolded-proteinresponse signals converge on death receptor 5 to control apoptosis*. Science (New York, NY) 2014, 345, 98.

163. Urano, F.; Wang, X.; Bertolotti, A.; Zhang, Y.; Chung, P.; Harding, H.P.; Ron, D. *Coupling of stress in the ER to activation of JNK protein kinases by transmembrane protein kinase IRE1*. Science 2000, 287, 664–666.

164. Saveljeva, S.; Mc Laughlin, S.L.; Vandenabeele, P.; Samali, A.; Bertrand, M.J.M. *Endoplasmic reticulum stress induces ligand-independent TNFR1-mediated necroptosis in L929 cells*. Cell Death Dis 2015, 6, e1587.

165. Logue, S.E.; Cleary, P.; Saveljeva, S.; Samali, A. *New directions in ER stress-induced cell death*. Apoptosis 2013, 18, 537–546.

166. Ghosh, R.; Wang, L.; Wang, E.S.; Perera, B.G.; Igbaria, A.; Morita, S.; Prado, K.; Thamsen, M.; Caswell, D.; Macias, H. et al. *Allosteric inhibition of the IRE1alpha RNase preserves cell viability and function during endoplasmic reticulum stress*. Cell 2014, 158, 534–548.

167. Cano-González, A.; Mauro-Lizcano, M.; Iglesias-Serret, D.; Gil, J.; López-Rivas, A. *Involvement of both caspase-8 and Noxa-activated pathways in Endoplasmic Reticulum stress-induced apoptosis in triple-negative breast tumor cells*. Cell Death Dis. 2018, 9, 134.

168. Aleo, E.; Henderson, C.J.; Fontanini, A.; Solazzo, B.; Brancolini, C. *Identification of new compounds that trigger apoptosome-independent caspase activation and apoptosis*. Cancer Res. 2006, 66, 9235–9244.

169. Manini, I.; Sgorbissa, A.; Potu, H.; Tomasella, A.; Brancolini, C. *The DeISGylase USP18 limits TRAIL-induced apoptosis through the regulation of TRAIL levels: Cellular levels of TRAIL influences responsiveness to TRAIL-induced apoptosis*. Cancer Biol. Ther. 2013, 14, 1158–1166.

170. Chang, T.K.; Lawrence, D.A.; Lu, M.; Tan, J.; Harnoss, J.M.; Marsters, S.A.; Liu, P.; Sandoval, W.; Martin, S.E.; Ashkenazi, A. *Coordination between two branches of the unfolded protein response determines apoptotic cell fate*. Mol. Cell 2018, 71, 629–636.e5.

171. Zhu, Z.C.; Liu, J.W.; Yang, C.; Li, M.J.;Wu, R.J.; Xiong, Z.Q. *Targeting KPNB1 overcomes TRAIL resistance by regulating DR5, Mcl-1 and FLIP in glioblastoma cells*. Cell Death Dis. 2019, 10, 118.

172. Lam, M.; Marsters, S.A.; Ashkenazi, A.; Walter, P. *Misfolded proteins bind and activate Death Receptor 5 to trigger apoptosis during unresolved endoplasmic reticulum stress*. Elife 2020, 9, e52291.

173. Sullivan, G.P.; O'Connor, H.; Henry, C.M.; Davidovich, P.; Clancy, D.M.; Albert, M.L.; Cullen, S.P.; Martin, S.J. *TRAIL receptors serve as stress-associated molecular patterns to promote ER-stress-induced inflammation*. Dev. Cell 2020, 52, 714–730.e5.

174. Von Karstedt, S.;Walczak, H. *An unexpected turn of fortune: Targeting TRAIL-Rs in KRAS-driven cancer*. Cell Death Discov. 2020, 6, 14.

175. Zong, W.X.; Li, C.; Hatzivassiliou, G.; Lindsten, T.; Yu, Q.C.; Yuan, J.; Thompson, C.B. *Bax and Bak can localize to the endoplasmic reticulum to initiate apoptosis*. J Cell Biol 2003, 162, 59–69.

176. Kim, H.; Tu, H.C.; Ren, D.; Takeuchi, O.; Jeffers, J.R.; Zambetti, G.P.; Hsieh, J.J.; Cheng, E.H. *Stepwise activation of BAX and BAK by tBID, BIM, and PUMA initiates mitochondrial apoptosis*. Mol Cell 2009, 36, 487–499.

177. Klee, M.; Pallauf, K.; Alcala, S.; Fleischer, A.; Pimentel-Muinos, F.X. *Mitochondrial apoptosis induced by BH3-only molecules in the exclusive presence of endoplasmic reticular Bak*. EMBO 2009, J 28, 1757–1768.

178. Lopes, U.G.; Erhardt, P.; Yao, R.; Cooper, G.M. *p53-dependent induction of apoptosis by proteasome inhibitors*. J. Biol. Chem. 1997, 272, 12893–12896.

179. Rastogi, N.; Duggal, S.; Singh, S.K.; Porwal, K.; Srivastava, V.K.; Maurya, R.; Bhatt, M.L.; Mishra, D.P. *Proteasome inhibition mediates p53 reactivation and anti-cancer activity of 6-gingerol in cervical cancer cells*. Oncotarget 2015, 6, 43310–43325.

180. Brancolini, C. *Inhibitors of the Ubiquitin-Proteasome System and the cell death machinery: How many pathways are activated?* Curr. Mol. Pharmacol. 2008, 1, 24–37.

181. Qiao, S.; Lamore, S.D.; Cabello, C.M.; Lesson, J.L.; Muñoz-Rodriguez, J.L.; Wondrak, G.T. *Thiostrepton is an inducer of oxidative and proteotoxic stress that impairs viability of human melanoma cells but not primary melanocytes*. Biochem. Pharmacol. 2012, 83, 1229–1240.

182. Arai, S.; Varkaris, A.; Nouri, M.; Chen, S.; Xie, L.; Balk, S.P. *MARCH5 mediates NOXA-dependent MCL1 degradation driven by kinase inhibitors and integrated stress response activation*. Elife 2020, 9, e54954.

183. Djajawi, T.M.; Liu, L.; Gong, J.N.; Huang, A.S.; Luo, M.J.; Xu, Z.; Okamoto, T.; Call, M.J.; Huang, D.C.S.; van Delft, M.F. *MARCH5 requires MTCH2 to coordinate proteasomal turnover of the MCL1:NOXA complex*. Cell Death Di er. 2020.

184. Allagnat, F.; Cunha, D.; Moore, F.; Vanderwinden, J.M.; Eizirik, D.L.; Cardozo, A.K. *Mcl-1 downregulation by pro-inflammatory cytokines and palmitate is an early event contributing to beta-cell apoptosis*. Cell Death Differ 2011, 18, 328–337.

185. Ramırez-Peinado, S.; Alcazar-Limones, F.; Lagares-Tena, L.; El Mjiyad, N.; Caro-Maldonado, A.; Tirado, O.M.; Mu~noz-Pinedo, C. *2-deoxyglucose induces noxadependent apoptosis in alveolar rhabdomyosarcoma*. Cancer Res 2011, 71, 6796–6806.

186. Jiang, C.C.; Lucas, K.; Avery-Kiejda, K.A.; Wade, M.; deBock, C.E.; Thorne, R.F.; Allen, J.; Hersey, P.; Zhang, X.D. *Up-regulation of Mcl-1 is critical for survival of human melanoma cells upon endoplasmic reticulum stress*. Cancer Res 2008, 68, 6708–6717.

187. Vaux, D.L.; Silke, J. IAPs, *RINGs and ubiquitylation*. Nat. Rev. Mol. Cell Biol. 2005, 6, 287–297.

188. Scomazzon, S.P.; Riccio, A.; Santopolo, S.; Lanzilli, G.; Coccia, M.; Rossi, A.; Santoro, M.G. *The zinc-finger AN1-type domain 2a gene acts as a regulator of cell survival in human melanoma: Role of E3-ligase cIAP2*. Mol. Cancer Res. 2019, 17, 2444–2456.

189. Yamamoto, K.; Ichijo, H.; Korsmeyer, S.J. *BCL-2 is phosphorylated and inactivated by an ASK1/Jun Nterminal protein kinase pathway normally activated at G(2)/M*. Mol Cell Biol 1999, 19, 8469–8478.

190. Fan, M.; Goodwin, M.; Vu, T.; Brantley-Finley, C.; Gaarde, W.A.; Chambers, T.C. *Vinblastine-induced phosphorylation of Bcl-2 and Bcl-XL is mediated by JNK and occurs in parallel with inactivation of the Raf-1/MEK/ERK cascade*. J Biol Chem 2000, 275, 29980–29985.

191. Morsi, R.Z.; Hage-Sleiman, R.; Kobeissy, H.; Dbaibo, G. Noxa: *Role in cancer pathogenesis and treatment*. Curr. Cancer Drug Targets 2018, 18, 914–928.

192. Oda, E.; Ohki, R.; Murasawa, H.; Nemoto, J.; Shibue, T.; Yamashita, T.; Tokino, T.; Taniguchi, T.; Tanaka, N. *Noxa, a BH3-only member of the Bcl-2 family and candidate mediator of p53-induced apoptosis*. Science 2000, 288, 1053–1058.

193. Qin, J.Z.; Zi ra, J.; Stennett, L.; Bodner, B.; Bonish, B.K.; Chaturvedi, V.; Bennett, F.; Pollock, P.M.; Trent, J.M.; Hendrix, M.J.C.; et al. *Proteasome inhibitors trigger NOXA-mediated apoptosis in melanoma and myeloma cells*. Cancer Res. 2005, 65, 6282–6293.

194. Fernandez, Y.; Verhaegen, M.; Miller, T.P.; Rush, J.L.; Steiner, P.; Opipari, A.W.J.; Lowe, S.W.; Soengas, M.S. *Differential regulation of Noxa in normal melanocytes and melanoma cells by proteasome inhibition: Therapeutic implications*. Cancer Res. 2005, 65, 6294–6304.

195. Vela, L.; Gonzalo, O.; Naval, J.; Marzo, I. *Direct interaction of Bax and Bak proteins with Bcl-2 Homology Domain 3 (BH3)-only proteins in living cells revealed by fluorescence complementation*. J. Biol. Chem. 2013, 288, 4935–4946.

196. Chen, H.C.; Kanai, M.; Inoue-Yamauchi, A.; Tu, H.C.; Huang, Y.; Ren, D.; Kim, H.; Takeda, S.; Reyna, D.E.; Chan, P.M.; et al. *An interconnected hierarchical model of cell death regulation by the BCL-2 family*. Nat. Cell Biol. 2015, 17, 1270–1281.

197. Wang, Q.; Mora-Jensen, H.; Weniger, M.A.; Perez-Galan, P.; Wolford, C.; Hai, T.; Ron, D.; Chen, W.; Trenkle, W.; Wiestner, A. et al. *ERAD inhibitors integrate ER stress with an epigenetic mechanism to activate BH3-only protein NOXA in cancer cells*. Proc Natl Acad Sci 2009, 106, 2200–2205.

198. Verfaillie, T.; van Vliet, A.; Garg, A.D.; Dewaele, M.; Rubio, N.; Gupta, S.; de Witte, P.; Samali, A.; Agostinis, P. *Pro-apoptotic signaling induced by photo-oxidative ER stress is amplified by Noxa, not Bim*. Biochem Biophys Res Commun 2013, 438, 500–506.

199. Zhang, L.; Lopez, H.; George, N.M.; Liu, X.; Pang, X.; Luo, X. *Selective involvement of BH3-only proteins and differential targets of Noxa in diverse apoptotic pathways*. Cell Death Differ 2010, 18, 864–873.

200. Guang, M.H.Z.; Kavanagh, E.L.; Dunne, L.P.; Dowling, P.; Zhang, L.; Lindsay, S.; Bazou, D.; Goh, C.Y.; Hanley, C.; Bianchi, G.; et al. *Targeting proteotoxic stress in cancer: A review of the role that protein quality control pathways play in oncogenesis*. Cancers 2019, 11, 66.

201. Puthalakath, H.; O'Reilly, L.A.; Gunn, P.; Lee, L.; Kelly, P.N.; Huntington, N.D.; Hughes, P.D.; Michalak, E.M.; McKimm-Breschkin, J.; Motoyama, N.; et al. *ER stress triggers apoptosis by activating BH3-only protein Bim*. Cell 2007, 129, 1337–1349.

202. Li, J.; Lee, B.; Lee, A.S. *Endoplasmic reticulum stress-induced apoptosis: Multiple pathways and activation of p53-up-regulated modulator of apoptosis (PUMA) and Noxa by p53*. J. Biol. Chem. 2006, 281, 7260–7270.

203. Llambi, F.; Wang, Y.M.; Victor, B.; Yang, M.; Schneider, D.M.; Gingras, S.; Parsons, M.J.; Zheng, J.H.; Brown, S.A.; Pelletier, S.; et al. *BOK is a non-canonical BCL-2 family effector of apoptosis regulated by ER-associated degradation*. Cell 2016, 165, 421–433.

204. Sopha, P.; Ren, H.Y.; Grove, D.E.; Cyr, D.M. *Endoplasmic Reticulum stress-induced degradation of DNAJB12 stimulates BOK accumulation and primes cancer cells for apoptosis*. J. Biol. Chem. 2017, 292, 11792–11803.

205. Thangameeran, S.I.M.; Tsai, S.T.; Hung, H.Y.; Hu, W.F.; Pang, C.Y.; Chen, S.Y.; Liew, H.K. *A Role for Endoplasmic Reticulum Stress in Intracerebral Hemorrhage*. Cells 2020, 9(3), 750.

206. Ciotti, S.; Iuliano, L.; Cefalù, S.; Comelli, M.; Mavelli, I.; Di Giorgio, E.; Brancolini, C. *GSK3 is a key regulator of the ROS-dependent necrotic death induced by the quinone DMNQ*. Cell Death Dis. 2020, 11, 2.

207. Del Re, D.P.; Amgalan, D.; Linkermann, A.; Liu, Q.; Kitsis, R.N. *Fundamental mechanisms of regulated cell death and implications for heart disease*. Physiol. Rev. 2019, 99, 1765–1817.

208. Fontanini, A.; Foti, C.; Potu, H.; Crivellato, E.; Maestro, R.; Bernardi, P.; Demarchi, F.; Brancolini, C. *The isopeptidase inhibitor G5 triggers a caspase-independent necrotic death in cells resistant to apoptosis: A comparative study with the proteasome inhibitor bortezomib*. J. Biol. Chem. 2009, 284, 8369–8381.

209. Tomasella, A.; Blangy, A.; Brancolini, C. *A receptor-interacting protein 1 (RIP1)-independent necrotic death under the control of protein phosphatase PP2A that involves the reorganization of Actin cytoskeleton and the action of Cofilin-1*. J. Biol. Chem. 2014, 289, 25699–25710.

210. Ramdzan, Y.M.; Trubetskov, M.M.; Ormsby, A.R.; Newcombe, E.A.; Sui, X.; Tobin, M.J.; Bongiovanni, M.N.; Gras, S.L.; Dewson, G.; Miller, J.M.L.; et al. *Huntingtin inclusions trigger cellular quiescence, deactivate apoptosis, and lead to delayed necrosis*. Cell Rep. 2017, 19, 919–927.

211. Wang,W.; Li, S.;Wang, H.; Li, B.; Shao, L.; Lai, Y.; Horvath, G.;Wang, Q.; Yamamoto, M.; Janicki, J.S.; et al. *Nrf2 enhances myocardial clearance of toxic ubiquitinated proteins*. J. Mol. Cell. Cardiol. 2014, 72, 305–315.

212. Han, J.H.; Park, J.; Myung, S.H.; Lee, S.H.; Kim, H.Y.; Kim, K.S.; Seo, Y.W.; Kim, T.H. *Noxa mitochondrial targeting domain induces necrosis via VDAC2 and mitochondrial catastrophe*. Cell Death Dis. 2019, 10, 519.

213. Schwarzer, R.; Laurien, L.; Pasparakis, M. *New insights into the regulation of apoptosis, necroptosis, and pyroptosis by Receptor Interacting Protein Kinase 1 and caspase-8*. Curr. Opin. Cell Biol. 2020, 63, 186–193.

214. Rizzi, F.; Naponelli, V.; Silva, A.; Modernelli, A.; Ramazzina, I.; Bonacini, M.; Tardito, S.; Gatti, R.; Uggeri, J.; Bettuzzi, S. *Polyphenon E(R), a standardized green tea extract, induces endoplasmic reticulum stress, leading to death of immortalized PNT1a cells by anoikis and tumorigenic PC3 by necroptosis*. Carcinogenesis 2014, 35, 828–839.

215. Rojas-Rivera, D.; Delvaeye, T.; Roelandt, R.; Nerinckx, W.; Augustyns, K.; Vandenabeele, P.; Bertrand, M.J.M. *When PERK inhibitors turn out to be new potent RIPK1 inhibitors: Critical issues on the specificity and use of GSK2606414 and GSK2656157*. Cell Death Dier. 2017, 24, 1100–1110.

216. Luan, Q.; Jin, L.; Jiang, C.C.; Tay, K.H.; Lai, F.; Liu, X.Y.; Liu, Y.L.; Guo, S.T.; Li, C.Y.; Yan, X.G.; et al. *RIPK1 regulates survival of human melanoma cells upon endoplasmic reticulum stress through autophagy*. Autophagy 2015, 11, 975–994.

217. Cheng, S.B.; Nakashima, A.; Huber, W.J.; Davis, S.; Banerjee, S.; Huang, Z.; Saito, S.; Sadovsky, Y.; Sharma, S. *Pyroptosis is a critical inflammatory pathway in the placenta from early onset preeclampsia and in human trophoblasts exposed to hypoxia and endoplasmic reticulum stressors*. Cell Death Dis. 2019, 10, 927.

218. Li, J.; Cao, F.; Yin, H.L.; Huang, Z.J.; Lin, Z.T.; Mao, N.; Sun, B.; Wang, G. *Ferroptosis: Past, present and future*. Cell Death Dis. 2020, 11, 88.

219. Bebber, C.M.; Müller, F.; Clemente, L.P.; Weber, J.; von Karstedt, S. *Ferroptosis in cancer cell biology*. Cancers 2020, 12, 164.

220. Lee, Y.S.; Lee, D.H.; Choudry, H.A.; Bartlett, D.L.; Lee, Y.J. *Ferroptosis-induced endoplasmic reticulum stress: Cross-talk between ferroptosis and apoptosis*. Mol. Cancer Res. 2018, 16, 1073–1076.

221. Chen, Y.; Mi, Y.; Zhang, X.; Ma, Q.; Song, Y.; Zhang, L.; Wang, D.; Xing, J.; Hou, B.; Li, H.; et al. *Dihydroartemisinin-induced unfolded protein response feedback attenuates ferroptosis via PERK/ATF4/HSPA5 pathway in glioma cells*. J. Exp. Clin. Cancer Res. 2019, 38, 402.

222. Brigelius-Flohé, R.; Flohé, L. *Regulatory phenomena in the glutathione peroxidase superfamily*. Antioxid. Redox Signal. 2019.

223. Vitale, M.; Bakunts, A.; Orsi, A.; Lari, F.; Tadè, L.; Danieli, A.; Rato, C.; Valetti, C.; Sitia, R.; Raimondi, A.; et al. *Inadequate BiP availability defines endoplasmic reticulum stress*. Elife 2019, 8, e41168.

224. Li, J.; Labbadia, J.; Morimoto, R.I. Rethinking *HSF1 in stress, development, and organismal health*. Trends Cell Biol. 2017, 27, 895–905.

225. Gaglia, G.; Rashid, R.; Yapp, C.; Joshi, G.N.; Li, C.G.; Lindquist, S.L.; Sarosiek, K.A.; Whitesell, L.; Sorger, P.K.; Santagata, S. *HSF1 phase transition mediates stress adaptation and cell fate decisions*. Nat. Cell Biol. 2020, 22, 151–158.

226. Schubert, U.; Anton, L.C.; Gibbs, J.; Norbury, C.C.; Yewdell, J.W.; Bennink, J.R. *Rapid degradation of a large fraction of newly synthesized proteins by proteasomes*. Nature 2000, 404, 770–774.

227. Cenci, S.; Sitia, R. *Managing and exploiting stress in the antibody factory*. FEBS Lett. 2007, 581, 3652–3657.

228. Ruggero, D. *Translational control in cancer etiology*. Cold Spring Harb. Perspect. Biol. 2013, 5, a012336.

229. Saxton, R.A.; Sabatini, D.M. *mTOR signaling in growth, metabolism, and disease*. Cell 2017, 168, 960–976.

230. Chui, M.H.; Doodnauth, S.A.; Erdmann, N.; Tiedemann, R.E.; Sircoulomb, F.; Drapkin, R.; Shaw, P.; Rottapel, R. *Chromosomal instability and mTORC1 activation through PTEN loss contribute to proteotoxic stress in ovarian carcinoma*. Cancer Res. 2019, 79, 5536–5549.

231. Llinàs-Arias, P.; Rosselló-Tortella, M.; López-Serra, P.; Pérez-Salvia, M.; Setién, F.; Marin, S.; Muñoz, J.P.; Junza, A.; Capellades, J.; Calleja-Cervantes, M.E.; et al. *Epigenetic loss of the endoplasmic reticulumassociated degradation inhibitor SVIP induces cancer cell metabolic reprogramming*. JCI Insight 2019, 5, e125888.

232. Tsvetkov, P.; Detappe, A.; Cai, K.; Keys, H.R.; Brune, Z.; Ying, W.; Thiru, P.; Reidy, M.; Kugener, G.; Rossen, J.; et al. *Mitochondrial metabolism promotes adaptation to proteotoxic stress*. Nat. Chem. Biol. 2019, 15, 681–689.

233. Bastola, P.; Oien, D.B.; Cooley, M.; Chien, J. *Emerging cancer therapeutic targets in protein homeostasis*. AAPS J. 2018, 20, 94.

234. Xie, J.L.; Jarosz, D.F. *Mutations, protein homeostasis, and epigenetic control of genome integrity*. DNA Repair 2018, 71, 23–32.

235. Pfau, S.J.; Amon, A. *Chromosomal instability and aneuploidy in cancer: From yeast to man*. EMBO Rep. 2012, 13, 515–527.

236. Brennan, C.M.; Vaites, L.P.;Wells, J.N.; Santaguida, S.; Paulo, J.A.; Storchova, Z.; Harper, J.W.; Marsh, J.A.; Amon, A. *Protein aggregation mediates stoichiometry of protein complexes in aneuploid cells*. Genes Dev. 2019, 33, 1031–1047.

237. Donnelly, N.; Passerini, V.; Durrbaum, M.; Stingele, S.; Storchova, Z. *HSF1 deficiency and impaired HSP90-dependent protein folding are hallmarks of aneuploid human cells*. EMBO J. 2014, 33, 2374–2387.

238. Zhu, J.; Tsai, H.J.; Gordon, M.R.; Li, R. *Cellular stress associated with aneuploidy*. Dev. Cell 2018, 44, 420–431.

239. Mantovani, F.; Collavin, L.; Del Sal, G. *Mutant p53 as a guardian of the cancer cell*. Cell Death Dier. 2019, 26,199–212.

240. Harris, I.S.; Endress, J.E.; Colo , J.L.; Selfors, L.M.; McBrayer, S.K.; Rosenbluth, J.M.; Takahashi, N.; Dhakal, S.; Koduri, V.; Oser, M.G.; et al. *Deubiquitinases maintain protein homeostasis and survival of cancer cells upon glutathione depletion*. Cell Metab. 2019, 29, 1166–1181.e6.

241. Chen, L.; Yang, X. *TRIM11 cooperates with HSF1 to suppress the anti-tumor e ect of proteotoxic stress drugs*. Cell Cycle 2019, 18, 60–68.

242. Chatterjee, S.; Burns, T.F. *Targeting Heat Shock Proteins in cancer: A promising therapeutic approach*. Int. J. Mol. Sci. 2017, 18, 1978.

243. Gomez-Pastor, R.; Burchfiel, E.T.; Thiele, D.J. *Regulation of heat shock transcription factors and their roles in physiology and disease*. Nat. Rev. Mol. Cell Biol. 2018, 19, 4–19.

244. Dias, M.H.; Fonseca, C.S.; Zeidler, J.D.; Albuquerque, L.L.; da Silva, M.S.; Cararo-Lopes, E.; Reis, M.S.; Noël, V.; Dos Santos, E.O.; Prior, I.A.; et al. *Fibroblast growth factor 2 lethally sensitizes cancer cells tostress-targeted therapeutic inhibitors*. Mol. Oncol. 2019, 13, 290–306.

245. Tomasella, A.; Picco, R.; Ciotti, S.; Sgorbissa, A.; Bianchi, E.; Manfredini, R.; Benedetti, F.; Trimarco, V.; Frezzato, F.; Trentin, L.; et al. *The isopeptidase inhibitor 2cPE triggers proteotoxic stress and ATM activation in chronic lymphocytic leukemia cells*. Oncotarget 2016, 19, 45429–45443.

246. Majera, D.; Skrott, Z.; Bouchal, J.; Bartkova, J.; Simkova, D.; Gachechiladze, M.; Steigerova, J.; Kurfurstova, D.; Gursky, J.; Korinkova, G.; et al. *Targeting genotoxic and proteotoxic stress-response pathways in human prostate cancer by clinically available PARP inhibitors, vorinostat and disulfiram*. Prostate 2019, 79, 352–362.

247. Yallowitz, A.; Ghaleb, A.; Garcia, L.; Alexandrova, E.M.; Marchenko, N. *Heat Shock Factor 1 confers resistance to lapatinib in ERBB2-positive breast cancer cells*. Cell Death Dis. 2018, 9, 621.

248. Urra, H.; Dufey, E.; Avril, T.; Chevet, E.; Het, C. *Endoplasmic Reticulum Stress and the Hallmarks of Cancer*. Trends Cancer. 2016, 2(5), 252-262.

249. Nanduri; B.; Suvarnapunya, A.E.; Venkatesan, M.; Edelmann, M.J. *Deubiquitinating enzymes as promising drug targets for infectious diseases*. Curr Pharm Des. 2013, 19(18), 3234-47.

250. Weathington, N.M.; Mallampalli, R.K. *Emerging therapies targeting the ubiquitin proteasome system in cancer*. J Clin Invest. 2014, 124(1), 6-12.

251. Johnson, D.E. *The ubiquitin-proteasome system: opportunities for therapeutic intervention in solid tumors*. Endocr Relat Cancer. 2015, 22(1), T1-17.

252. Kyle, R.A.; Rajkumar, S.V. *Multiple myeloma*. N Engl J Med. 2004, 351(18), 1860-73.

253. Milano, A.; Iaffaioli, R.V.; Caponigro, F. *The proteasome: a worthwhile target for the treatment of solid tumours?* Eur J Cancer. 2007, 43(7), 1125-33.

254. Zhang, X.; Linder, S.; Bazzaro, M. *Drug Development Targeting the Ubiquitin–Proteasome System (UPS) for the Treatment of Human Cancers*. Cancers (Basel). 2020, 12(4), 902.

255. Papadopoulos, K.P.; Siegel, D.S.; Vesole, D.H.; Lee, P.; Rosen, S.T.; Zojwalla, N.; Holahan, J.R.; Lee, S.; Wang, Z.; Badros, A. *Phase I study of 30-minute infusion of carfilzomib as single agent or in combination with low-dose dexamethasone in patients with relapsed and/or refractory multiple myeloma*. J Clin Oncol. 2015, 33(7), 732-9.

256. Zang, Y.; Thomas, S.M.; Chan, E.T.; Kirk, C.J.; Freilino, M.L.; DeLancey, H.M.; Grandis, J.R.; Li, C.; Johnson, D.E. *Carfilzomib and ONX 0912 inhibit cell survival and tumor growth of head and neck cancer and their activities are enhanced by suppression of Mcl-1 or autophagy*. Clin Cancer Res. 2012, 18(20), 5639-49.

257. Cersosimo, U.; Sgorbissa, A.; Foti, C.; Drioli, S.; Angelica, R.; Tomasella, A.; Picco, R.; Semrau, M.S.; Storici, P.; Benedetti, F.; Berti, F.; Brancolini, C. *Synthesis, characterization, and optimization for in vivo delivery of a nonselective isopeptidase inhibitor as new antineoplastic agent*. J Med Chem. 2015, 58(4), 1691-704.

258. Foti, C.; Florean, C.; Pezzutto, A.; Roncaglia, P.; Tomasella, A.; Gustincich, S.; Brancolini, C. *Characterization of caspase-dependent and caspase-independent deaths in glioblastoma cells treated with inhibitors of the ubiquitin-proteasome system*. Mol Cancer Ther. 2009, 8(11), 3140-50.

259. Verbitski, S.M.; Mullally, J.E.; Fitzpatrick, F.A.; Ireland, C.M. *Punaglandins, chlorinated prostaglandins, function as potent Michael receptors to inhibit ubiquitin isopeptidase activity*. J Med Chem. 2004, 47(8), 2062-70.

260. Ciotti, S.; Sgarra, R.; Sgorbissa, A.; Penzo, C.; Tomasella, A.; Casarsa, F.; Benedetti, F.; Berti, F.; Manfioletti, G.; Brancolini, C. *The binding landscape of a partially-selective isopeptidase inhibitor with potent pro-death activity, based on the bis(arylidene)cyclohexanone scaffold*. Cell Death Dis. 2018, 9(2), 184.

261. Ravi, R.; Bedi, A. *NF-kappaB in cancer--a friend turned foe*. Drug Resist Updat. 2004, 7(1), 53-67.

262. Ganten, T.M.; Koschny, R.; Haas, T.L.; Sykora, J.; Li-Weber, M.; Herzer, K.; Walczak, H. *Proteasome inhibition sensitizes hepatocellular carcinoma cells, but not human hepatocytes, to TRAIL*. Hepatology. 2005, 42(3), 588-97.

263. Sayers, T.J.; Brooks, A.D.; Koh, C.Y.; Ma, W.; Seki, N.; Raziuddin, A.; Blazar, B.R.; Zhang, X.; Elliott, P.J.; Murphy, W.J. *The proteasome inhibitor PS-341 sensitizes neoplastic cells to TRAIL-mediated apoptosis by reducing levels of c-FLIP*. Blood. 2003, 102(1), 303-10.

264. Furnari, F.B.; Fenton, T.; Bachoo, R.M.; Mukasa, A.; Stommel, J.M.; Stegh, A.; Hahn, W.C.; Ligon, K.L.; Louis, D.N.; Brennan, C.; Chin, L.; DePinho, R.A.; Cavenee, W.K. *Malignant astrocytic glioma: genetics, biology, and paths to treatment*. Genes Dev. 2007, 21(21), 2683-710.

265. Ambach, A.; Saunus, J.; Konstandin, M.; Wesselborg, S.; Meuer, S.C.; Samstag, Y. *The serine phosphatases PP1 and PP2A associate with and activate the actin-binding protein cofilin in human T lymphocytes*. Eur J Immunol. 2000, 30(12), 3422-31.

266. Iuliano, L.; Drioli, S.; Pignochino, Y.; Cafiero, C.M.; Minisini, M.; D'Este, F.; Picco, R.; Dalla, E.; Giordano, G.; Grignani, G.; Di Giorgio, E.; Benedetti, F.; Felluga, F.; Brancolini, C. *Enhancing Proteotoxic Stress in Leiomyosarcoma Cells Triggers Mitochondrial Dysfunctions, Cell Death, and Antitumor Activity in vivo*. Mol Cancer Ther. 2021, 20(6), 1039-1051.

267. Xue, M.; Feng, L. *The Role of Unfolded Protein Response in Coronavirus Infection and Its Implications for Drug Design*. Front Microbiol. 2021, 12, 808593.

268. Toma-Jonik, A.; Vydra, N.; Janus, P.; Widłak, W. *Interplay between HSF1 and p53 signaling pathways in cancer initiation and progression: non-oncogene and oncogene addiction*. Cellular Oncology. 2019, volume 42, pages 579–589.

269. Pautier, P; Floquet, A.; Chevreau, C.; Penel, N.; Guillemet, C; et al. *A single-arm multicentre phase II trial of doxorubicin in combination with trabectedin in the first-line treatment for leiomyosarcoma with long-term follow-up and impact of cytoreductive surgery*. ESMO Open. 2021, 6(4), 100209.

270. Pautier, P.; Penel, N.; Ray-Coquard, I; Italiano, A.; Bompas, E.; et al. *A phase II of gemcitabine combined with pazopanib followed by pazopanib maintenance, as second-line treatment in patients with advanced leiomyosarcomas: A unicancer French Sarcoma Group study (LMS03 study)*. Eur J Cancer . 2020, 125, 31-37.

271. Xing, Y.; Lin, N.U.; Maurer, M.A.; Chen, H.; Mahvash, A.; et al. *Phase II trial of AKT inhibitor MK-2206 in patients with advanced breast cancer who have tumors with PIK3CA or AKT mutations, and/or PTEN loss/PTEN mutation*. Breast Cancer Res. 2019, 21(1), 78.

272. Wright, T.D.; Raybuck, C.; Bhatt, A.; Monlish, D.; Chakrabarty, S.; et al. *Pharmacological inhibition of the MEK5/ERK5 and PI3K/Akt signaling pathways synergistically reduces viability in triple-negative breast cancer*. J Cell Biochem. 2020, 121(2), 1156-1168.

273. Liu, Q.; Kang, S.A.; Thoreen, C.C.; Hur, W.; Wang, J.; et al. *Development of ATP-competitive mTOR Inhibitors*. Methods Mol Biol. 2012, 821, 447–460.

274. Sun, Z.; Jiang, Q.; Li, J.; Guo, J. *The potent roles of salt-inducible kinases (SIKs) in metabolic homeostasis and tumorigenesis*. Signal Transduction and Targeted Therapy. 2020, volume 5, Article number: 150.

275. Jackson, S.; Baker, E.H.; Gross, A.M.; Whitcomb, P.; Baldwin, A.; et al. *The MEK inhibitor selumetinib reduces spinal neurofibroma burden in patients with NF1 and plexiform neurofibromas*. Neurooncol Adv. 2020, 2(1), vdaa095.

276. Marks, P.A. *Discovery and development of SAHA as an anticancer agent*. Oncogene. 2007, 26(9), 1351-6.

277. Wu, C.P.; Lusvarghi, S.; Wang, J.C.; Hsiao, S.H.; Huang, Y.H.; Hung, T.H.; Ambudkar, S.V. *The Selective Class IIa Histone Deacetylase Inhibitor TMP195 Resensitizes ABCB1- and ABCG2-Overexpressing Multidrug-Resistant Cancer Cells to Cytotoxic Anticancer Drugs*. Int J Mol Sci. 2020, 21(1), 238.

278. Redmann, M; Benavides, G.A.; Berryhill, T.F.; Wani, WY.; Ouyang, X.; et al. *Inhibition of autophagy with bafilomycin and chloroquine decreases mitochondrial quality and bioenergetic function in primary neurons*. Redox Biol. 2017, 11, 73-81.

279. Muenchow, A.; Weller, S.; Hinterleitner, C.; Malenke, E.; Bugl, S.; et al. *The BCL-2 selective inhibitor ABT-199 sensitizes soft tissue sarcomas to proteasome inhibition by a concerted mechanism requiring BAX and NOXA*. Cell Death & Disease. 2020, volume 11, Article number: 701.

280. Ritter, V.; Krautter, F.; Klein, D.; Jendrossek, V.; Rudner, J. *Bcl-2/Bcl-xL inhibitor ABT-263 overcomes hypoxia-driven radioresistence and improves radiotherapy*. Cell Death Dis. 2021, 12(7), 694.

281. Sun, H.; Lin, D.C.; Guo, X.; Masouleh, B.K.; Gery, S.; et al. *Inhibition of IRE1α-driven pro-survival pathways is a promising therapeutic application in acute myeloid leukemia*. Oncotarget. 2016, 7(14), 18736-49.

282. Mimura, N; Fulciniti, M.; Gorgun, G.; Tai, Y.T.; Cirstea, D.; et al. *Blockade of XBP1 splicing by inhibition of IRE1α is a promising therapeutic option in multiple myeloma*. Blood. 2012, 119(24), 5772–5781.

283. Longley, D.B.; Johnston, P.G. *Molecular mechanisms of drug resistance*. J Pathol. 2005, 205, 275–292.

284. Jeyasuria, P.; Subedi, K.; Suresh, A.; Condon, J.C. *Elevated levels of uterine anti-apoptotic signaling may activate NFKB and potentially confer resistance to caspase 3-mediated apoptotic cell death during pregnancy in mice*. Biol Reprod. 2011, 85(2), 417-24.

285. Reader, J.; Harper, A.K.; Legesse, T.; Staats, P.N.; Goloubeva, O.; et al. *EP4 and Class III β-Tubulin Expression in Uterine Smooth Muscle Tumors: Implications for Prognosis and Treatment*. Cancers (Basel). 2019, 11(10), 1590.

286. Rello-Varona, S.; Herrero-Martín, D.; Lagares-Tena, L.; López-Alemany, R.; Mulet-Margalef, N.; et al. *The importance of being dead: cell death mechanisms assessment in anti-sarcoma therapy*. Front. Oncol. 2015.

287. Bodner, K.; Bodner-Adler, B.; Kimberger, O.; Czerwenka, K.; Mayerhofer, K. *Bcl-2 receptor expression in patients with uterine smooth muscle tumors: an immunohistochemical analysis comparing leiomyoma, uterine smooth muscle tumor of uncertain malignant potential, and leiomyosarcoma*. J Soc Gynecol Investig. 2004, 11(3), 187-91.

288. Hemming, M.L.; Fan, C.; Raut, C.P.; Demetri, G.D.; Armstrong, S.A.; Sicinska, E.; George, S. *Oncogenic Gene-Expression Programs in Leiomyosarcoma and Characterization of Conventional, Inflammatory, and Uterogenic Subtypes*. Mol Cancer Res. 2020, 18(9), 1302-1314.

289. Barlin, J.N.; Zhou, Q.C.; Leitao, M.M.; Bisogna, M.; Olvera, N.; et al. *Molecular Subtypes of Uterine Leiomyosarcoma and Correlation with Clinical Outcome*. Neoplasia. 2015, 17(2), 183–189.

290. Yang, J.; Li, C.; Zhou, J.; Liu, X.; Wang, S. *Identification of Prognostic Genes in Leiomyosarcoma by Gene Co-Expression Network Analysis*. Front Genet. 2020, 10, 1408.

291. Heffeter, P.; Atil, B.; Kryeziu, K.; Groza, D.; Koellensperge, G.; et al. *The ruthenium compound KP1339 potentiates the anticancer activity of sorafenib in vitro and in vivo*. Eur J Cancer. 2013, 49(15), 3366–3375.

292. Liese, J.; Hinrichs, T.M.; Lange, M.; Fulda, S. *Cotreatment with sorafenib and oleanolic acid induces reactive oxygen species-dependent and mitochondrial-mediated apoptotic cell death in hepatocellular carcinoma cells* Anticancer Drugs. 2019, 30(3), 209-217.

293. Zhang, D.; De Veirman, K.; Fan, R.; Jian, Q.; Zhang, Y.; et al. *ER stress arm XBP1s plays a pivotal role in proteasome inhibition-induced bone formation*. Stem Cell Research & Therapy. 2020, volume 11, Article number: 516.

294. Zhang, C.; van Leeuwen, W.; Blotenburg, M.; Aguilera-Gomez, A.; Brussee, S.; et al. *Activation of IRE1, PERK and salt-inducible kinases leads to Sec body formation in Drosophila S2 cells*. J Cell Sci. 2021, 134(17), jcs258685.

295. Bon, H; Wadhwa, K.; Schreiner, A.; Osborne, M.; Carroll, T.; et al. *Salt-inducible kinase 2 regulates mitotic progression and transcription in prostate cancer*. Mol Cancer Res. 2015, 13(4), 620-635.

296. Yang, F.C.; Lin, Y.H.; Chen, W.H.; Huang, J.Y.; Chang, H.Y.; et al. *Interaction between salt-inducible kinase 2 (SIK2) and p97/valosin-containing protein (VCP) regulates endoplasmic reticulum (ER)-associated protein degradation in mammalian cells*. J Biol Chem. 2013, 288(47), 33861-33872.

8 ACKNOWLEDGMENTS

First of all I want to thank my Supervisor Prof. Claudio Brancolini for guiding me during all my time as a PhD student, indeed all his knowledge and all his passion for the scientific work are for me an example of how people have to face all the problems not only in the research field.

I want to thank my external reviewer Prof. Marco Corazzari for his important and critical advises regarding my PhD project.

A special thanks to the Bioinformatic Unit of the Department of Medical Area of the University of Udine, Dott. Emiliano Dalla and Dott. Raffaella Picco, for their fundamental role in the analysis of the bioinformatics data, and to Dott. Francesca D'Este for helping us in images with the microscope.

A very big thank to all the PhD students of the Kolbe family whom give me everytime fantastic and joyful moments. I sincerely want to thank all my lab mates of the CB lab from the bachelor students, to the master students to all past and present PhD students and Post-Docs. In particular, I want to thank Teresa, Eros, Martina, Liliana, Vanessa, Eleonora, Sowmya, Hari, Valentina: you all are my second family. A special thanks also to Sonia for introducing me in this fantastic world of G5 and derivatives and for giving me the opportunity to continue her work.

I deeply want to thank my family and my closest friends for supporting me throughout my PhD, I hope that I will make you proud of me.

9 PUBLICATIONS

1. **Cell Death Dis. 2020, 11, 2**.

GSK3 is a key regulator of the ROS-dependent necrotic death induced by the quinone DMNQ.

Ciotti, S.; ***IULIANO, L***.; Cefalù, S.; Comelli, M.; Mavelli, I.; Di Giorgio, E.; Brancolini, C.

2. **Cancers (Basel) 2020, Aug 23;12(9):2385.**

Proteotoxic Stress and Cell Death in Cancer Cells.

Brancolini, C.; ***IULIANO, L***.

3. **Mol Cancer Ther. 2021, Jun;20(6):1039-1051.**

Enhancing Proteotoxic Stress in Leiomyosarcoma Cells Triggers Mitochondrial Dysfunctions, Cell Death, and Antitumor Activity in vivo.

IULIANO, L.; Drioli, S.; Pignochino, Y.; Cafiero, C.M.; Minisini, M.; D'Este, F.; Picco, R.; Dalla, E.; Giordano, G.; Grignani, G.; Di Giorgio, E.; Benedetti, F.; Felluga, F.; Brancolini, C.

Ciotti et al. *Cell Death and Disease* (2020)11:2
https://doi.org/10.1038/s41419-019-2202-0

Cell Death & Disease

ARTICLE Open Access

GSK3β is a key regulator of the ROS-dependent necrotic death induced by the quinone DMNQ

Sonia Ciotti[1], Luca Iuliano[1], Sebastiano Cefalù[1], Marina Comelli[1], Irene Mavelli[1], Eros Di Giorgio[1] and Claudio Brancolini[1]

Abstract

Signaling pathways controlling necrosis are still mysterious and debated. We applied a shRNA-based viability screen to identify critical elements of the necrotic response. We took advantage from a small molecule (G5) that makes covalent adducts with free thiols by Michael addition and elicits multiple stresses. In cells resistant to apoptosis, G5 triggers necrosis through the induction of protein unfolding, glutathione depletion, ER stress, proteasomal impairments, and cytoskeletal stress. The kinase GSK3β was isolated among the top hits of the screening. Using the quinone DMNQ, a ROS generator, we demonstrate that GSK3β is involved in the regulation of ROS-dependent necrosis. Our results have been validated using siRNA and by knocking-out GSK3β with the CRISPR/Cas9 technology. In response to DMNQ GSK3β is activated by serine 9 dephosphorylation, concomitantly to Akt inactivation. During the quinone-induced pro-necrotic stress, GSK3β gradually accumulates into the nucleus, before the collapse of the mitochondrial membrane potential. Accumulation of ROS in response to DMNQ is impaired by the absence of GSK3β. We provide evidence that the activities of the obligatory two-electrons reducing flavoenzymes, NQO1 (NAD(P)H quinone dehydrogenase 1) and NQO2 are required to suppress DMNQ-induced necrosis. In the absence of GSK3β the expression of NQO1 and NQO2 is dramatically increased, possibly because of an increased transcriptional activity of NRF2. In summary, GSK3β by blunting the anti-oxidant response and particularly *NQO1* and *NQO2* expression, favors the appearance of necrosis in response to ROS, as generated by the quinone DMNQ.

Introduction

In multicellular organisms cell death processes regulate organogenesis and tissue homeostasis. These forms of cellular demise have been generally considered as programmed cell death[1,2]. Noxious insults can also trigger cell death, as the result of an unmanageable damage. These varieties of cell elimination belong to the group of the accidental cell death[3,4]. Programmed and accidental cell deaths can be accomplished by the engagement of distinct signaling pathways, which activate both common and distinct molecular machineries devoted to cells elimination[1,5–7]. Apoptosis is a cell autonomous and evolutionary conserved genetic program, evolved to finalize a harmonious cellular disassembling.

In cells deficient for apoptosis cell death can still occur through alternative mechanisms. Moreover, certain stimuli can directly engage alternative death pathways such as ferroptosis or necroptosis[6–9]. Necrosis can also be triggered by noxious insults and apoptosis and necrosis can, in some conditions, co-exist. Despite the mechanisms controlling cell death by apoptosis are well-known, the existence of specific molecular players regulating necrosis is still debated[8].

G5 is a non-selective isopeptidases inhibitor that can react with cellular thiols, thus eliciting multiple cellular stresses[10–15]. G5 belongs to a family of compounds that have been synthetized and investigated for the ability to commend accidental death in cancer cells, with therapeutic perspectives[16–22]. Protein misfolding, ER-stress, deubiquitinases inhibition and accumulation of poly-ubiquitylated proteins, glutathione depletion, alterations of the actin cytoskeleton and of the cell adhesion mark the cellular response to G5. In cells resistant to apoptosis this

Correspondence: Claudio Brancolini (claudio.brancolini@uniud.it)
[1]Department of Medicine, Università degli Studi di Udine. P.le Kolbe 4, 33100 Udine, Italy
Edited by A. Finazzi-Agrò

Official journal of the Cell Death Differentiation Association

SPRINGER NATURE CDDpress

plethora of stresses can result in a necrotic death, which is distinguishable from necroptosis[11,13,14]. However, few additional data are available about the signaling networks transducing this peculiar form of necrosis.

G5, due to its pleiotropic effects, represents an ideal compound to identify genes controlling different stress signaling pathways that ultimately conduct to a necrotic death. For this reason, we conducted a functional shRNA-based screening aimed to identify genes that can influence cell survival in response to this compound. We used as a model the glioblastoma cell line U87MG, which activates necrosis when treated with high doses of G5[12,14].

Results

shRNA screen to identify elements of the necrotic death induced by the proteotoxic stressor G5

To identify genes controlling G5-induced necrosis, we conducted a shRNA-based survival screen, using Cellecta's Lentiviral shRNA Library Module 1. This module targets 5046 signaling pathway associated genes and consists of 27.500 shRNAs. For every target are present from 5 to 6 different shRNAs. U87MG cells were chosen as cellular model, because of their propensity to die by necrosis in response to G5[12]. The screen was based on the hypothesis that U87MG cells expressing a shRNA, targeting a gene necessary for the G5-induced cell death, would show a survival advantage and would be over-represented after sequencing.

The infection and the selection scheme is described in Fig. 1a. Briefly, after 2 days of recovery from infections, cells were treated with puromycin and, after 3 days of selection, G5 was added for 60 h. Genomic DNA was extracted from the surviving cells and the abundance of every integrated shRNA-specific barcode was amplified by PCR with vector-specific primers and identified using high-throughput (HT) sequencing. The deconvolution and normalization of the reads for each barcode, respect to control shRNAs (against the Luciferase), has revealed the identity of the most enriched shRNAs. The relevant "hits" were defined when at least three different shRNAs were enriched in comparison to the median value of the control shRNAs targeting the luciferase (1541 reads) or the median value for all shRNAs (1490 reads). In order to isolate genes that could play key functions in transducing the necrotic signal, we imposed that the second shRNAs was to be enriched >3 fold compared to the median value. In this manner we selected 371 genes (Fig. 1b and Table S1). Among the top target genes we identified: *RNASEL*, *POU5F1*, *GSK3B*, *CAPN1*, and *DUSP10*. We focused the attention on glycogen synthase kinase-3 β (GSK3β) for two main reasons. First GSK3β can be activated under specific stress-conditions and it is involved in the regulation of cell death pathways in different cellular contexts[23–27]. Second, among other represented hits interacting proteins, regulators and substrates of GSK3β were found. These include Calpain-1 (CAPN1)[28], the protein phosphatase-1 (PPP1)[29], and the substrate MAP2 (Fig. 1c)[30].

Validation of CAPN1 and GSK3β as genes transducing G5-induced necrosis

The involvement of CAPN1 in different necrotic responses is well established[31]. To validate CAPN1 as an effector of the G5-induced necrosis, we silenced its expression using a siRNA targeting a different region of the gene. In addition, a siRNA against PP2AC was used as positive control[13].

In comparison with the control transfected cells, U87MG cells silenced for CAPN1 or PP2AC were partially protected from G5-induced cell death (Fig. 1d). The potency of the silencing was confirmed by the reduction of the respective protein levels (Fig. 1e).

Next, we validated GSK3β as an element of the G5-induced cell death pathway. Its expression was silenced in U87MG and U87MG/BCL-XL cells, with a siRNA targeting a different sequence, respect to those recognized by the shRNAs isolated with the screening. U87MG/BCL-XL cells were used to further exclude the induction of apoptosis. In both cell lines the silencing of GSK3β only modestly decreased G5-induced necrosis (Fig. 1f).

The modest impact of GSK3β silencing in the necrotic pathway triggered by G5 could be the consequence of the low silencing efficiency. In fact, ~40% of the mRNA is still expressed after transfection (Fig. 1g). To unambiguously clarify this point, we applied the CRISPR/Cas9 system to knock-out GSK3β in U87MG cells (Fig S1a). After the screening of 253 clones, a $GSK3\beta^{-/-}$ clone (number 19) was identified. The immunoblot analysis demonstrates the complete absence of the GSK3β protein in these cells in comparison with two clones of $GSK3\beta^{+/+}$ cells, which underwent the same selection (Fig. 1h). The $GSK3\beta^{+/+}$ control U87MG cells were infected with Cas9 without the sgRNA (indicated as control cells). Clone 63 was infected with both Cas9 and the sgRNA but resulted as a clone still WT for GSK3β, after the screening (indicated as WT cells). Genomic DNA Sanger sequencing of *GSK3β* loci in the three cell lines demonstrated the insertion of a T in the exon 1, two nucleotides after the PAM, in the KO clone and the presence of a WT GSK3β in the clone 63 and in the WT control (Fig. S1b). The insertion of a T causes the frameshift and the appearance of a STOP codon. Only the first 10 aa of GSK3β can be translated in the $GSK3\beta^{-/-}$ cells. This event explains the absence of the GSK3β protein (Fig. 1h). Having proved that $GSK3\beta^{-/-}$ cells do not show overt deficits in their proliferative capacity (Fig. S1c), U87MG/$GSK3\beta^{+/+}$ and U87MG/$GSK3\beta^{-/-}$ cells were treated with G5 for 24 h. Similarly to the silenced cells, U87MG/$GSK3\beta^{-/-}$ cells acquired some

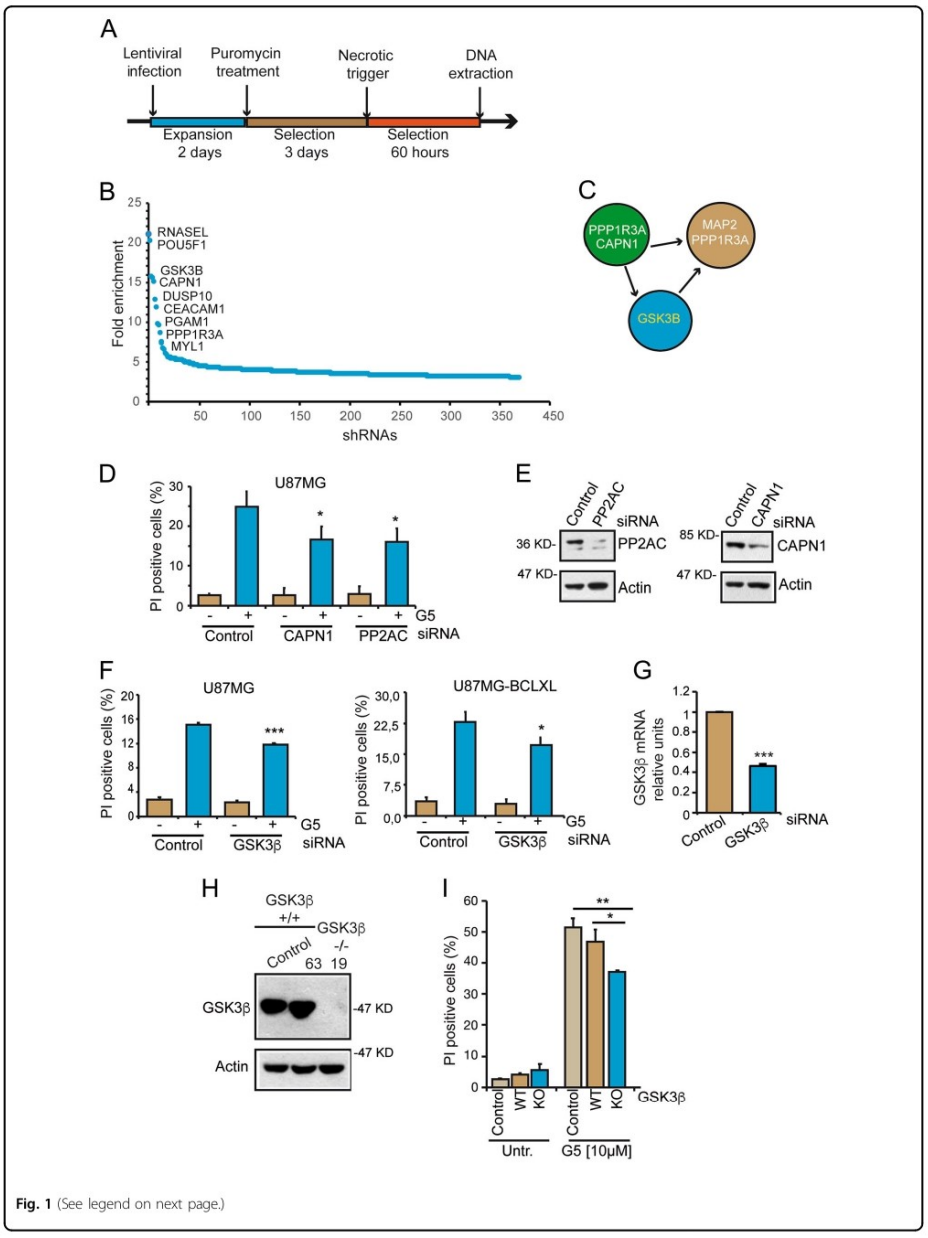

Fig. 1 (See legend on next page.)

(see figure on previous page)

Fig. 1 Screening protocol and targets validation. a Schematic representation of the screening protocol. 66×10^6 millions of cells were infected with the lentiviral particles containing the shRNA plasmids with a MOI of 0,1 for 2 days. For the selection of the expressing-shRNAs, cells were first grown in the presence of puromycin (2 μg/ml) for additional 3 days and subsequently treated with G5 (2.5 μM) for 60 h. Surviving cells were harvested to recover the genomic DNA. **b** Representation of the most enriched hits. Data are represented as fold enrichment respect to the median of all shRNAs. The enrichment is relative to the second most abundant shRNA. Only shRNA with a fold increase >3 are shown. **c** Hits that are in relationship with GSK3β as up-stream regulators or downstream effectors. **d** U87MG cells were silenced for CAPN1 and PP2AC and, after 48 h from transfection, they were treated with G5 (2.5 μM) for 24 h. Cell death was calculated as percentage of cells positive to PI staining using cytofluorimetric analysis. Data are from three experiments; +SD. **e** Cellular lysates from the silenced cells were analyzed by immunoblot. Antibodies anti-CAPN1, anti-PP2AC, and anti-Actin (as loading control) were used as indicated. **f** U87MG and U87MG-BCLXL cells were silenced for GSK3β. After 48 h they were treated with G5 (2.5 μM) for further 24 h. Cell death was calculated as percentage of cells positive to PI staining using cytofluorimetric analysis. Data are from three experiments; +SD. **g** qRT-PCR analysis of GSK3β mRNA levels in silenced cells. Data were from three experiments; +SD. **h** Immunoblot analysis of GSK3β levels in the indicated clones of U87MG cells, selected after CRISPR/Cas9 mediated knock-out. Actin was used as loading control. **i** Cytofluorimetric analysis were performed to measure the % of PI positivity in the different U87MG clones treated with G5 (10 μM) for 24 h. Data are presented as mean ± SD. $n = 3$.

resistance to G5-treatment (Fig. 1h). The moderate resistance to G5-treatment is evident only at high concentrations and after prolonged periods of treatment (24 h) with the drug (Fig. S2a, b). This observation further suggests the induction of a necrotic form of cell death. G5-induced cell death is poorly affected by inhibitors of necroptosis or of ferroptosis (Fig. S2a, b). In summary, GSK3β plays a partial contribution in transducing necrotic signals elicited by G5.

GSK3β is a critical transducer of DMNQ-induced oxidative death

G5 triggers pleiotropic stresses, which can drive cells to death through different pathways. Proteasome impairment, misfolding and proteotoxic stress, oxidative stress and cytoskeletal malfunctions are all hallmarks of the G5-induced cell death[11–14]. The partial impact of GSK3β could stem from the co-existence of these multiple pathways. Since GSK3β can be involved in regulating ROS-induced cell death[32–35], we hypothesized that its involvement in G5-induced death could depend on the ability of the compound of triggering oxidative stress. The impact of G5 on oxidative stress could be direct, through the depletion of glutathione or indirect, through the induction of protein misfolding[14]. To prove this hypothesis, we selected the redox-cycling 2,3-dimethoxy-1,4-naphthoquinone (DMNQ), a well-known inducer of oxidative stress. DMNQ toxicity is mediated by ROS production via one-electron-based redox cycling[36]. When U87MG cells were treated with DMNQ, *GSK3β*$^{-/-}$ cells showed a strong resistance to death (Fig. 2a). To exclude a clone-specific effect, the contribution of GSK3β to DMNQ-induced cell death was validated by RNAi. DMNQ-induced cell death was effectively compromised also after GSK3β silencing (Fig. 2b). The decreased level of GSK3β in the corresponding silenced cells was confirmed by the immunoblot analysis (Fig. 2c). Finally, we proved that also menadione, another quinone, requires GSK3β to efficiently trigger cell death (Fig. S3a). In summary, GSK3β plays a partial role during G5-induced cell death and a fundamental role during DMNQ-induced cell death.

GSK3β kinase activity is required for DMNQ-induced oxidative necrotic death

To further confirm the role of GSK3β in transducing DMNQ-induced oxidative death, we re-expressed GSK3β in U87MG/*GSK3β*$^{-/-}$ cells. The GSK3β wild type (WT) and its kinase dead mutant (KM), carrying the K85A aa substitution were both C-terminal GFP-tagged. As control we also expressed GSK3β and its mutant in U87MG/*GSK3β*$^{+/+}$ cells. Immunoblot analysis confirmed the expression of the different GSK3β fusions in *GSK3β*$^{-/-}$ and *GSK3β*$^{+/+}$ cells (Fig. 2d). The same cells expressing only the neomycin resistance gene were used as control (Neo cells). Cell death in response to DMNQ was recovered only in U87MG/*GSK3β*$^{-/-}$ cells re-expressing the GSK3β-WT. Restoring only GSK3β expression without the catalytic activity (KM mutant) was insufficient to recover the necrotic defect of the KO cells (Fig. 2e). DMNQ-induced cell death is largely caspase-independent and it is marginally affected by the Ferrostatin-1, an inhibitor of ferroptosis (Fig. S2c, d and Fig. S3c). On the opposite it is strongly dependent on the activity of RIP1, as previously reported[13]. Hence, GSK3β kinase activity is necessary to trigger cell death in response to DMNQ.

GSK3β can also influence cell death by apoptosis[37]. Therefore, to confirm that DMNQ specifically elicits necrosis also in cells overexpressing the kinase, we evaluated caspases activation, the key enzymes of the apoptotic pathway. Caspase-3 and Caspase-2 activation and HDAC4 processing (a caspase-3 substrate) were monitored by immunoblot. Cells were also treated with the combination TRAIL/bortezomib a renowned apoptotic stimulus[38]. Figure 2f shows that GSK3β-dependent, DMNQ-induced cell death, does not require caspase activation. On the opposite, U87MG cells, after incubation with TRAIL/bortezomib, strongly activate caspases.

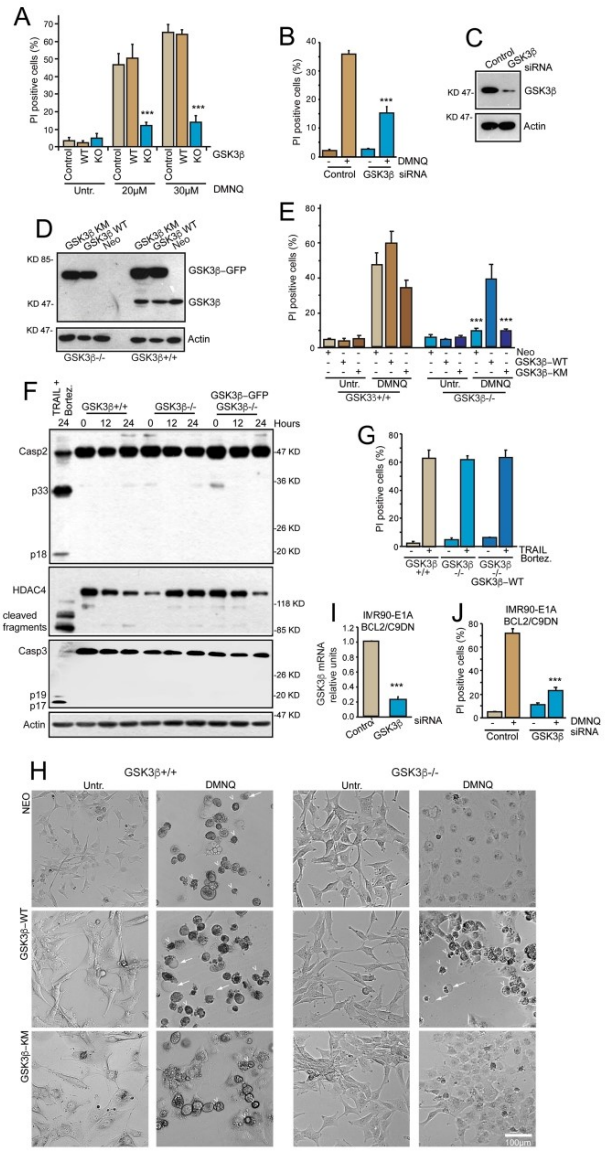

Fig. 2 (See legend on next page.)

(see figure on previous page)

Fig. 2 GSK3β is necessary for the necrotic response elicited by DMNQ. a Cytofluorimetric analysis measuring cell death percentages (PI positivity) in the different U87MG clones treated with the indicated concentrations of DMNQ for 24 h. Data are presented as mean ± SD. n = 3. **b** Cytofluorimetric analysis measuring cell death percentages (PI positivity). U87MG cells were transfected with siRNAs against GSK3β or control. After 48 h they were treated with 30 μM of DMNQ for further 24 h. Data are presented as mean ± SD. *n* = 3. **c** Immunoblot analysis of GSK3β levels in U87MG cells transfected with siRNAs against GSK3β or control. Actin was used as loading control. **d** Immunoblot analysis of GSK3β levels in U87MG *GSK3β*$^{+/+}$ and *GSK3β*$^{-/-}$ cells retrovirally infected with the GSK3β-GFP fusions WT or its catalytically inactive mutant K85A (KM). Actin was used as loading control. **e** Cytofluorimetric analysis measuring cell death percentages (PI positivity) in the indicated U87MG cell lines treated with 30 μM of DMNQ for 24 h. Data are presented as mean ± SD. *n* = 3. **f** Immunoblot analysis of Caspase-3, Caspase-2, and HDAC4 caspase-dependent processing in the indicated U87MG cell lines treated with 30 μM of DMNQ. Incubation with the combination TRAIL (2.5 ng/ml) and bortezomib (0.1 μM) for 20 h was used to trigger apoptosis. Actin was used as loading control. **g** Cytofluorimetric analysis measuring cell death percentages (PI positivity) in the indicated U87MG cell lines treated or not with the combination TRAIL (2.5 ng/ml) and bortezomib (0.1 μM) for 24 h. Data are presented as mean ± SD. *n* = 3. **h** Microscopic images of the indicated U87MG cell lines treated for 24 h with DMNQ (30 μM). Arrows point to membrane blistering and arrowheads to examples of necrotic cells. Phase contrast images were obtained with Leica DMi1 microscope with a 10x objective. **i** qRT-PCR analysis of GSK3β mRNA levels in the silenced IMR90-E1A//BCL2/C9DN cells. Data are from three experiments; +SD. **j** Cytofluorimetric analysis measuring cell death percentages (PI positivity). IMR90-E1A/BCL2/C9DN cells were transfected with siRNAs against GSK3β or control and after 48 h treated with 100 μM of DMNQ for further 24 h. Data are presented as mean ± SD. *n* = 3.

We also demonstrated that GSK3β is not required for TRAIL/bortezomib-induced apoptosis (Fig. 2h). DMNQ-induced cell death showed the features of necrosis, with the appearance of vacuolization and membrane blistering[11]. The appearance of these necrotic features is strictly dependent on the kinase activity of GSK3β (Fig. 2h).

Next, we proved that the role of GSK3β in transducing a necrotic signal is not limited to U87MG cells. We took advantage from IMR90-E1A cells expressing Bcl-2 and a dominant negative mutant of Caspase-9. These engineered cells are resistant to apoptosis and die by necrosis[39]. The role of GSK3β in the DMNQ-dependent necrotic response was confirmed also in human fibroblasts. When GSK3β was silenced in these cells (Fig. 2i), DMNQ was unable of triggering cell death (Fig. 2j).

DMNQ treatment activates GSK3β

To explore whether GSK3β is activated during DMNQ and G5-induced necrosis, the phosphorylation status of Ser-9 was evaluated. Once phosphorylated, Ser-9 inhibits the kinase activity of GSK3β, by acting as a pseudosubstrate[40,41]. Akt is the main up-stream regulator of GSK3β activity, through Ser-9 phosphorylation[40,42]. Hence, we also evaluated Akt activation levels by monitoring Thr-308 and Ser-473 phosphorylation status[13].

In DMNQ-treated cells an early and dramatic dephosphorylation of GSK3β Ser-9 was detected, as soon after 1 h from treatment, which became stronger after 3 h (Fig. 3a). The reappearance of Ser-9 phosphorylation after 6 h could mark the emerging of cells resistant to DMNQ treatment. Akt Thr-308 dephosphorylation parallels the behavior of Ser-9, thus suggesting a direct link between Akt inactivation and GSK3β activation in response to DMNQ. Akt Ser-473 phosphorylation remains unperturbed after DMNQ treatment (Fig. 3a).

Ser-9 dephosphorylation was observed also in response to G5. Here the decrease is modest at early times but appears more consistent at later time-points (12 h). This delayed activation of GSK3β parallels the inactivation of Akt (Fig. 3b). Overall, GSK3β activation, as monitored by Ser-9 phosphorylation, is modest in G5-treated compared to DMNQ-treated cells.

DMNQ-dependent mitochondrial dysfunctions: the role of GSK3β

DMNQ treatment triggers mitochondrial fragmentation, which depends on Drp1 activities[13]. Smac/DIABLO localization was used to monitor the mitochondrial morphology and the integrity of the outer mitochondrial membrane (OMM)[43]. In *GSK3β*$^{-/-}$ and *GSK3β*$^{+/+}$ U87MG cells the mitochondrial networks were similar (Fig. 3b). DMNQ treatment triggers mitochondrial fragmentation in both cell lines, which is therefore independent from GSK3β. By contrast, SMAC levels were clearly reduced in U87MG/*GSK3β*$^{+/+}$ compared to *GSK3β*$^{-/-}$ cells (Fig. 3c). Re-expression of GSK3β promoted the decrease of SMAC protein. The degradation of SMAC in response to DMNQ could be related to its release into the cytoplasm as a consequence of the OMM rupture[39]. The alteration of mitochondrial functionality was confirmed by the measure of the mitochondrial membrane potential ($\Delta\psi_m$). After 24 h of DMNQ treatment, $\Delta\psi_m$ is completely collapsed in *GSK3β*$^{+/+}$ cells but maintained in *GSK3β*$^{-/-}$ cells (Fig. 3d). As control, incubation with the mitochondrial uncoupler FCCP triggered mitochondrial membrane depolarization in a GSK3β independent manner (Fig. 3d).

$\Delta\psi_m$ dissipation and the nuclear translocation of GSK3β

GSK3β is a pleiotropic kinase involved in multiple signaling pathways. Although it is mainly a cytosolic protein, it can also localize in other subcellular compartments, including the nucleus and the mitochondria[44,45]. Particularly, GSK3β shuttles between the nucleus and the

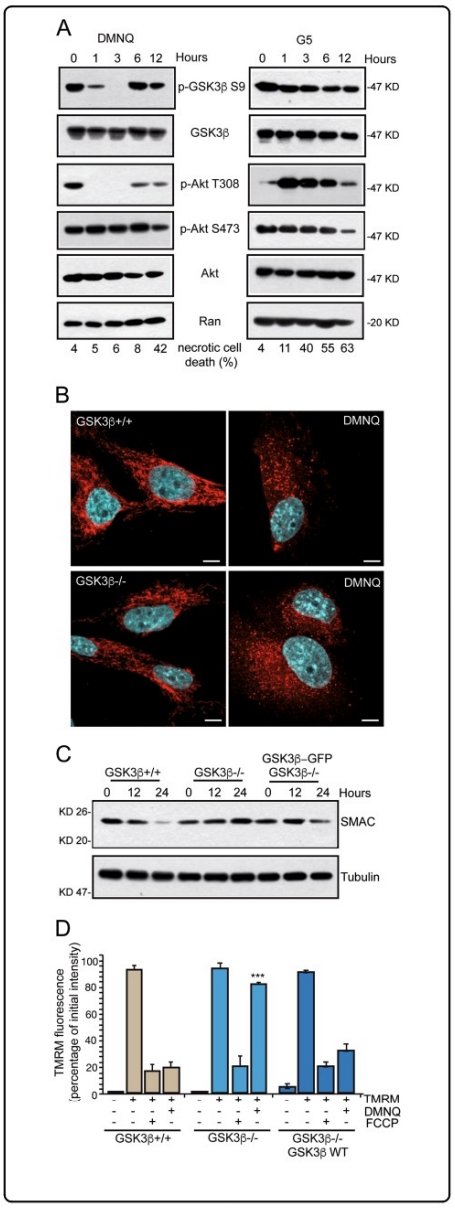

Fig. 3 GSK3β is activated by DMNQ treatment. a U87MG cells were treated with 30 μM DMNQ or 10 μM G5 for the indicated times. Cellular lysates were generated and immunoblots were performed with the indicated antibodies. In parallel cell death was scored by cytofluorimetric analysis and it is showed at the bottom. **b** U87MG *GSK3β*$^{+/+}$ and *GSK3β*$^{-/-}$ cells were treated or not with 30 μM DMNQ for 24 h. Immunofluorescence analysis was performed to visualize mitochondria morphology, using anti-SMAC antibodies (red). Nuclei were stained with Hoechst 33258 (cyan). Bar 10 μm. Confocal images are shown in pseudocolors and were acquired with a Leica SP8 LSM. **c** Immunoblot analysis of SMAC levels in the indicated U87MG cells treated with 30 μM DMNQ for the indicated time points. Actin was used as loading control. **d** Cytofluorimetric analysis of TMRM fluorescence. The indicated U87MG cells were incubated for 30 min with TMRM (1 μM). FCCP (10 μM) was used for 5 min. Data are from three experiments. Columns represent the percentage of initial intensity of TMRM fluorescence + SD.

cytoplasm and a decline of PI3K/Akt activity can favor its nuclear accumulation[44].

To monitor the subcellular localization of GSK3β in vivo during necrosis, U87MG/*GSK3β*$^{-/-}$ cells expressing the GSK3β-GFP were exposed to DMNQ and subjected to time-lapse confocal microscopy. We also measured in parallel the mitochondrial membrane potential, as a reference of the necrotic death. Figure 4a shows selected time-frames of the analysis, proving the progressive nuclear accumulation GSK3β-GFP, which becomes evident 1 h before the collapse of $\Delta\psi_m$. Figure 4b shows the individual traces for TMRM uptake and GSK3β-GFP localization in 10 typical U87MG/*GSK3β*$^{-/-}$ cells expressing GSK3β-GFP, in response to DMNQ. In all examples the progressive nuclear accumulation of GSK3β-GFP anticipates $\Delta\psi_m$ collapse. By contrast, when the same analysis was performed in untreated cells, nuclear accumulation of GSK3β-GFP was not observed and only "physiological fluctuations" of the $\Delta\psi_m$[46] were monitored (Fig. 4c). The integrity of the GSK3β-GFP chimera throughout the time of the analysis was verified by immunoblot (Fig. 4d). These data indicate that DMNQ triggers the nuclear accumulation of GSK3β-GFP before $\Delta\psi_m$ collapse.

DMNQ-triggered ROS generation requires GSK3β activity

The quinone DMNQ triggers ROS generation after one-electron reduction by several intracellular flavoenzymes such as the NADPH-cytochrome P450 reductase or nitric oxide synthetases. The product of the one-electron reduction, DMNQ•-, reacts rapidly with O_2 to form superoxide anion, O_2•-, regenerating DMNQ. This redox-cycle is critical for redox signaling and toxicity[36,47].

Therefore, we explored whether GSK3β activity was required to sustain the redox cycle. First, we demonstrated that potentiation of the antioxidant properties, by

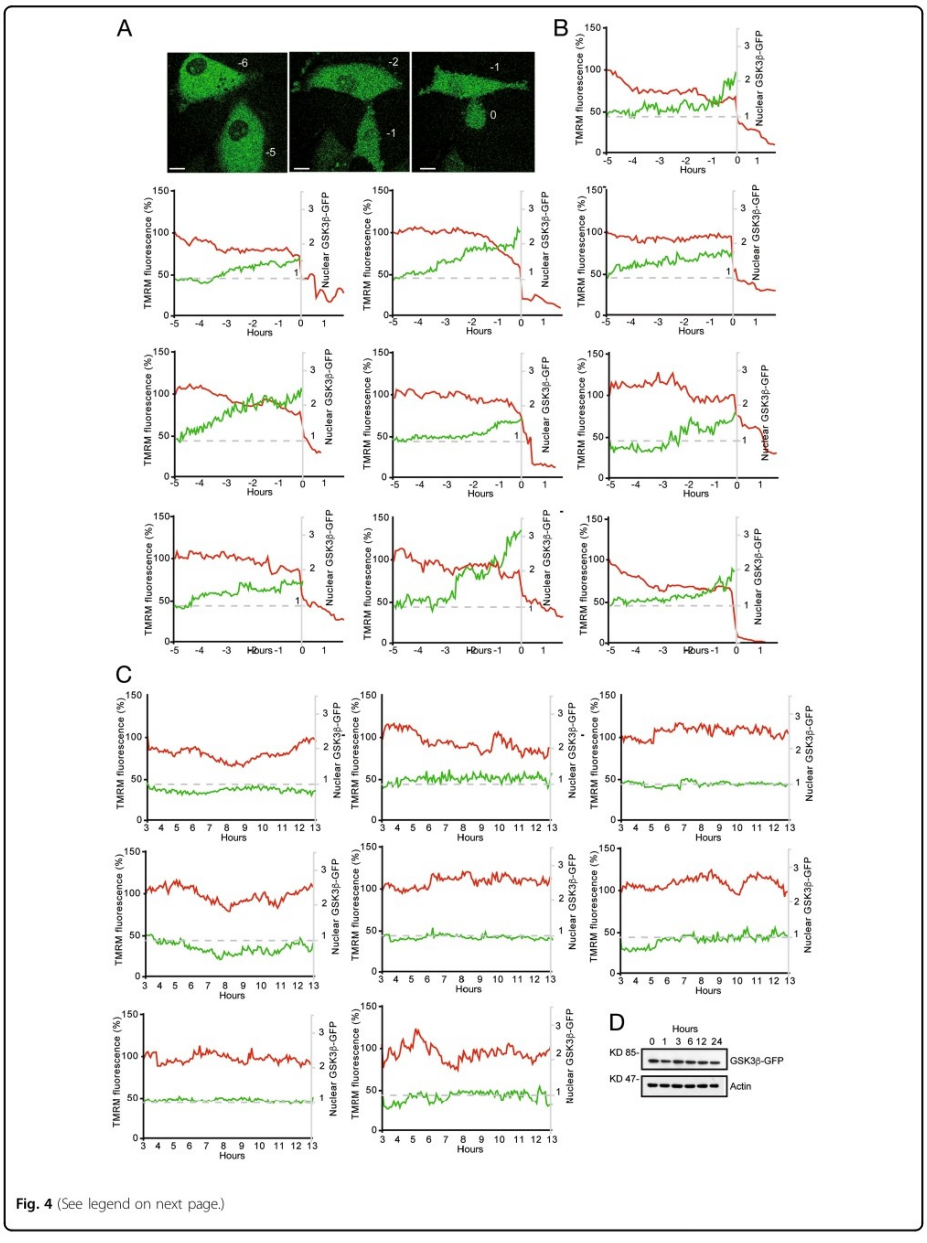

Fig. 4 (See legend on next page.)

(see figure on previous page)
Fig. 4 Nuclear translocation of GSK3β WT-GFP and mitochondrial Δψm dissipation at single cell level in vivo. a Representative frames of two U87MG/*GSK3β*$^{-/-}$ cells re-expressing GSK3βWT-GFP treated with 30 μM DMNQ. Numbers indicate h before $\Delta\psi_m$ dissipation. Bar 16 μm. **b** Individual traces of cellular TMRM fluorescence (red) and of the nuclear/cytosolic fluorescence of GSK3βWT-GFP (green) in U87MG/*GSK3β*$^{-/-}$ cells re-expressing GSK3βWT-GFP. Cells were treated with 30 μM DMNQ for 24 h. **c** Individual traces of cellular TMRM fluorescence (red) and of the nuclear/cytosolic fluorescence of GSK3βWT-GFP (green) in untreated U87MG/*GSK3β*$^{-/-}$ cells, re-expressing GSK3βWT-GFP. **d** Immunoblot analysis of GSK3βWT-GFP levels in U87MG/*GSK3β*$^{-/-}$ cells treated with 30 μM DMNQ for the indicated times. Actin was used as loading control.

treating cells with N-acetylcysteine (NAC), completely abrogates the GSK3β-dependent toxicity of DMNQ (Fig. 5a). Next, we compared DMNQ-induced ROS levels, using two different sensors: Carboxy-H_2DCFDA and Deep Red Dye, in the presence or absence of GSK3β. DMNQ, through its redox-cycling activity triggers a progressive increase of ROS (Fig. 5b). In the absence of GSK3β, after an initial increase, ROS levels dropped-down, reaching a condition similar to the untreated cells. Re-expression of GSK3β restored the ROS accumulation in response to DMNQ (Figs. 5c and S4).

We also monitored the appearance of ROS in response to G5. Differently from DMNQ, G5 triggers a rapid increase of ROS, within 1 h from treatment, that declines at later times. the contribution of GSK3β is significant also in the case of G5-generated ROS. However, it is much less pronounced, when compared to DMNQ (Fig. 5d).

ROS generation requires GSK3β activity to blunt the expression of NRF2-target genes involved in the anti-oxidant response

ROS generation by DMNQ can be prevented by obligatory two-electrons reducing flavoenzymes, such as NQO1 (NAD(P)H quinone dehydrogenase 1) and NQO2. These enzymes, by producing hydroquinones, prevents ROS generation by circumventing one-electron reductase-dependent redox cycling[47–49]. The strong impact of GSK3β on ROS generation could stem from its ability of influencing *NQO1* and *NQO2* activities. To verify this hypothesis, we analyzed the expression levels of the two enzymes in U87MG/*GSK3β*$^{-/-}$ and *GSK3β*$^{+/+}$ cells treated with DMNQ. qRT-PCR showed that only in response to DMNQ the expression levels of *NQO1* and *NQO2* dramatically increase in *GSK3β*$^{-/-}$ cells. By contrast, only *NQO2* expression is modestly up-regulated in *GSK3β*$^{+/+}$ cells (Fig. 5e). We also compared the expression of *HMOX1* and *GCLM*, two genes that belong to the anti-oxidant defense. *GCLM* is similarly and modestly up-regulated in the two cell lines whereas HMOX1 shows a behavior similar to *NQO2*.

The transcription of these genes in response to oxidative stressors is under the supervision of NRF2[50]. The activity of this transcription factor is subjected to multiple levels of controls, including half-life variations. In fact, NRF2 is subjected to proteasomal-mediated degradation, which is suppressed by the oxidative stress[50].

As expected DMNQ triggers the up-regulation of NRF2. However, in the absence of GSK3β, this up-regulation is more pronounced and sustained through the time (Fig. 5f).

To demonstrate the key role of *NQO1* and *NQO2* in the necrotic response triggered by DMNQ, U87MG/*GSK3β*$^{+/+}$, *GSK3β*$^{-/-}$ *or GSK3β*$^{-/-}$ expressing GSK3β-GFP were treated with dicoumarol a potent inhibitor of NQO1 and tacrine, a recently identified NQO2 inhibitor[51,52]. The resistance to DMNQ-induced necrosis observed in the absence of GSK3β was completely abolished by the inhibition of NQO1, as well as, after the inhibition of NQO2, although less efficiently (Fig. 5g).

In summary, GSK3β, through the regulation of NRF2 levels, can blunt the expression of *NQO1* and *NQO2*, two enzymes that prevent ROS generation. In this manner GSK3β can promote cell death by necrosis.

Discussion

Quinone compounds are ubiquitously diffused in the environment as elements of the food chains or as air pollutants, for example in the diesel exhaust particles[53]. Quinones can also be generated in the body as a result of some xenobiotic metabolism through the cytochrome P450 system[36]. DMNQ has been intensively studied as an example of quinones toxicity. DMNQ toxicity is mediated by ROS production via one-electron-based redox cycling. Several flavoenzymes, including NADPH-cytochrome P450 reductase and NADH-cytochrome b reductase, can fulfil the one-electron reduction of DMNQ[36,47,48]. For this reason DMNQ is also commonly used, as a tool, to investigate the cellular responses to the oxidative stress.

In this manuscript we have demonstrated that GSK3β is a key player of the DMNQ/ROS-induced necrotic death. We show that GSK3β is responsible for reducing the anti-oxidant response engaged by NRF2. This response leads the up-regulation of the obligatory two-electron reducing flavoenzymes NQO1 and NQO2[47,48,51,52]. These flavoenzymes are required to blunt the redox cycling activity of DMNQ. In the absence of GSK3β, NRF2 levels and the transcription of its targets *NQO1* and *NQO2* is strongly sustained. In this manner the cytotoxic effect of quinones is nullified (Fig. 6).

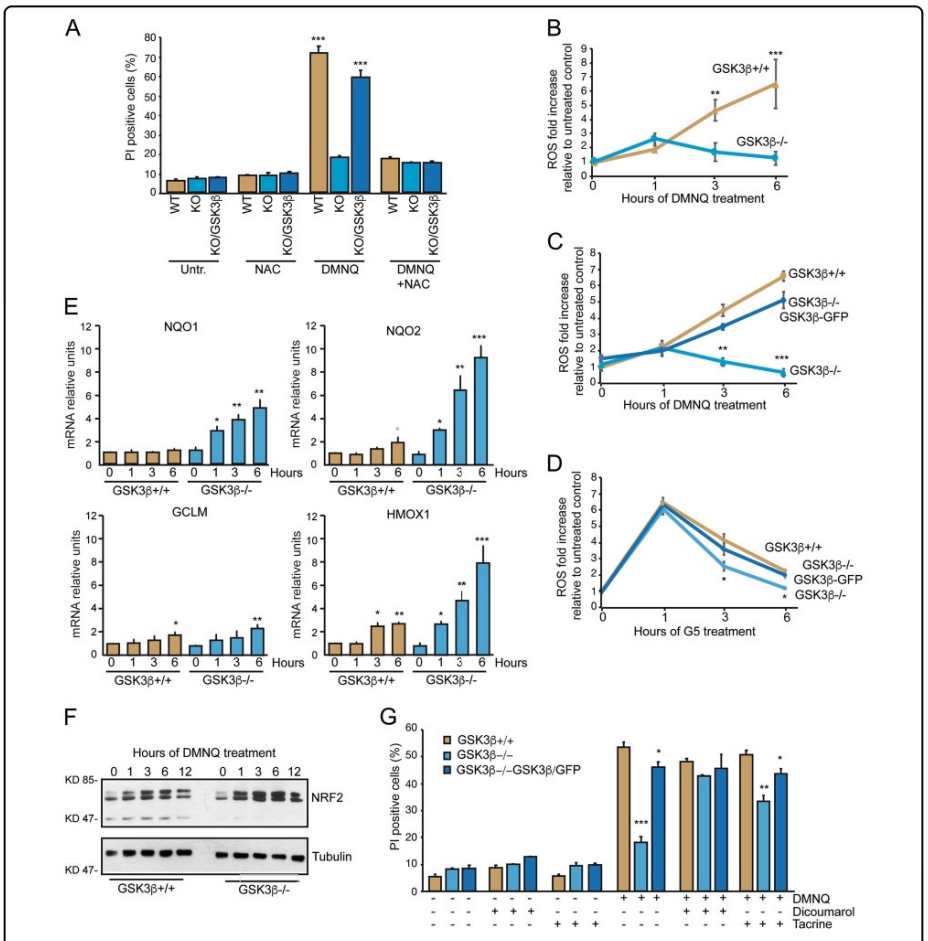

Fig. 5 GSK3β favors ROS generation in response to DMNQ. a Cytofluorimetric analysis measuring cell death percentages (PI positivity) in the indicated U87MG cell lines, treated or not with the indicated combinations of molecules. DMNQ was used 30 μM. N-acetylcysteine (NAC) was 5 mM. Incubation was for 24 h. Data are presented as mean ± SD. $n = 3$. **b** Levels of reactive oxygen species as measured by Carboxy-H_2DCFDA fluorescence in U87MG *GSK3β*$^{+/+}$ and *GSK3β*$^{-/-}$ cells treated with 30 μM DMNQ. **c** Levels of reactive oxygen species as measured by ROS Deep Red Dye fluorescence in the indicated U87MG cell lines treated with 30 μM DMNQ. **d** Levels of reactive oxygen species as measured by ROS Deep Red Dye fluorescence in the indicated U87MG cell lines treated with 10 μM G5. **e** Time-course analysis of *NQO1, NQO2, HMOX1* and *GCLM* mRNA expression levels. U87MG *GSK3β*$^{+/+}$ and *GSK3β*$^{-/-}$ cells were treated with 30 μM of DMNQ for the indicated times and the mRNA levels were monitored by qRT-PCR. Data are from three experiments; +SD. **f** Immunoblot analysis of NRF2 levels in U87MG *GSK3β*$^{+/+}$ and *GSK3β*$^{-/-}$ cells treated with 30 μM DMNQ for the indicated times. Actin was used as loading control. **g** Cytofluorimetric analysis measuring cell death percentages (PI positivity) in the indicated U87MG cell lines, treated or not with the indicated combinations of molecules. DMNQ was used 30 μM, Dicoumarol 100 μM, Tacrine 20 μM. Incubation was for 24 h. Data are presented as mean ± SD. $n = 3$.

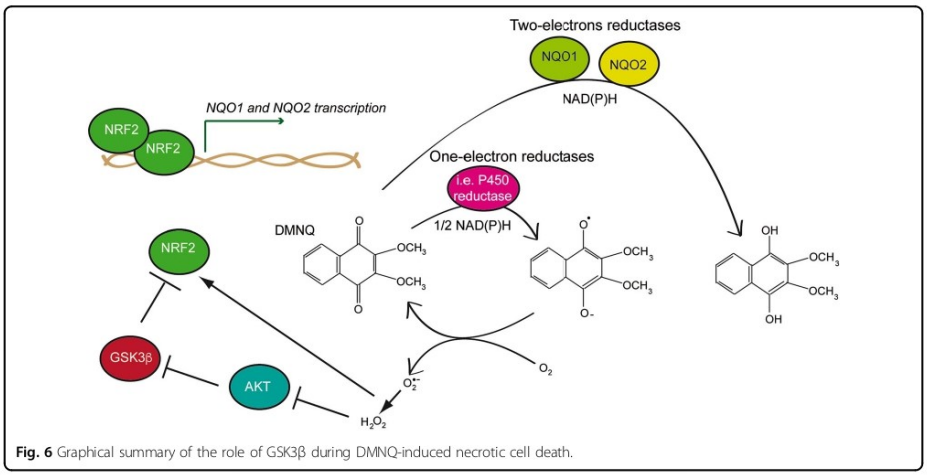

Fig. 6 Graphical summary of the role of GSK3β during DMNQ-induced necrotic cell death.

Our results suggest a model where high ROS levels, as generated by DMNQ, inhibit AKT[13,54] and consequently unleash GSK3β activity, which in turn, switches-off the NRF2 anti-oxidant responses[50,55,56]. Hence, the impact of GSK3β in this necrotic pathway is mainly exerted by suppressing a pro-survival signal (Fig. 6).

The described pathway is pathological relevant and it is implicated in other models of cell death elicited by oxidative stress. Examples are the ischemia and reperfusion injury in the brain[57], in hepatocytes[58,59], during diabetic nephropathies[60], in a model for Alzheimer disease[61] and in other models of neurological diseases[62,63].

The time-lapse analysis suggests that the DMNQ-dependent nuclear accumulation of GSK3β anticipates the $\Delta\psi_m$ collapse. Hence, it is plausible that GSK3β activation is coupled to its nuclear accumulation where it phosphorylates NRF2, a signal necessary for its nuclear exclusion, its poly-ubiquitylation and the subsequent proteasomal degradation[44,64].

GSK3β was identified after a high-throughput shRNA screening, aimed to define new players of the necrotic response induced by G5. Unexpectedly, the kinase plays only a minor role in this form of death. In agreement with our observation GSK3β activation is much less evident in response to G5 compared to DMNQ. Even though we have demonstrated that G5 is able to trigger oxidative stress.

We suggest that Akt could explanation this apparent paradox. Akt in response to G5 is not dephosphorylated at early time points, differently from DMNQ. Instead we confirmed a strong increase of Thr 308 phosphorylation, as previously reported[13]. The two cysteine residues 310 and 296 found in the T-loop region are critical for Akt activity. We have recently shown that G5 can directly target Akt, possibly by reacting with these cysteines residues[15]. Hence G5 could directly interfere with Akt activities. How it could occur and which could be the consequence on Akt activity, deserve further investigations.

Finally, we have not completely unveiled the molecular basis of the necrotic pathway elicited by G5. GSK3β and the oxidative stress probably play only a secondary or additive role in this pathway. During the investigation of the role of GSK3β, we also tested the contribution of other genes, which were included among the top hits of the screening. Transfection of isolated siRNAs only minimally reduced G5-induced cell death. It is plausible that, the simultaneous induction of multiple stresses by G5 causes multiple cellular dysfunctions that ultimately trigger necrosis. Under this condition, ablation of a single gene is not enough to rescue cells from the death commitment.

Materials and methods

Cell culture conditions and reagents

The cell lines used in this article were Uppsala 87 Malignant Glioma (U87MG) glioblastoma cell line, IMR90-E1A lung fibroblast cell line, Human Embryonic Kidney cells 293 T1 (HEK293T1) cell line and Phoenix Amphotropic (AMPHO) embryonic kidney cell line. All cell lines were cultured at 37 °C in 5% CO_2 atmosphere in Dulbecco's Modified Eagle's Medium (DMEM), (Sigma-Aldrich) supplemented with 10% fetal bovine serum

(FBS); glutamine (2 mmol/L), penicillin (100 U/mL) and streptomycin (100 µg/mL) (Euroclone). All cell lines were tested for mycoplasma contamination and resulted as mycoplasma free. U87MG cells were authenticated by gene expression profile. U87MG/BCL-XL and IMR90/E1A/BCL-2/C9DN cells, expressing a dominant negative mutant of caspase-9 were previously described[11,12] and verified for the expression of the transgenes. The following chemicals were used: 4H-thiopyran-4-one, tetrahydro-3,5-bis[(4-nitrophenyl) methylene]-1,1-dioxide (G5)[10]; 2,3-dimethoxy-1,4-naphthoquinone (DMNQ); carbonilcyanide *p*-triflouromethoxyphenylhydrazone (FCCP); NAC; Propidium Iodide (PI), Ferrostatin-1 and DMSO (Sigma Aldrich); Tetramethyl Rhodamine Methyl-ester (TMRM) (Life Technologies); Bortezomib (LC Laboratories); TNF-related apoptosis-inducing ligand (TRAIL)[65]; G418 (Euroclone); Hygromycin (PanReac-AppliChem); Dicoumarol and Tacrine (Santa Cruz Biotechnology); Necrostatin-1 (Enzo Life Sciences); Boc-D-FMK (Abcam).

shRNA library screening

U87MG cells were transduced with DECIPHER Pooled shRNA library-Human Module 1 (Cellecta, Mountain View, CA, USA) composed by 27500 shRNAs targeting 5043 genes (5–6 shRNAs/mRNA). The HTS3 (DECIPHER pRSI9-U6-(sh)-HTS3-UbiC-TagRFP-2A-Puro-dW) cassette of each shRNA contains the U6 RNA polymerase III promoter to drive shRNAs expression, the fluorescence protein (RFP) and the puromycin resistance. All shRNAs have unique 18-nucleotide DNA barcode sequences, which facilitate their identification after HT sequencing. The HEK293T1 packaging cells were transfected with 60 µg of the plasmid shRNAs library and 300 µg of the packaging plasmid mix (Cellecta Inc., psPAX2: pMD2.G), in DMEM without serum or antibiotics and in the presence of Plus Reagent^{TM} and Lipofectamin^{TM} (Life Technologies). The concentrated lentiviral particles were re-suspended in PBS with 10% FBS and stored at −80 °C for the lentiviral titer estimation. After the calculation of the Transduction Units, 66×10^6 cells were transduced with the shRNA library at MOI of 0.1 to ensure that ~90% of the cells are infected with one shRNA-carrying virus. After 48 h, infected cells were selected by adding Puromycin (2 µg/ml) for 72 h. Later, the selected cells were treated with G5 (2.5 µM) for 60 h. Genomic DNA (gDNA) was purified from the surviving cells using the QIAamp DNA Micro Kit (Qiagen, Hilden, Germany). Pooled barcodes were PCR-amplified from 100 µg of gDNA and identified after Illumina sequencing by deconvolution analysis. Positive hits were selected as genes when at least two different shRNAs scored higher frequencies in comparison to the average of the control luciferase ($n \geq 3$).

RNA interference

The RNA interference (RNAi) was performed using the following siRNAs direct against: CAPN1 (Santa Cruz Biotechnology); PP2Ac (Life Technologies); GSK3β (Fw 5′-GCAUUUAUCGUUAACCUAA-3′, Rv 5′-UUAGGUUAACGA UAAAUGC - 3′, Sigma Aldrich); or the relative control siRNAs. U87MG, U87MG/BCL-XL and IMR90/E1A/BCL-2/C9DN cells were transfected 24 h after seeding. Six hours later the medium was changed, and after 48 h of silencing, cells were treated with G5 or DMNQ for further 24 h. RNA was extracted and the protein lysates were collected for the subsequent analysis.

Drug treatments, PI- and TMRM-assay

For cytofluorimetric analysis, drug treated cells were collected in PBS and incubated with propidium iodide (PI) for 5 min at room temperature. PI fluorescence was determined by the FACSCalibur flow cytometer (BD, San Jose, CA,) at the excitation wavelength of 585 nm. For TMRM assay, cells were incubated with TMRM (1 µM) for 30 min. TMRM fluorescence was determined by flow cytometer at the excitation wavelength of 488 nm.

Cell lysis and Western Blotting

The cellular lysis was performed using an SDS denaturing lysis solution in which the protease inhibitor cocktail (PIC), phenylmethane sulfonyl fluoride (PMSF), Na_3VO_4 and β-mercaptoethanol were added. After SDS/PAGE electrophoresis proteins were transferred to a 0.2 µm-pore-sized nitrocellulose membrane. Immunoblotting was performed as previously described[11]. The used primary antibodies were: anti-PP2Ac (Upstate, 05-545); anti-actin (Sigma-Aldrich, A2066); anti-CAPN1 (sc-271313), anti-GSK3β (sc-377213) and anti-NRF2 (sc-365949) (Santa Cruz Biotechnology); anti-p-GSK3β S9 (9336), anti-p-Akt T308 (4056); anti-p-Akt T473 (9271), anti-Akt (9272), anti-Caspase-3 (9662) (Cell Signaling Technology), anti-Smac/DIABLO[39] and anti-HDAC4[66]; anti-Caspase-2[67]; anti-tubulin[67]. The same membranes were incubated with the horseradish peroxidase-conjugated secondary antibody for 1 h at room temperature. The used secondary antibodies were goat anti-mouse or goat anti-rabbit (Sigma Aldrich). Finally, the blots were developed using Super Signal West Dura as recommended by the vendor (Pierce Waltham, MA, USA).

RNA extraction and qRT-PCR

Cells were lysed using Tri-Reagent (Molecular Research Center). 1.0 µg of total RNA was retro-transcribed by using 100 units of M-MLV Reverse transcriptase (Life Technologies). qRT-PCRs were performed using SYBR green technology (KAPA Biosystems). Data were analyzed

by comparative threshold cycle using *HPRT* and *GAPDH* as normalizer.

Generation of GSK3β knock-out U87MG cells

U87MG cells null for GSK3β were achieved using the CRISPR/Cas9 technology. The single guide RNA (sgRNA) 5′-CCTTTGCGGAGAGCTGCAAG-3′ was designed using "CRISPR design" tool (http://crispr.mit.edu/). Lentiviral infections and selections were performed as previously described[68]. The KO clones were screened by PCR, immunoblots and validated by Sanger sequencing.

Generation of U87MG/GSK3β$^{-/-}$ cells expressing GSK3β WT and its mutant K/M fused to GFP

The coding sequence of GSK3β was amplified by PCR from Vectors encoding wild-type and kinase-dead GSK3β previously described[69], using the following primers (Sigma-Aldrich): - AGATCTATGTCAGGGCGGCCC AG, as forward primer containing a restriction site for *Bgl*II; - GAATTCTGGTGGAGTTGGAAGCTGATG, as reverse primer containing the *Eco*RI site. GSK3β WT and the kinase defective mutant KM were cloned into pEGFP-N1 plasmid. Next the two fusions (GSK3β/WT-GFP and GSK3β/KM-GFP) digested *Bgl*II and *Xho*I were subcloned into the retroviral vector pWZL-Neo. U87MG cells expressing BCL-XL, GSK3β-WT-GFP or GSK3β/KM-GFP constructs were generated by retroviral infection as previously described[12]. G418 (1000 μg/ml) for the selection of GSK3β-WT-GFP or KM-GFP expressing cells and Hygromycin (200 μg/ml) for the selection of BCL-XL expressing cells were used. As control U87MG cells were infected with pWZL-Hygro and pWZL-Neo retroviral vectors and selection performed as above described.

Immunofluorescences and time-lapse microscopy

U87MG cells were fixed with 3% paraformaldehyde and permeabilized with 0.5% Triton X-100. The primary antibody was anti-Smac/DIABLO, and the secondary antibody was Alexa Fluor 546-conjugated anti-rabbit (Life Technologies). Cells were imaged with a Leica confocal microscopy SP2 or SP8.

For time-lapse analysis TMRM (20 nM)[39] was used and DMNQ (30 μM) added 1 h before the analysis. The images were collected every 5 min for 24 h using a Leica SP8 confocal microscope (Leica Microsystems) equipped with a stage top incubator controlling temperature, CO_2 and humidity (Okolab). Image analysis was performed using the Leica Acquired Software X (LASX). For the TMRM $\Delta\psi_m$ analysis, the fluorescence of the mitochondria was evaluated through drawing a region around the cell (Region Of Interest; ROI) and measuring its Mean fluorescence Intensity ($MI_{TMRMcell}$). The fluorescence of the background (BK_{TMRM}), which is another ROI located in a non-fluorescent region, was subtracted to the $MI_{TMRMcell}$ and the obtained data was multiplied for the area of the cell ($Area_{cell}$), according to the following equation:

$$\text{TMRM fluorescence } (\%) = (MI_{TMRMcell} - BK_{TMRM}) * Area_{cell}$$

A similar calculation was used to quantify the increase of nuclear fluorescence of GSK3β-GFP, according to the following formula:

$$\text{Nuclear GSK3}\beta - \text{GFP} = \left(MI_{GSK3\beta-GFPnucl} - BK_{GSK3\beta-GFP}\right) * Area_{nucl} \Big/ \left(MI_{GSK3\beta-GFPcytosol} - BK_{GSK3\beta-GFPcytosol}\right) * Area_{cytosol}$$

ROS accumulation measurement

The reactive oxygen species (ROS) accumulation was evaluated using two different probes following the manufacturer's instructions: 6-carboxy-2',7'-dichlorodihydrofluorescein diacetate (Carboxy-H_2DCFDA) (Life Technologies) and the ROS Deep Red Dye from the Cellular Reactive Oxygen Species Detection Assay Kit Deep Red Fluorescence (Abcam). Carboxy-H_2DCFDA and ROS Deep Red Dye fluorescence were determined by the FACSCalibur flow cytometer (BD) at the excitation wavelength of 495 nm for Carboxy-H_2DCFDA and 650 nm for the ROS Deep Red Dye.

Statistics

Results were expressed as means ± standard deviations (SD) from at least three independent experiments. Statistical analysis of differences between groups was performed using the Student's t test of Excel software (two-samples, two-tailed distribution, equal variance), with p values represented as: $^{*}p < 0.05$; $^{**}p < 0.01$; $^{***}p < 0.005$. Measurements were obtained in double-blind.

Acknowledgements

This work was supported by grant from Regione Friuli-Venezia Giulia POR FESR 2014-2020 ATeNA. We thank Raffaella Picco (DAME UniUD) for helping in data analysis.

Conflict of interest

The authors declare that they have no conflict of interest.

Supplementary Information accompanies this paper at (https://doi.org/10.1038/s41419-019-2202-0).

Received: 9 July 2019 Revised: 11 December 2019 Accepted: 12 December 2019
Published online: 02 January 2020

References

1. Tuzlak, S., Kaufmann, T. & Villunger, A. Interrogating the relevance of mitochondrial apoptosis for vertebrate development and postnatal tissue homeostasis. *Genes Dev.* **30**, 2133–2151 (2016).
2. Lindsten, T. & Thompson, C. B. Cell death in the absence of Bax and Bak. *Cell Death Differ.* **13**, 1272–1276 (2006).
3. Jorgensen, I., Rayamajhi, M. & Miao, E. A. Programmed cell death as a defence against infection. *Nat. Rev. Immunol.* **17**, 151–164 (2017).
4. Redza-Dutordoir, M. & Averill-Bates, D. A. Activation of apoptosis signalling pathways by reactive oxygen species. *Biochim. Biophys. Acta* **1863**, 2977–2992 (2016).
5. Feamhead, H. O., Vandenabeele, P. & Vanden Berghe, T. How do we fit ferroptosis in the family of regulated cell death? *Cell Death Differ.* **24**, 1991–1998 (2017).
6. Green, D. R. & Llambi, F. Cell death signaling. *Cold Spring Harb. Perspect. Biol.* **7**, a006080 (2015).
7. Tang, D., Kang, R., Berghe, T. V., Vandenabeele, P. & Kroemer, G. The molecular machinery of regulated cell death. *Cell Res.* **29**, 347–364 (2019).
8. Conrad, M. et al. Regulation of lipid peroxidation and ferroptosis in diverse species. *Genes Dev.* **32**, 602–619 (2018).
9. Friedmann Angeli, J. P., Krysko, D. V. & Conrad, M. Ferroptosis at the crossroads of cancer-acquired drug resistance and immune evasion. *Nat. Rev. Cancer* **19**, 405–414 (2019).
10. Aleo, E., Henderson, C. J., Fontanini, A., Solazzo, B. & Brancolini, C. Identification of new compounds that trigger apoptosome-independent caspase activation and apoptosis. *Cancer Res.* **66**, 9235–9244 (2006).
11. Fontanini, A. et al. The isopeptidase inhibitor G5 triggers a caspase-independent necrotic death in cells resistant to apoptosis: a comparative study with the proteasome inhibitor bortezomib. *J. Biol. Chem.* **284**, 8369–8381 (2009).
12. Foti, C. et al. Characterization of caspase-dependent and caspase-independent deaths in glioblastoma cells treated with inhibitors of the ubiquitin-proteasome system. *Mol. Cancer Ther.* **8**, 3140–3150 (2009).
13. Tomasella, A., Blangy, A. & Brancolini, C. A receptor-interacting protein 1 (RIP1)-independent necrotic death under the control of protein phosphatase PP2A that involves the reorganization of actin cytoskeleton and the action of cofilin-1. *J. Biol. Chem.* **289**, 25699–25710 (2014).
14. Tomasella, A. et al. The isopeptidase inhibitor 2cPE triggers proteotoxic stress and ATM activation in chronic lymphocytic leukemia cells. *Oncotarget* **7**, 45429–45443 (2016).
15. Ciotti, S. et al. The binding landscape of a partially-selective isopeptidase inhibitor with potent pro-death activity, based on the bis(arylidene)cyclohexanone scaffold. *Cell Death Dis.* **9**, 184 (2018).
16. Anchoori, R. K. et al. Stressing the ubiquitin-proteasome system without 20S proteolytic inhibition selectively kills cervical cancer cells. *PLoS ONE* **6**, 23888 (2011).
17. Shukla, N. et al. Proteasome addiction defined in ewing sarcoma is effectively targeted by a novel class of 19S proteasome inhibitors. *Cancer Res.* **76**, 4525–4534 (2016).
18. Coughlin, K. et al. Small-molecule RA-9 inhibits proteasome-associated DUBs and ovarian cancer in vitro and in vivo via exacerbating unfolded protein responses. *Clin. Cancer Res.* **20**, 3174–3186 (2014).
19. Cersosimo, U. et al. Synthesis, characterization, and optimization for in vivo delivery of a nonselective isopeptidase inhibitor as new antineoplastic agent. *J. Med. Chem.* **58**, 1691–1704 (2015).
20. D'Arcy, P. et al. Inhibition of proteasome deubiquitinating activity as a new cancer therapy. *Nat. Med.* **17**, 1636–1640 (2011).
21. Wang, X. et al. The 19S Deubiquitinase inhibitor b-AP15 is enriched in cells and elicits rapid commitment to cell death. *Mol. Pharmacol.* **85**, 932–945 (2014).
22. Karki, S. S. et al. Synthesis and biological evaluation of novel 2-aralkyl-5-substituted-6-(4'-fluorophenyl)-imidazo[2,1-b][1,3,4]thiadiazole derivatives as potent anticancer agents. *Eur. J. Med. Chem.* **46**, 2109–2116 (2011).
23. Robertson, H., Hayes, J. D. & Sutherland, C. A partnership with the proteasome; the destructive nature of GSK3. *Biochem. Pharmacol.* **147**, 77–92 (2018).
24. Reddy, P. H. Amyloid beta-induced glycogen synthase kinase 3β phosphorylated VDAC1 in Alzheimer's disease: implications for synaptic dysfunction and neuronal damage. *Biochim Biophys. Acta* **1832**, 1913–1921 (2013).
25. Ghaderi, S. et al. Role of glycogen synthase kinase following myocardial infarction and ischemia-reperfusion. *Apoptosis* **22**, 887–897 (2017).
26. Wakatsuki, S., Tokunaga, S., Shibata, M. & Araki, T. GSK3B-mediated phosphorylation of MCL1 regulates axonal autophagy to promote Wallerian degeneration. *J. Cell Biol.* **216**, 477–493 (2017).
27. Gu, C. et al. P7C3 inhibits GSK3β activation to protect dopaminergic neurons against neurotoxin-induced cell death in vitro and in vivo. *Cell Death Dis.* **8**, 2858 (2017).
28. Goñi-Oliver, P., Lucas, J. J., Avila, J. & Hernández, F. N-terminal cleavage of GSK-3 by calpain: a new form of GSK-3 regulation. *J. Biol. Chem.* **282**, 22406–22413 (2007).
29. Felgueiras, J. & Fardilha, M. Phosphoprotein phosphatase 1-interacting proteins as therapeutic targets in prostate cancer. *World J. Pharm.* **3**, 120–139 (2014).
30. Sánchez, C., Tompa, P., Szücs, K., Friedrich, P. & Avila, J. Phosphorylation and dephosphorylation in the proline-rich C-terminal domain of microtubule-associated protein 2. *Eur. J. Biochem.* **241**, 765–771 (1996).
31. Cheng, S. Y., Wang, S. C., Lei, M., Wang, Z. & Xiong, K. Regulatory role of calpain in neuronal death. *Neural Regen. Res.* **13**, 556–562 (2018).
32. Juhaszova, M. et al. Glycogen synthase kinase-3beta mediates convergence of protection signaling to inhibit the mitochondrial permeability transition pore. *J. Clin. Invest.* **113**, 1535–1549 (2004).
33. Mobasher, M. A. et al. Protein tyrosine phosphatase 1B modulates GSK3β/Nrf2 and IGFIR signaling pathways in acetaminophen-induced hepatotoxicity. *Cell Death Dis.* **4**, e626 (2013).
34. Rizvi, F., Shukla, S. & Kakkar, P. Essential role of PH domain and leucine-rich repeat protein phosphatase 2 in Nrf2 suppression via modulation of Akt/GSK3β/Fyn kinase axis during oxidative hepatocellular toxicity. *Cell Death Dis.* **5**, e1153 (2014).
35. Sunaga, D. et al. Accelerated recovery of mitochondrial membrane potential by GSK-3β inactivation affords cardiomyocytes protection from oxidant-induced necrosis. *PLoS ONE* **9**, e112529 (2014).
36. Watanabe, N. & Forman, H. J. Autoxidation of extracellular hydroquinones is a causative event for the cytotoxicity of menadione and DMNQ in A549-S cells. *Arch. Biochem. Biophys.* **411**, 145–157 (2003).
37. Ding, Q. et al. Degradation of Mcl-1 by beta-TrCP mediates glycogen synthase kinase 3-induced tumor suppression and chemosensitization. *Mol. Cell Biol.* **27**, 4006–4017 (2007).
38. Unterkircher, T. et al. Bortezomib primes glioblastoma, including glioblastoma stem cells, for TRAIL by increasing tBid stability and mitochondrial apoptosis. *Clin. Cancer Res.* **17**, 4019–4030 (2011).
39. Henderson, C. J. et al. Caspase activation and apoptosis in response to proteasome inhibitors. *Cell Death Differ.* **12**, 1240–1254 (2005).
40. Cross, D. A., Alessi, D. R., Cohen, P., Andjelkovich, M. & Hemmings, B. A. Inhibition of glycogen synthase kinase-3 by insulin mediated by protein kinase B. *Nature* **378**, 785–789 (1995).
41. Frame, S., Cohen, P. & Biondi, R. M. A common phosphate binding site explains the unique substrate specificity of GSK3 and its inactivation by phosphorylation. *Mol. Cell* **7**, 1321–1327 (2001).
42. Alessi, D. R. & Cohen, P. Mechanism of activation and function of protein kinase B. *Curr. Opin. Genet. Dev.* **8**, 55–62 (1998).
43. Du, C., Fang, M., Li, Y., Li, L. & Wang, X. Smac, a mitochondrial protein that promotes cytochrome c-dependent caspase activation by eliminating IAP inhibition. *Cell* **102**, 33–42 (2000).
44. Bechard, M., Trost, R., Singh, A. M. & Dalton, S. Frat is a phosphatidylinositol 3-kinase/Akt-regulated determinant of glycogen synthase kinase 3β subcellular localization in pluripotent cells. *Mol. Cell Biol.* **32**, 288–296 (2012).
45. Tanno, M. et al. Translocation of glycogen synthase kinase-3β (GSK-3β), a trigger of permeability transition, is kinase activity-dependent and mediated by interaction with voltage-dependent anion channel 2 (VDAC2). *J. Biol. Chem.* **289**, 29285–29296 (2014).
46. Hüser, J. & Blatter, L. A. Fluctuations in mitochondrial membrane potential caused by repetitive gating of the permeability transition pore. *Biochem. J.* **343**, 311–317 (1999).
47. Watanabe, N., Dickinson, D. A., Liu, R. M. & Forman, H. J. Quinones and glutathione metabolism. *Methods Enzymol.* **378**, 319–340 (2004).
48. Deller, S., Macheroux, P. & Sollner, S. Flavin-dependent quinone reductases. *Cell Mol. Life Sci.* **65**, 141–160 (2008).
49. Bedard, K. & Krause, K. H. The NOX family of ROS-generating NADPH oxidases: physiology and pathophysiology. *Physiol. Rev.* **87**, 245–313 (2007).
50. Schmidlin, C. J., Dodson, M. B., Madhavan, L. & Zhang, D. D. Redox regulation by NRF2 in aging and disease. *Free Radic. Biol. Med.* **134**, 702–707 (2019).

51. Asher, G., Lotem, J., Kama, R., Sachs, L. & Shaul, Y. NQO1 stabilizes p53 through a distinct pathway. *Proc. Natl Acad. Sci. USA* **99**, 3099–3104 (2002).
52. den Braver-Sewradj, S. P. Reduction and scavenging of chemically reactive drug metabolites by NAD(P)H:Quinone Oxidoreductase 1 and NRH:Quinone Oxidoreductase 2 and variability in hepatic concentrations. *Chem. Res. Toxicol.* **31**, 116–126 (2018).
53. Kumagai, Y., Abiko, Y. & Cong, N. L. Chemical toxicology of reactive species in the atmosphere: two decades of progress in an electron acceptor and an electrophile. *J. Toxicol. Sci.* **41**, SP37–SP47 (2016).
54. Luanpitpong, S. et al. Regulation of lung cancer cell migration and invasion by reactive oxygen species and caveolin-1. *J. Biol. Chem.* **285**, 38832–38840 (2010).
55. Rada, P. et al. Structural and functional characterization of Nrf2 degradation by the glycogen synthase kinase 3/β-TrCP axis. *Mol. Cell Biol.* **32**, 3486–3499 (2012).
56. Gong, P. & Cederbaum, A. I. Transcription factor Nrf2 protects HepG2 cells against CYP2E1 plus arachidonic acid-dependent toxicity. *J. Biol. Chem.* **281**, 14573–14579 (2006).
57. Chen, X. et al. GSK-3β downregulates Nrf2 in cultured cortical neurons and in a rat model of cerebral ischemia-reperfusion. *Sci. Rep.* **6**, 20196 (2016).
58. Xing, H. Y. et al. The cytoprotective effect of hyperoside against oxidative stress is mediated by the Nrf2-ARE signaling pathway through GSK-3β inactivation. *PLoS ONE* **10**, e0145183 (2015).
59. Jiang, Y. et al. Therapeutic targeting of GSK3β enhances the Nrf2 antioxidant response and confers hepatic cytoprotection in hepatitis C. *Gut* **64**, 168–179 (2015).
60. Mathur, A., Pandey, V. K. & Kakkar, P. Activation of GSK3β/β-TrCP axis via PHLPP1 exacerbates Nrf2 degradation leading to impairment in cell survival pathway during diabetic nephropathy. *Free Radic. Biol. Med.* **120**, 414–424 (2018).
61. Farr, S. A. et al. Antisense oligonucleotide against GSK-3β in brain of SAMP8 mice improves learning and memory and decreases oxidative stress: Involvement of transcription factor Nrf2 and implications for Alzheimer disease. *Free Radic. Biol. Med.* **67**, 387–395 (2014).
62. Ranea-Robles, P. et al. Aberrant regulation of the GSK-3β/NRF2 axis unveils a novel therapy for adrenoleukodystrophy. *EMBO Mol. Med.* **10**, e8604 (2018).
63. Rojo, A. I. et al. Functional interference between glycogen synthase kinase-3 beta and the transcription factor Nrf2 in protection against kainate-induced hippocampal cell death. *Mol. Cell Neurosci.* **39**, 125–132 (2008).
64. Meares, G. P. & Jope, R. S. Resolution of the nuclear localization mechanism of glycogen synthase kinase-3: functional effects in apoptosis. *J. Biol. Chem.* **282**, 16989–17001 (2007).
65. Sgorbissa, A., Tomasella, A., Potu, H., Manini, I. & Brancolini, C. Type I IFNs signaling and apoptosis resistance in glioblastoma cells. *Apoptosis* **16**, 1229–1244 (2011).
66. Paroni, G. et al. Caspase-dependent regulation of histone deacetylase 4 nuclear-cytoplasmic shuttling promotes apoptosis. *Mol. Biol. Cell* **15**, 2804–2818 (2004).
67. Paroni, G., Henderson, C., Schneider, C. & Brancolini, C. Caspase-2-induced apoptosis is dependent on caspase-9, but its processing during UV- or tumor necrosis factor-dependent cell death requires caspase-3. *J. Biol. Chem.* **276**, 21907–21915 (2001).
68. Di Giorgio, E. et al. The co-existence of transcriptional activator and transcriptional repressor MEF2 complexes influences tumor aggressiveness. *PLoS Genet.* **13**, e1006752 (2017).
69. Diehl, J. A., Cheng, M., Roussel, M. F. & Sherr, C. J. Glycogen synthase kinase-3beta regulates cyclin D1 proteolysis and subcellular localization. *Genes Dev.* **12**, 3499–3511 (1998).

cancers

MDPI

Review

Proteotoxic Stress and Cell Death in Cancer Cells

Claudio Brancolini * and Luca Iuliano

Department of Medicine, Università degli Studi di Udine, p.le Kolbe 4—33100 Udine, Italy; iuliano.luca@spes.uniud.it
* Correspondence: claudio.brancolini@uniud.it

Received: 14 July 2020; Accepted: 20 August 2020; Published: 23 August 2020

check for updates

Abstract: To maintain proteostasis, cells must integrate information and activities that supervise protein synthesis, protein folding, conformational stability, and also protein degradation. Extrinsic and intrinsic conditions can both impact normal proteostasis, causing the appearance of proteotoxic stress. Initially, proteotoxic stress elicits adaptive responses aimed at restoring proteostasis, allowing cells to survive the stress condition. However, if the proteostasis restoration fails, a permanent and sustained proteotoxic stress can be deleterious, and cell death ensues. Many cancer cells convive with high levels of proteotoxic stress, and this condition could be exploited from a therapeutic perspective. Understanding the cell death pathways engaged by proteotoxic stress is instrumental to better hijack the proliferative fate of cancer cells.

Keywords: UPR; NOXA; DR5; BCL2; apoptosis; necroptosis; ferroptosis; proteotoxic stress

1. Proteotoxic Stress: An Introduction

Proteins are key macromolecules that play fundamental roles in almost every cellular process, from gene expression to cell/tissue protection [1]. The important and relentless actions of proteins oblige cells to supervise and guarantee their correct folding and assembling. Protein homeostasis or proteostasis is the fundamental cellular effort aimed at reaching this goal. Proteostasis is governed through a complex network of regulative mechanisms and is an essential task for cell survival [2]. The vast majority of proteins need to assume a peculiar thermodynamically stable three-dimensional structure that depends on their amino acid sequence [3]. During the folding process, proteins, particularly those presenting complex domains, can often produce folded intermediates. These intermediates can expose hydrophobic amino acid residues, thus becoming more susceptible to being stacked into a misfolded condition, a circumstance that can lead to the formation of misfolded aggregates [4].

Cells use a complex network, called the proteostasis network (PN), in order to monitor protein homeostasis. PN includes molecular chaperones and proteolytic machinery. These gene families promptly cooperate to guarantee regular proteostasis. In this manner, PN coordinates protein synthesis with folding and, if necessary, it can trigger protein degradation [5–7]. The importance of proteostasis maintenance becomes evident in the presence of PN dysfunctions. Inefficiency in these monitoring activities is responsible for several pathologies, including neurodegenerative diseases. Frequently, these deficiencies are age-dependent, with significant social and economic costs [7–10].

Molecular chaperones supervise protein folding, a process that requires ATP hydrolysis and a high cost in terms of energy. In particular, the chaperones of the heat shock protein (HSP) family help protein folding and are fundamental when critical conditions such as heat stress, oxidative stress, or hypoxia emerge [1]. These particular proteins are defined as HSPs because their expression is dramatically upregulated when cells are exposed to high temperatures or other forms of stress. The human genome encodes for about 330 chaperones and cochaperones [11]. The most known

classes of chaperones include the ATP-dependent HSP70s, HSP90s, HSP60s (also called chaperonins), and HSP100s and the ATP-independent small HSPs (sHSPs) [11]. In many cases, chaperones are assisted in their activities by regulatory proteins called cochaperones, a large protein family that includes 244 different members. Some examples of cochaperones are the HSP40s (49 proteins) as regulators of the HSP70s and the tetratricopeptide repeat proteins (TPRs; 114 proteins) as regulators of the HSP90s. In general, cochaperones assist the functions of the chaperones by providing more selectivity and specificity toward the substrate [11,12].

Chaperones function as the main players in the maintenance of proteostasis by facilitating the folding of proteins. They usually bind to the hydrophobic polypeptide segments exposed by unfolded or not-completely-folded proteins, thus avoiding their aggregation throughout the folding process [1]. HSP70s and HSP90s are the most important members of the ATP-dependent chaperones. During the folding, they work through ATP-regulated cycles of binding and release from the target protein. This process ends when proteins are finally able to obtain their correct structure [2,13]. Moreover, some proteins are incapable of folding without the presence of chaperones, and this event determines the limit of the Anfinsen dogma. An example of this type of protein is the cytoskeletal actin [14].

Chaperones can do their duties either in cooperation with the ribosome, for example, the mammalian ribosome-associated complex (RAC) and some specialized HSP70s (HSP70L1) [15,16], or, once the polypeptide is released, alone. This is the case of HSP70s, HSP90s, and the TRiC/CCT chaperonin. In particular, TRiC are complexes structured as a double-ring that encircle, for a short time, the unfolded protein in a structure similar to a cage. In this manner, TRiC allow the correct folding and avoid the formation of aggregates [2,17]. In addition, the ATP-independent sHSPs work as a support in the maintenance of the proteins in a stable state. Through this strategy, proteins will not go under aggregation processes [18].

In general, proteins can be divided into proteins that fold easily and quickly after the interaction with the upstream chaperones, like HSP70s, and proteins that require more help during the process. The first group of proteins does not need downstream chaperones; instead, the second group of proteins is not able to complete the folding correctly and needs more specialized chaperones, like HSP90s or the chaperonins, to achieve the proper structure [19]. These "difficult" proteins are usually larger than the average and comprehend multiple domains or domains, which have complex topologies of folding. For these reasons, they need a strong interaction with the chaperones and also with the cochaperones, generating an interconnected network called "chaperome" [20].

The human PN has not yet been completely characterized in all its parts. However, investigations aimed at dissecting the network of proteins interacting with HSP90s have revealed the presence of E3 ligases (enzymes involved in the last step of ubiquitin-conjugation). This finding highlights the close relationship between the folding and protein degradation processes [21]. A detailed study, which involved about 70 chaperones, cochaperones, and proteins of the quality-control compartment, has illustrated that there is a hierarchical organization within PN. This organization is centered on the interconnected chaperone systems of HSP70 and HSP90 [22]. Another study revealed that the chaperone network can be rewired after oncogenic transformation in a new network of interactions defined as "epichaperome", which can favor cancer cell survival [23].

Importantly, the chaperone systems have evolved several mechanisms to compensate when a single chaperone fails or is disabled. This aspect is also important from a therapeutic perspective when specific inhibitors against a chaperone are evaluated [24]. For example, the inhibition of HSP90 can promote the binding of the unfolded proteins to Hsc70, the constitutively expressed HSP70 [22]. Furthermore, between members of the BAG family of cochaperones, which act as nucleotide exchange factors of HSP70, BAG2 is the only one that has a similar substrate range to Hsc70. This evidence permits us to conclude that BAG2 could be a general cofactor, which is important in the folding mechanism of Hsc70 substrate proteins. Finally, among the interactors of Hsc70, the E3 ligase CHIP (Carboxy Terminus of HSP70-Interacting Protein) has been identified, thus further confirming the correlation between the chaperones and the ubiquitin–proteasome system (UPS) [25,26].

2. The Protein Quality System

In order to maintain the proteostasis, eukaryotic cells have evolved several systems monitoring quality control. These systems are different from the folding/re-folding actions of chaperones and are involved in the degradation of damaged and misfolded proteins. The most important system is represented by UPS. It works in cooperation with the lysosomal system [27,28] and plays a crucial role in several cellular processes by controlling the physiological turnover of proteins [29]. The degradation of the proteins through UPS is due to the presence of a ubiquitin tag, which is conjugated through a multistep process called ubiquitylation. A ubiquitin moiety is initially covalently linked onto Lys residues of target proteins (isopeptide-bond) and, next, elongated through the use of specific Lys of the ubiquitin itself, most frequently Lys 48. The ubiquitylation requires the coordinated action of three enzymes. The E1 ubiquitin-activating enzymes, E2 ubiquitin-conjugation enzymes, and E3 ubiquitin ligase enzymes [30–32]. After ubiquitylation, the tagged proteins are translocated to the 26S proteasome, an ATP-dependent protease complex found in the cytosol and in the nucleus of all eukaryotic cells. The proteasome is composed of about 50 different subunits, but it is possible to define two critical subcomplexes: the 20S catalytic core and one or two 19S regulatory subunits. The 19S particles are bound to one or both ends of the 20S component [33–35]. The ubiquitin tag is recognized by the 19S regulatory subunits, and, here, it is recycled by the action of deubiquitinases (DUBs). Three DUBs are associated with the 19S regulatory subunits: RPN11/POH1, USP14, and UCH-L5 [36–38]. This process is crucial for the degradation since the presence of the ubiquitin chain would impact sterically on the translocation from the 19S regulatory subunits to the 20S catalytic core. In fact, small molecules that inhibit these DUBs trigger cell death responses, similar to inhibitors of the catalytic portion such as bortezomib, carfilzomib, and ixazomib [36,39–41].

The 20S catalytic core is constituted by two heptameric rings of β-subunits and two heptameric rings of α-subunits. The α-subunits have a structural role, and the β-subunits have a catalytic role instead. In particular, β1 has a caspase-like activity, β2 has a trypsin-like activity, and β5 has a chymotrypsin-like activity [42–44]. A recent analysis of the proteasome and its substrates, through cryoelectron microscopy, offers a new intriguing sight into this complex process [45–47]. Because of the necessity of substrate unfolding, the proteasome is incapable of degrading the aggregated proteins directly. Normally, once bound to the proteasome, the substrate is unfolded by the action of six ATPase subunits (Rpt1–6) [48]. Hence, an obligatory prerequisite step for UPS-dependent degradation is substrate disaggregation through the chaperones network. The second example of such cooperation is the direct interaction between the E3 ligase CHIP and HSP70. CHIP can thus ubiquitylate chaperone–client proteins. However, this modification may still be inverted by DUBs [49]. How these conflicting mechanisms are controlled will be important for a better understanding of the protein quality control machinery.

In summary, even in the presence of UPS, protein misfolding can induce the creation of insoluble aggregates, particularly under stress situations. By contrast, autophagy can directly eliminate these aggregates via lysosomal degradation [50]. The complex molecular system involved in this task is defined as the autophagy lysosomal pathway (ALP). It includes core ATG products and additional factors, with a total of about 500 components [51]. The aggregated proteins can be accumulated in ubiquitin-positive regions, where the autophagic system is recruited by chaperones in a process known as chaperone-assisted selective autophagy (CASA) [52–54]. In normal unstressed conditions, the soluble proteins that need to be degraded can also be eliminated by a different type of autophagy, defined as chaperone-mediated autophagy (CMA). This response first involves the action of Hsc70, which can recognize the substrate and then the lysosomal translocation, operating through the lysosomal receptor LAMP2A (lysosome-associated membrane protein 2A). CMA avoids the formation of the autophagosome [55]. Although both UPS and ALP display an important grade of specificity toward their variety of substrates, they are connected to each other. They often compensate for each other when one of these two pathways is not working properly [56–59].

3. Cellular Responses to the Unfolded Proteins

Despite the presence of the chaperone systems, some errors occur during folding and many stressors such as heat, heavy metal ions, oxygen radicals, and mutations can hamper the correct folding. A misfolded or unfolded protein is not functional and can elicit a pathological condition derived from its aggregation [1,60–63]. Folding maturation in the endoplasmic reticulum (ER) is a difficult task. Proteins of the secretory pathway, if unable to fold correctly, are retained in ER and then retro-translocated to the proteasome for their degradation. The process is called ER-associated degradation (ERAD) [64]. A fundamental role in ERAD is played by the cytosolic ATPase p97 (VCP/Cdc48). This ATPase is involved in delivering the ubiquitylated unfolded proteins from ER to the proteasome through ATP hydrolysis [65]. If this system is overloaded, the accumulation of incorrectly folded proteins occurs in ER, thus leading to ER dysfunctions, including an altered redox equilibrium. These conditions are responsible for the induction of ER stress [66–70]. In response to ER stress, cells activate UPR (unfolded protein response) [71,72]. This adaptive response is important for sustaining cell survival. To this end, UPR blocks protein translation, increases the activation of chaperones, and potentiates the ERAD pathway. Through UPR, cells avoid the accumulation of misfolded proteins and restore the physiological condition of proteostasis. As explained above, UPR allows cells to survive the stress condition [64,70–73]. UPR is governed by three sensors: PERK (protein kinase RNA-like ER kinase), IRE1 (inositol-requiring enzyme 1) and ATF6 (activating transcription factor 6) [64,74,75]. All these sensors work in parallel to decrease ER stress. PERK and IRE1 activation can decrease protein synthesis with the consequent reduction in the number of proteins that can enter ER. The activation of ATF6 can upregulate the transcription of different chaperones involved in controlling protein folding [64].

PERK is a serine/threonine kinase that has several substrates. The best characterized is the eukaryotic translation initiation factor-2 alpha (eIF2α). PERK is able to phosphorylate eIF2α at serine 51 [70,71,76], thus blocking the CAP-dependent translation and diminishing ER stress [64]. Another notable substrate is NRF2 (nuclear factor erythroid-derived 2), the master regulator of redox homeostasis [77]. PERK can phosphorylate NRF2 on Thr 80, localized within the Neh2 domain [78]. This favors the activation of NRF2 and its nuclear import. From the nucleus, NRF2 coordinates the expression of the antioxidant response by binding the antioxidant response elements (AREs) present in the regulatory regions of several genes [79]. Additional studies have revealed that FOXO transcription factors [80,81] and diacylglycerol [82,83] can also be phosphorylated by PERK in order to reduce ER stress. Other PERK-related kinases exist that can supervise different stress conditions. Protein kinase R (PKR) is involved in the antiviral response, GCN2/EIF2AK4 (eukaryotic translation initiation factor 2 alpha kinase 4) is involved in sensing amino acid pool depletion, and, finally, HRI/EIF2AK1 (eukaryotic translation initiation factor 2 alpha kinase 1) is activated by heavy metals, heat shock, and proteasome inhibition [84]. All these kinases phosphorylate eIF2α, reduce translation, and diminish proteotoxic stress. Interestingly, HRI also confers resistance to UPS inhibitors such as bortezomib [85].

BiP/GRP78, a HSP70 family member localized into ER, is a master regulator of UPR in response to ER stress. It monitors the release and activation of the three sensors PERK, IRE1, and ATF6 [86,87]. PERK, IRE1, and ATF6 are constitutive clients of Bip/GRP78. The increase in protein unfolding, by incessantly sequestering BiP/GRP78, unleashes the three sensors and activates UPR. After the disassociation from BiP/GRP78, PERK can dimerize, and this favors its autophosphorylation and activation [88]. The activated form of IRE1, after BiP/GRP78 release, has an endoribonuclease activity that can splice a 26-base intron contained in the mRNA of the X-box binding protein 1 (XBP-1) [89]. The mature XBP-1 acts as a TF that supervises the transcription of genes involved in ERAD and protein folding [90]. Finally, the dissociation of ATF6 from BiP/GRP78 permits its translocation from ER to Golgi, where it is processed. The cleaved ATF6 can enter the nucleus where it acts as a TF to transcribe genes such as GRP78 and GRP94, which augment the ER-folding potential [91]. This sophisticated adaptive response allows cells to survive stress conditions. However, if the proteostasis restoration fails, a permanent and sustained activation of UPR can be deleterious. Initially engaged to permit cell survival, UPR can switch to triggering cell death [64,74,92].

4. Cell Death Pathways Activated by Proteotoxic Stress

The induction of proteotoxic stress through the use of small compounds/drugs achieves a therapeutic interest, particularly from an antitumor perspective [93]. In order to better synergize the induction of proteotoxic stress with the available therapies, it is fundamental to dissect the molecular mechanisms controlling cell death in response to proteotoxic stress.

4.1. The Extrinsic Pathway of Caspase Activation

It is well established that proteotoxic stress engages the mitochondrial pathway of caspase activation [94]. However, proteotoxic stress is a broad and complex pro-death insult; additionally, the extrinsic pathway is involved [95]. This role was suggested by early studies reporting the upregulation of TNFRSF10B/DR5, the TRAIL receptor, in response to ER-stressors/PERK activation, UPS inhibitors, as well as the influence of caspase-8 inhibitors on proteotoxic stress-induced cell death [39,95–101]. More recently, it has been proposed that UPR not only upregulates DR5 expression but misfolded proteins can directly engage with DR5 in the ER–Golgi intermediate compartment to drive the assembly of DR5 in complexes competent for caspase-8 activation (Figure 1). This activation can occur independently from the binding of its canonical extracellular ligand Apo2L/TRAIL [102]. Although the mechanism involved in such activation is unknown, a plausible hypothesis points to the release of an autoinhibitory activity that normally prevents spontaneous activation of the receptor. The increased levels of expression, the trapping in a particular membrane domain, and the priming effect of misfolded proteins could be the culprits [102,103].

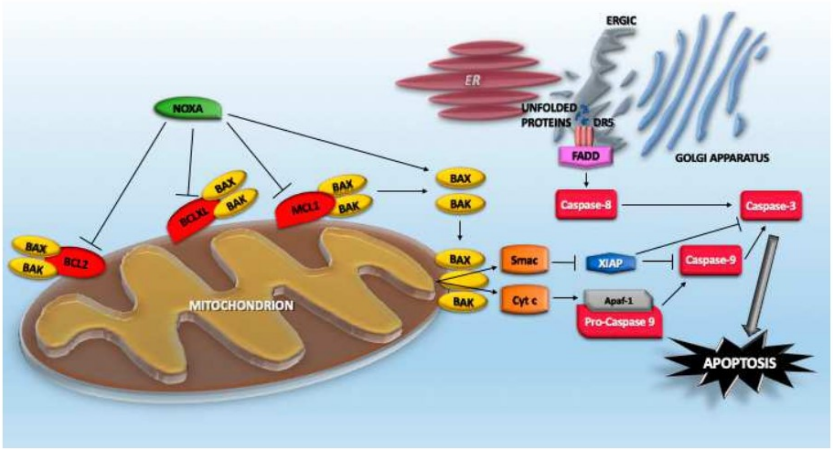

Figure 1. Apoptotic pathways engaged by proteotoxic stress.

In the receptor-independent activation of caspase-8 following ER stress, a contribution of RIPK1 (receptor interacting serine/threonine kinase 1) has also been proposed. The contribution appears indirect and is sustained by the use of Ripk1-deficient murine cells. The involvement of Ripk-1 in ER stressor-induced apoptosis is still mysterious. It is independent of the kinase activity from cIAP1/2 (BIRC1/2—baculoviral IAP repeat containing 1 and 2)-mediated ubiquitylation and does not involve the direct regulation of JNK/MAPK8 or CHOP [104]. ER stress can also promote inflammatory responses in the presence of chemotherapeutic regiments. Here, again, ER stress elicits TRAIL receptor upregulation, which results in a caspase-8/FADD/RIPK1-dependent activation of NF-κB. Similar to cell death, inflammatory cytokine production occurs in a ligand-independent manner. The importance of this

response is testified by the protection observed in $DR5^{-/-}$ mice from taxol-induced inflammation [103]. These studies confirm that similar to other observations, the engagement of DR5 can result in different cellular responses that are context-dependent [105].

4.2. The ATF Network

A huge plethora of studies have indicated that cell death induced by proteotoxic stress can follow different routes. Certainly, the foremost investigated signaling pathway linking proteotoxic stress to apoptosis regards ER stress and the consequent UPR. A key element of this pathway is represented by ATF4 (activating transcription factor 4), a TF that belongs to the cAMP response element-binding protein (CREB)-2 family [106]. As explained above, eIF2α phosphorylation results in the attenuation of the cap-dependent protein translation, as well as the specific translation of selected mRNAs, including ATF4 itself. Normally, ATF4 protein is almost undetectable due to its very short half-life and low translation efficiency [107,108]. In fact, ATF4 levels dramatically increase in response to proteasome inhibitors because of the double effect exerted by UPR activation and the suppression of its degradation [109]. ATF4 is structured into different domains, which comprise a basic/leucine zipper domain (bZIP domain) that binds DNA. ATF4 interacts with several partners that influence its variegated transactivation activities and its stability [106,107]. As a consequence, ATF4 controls the expression of a wide range of genes that play different roles in resolving proteotoxic stress. Some of these genes are directly transcribed by ATF4, others indirectly through the action of other TFs (Figure 2). An example of a TF regulated by ATF4 is CHOP/GADD153 (CCAAT-enhancer-binding protein homologous protein), an important player of the apoptotic response [110]. Again, translation of CHOP mRNA is sustained by eIF2α phosphorylation that allows the escape from a poor translation initiation sequence [111]. Interestingly, this signaling arm is also involved in controlling ferroptosis through both GCN2-dependent and -independent mechanisms, which are elicited by cysteine depletion [112,113].

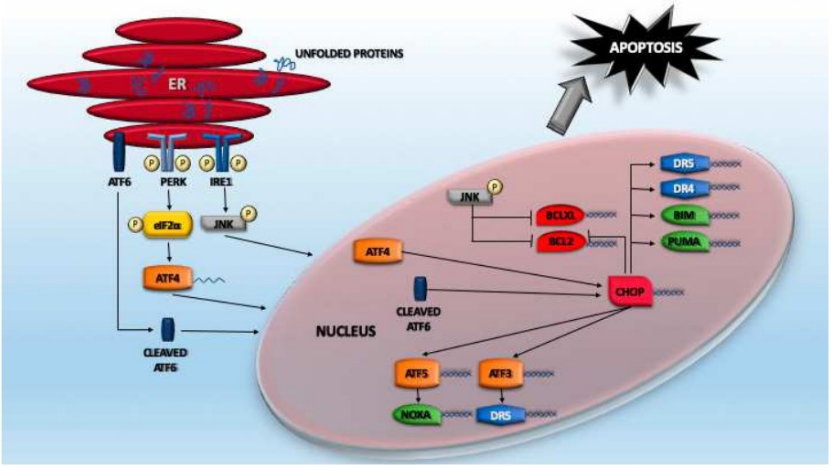

Figure 2. The activating transcription factor (ATF) network in response to proteotoxic stress.

ATF4 can also trigger cell death independently from CHOP. It can promote the downregulation of the IAP family member XIAP (X-linked inhibitor of apoptosis) in a still-undefined manner. These proteins can bind and block caspase activities but can also, through a RING zinc finger domain with E3 ubiquitin ligase activity, promote ubiquitylation and the subsequent proteasomal degradation of their substrates, including caspases [114].

CHOP supervises the expression of a collection of genes. Interestingly, some of these genes are shared with ATF4, thus suggesting the existence of a feed-forward mechanism to sustain proteotoxic-dependent gene expression [115]. Similarly, the control operated by ATF6 on CHOP transcription can be viewed as a cooperative mechanism to resolve proteotoxic stress [116]. A gene under the direct transcriptional control of CHOP is DR5 [103,117,118]. A CHOP-binding site is present in the 5′-flanking region (position –281 and –216 from TSS) of the DR5 gene [117]. Moreover, ATF3, another ATF/CREB family TF that facilitates apoptotic cell death, is involved in the ER stress-mediated DR5 induction in human p53-deficient colorectal cancer cells [119,120]. TRAIL-R1/DR4 is also engaged by ER stress, although with less relevance. CHOP/ATF4 can also promote DR4 upregulation, although with differences among models and cell lines and via both transcriptional and post-transcriptional mechanisms [121,122].

ATF5 is another ATF/CREB family member under CHOP/ATF4 control (Figure 2). Transcriptional upregulation occurs via the direct binding of CARE elements in the ATF5 promoter [115,123]. Similar to ATF4 and CHOP, ATF5 is preferentially translated once eIF2 is phosphorylated. Among the ATF5-dependent genes involved in apoptosis, the BH3-only protein NOXA/PMAIP1 can be found [123]. Experimental downregulation of each of these TFs (ATF3, ATF4, ATF5, and CHOP) results in the abrogation of NOXA induction in response to proteotoxic stress. Hence, they all contribute to sustaining the feed-forward loop that drives apoptosis [115,123,124].

4.3. The BCL2 Family Members

NOXA/PMAIP1 is a BCL-2 proapoptotic family member that plays important roles in different apoptotic responses. NOXA is the smallest of BH3-only proteins (54 residues), and its expression is dramatically upregulated after proteotoxic stress [125]. Initially identified as a TP53 target gene [126], further studies have demonstrated that its transcription can be potently upregulated by TP53-independent mechanisms under different stress conditions, including oncogenic transformation and proteotoxic stress [127–130]. NOXA depletion impairs apoptosis in response to proteotoxic stress. NOXA can act as either sensitizer and activator by virtue of its BH3 domain, which is inserted into the hydrophobic-binding groove of multidomain proapoptotic or antiapoptotic BCL2 family members. As a sensitizer, it interacts with MCL1, BCLXL, and BCL2A1 (Figure 1). In this manner, NOXA interrupts the sequestration operated by these antiapoptotic proteins against multidomain proapoptotic proteins such as BAX and BAK. As a consequence, NOXA unleashes the pro-death activities (oligomerization and channel formation) of BAX/BAK. In contrast, as an activator, NOXA directly binds and activates BAX/BAK [131–134]. Curiously, murine Noxa contains two BH3 domains (A and B, encoded by exons 2 and 3), with only the BH3 domain B conserved in humans [126].

Additional mechanisms are used by proteotoxic stress to engage the mitochondrial pathway of caspase activation. BIM/BCL2L11 and PUMA/BBC3 are other BH3-only proteins, of which upregulation was reported in several models of proteotoxic stress and, particularly, during ER stress. The ablation of these proteins influences the death response to proteotoxic stress [84,93,94]. BIM was reported as being a transcriptional target of CHOP [135]. Similarly, PUMA expression is induced through transcriptional upregulation in response to an ER stress stimulus in a variety of human cell lines [136,137]. In addition to the action on BH3-only proteins, proteotoxic stress can downregulate BCL2 at a transcriptional level through CHOP [138] (Figure 1). Moreover, JNK activation via the IRE1 pathway triggers BCL2 and BCLXL phosphorylation and their subsequent inactivation [139,140]. Among the different routes that proteotoxic stress can engage to trigger apoptosis, the regulation of BOK (BCL2 family apoptosis regulator BOK) must also be included. This proapoptotic BCL2 family member is normally expressed at low levels. In fact, it is constitutively degraded, with a short half-life of 15 min. During proteotoxic stress, E3 ligases such as gp78, which mediates BOK degradation, become saturated because of the accumulation of misfolded proteins. Hence, BOK can accumulate to favor mitochondrial outer membrane permeabilization [141]. Normally, DNAJB12 (JB12) contributes to maintain low levels of

BAK and to sustain the survival of cancer cells. This chaperon is an ER-associated Hsp40 family protein that recruits Hsp70 to the ER surface in the protein quality control system [142].

4.4. Additional Cell Death Responses

When proteotoxic stress advances, UPS becomes clogged by the accumulation of polyubiquitylated proteins. Blocking the proteasome affects the expression of unstable signaling proteins and, therefore, signaling pathways controlling cell survival and cell death are modulated. Two important UPS targets, controlling the survival/death switch, are the inhibitors of NF-kB, IkBα [143], and TP53 [144]. Furthermore, elements of the apoptotic machinery, both pro- and antiapoptotic, such as NOXA, BIM, and MCL1, also accumulate in response to UPS saturation [29,145,146]. MCL1 stabilization represents the dark side in the anticancer effect engaged by UPS inhibitors. Interestingly, multiple kinase inhibitors, such as erlotinib, rapidly enhance UPS-dependent degradation of MCL1. Erlotinib upregulates NOXA expression, which, in turn, through the action of the mitochondria-associated ubiquitin ligase MARCH5 supervises MCL1 degradation [147,148]. Similar to MCL1, other pro-survival proteins such as IAPs (XIAP, cIAP1, and cIAP2 in mammals) accumulate in response to proteotoxic stress-dependent UPS saturation [149]. The activities of these proteins can be instrumental in maintaining cell survival under stress conditions. For example, AIRAP, a proteotoxic-stress gene regulated by the master TF HSF1 (heat-shock factor 1), can regulate cell survival by controlling the levels of cIAP2 [150]. The switch between cell survival/death must also imply control over IAPs. An example is the ability of tunicamycin and thapsigargin (two ER stressors) to reduce XIAP levels in a number of mammalian cell lines [114]. XIAP translation can be reduced in a PERK-mediated manner, and ATF4 promotes its degradation, a new scenario that can contribute to reducing the threshold required for caspase activation.

As indirect consequences elicited by proteotoxic stress can favor cell death, the accumulation of ROS and the alterations of calcium homeostasis must be mentioned. These cofactors can be the deleterious corollaries of the progressive impairments in the clearance capacities normally operated by UPS and autophagy. Accumulation of unfolded proteins and aggregates impact ER and mitochondrial functions, thus leading to alterations in ROS and calcium levels that, in turn, engage further signaling events leading to cell death. How these events integrate with classic apoptotic signaling is not clear. In some studies, induction of oxidative stress can be observed in the initial phases of proteotoxic stress [84,151,152]. Certainly, the augmented levels of ROS and calcium can be responsible for the induction of alternative forms of death in response to the proteotoxic stress observed in different studies [153,154]. In general, the appearance of nonapoptotic or alternative forms of cell death in response to proteotoxic stress is a less investigated item [155–157]. Frequently, these necrotic-like responses appear when apoptosis is defective. Interestingly, in a model of toxicity elicited by mutant Huntingtin, a new hypothesis to explain the apoptotic/necrotic switch has been proposed. If the sequestered mutant protein is soluble, cells are characterized by hyperpolarized mitochondrial membrane potential and increased levels of reactive oxygen species, and cell death occurs via apoptosis. Instead, when mutant Huntingtin is present as aggregates, where other cellular proteins can be sequestered, a collapse in mitochondrial potential, cellular quiescence, and deactivated apoptosis occur. Overall, this response curtails cellular metabolism and leads to a slow death by necrosis [158]. Clearly, this model must be verified with general inducers of proteotoxic stress, but it is an interesting hypothesis that deserves further study. Necrotic proteotoxicity can be hampered by NRF2, possibly through the formation of autophagosomes aimed at decreasing the ubiquitylated protein aggregates [159]. Finally, in the necrotic arena, a new role of NOXA cannot be excluded, since its mitochondrial targeting domain (MTD) can trigger mitochondrial fragmentation and necrosis [160].

Necroptosis is a specific form of cell death activated through the serine/threonine kinases RIPK1 and RIPK3 and the pseudokinase MLKL [161]. Compounds that trigger necroptosis can also activate UPR [162,163]. This observation suggests some links between proteotoxic stress and necroptosis. However, as similarly discussed below for ferroptosis, it is not simple to discriminate if UPR engagement is within a pro-survival effort rather than an effective contribution to the cell death process. Importantly,

a study aimed at investigating the involvement of UPR in the "classical necroptosis" induced by TNF-α discovered that two commonly used PERK inhibitors, GSK2606414 and GSK2656157, are indeed potent RIPK1 inhibitors [164]. Certainly, RIPK1, in its pleiotropic activities, can also antagonize proteotoxic stress-induced cell death. Overexpression of RIPK1 enhances the induction of autophagy and confers resistance of melanoma cells to ER stress-induced cell death [165]. Finally, during UPR and ER stress induced by hypoxia, which characterize preeclampsia, the contribution of necroptosis has been excluded. Instead, pyroptosis linked to the activation of the NLRP3 inflammasome, through the activity of thioredoxin-interacting protein (TXNIP), has been proposed [166].

Ferroptosis is a specific form of iron-dependent cell death, characterized by the accumulation of lipid peroxides due to the failure of glutathione-dependent antioxidant defenses [167,168]. Few data are available about the implications of ferroptosis in the proteotoxic stress-induced cell death. It is possible that connections exist, as recently discussed [169]. In particular, if we take into account that different ferroptotic agents can also trigger UPR [170,171], the involvement of UPR, at least in the initial phase, can be viewed as a pro-survival strategy [172], as discussed above for necroptosis. On the other hand, ROS could be the link between ferroptosis and proteotoxic stress. For example, glutathione peroxidases can regulate ferroptosis through their ability to reduce hydroperoxy groups in complex lipids and to silence lipoxygenases. However, they can also play a part during the oxidative protein-folding control in ER by reacting with protein isomerase as an alternate substrate [173].

A final important point concerns the heterogenous response of cell populations to proteotoxic stress. It is well known that although exposed to the same intensity of proteotoxic stress, some cells die while others survive. Clearly, the availability of a pool of chaperones is a critical condition. Particularly, for ER stress, the ER resident chaperone BIP is a key factor during the switch from proteostasis to proteotoxicity [174]. HSF1 is the master regulator of chaperone expression in response to proteotoxic stress. Under stress conditions, HSF1 is phosphorylated and it trimerizes and binds regulative elements in chaperone genes, thus driving their transcription [175]. Recently, a model has been proposed where membrane-less organelle foci of HSF1 regulate the cell decision in terms of survival/death. In the presence of prolonged stress, the biophysical properties of HSF1 foci can undergo a change. Small, fluid condensates enlarge into indissoluble gel-like arrangements, where HSF1 is immobilized. Consequently, chaperone gene expression decreases, leading to cell death by apoptosis [176].

5. Proteotoxic Stress in Cancer Cells

For a detailed discussion on proteotoxic stress and cancer, we refer to previously published reviews, some of them cited thereafter. In this section, we would like to provide only a general overview of this topic.

The protein synthesis process is intrinsically prone to errors. It has been estimated that in mammalian cells, more than 30% of newly synthesized proteins are degraded by the proteasome within minutes from their translation [177]. These quickly degraded proteins are called defective ribosomal proteins (DRiPs) or rapidly degraded polypeptides (RDPs). If not removed, DRiPs can increase proteasome loading and the consequent induction of proteotoxic stress [178]. Cancer cells generally boost protein synthesis and, therefore, DRiPs accumulate more rapidly than in normal cells [93,179]. For example, cancer cells frequently overactivate the mTORC1 pathway. This pathway is required to promote elevated levels of protein synthesis, a condition that obliges cancer cells to pay tribute to the proteasome to avoid the accumulation of misfolded proteins. This dependence from the proteasome has been exploited to kill cancer cells via small compounds blocking UPS [36,180–182]. The fundamental role of the proteostasis in cancer cells is further underlined by the formation of immunoproteasomes as a secondary mechanism to manage the increased proteotoxic stress arising in mutated cells for RAS, PTEN, TSC1, or mTORC1 [180,183]. Environmental conditions, which are commonly exacerbated in tumors, such as hypoxia, oxidative stress, and nutrient deprivation, are additional inducers of protein misfolding and proteotoxic stress [84,94,178].

A still poorly explored aspect of proteotoxic stress is its connection with cellular metabolism [184,185]. It seems that the switch towards an oxidative metabolism rather than glycolysis renders cancer cells resistant to the UPS inhibitor bortezomib. The regulation of the mitochondrial state could represent an additional mechanism of adaptation to proteotoxic stress that could be addressed from a therapeutic perspective [186].

In addition to the amplified levels of protein synthesis and the environmental conditions, genetic alterations accumulated in cancer are other sources of proteotoxic stress. Aneuploidy, copy number variations, and point mutations are common genetic alterations in cancers that can induce proteotoxic stress [187–191]. Aneuploidy is also associated with many types of stresses in cancer cells, which include both metabolic and oxidative stresses [192]. In aneuploid cells, protein complex stoichiometry imbalances are important causes of protein aggregation and proteotoxic stress induction. The uncoordinated expression of a single subunit of protein complexes, encoded on excess chromosomes, leads to its aggregate state. The excess subunits are degraded, or they aggregate, with protein aggregation nearly as effective as protein degradation for lowering the levels of excess proteins [193]. In aneuploid cells, the induction of HSF1 is also, in some way, compromised. This deficit is transduced in the impaired expression of HSP90, accumulation of misfolded proteins, and the appearance of proteotoxic stress [194]. Similarly, overexpression of genes, as well as the accumulation of mutations in coding regions, can alter normal proteostasis [195]. These mutations would produce protein variants that are more prone to misfolding, degradation, and aggregation [191].

Cancer cells convive with proteotoxic stress by upregulating all the possible mechanisms that are able to maintain proteostasis [196–204]. As a consequence, cancer cells are more dependent on the presence of HSPs from UPS for their growth and survival [205,206]. Among HSPs, HSP90s and HSP70s are critical for escaping from antiproliferative signals, resisting cell death, and evading senescence. Additionally, these chaperones are involved in many distinct tracts of cancer cells, including drug resistance, angiogenesis, and metastasis [207,208]. Clearly, impacting these adaptive mechanisms has important consequences to the survival of cancer cells [209,210]. This dependence has attracted interest in developing therapeutic approaches aimed at switching-off these adaptations and thus unleashing all the dramatic consequences of the unresolved proteotoxic stress [210–218]. In some circumstances, adaptations to proteotoxic stress can favor the resistance to other therapeutic regiments, as observed for HSF1 and the resistance to the receptor tyrosine kinase (RTK) inhibitor lapatinib in breast cancer [219]. Interestingly, the master regulators of ER stress and UPR (ATF3/4/5/6 and CHOP) are highly expressed in a fraction of bladder, kidney, and prostate cancers, indicative of high levels of proteotoxic stress (Figure 3A). These subgroups of tumors exhibit aggressive behavior characterized by a reduction of overall survival (Figure 3B).

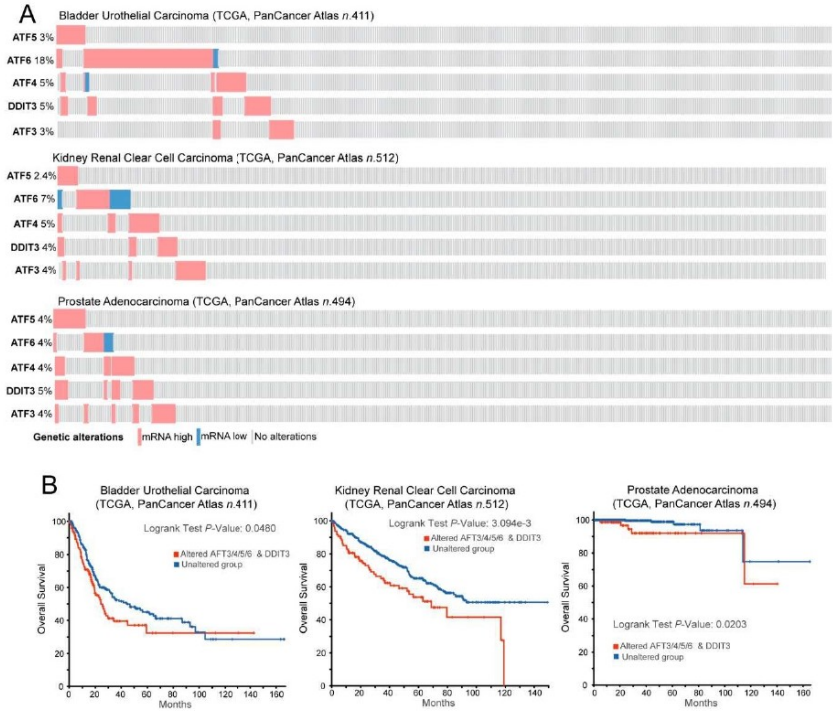

Figure 3. ATF factors in cancer. (**A**) Oncoprint of mRNA expression variations for the indicated TFs. Data were obtained from the TCGA database and include RNAseq data from patients, as indicated. The heatmap shows the alterations in the expression levels and was generated through cBioPortal (http://www.cbioportal.org). mRNA expression z-scores are relative to diploid samples (RNA Seq V2 RSEM). (**B**) Kaplan–Meier survival analysis related to the alterations in the mRNA levels of the ATF network. All cases were analyzed and clustered into two groups according to ATF3/4/5/6 and DDIT3/CHOP alterations in the expression levels, as illustrated in (**A**). Data were generated through cBioPortal (http://www.cbioportal.org).

6. Conclusions

Proteostasis is a fundamental task for every cell. The evolution has sculptured elaborate interconnected mechanisms to maintain proteostasis. Some of these mechanisms have been highly conserved through evolution and, with the appearance of eukaryotic cells, each subcellular compartment has evolved a dedicated set of strategies [220,221]. Proteostasis alterations and the induction of proteotoxic stress are responsible for several pathological conditions, particularly in neurodegenerative diseases, including Huntington's, Parkinson's, amyotrophic lateral sclerosis, and Alzheimer's diseases [222]. On the other hand, small compounds that are able to trigger proteotoxic stress or target the machinery resolving proteotoxic stress are actively investigated as anticancer agents [93]. Undoubtedly, the central role played by proteotoxic stress in the cell life/death decision guarantees that by studying its regulation or developing new compounds aimed to improve or impair its appearance, benefits for the human health will be generated.

Author Contributions: All authors have read and agreed to the published version of the manuscript. C.B. conceptualized and designed the review. L.I. and C.B. wrote the paper and created the figures.

Funding: This research was funded by Interreg Italia–Osterreich rITAT1054 EPIC in a grant to C.B.

Conflicts of Interest: The authors declare no conflict of interest. The funders had no role in the design of the study; in the collection, analyses, or interpretation of data; in the writing of the manuscript, or in the decision to publish the results.

References

1. Amm, I.; Sommer, T.; Wolf, D.H. Protein quality control and elimination of protein waste: The role of the ubiquitin-proteasome system. *Biochim. Biophys. Acta* **2014**, *1843*, 182–196. [CrossRef]
2. Balchin, D.; Hayer-Hartl, M.; Hartl, F.U. In vivo aspects of protein folding and quality control. *Science* **2016**, *353*, aac4354. [CrossRef]
3. Anfinsen, C.B. Principles that govern the folding of protein chains. *Science* **1973**, *181*, 223–230. [CrossRef]
4. Ellis, R.J.; Minton, A.P. Protein aggregation in crowded environments. *Biol. Chem.* **2006**, *387*, 485–497. [CrossRef] [PubMed]
5. Morimoto, R.I. Proteotoxic stress and inducible chaperone networks in neurodegenerative disease and aging. *Genes Dev.* **2008**, *22*, 1427–1438. [CrossRef] [PubMed]
6. Gokhale, S.; Nyayanit, D.; Gadgil, C. A systems view of the protein expression process. *Syst. Synth. Biol.* **2011**, *5*, 139–150. [CrossRef] [PubMed]
7. Hipp, M.S.; Kasturi, P.; Hartl, F.U. The proteostasis network and its decline in ageing. *Nat. Rev. Mol. Cell Biol.* **2019**, *20*, 421–435. [CrossRef]
8. Taylor, R.C.; Dillin, A. Aging as an event of proteostasis collapse. *Cold Spring Harb. Perspect. Biol.* **2011**, *3*, a004440. [CrossRef]
9. Labbadia, J.; Morimoto, R.I. The biology of proteostasis in aging and disease. *Annu. Rev. Biochem.* **2015**, *84*, 435–464. [CrossRef]
10. Higuchi-Sanabria, R.; Frankino, P.A.; Paul, J.W., III; Tronnes, S.U.; Dillin, A. A futile battle? Protein quality control and the stress of aging. *Dev. Cell* **2018**, *44*, 139–163. [CrossRef]
11. Brehme, M.; Voisine, C.; Rolland, T.; Wachi, S.; Soper, J.H.; Zhu, Y.; Orton, K.; Villella, A.; Garza, D.; Vidal, M.; et al. A chaperome subnetwork safeguards proteostasis in aging and neurodegenerative disease. *Cell Rep.* **2014**, *9*, 1135–1150. [CrossRef] [PubMed]
12. Bohush, A.; Bieganowski, P.; Filipek, A. Hsp90 and its co-chaperones in neurodegenerative diseases. *Int. J. Mol. Sci.* **2019**, *20*, 4976. [CrossRef] [PubMed]
13. Hartl, F.U.; Bracher, A.; Hayer-Hartl, M. Molecular chaperones in protein folding and proteostasis. *Nature* **2011**, *475*, 324–332. [CrossRef] [PubMed]
14. Balchin, D.; Miličić, G.; Strauss, M.; Hayer-Hartl, M.; Hartl, F.U. Pathway of actin folding directed by the eukaryotic chaperonin TRiC. *Cell* **2018**, *174*, 1507–1521. [CrossRef] [PubMed]
15. Preissler, S.; Deuerling, E. Ribosome-associated chaperones as key players in proteostasis. *Trends Biochem. Sci.* **2012**, *37*, 274–283. [CrossRef] [PubMed]
16. Kramer, G.; Shiber, A.; Bukau, B. Mechanisms of cotranslational maturation of newly synthesized proteins. *Annu. Rev. Biochem.* **2019**, *88*, 337–364. [CrossRef]
17. Hayer-Hartl, M.; Bracher, A.; Hartl, F.U. The GroELGroES chaperonin machine: A nano-cage for protein folding. *Trends Biochem. Sci.* **2016**, *41*, 62–76. [CrossRef]
18. Carra, S.; Alberti, S.; Arrigo, P.A.; Benesch, J.L.; Benjamin, I.J.; Boelens, W.; Bartelt-Kirbach, B.; Brundel, B.; Buchner, J.; Bukau, B.; et al. The growing world of small heat shock proteins: From structure to functions. *Cell Stress Chaperones* **2017**, *22*, 601–611. [CrossRef]
19. Hartl, F.U. Molecular chaperones in cellular protein folding. *Nature* **1996**, *381*, 571–579. [CrossRef]
20. Powers, E.T.; Balch, W.E. Diversity in the origins of proteostasis networks—A driver for protein function in evolution. *Nat. Rev. Mol. Cell Biol.* **2013**, *14*, 237–248. [CrossRef]
21. Taipale, M.; Krykbaeva, I.; Koeva, M.; Kayatekin, C.; Westover, K.D.; Karras, G.I.; Lindquist, S. Quantitative analysis of HSP90-client interactions reveals principles of substrate recognition. *Cell* **2012**, *150*, 987–1001. [CrossRef] [PubMed]

22. Taipale, M.; Tucker, G.; Peng, J.; Krykbaeva, I.; Lin, Z.Y.; Larsen, B.; Choi, H.; Berger, B.; Gingras, A.C.; Lindquist, S. A quantitative chaperone interaction network reveals the architecture of cellular protein homeostasis pathways. *Cell* **2014**, *158*, 434–448. [CrossRef] [PubMed]
23. Rodina, A.; Wang, T.; Yan, P.; Gomes, E.D.; Dunphy, M.P.; Pillarsetty, N.; Koren, J.; Gerecitano, J.F.; Taldone, T.; Zong, H.; et al. The epichaperome is an integrated chaperome network that facilitates tumour survival. *Nature* **2016**, *538*, 397–401. [CrossRef] [PubMed]
24. De Thonel, A.; Mezger, V.; Garrido, C. Implication of Heat Shock Factors in tumorigenesis: Therapeutical potential. *Cancers* **2011**, *3*, 1158–1181. [CrossRef] [PubMed]
25. Esser, C.; Alberti, S.; Höhfeld, J. Cooperation of molecular chaperones with the ubiquitin/proteasome system. *Biochim. Biophys. Acta* **2004**, *1695*, 171–188. [CrossRef] [PubMed]
26. Kundrat, L.; Regan, L. Balance between folding and degradation for Hsp90-dependent client proteins: A key role for CHIP. *Biochemistry* **2010**, *49*, 7428–7438. [CrossRef]
27. Hershko, A.; Ciechanover, A. The ubiquitin system. *Annu. Rev. Biochem.* **1998**, *67*, 425–479. [CrossRef]
28. Ciechanover, A. The ubiquitin proteolytic system: From a vague idea, through basic mechanisms, and onto human diseases and drug targeting. *Neurology* **2006**, *66*, S7–S19. [CrossRef]
29. Demarchi, F.; Brancolini, C. Altering protein turnover in tumor cells: New opportunities for anti-cancer therapies. *Drug Resist. Updates* **2005**, *8*, 359–368. [CrossRef]
30. Chowdhury, M.; Enenkel, C. Intracellular dynamics of the Ubiquitin-Proteasome-System. *F1000Research* **2015**, *4*, 367. [CrossRef]
31. Morreale, F.E.; Walden, H. Types of ubiquitin ligases. *Cell* **2016**, *165*, 248.e1. [CrossRef] [PubMed]
32. Buetow, L.; Huang, D.T. Structural insights into the catalysis and regulation of E3 ubiquitin ligases. *Nat. Rev. Mol. Cell Biol.* **2016**, *17*, 626–642. [CrossRef] [PubMed]
33. Glickman, M.H.; Ciechanover, A. The ubiquitin-proteasome proteolytic pathway: Destruction for the sake of construction. *Physiol. Rev.* **2002**, *82*, 373–428. [CrossRef] [PubMed]
34. Nandi, D.; Tahiliani, P.; Kumar, A.; Chandu, D. The ubiquitin-proteasome system. *J. Biosci.* **2006**, *31*, 137–155. [CrossRef]
35. D'Arcy, P.; Wang, X.; Linder, S. Deubiquitinase inhibition as a cancer therapeutic strategy. *Pharmacol. Ther.* **2015**, *147*, 32–54. [CrossRef]
36. Sgorbissa, A.; Potu, H.; Brancolini, C. Isopeptidases in anticancer therapy: Looking for inhibitors. *Am. J. Transl. Res.* **2010**, *2*, 235–247.
37. Rehman, S.A.A.; Kristariyanto, Y.A.; Choi, S.Y.; Labib, K.; Hofmann, K.; Kulathu, Y. MINDY-1 is a member of an evolutionarily conserved and structurally distinct new family of deubiquitinating enzymes. Molecular. *Cell* **2016**, *63*, 146–155. [CrossRef]
38. Kuo, C.L.; Goldberg, A.L. Ubiquitinated proteins promote the association of proteasomes with the deubiquitinating enzyme Usp14 and the ubiquitin ligase Ube3c. *Proc. Natl. Acad. Sci. USA* **2017**, *114*, E3404–E3413. [CrossRef]
39. Aleo, E.; Henderson, C.J.; Fontanini, A.; Solazzo, B.; Brancolini, C. Identification of new compounds that trigger apoptosome-independent caspase activation and apoptosis. *Cancer Res.* **2006**, *66*, 9235–9244. [CrossRef]
40. Tian, Z.; D'Arcy, P.; Wang, X.; Ray, A.; Tai, Y.T.; Hu, Y.; Carrasco, R.D.; Richardson, P.; Linder, S.; Chauhan, D.; et al. A novel small molecule inhibitor of deubiquitylating enzyme USP14 and UCHL5 induces apoptosis in multiple myeloma and overcomes bortezomib resistance. *Blood* **2014**, *123*, 706–716. [CrossRef]
41. Zhang, X.; Pellegrini, P.; Saei, A.A.; Hillert, E.K.; Mazurkiewicz, M.; Olofsson, M.H.; Zubarev, R.A.; D'Arcy, P.; Linder, S. The deubiquitinase inhibitor b-AP15 induces strong proteotoxic stress and mitochondrial damage. *Biochem. Pharmacol.* **2018**, *156*, 291–301. [CrossRef]
42. Baumeister, W.; Walz, J.; Zühl, F.; Seemüller, E. The proteasome: Paradigm of a self-compartmentalizing protease. *Cell* **1998**, *92*, 367–380. [CrossRef]
43. Voges, D.; Zwickl, P.; Baumeister, W. The 26S proteasome: A molecular machine designed for controlled proteolysis. *Annu. Rev. Biochem.* **1999**, *68*, 1015–1068. [CrossRef] [PubMed]
44. Kisselev, A.F.; Akopian, T.N.; Castillo, V.; Goldberg, A.L. Proteasome active sites allosterically regulate each other, suggesting a cyclical bite-chew mechanism for protein breakdown. *Mol. Cell* **1999**, *4*, 395–402. [CrossRef]

45. Beck, F.; Unverdorben, P.; Bohn, S.; Schweitzer, A.; Pfeifer, G.; Sakata, E.; Nickell, S.; Plitzko, J.M.; Villa, E.; Baumeister, W.; et al. Near-atomic resolution structural model of the yeast 26S proteasome. *Proc. Natl. Acad. Sci. USA* **2012**, *109*, 14870–14875. [CrossRef] [PubMed]
46. de la Peña, A.H.; Goodall, E.A.; Gates, S.N.; Lander, G.C.; Martin, A. Substrate-engaged 26S proteasome structures reveal mechanisms for ATP-hydrolysis-driven translocation. *Science* **2018**, *362*, eaav0725. [CrossRef]
47. Dong, Y.; Zhang, S.; Wu, Z.; Li, X.; Wang, W.L.; Zhu, Y.; Stoilova-McPhie, S.; Lu, Y.; Finley, D.; Mao, Y. Cryo-EM structures and dynamics of substrate-engaged human 26S proteasome. *Nature* **2019**, *565*, 49–55. [CrossRef] [PubMed]
48. Tomita, T.; Matouschek, A. Substrate selection by the proteasome through initiation regions. *Protein Sci.* **2019**, *28*, 1222–1232. [CrossRef]
49. Mevissen, T.E.T.; Komander, D. Mechanisms of deubiquitinase specificityand regulation. *Annu. Rev. Biochem.* **2017**, *86*, 159–192. [CrossRef]
50. Galluzzi, L.; Baehrecke, E.H.; Ballabio, A.; Boya, P.; Bravo-San Pedro, J.M.; Cecconi, F.; Choi, A.M.; Chu, C.T.; Codogno, P.; Colombo, M.I.; et al. Molecular definitions of autophagy and related processes. *EMBO J.* **2017**, *36*, 1811–1836. [CrossRef]
51. García-Prat, L.; Martínez-Vicente, M.; Perdiguero, E.; Ortet, L.; Rodríguez-Ubreva, J.; Rebollo, E.; Ruiz-Bonilla, V.; Gutarra, S.; Ballestar, E.; Serrano, A.L.; et al. Autophagy maintains stemness by preventing senescence. *Nature* **2016**, *529*, 37–42. [CrossRef] [PubMed]
52. Carra, S.; Seguin, S.J.; Lambert, H.; Landry, J. HspB8 chaperone activity toward poly(Q)-containing proteins depends on its association with Bag3, a stimulator of macroautophagy. *J. Biol. Chem.* **2008**, *283*, 1437–1444. [CrossRef] [PubMed]
53. Gamerdinger, M.; Hajieva, P.; Kaya, A.M.; Wolfrum, U.; Hartl, F.U.; Behl, C. Protein quality control during aging involves recruitment of the macroautophagy pathway by BAG3. *EMBO J.* **2009**, *28*, 889–901. [CrossRef] [PubMed]
54. Arndt, V.; Dick, N.; Tawo, R.; Dreiseidler, M.; Wenzel, D.; Hesse, M.; Fürst, D.O.; Saftig, P.; Saint, R.; Fleischmann, B.K.; et al. Chaperone-assisted selective autophagy is essential for muscle maintenance. *Curr. Biol.* **2010**, *20*, 143–148. [CrossRef] [PubMed]
55. Kaushik, S.; Cuervo, A.M. The coming of age of chaperone-mediated autophagy. *Nat. Rev. Mol. Cell Biol.* **2018**, *19*, 365–381. [CrossRef] [PubMed]
56. Suraweera, A.; Münch, C.; Hanssum, A.; Bertolotti, A. Failure of amino acid homeostasis causes cell death following proteasome inhibition. *Mol. Cell* **2012**, *48*, 242–253. [CrossRef]
57. Zhang, T.; Shen, S.; Qu, J.; Ghaemmaghami, S. Global analysis of cellular protein flux quantifies the selectivity of basal autophagy. *Cell Rep.* **2016**, *14*, 2426–2439. [CrossRef]
58. Dikic, I. Proteasomal and autophagic degradation systems. *Annu. Rev. Biochem.* **2017**, *86*, 193–224. [CrossRef]
59. Li, J.; Zhang, D.; Wiersma, M.; Brundel, B.J.J.M. Role of autophagy in proteostasis: Friend and foe in cardiac diseases. *Cells* **2018**, *7*, 279. [CrossRef]
60. Hershko, A.; Ciechanover, A.; Varshavsky, A. Basic medical research award. The ubiquitin system. *Nat. Med.* **2000**, *6*, 1073–1081. [CrossRef]
61. Pickart, C.M.; Eddins, M.J. Ubiquitin: Structures, functions, mechanisms. *Biochim. Biophys. Acta* **2004**, *1695*, 55–72. [CrossRef] [PubMed]
62. Wilkinson, J.C.; Wilkinson, A.S.; Scott, F.L.; Csomos, R.A.; Salvesen, G.S.; Duckett, C.S. Neutralization of Smac/Diablo by Inhibitors of Apoptosis (IAPs): A caspase-independent mechanism for apoptotic inhibition. *J. Biol. Chem.* **2004**, *279*, 51082–51090. [CrossRef] [PubMed]
63. Peng, C.; Trojanowski, J.Q.; Lee, V.M. Protein transmission in neurodegenerative disease. *Nat. Rev. Neurol.* **2020**, *16*, 199–212. [CrossRef] [PubMed]
64. Walter, P.; Ron, D. The Unfolded Protein Response: From stress pathway to homeostatic regulation. *Science* **2011**, *334*, 1081–1086. [CrossRef]
65. Auner, H.W.; Moody, A.M.; Ward, T.H.; Kraus, M.; Milan, E.; May, P.; Chaidos, A.; Driessen, C.; Cenci, S.; Dazzi, F.; et al. Combined inhibition of p97 and the proteasome causes lethal disruption of the secretory apparatus in multiple myeloma cells. *PLoS ONE* **2013**, *8*, e74415. [CrossRef] [PubMed]
66. Obeng, E.A.; Carlson, L.M.; Gutman, D.M.; Harrington, W.J., Jr.; Lee, K.P.; Boise, L.H. Proteasome inhibitors induce a terminal unfolded protein response in multiple myeloma cells. *Blood* **2006**, *107*, 4907–4916. [CrossRef] [PubMed]

67. Rajasekaran, N.S.; Connell, P.; Christians, E.S.; Yan, L.J.; Taylor, R.P.; Orosz, A.; Zhang, X.Q.; Stevenson, T.J.; Peshock, R.M.; Leopold, J.A.; et al. Human alpha B-crystallin mutation causes oxido-reductive stress and protein aggregation cardiomyopathy in mice. *Cell* **2007**, *130*, 427–439. [CrossRef]
68. Malhotra, J.D.; Kaufman, R.J. Endoplasmic reticulum stress and oxidative stress: A vicious cycle or a double-edged sword? *Antioxid. Redox Signal.* **2007**, *9*, 2277–2293. [CrossRef]
69. Kannan, S.; Muthusamy, V.R.; Whitehead, K.J.; Wang, L.; Gomes, A.V.; Litwin, S.E.; Kensler, T.W.; Abel, E.D.; Hoidal, J.R.; Rajasekaran, N.S. Nrf2 deficiency prevents reductive stress-induced hypertrophic cardiomyopathy. *Cardiovasc. Res.* **2013**, *100*, 63–73. [CrossRef]
70. Ri, M. Endoplasmic-reticulum stress pathway-associated mechanisms of action of proteasome inhibitors in multiple myeloma. *Int. J. Hematol.* **2016**, *104*, 273–280. [CrossRef]
71. Lafont, E. Stress management: Death receptor signalling and cross-talks with the unfolded protein response in cancer. *Cancers* **2020**, *12*, 1113. [CrossRef] [PubMed]
72. Hetz, C.; Zhang, K.; Kaufman, R.J. Mechanisms, regulation and functions of the unfolded protein response. *Nat. Rev. Mol. Cell Biol.* **2020**. [CrossRef] [PubMed]
73. Rao, R.V.; Ellerby, H.M.; Bredesen, D.E. Coupling endoplasmic reticulum stress to the cell death program. *Cell Death Differ.* **2004**, *11*, 372–380. [CrossRef] [PubMed]
74. Kaufman, R.J. Orchestrating the unfolded protein response in health and disease. *J. Clin. Investig.* **2002**, *110*, 1389–1398. [CrossRef] [PubMed]
75. Harding, H.P.; Calfon, M.; Urano, F.; Novoa, I.; Ron, D. Transcriptional and translational control in the mammalian unfolded protein response. *Annu. Rev. Cell Dev. Biol.* **2002**, *18*, 575–599. [CrossRef]
76. Szegezdi, E.; Logue, S.E.; Gorman, A.M.; Samali, A. Mediators of endoplasmic reticulum stress-induced apoptosis. *EMBO Rep.* **2006**, *7*, 880–885. [CrossRef] [PubMed]
77. Furukawa, M.; Xiong, Y. BTB protein Keap1 targets antioxidant transcription factor Nrf2 for ubiquitination by the Cullin 3-Roc1 ligase. *Mol. Cell. Biol.* **2005**, *25*, 162–171. [CrossRef]
78. Bobrovnikova-Marjon, E.; Grigoriadou, C.; Pytel, D.; Zhang, F.; Ye, J.; Koumenis, C.; Cavener, D.; Diehl, J.A. PERK promotes cancer cell proliferation and tumor growth by limiting oxidative DNA damage. *Oncogene* **2010**, *29*, 3881–3895. [CrossRef]
79. Xing, H.Y.; Cai, Y.Q.; Wang, X.F.; Wang, L.L.; Li, P.; Wang, G.Y.; Chen, J.H. The cytoprotective effect of hyperoside against oxidative stress is mediated by the Nrf2-ARE signaling pathway through GSK-3β inactivation. *PLoS ONE* **2015**, *10*, e0145183. [CrossRef]
80. Zhang, W.; Hietakangas, V.; Wee, S.; Lim, S.C.; Gunaratne, J.; Cohen, S.M. ER stress potentiates insulin resistance through PERK-mediated FOXO phosphorylation. *Genes Dev.* **2013**, *27*, 441–449. [CrossRef]
81. You, S.; Li, H.; Hu, Z.; Zhang, W. eIF2α kinases PERK and GCN2 act on FOXO to potentiate FOXO activity. *Genes Cells* **2018**, *23*, 786–793. [CrossRef] [PubMed]
82. Bobrovnikova-Marjon, E.; Pytel, D.; Riese, M.J.; Vaites, L.P.; Singh, N.; Koretzky, G.A.; Witze, E.S.; Diehl, J.A. PERK utilizes intrinsic lipid kinase activity to generate phosphatidic acid, mediate Akt activation, and promote adipocyte differentiation. *Mol. Cell. Biol.* **2012**, *32*, 2268–2278. [CrossRef] [PubMed]
83. Pytel, D.; Gao, Y.; Mackiewicz, K.; Katlinskaya, Y.V.; Staschke, K.A.; Paredes, M.C.G.; Yoshida, A.; Qie, S.; Zhang, G.; Chajewski, O.S.; et al. PERK is a haploinsufficient tumor suppressor: Gene dose determines tumor-suppressive versus tumor promoting properties of PERK in melanoma. *PLoS Genet.* **2016**, *12*, e1006518. [CrossRef] [PubMed]
84. McConkey, D.J. The integrated stress response and proteotoxicity in cancer therapy. *Biochem. Biophys. Res. Commun.* **2017**, *482*, 450–453. [CrossRef] [PubMed]
85. White, M.C.; Schroeder, M.D.; Zhu, K.; Xiong, K.; McConkey, D.J. HRI-mediated translational repression reduces proteotoxicity and sensitivity to Bortezomib in human pancreatic cancer cells. *Oncogene* **2018**, *37*, 4413–4427. [CrossRef]
86. Wang, M.; Wey, S.; Zhang, Y.; Ye, R.; Lee, A.S. Role of the unfolded protein response regulator GRP78/BiP indevelopment, cancer, and neurological disorders. *Antioxid. Redox Signal.* **2009**, *11*, 2307–2316. [CrossRef]
87. Couillault, C.; Fourquet, P.; Pophillat, M.; Ewbank, J.J. A UPR-independent infection-specific role for a BiP/GRP78 protein in the control of antimicrobial peptide expression in C. elegans epidermis. *Virulence* **2012**, *3*, 299–308. [CrossRef]
88. Rutkowski, D.T.; Kaufman, R.J. A trip to the ER: Coping with stress. *Trends Cell Biol.* **2004**, *14*, 20–28. [CrossRef]

89. Yoshida, H.; Matsui, T.; Yamamoto, A.; Okada, T.; Mori, K. XBP1 mRNA is induced by ATF6 and spliced by IRE1 in response to ER stress to produce a highly active transcription factor. *Cell* **2001**, *107*, 881–891. [CrossRef]
90. Lee, A.H.; Iwakoshi, N.N.; Glimcher, L.H. XBP-1 regulates a subset of endoplasmic reticulum resident chaperone genes in the unfolded protein response. *Mol. Cell. Biol.* **2003**, *23*, 7448–7459. [CrossRef]
91. Hillary, R.F.; FitzGerald, U. A lifetime of stress: ATF6 in development and homeostasis. *J. Biomed. Sci.* **2018**, *25*, 48. [CrossRef] [PubMed]
92. Ron, D. Translational control in the endoplasmic reticulum stress response. *J. Clin. Investig.* **2002**, *110*, 1383–1388. [CrossRef] [PubMed]
93. Guang, M.H.Z.; Kavanagh, E.L.; Dunne, L.P.; Dowling, P.; Zhang, L.; Lindsay, S.; Bazou, D.; Goh, C.Y.; Hanley, C.; Bianchi, G.; et al. Targeting proteotoxic stress in cancer: A review of the role that protein quality control pathways play in oncogenesis. *Cancers* **2019**, *11*, 66. [CrossRef] [PubMed]
94. Iurlaro, R.; Munoz-Pinedo, C. Cell death induced by endoplasmic reticulum stress. *FEBS J.* **2016**, *283*, 2640–2652. [CrossRef]
95. Cano-González, A.; Mauro-Lizcano, M.; Iglesias-Serret, D.; Gil, J.; López-Rivas, A. Involvement of both caspase-8 and Noxa-activated pathways in Endoplasmic Reticulum stress-induced apoptosis in triple-negative breast tumor cells. *Cell Death Dis.* **2018**, *9*, 134. [CrossRef]
96. Zhu, G.Y.; Li, Y.W.; Tse, A.K.W.; Hau, D.K.P.; Leung, C.H.; Yu, Z.L.; Fong, W.L. 20(s)-protopanaxadiol, a metabolite of ginsenosides, induced cell apoptosis through Endoplasmic Reticulum stress in human hepatocarcinoma HepG2 cells. *Eur. J. Pharmacol.* **2011**, *668*, 88–98. [CrossRef]
97. Manini, I.; Sgorbissa, A.; Potu, H.; Tomasella, A.; Brancolini, C. The DeISGylase USP18 limits TRAIL-induced apoptosis through the regulation of TRAIL levels: Cellular levels of TRAIL influences responsiveness to TRAIL-induced apoptosis. *Cancer Biol. Ther.* **2013**, *14*, 1158–1166. [CrossRef]
98. Martín-Pérez, R.; Palacios, C.; Yerbes, R.; Cano-González, A.; Iglesias-Serret, D.; Gil, J.; Reginato, M.J.; López-Rivas, A. Activated ERBB2/HER2 licenses sensitivity to apoptosis upon Endoplasmic Reticulum stress through a PERK-dependent pathway. *Cancer Res.* **2014**, *74*, 1766–1777. [CrossRef]
99. Lu, M.; Lawrence, D.A.; Marsters, S.; Acosta-Alvear, D.; Kimmig, P.; Mendez, A.S.; Paton, A.W.; Paton, J.C.; Walter, P.; Ashkenazi, A. Opposing unfolded-protein-response signals converge on death receptor 5 to control apoptosis. *Science* **2014**, *345*, 98–101. [CrossRef]
100. Chang, T.K.; Lawrence, D.A.; Lu, M.; Tan, J.; Harnoss, J.M.; Marsters, S.A.; Liu, P.; Sandoval, W.; Martin, S.E.; Ashkenazi, A. Coordination between two branches of the unfolded protein response determines apoptotic cell fate. *Mol. Cell* **2018**, *71*, 629–636.e5. [CrossRef]
101. Zhu, Z.C.; Liu, J.W.; Yang, C.; Li, M.J.; Wu, R.J.; Xiong, Z.Q. Targeting KPNB1 overcomes TRAIL resistance by regulating DR5, Mcl-1 and FLIP in glioblastoma cells. *Cell Death Dis.* **2019**, *10*, 118. [CrossRef] [PubMed]
102. Lam, M.; Marsters, S.A.; Ashkenazi, A.; Walter, P. Misfolded proteins bind and activate Death Receptor 5 to trigger apoptosis during unresolved endoplasmic reticulum stress. *Elife* **2020**, *9*, e52291. [CrossRef] [PubMed]
103. Sullivan, G.P.; O'Connor, H.; Henry, C.M.; Davidovich, P.; Clancy, D.M.; Albert, M.L.; Cullen, S.P.; Martin, S.J. TRAIL receptors serve as stress-associated molecular patterns to promote ER-stress-induced inflammation. *Dev. Cell* **2020**, *52*, 714–730.e5. [CrossRef] [PubMed]
104. Estornes, Y.; Aguileta, M.A.; Dubuisson, C.; De Keyser, J.; Goossens, V.; Kersse, K.; Samali, A.; Vandenabeele, P.; Bertrand, M.J.M. RIPK1 promotes death receptor-independent caspase-8-mediated apoptosis under unresolved ER stress conditions. *Cell Death Dis.* **2015**, *6*, e1798. [CrossRef]
105. Von Karstedt, S.; Walczak, H. An unexpected turn of fortune: Targeting TRAIL-Rs in KRAS-driven cancer. *Cell Death Discov.* **2020**, *6*, 14. [CrossRef]
106. Pitale, P.M.; Gorbatyuk, O.; Gorbatyuk, M. Neurodegeneration: Keeping ATF4 on a tight leash. *Front. Cell. Neurosci.* **2017**, *11*, 410. [CrossRef]
107. Rzymski, T.; Milani, M.; Singleton, D.C.; Harris, A.L. Role of ATF4 in regulation of autophagy and resistance to drugs and hypoxia. *Cell Cycle* **2009**, *8*, 3838–3847. [CrossRef]
108. Lassot, I.; Ségéral, E.; Berlioz-Torrent, C.; Durand, H.; Groussin, L.; Hai, T.; Benarous, R.; Margottin-Goguet, F. ATF4 degradation relies on a phosphorylation-dependent interaction with the SCF(betaTrCP) ubiquitin ligase. *Mol. Cell. Biol.* **2001**, *21*, 2192–2202. [CrossRef]

109. Wang, Q.; Mora-Jensen, H.; Weniger, M.A.; Perez-Galan, P.; Wolford, C.; Hai, T.; Ron, D.; Chen, W.; Trenkle, W.; Wiestner, A.; et al. ERAD inhibitors integrate ER stress with an epigenetic mechanism to activate BH3-only protein NOXA in cancer cells. *Proc. Natl. Acad. Sci. USA* **2009**, *106*, 2200–2205. [CrossRef]
110. Cnop, M.; Toivonen, S.; Igoillo-Esteve, M.; Salpea, P. Endoplasmic reticulum stress and eIF2α phosphorylation: The Achilles heel of pancreatic β cells. *Mol. Metab.* **2017**, *6*, 1024–1039. [CrossRef]
111. Palam, L.R.; Baird, T.D.; Wek, R.C. Phosphorylation of eIF2 facilitates ribosomal bypass of an inhibitory upstream ORF to enhance CHOP translation. *J. Biol. Chem.* **2011**, *286*, 10939–10949. [CrossRef] [PubMed]
112. Pathak, S.S.; Liu, D.; Li, T.; de Zavalia, N.; Zhu, L.; Li, J.; Karthikeyan, R.; Alain, T.; Liu, A.C.; Storch, K.F.; et al. The eIF2α kinase GCN2 modulates period and rhythmicity of the circadian clock by translational control of Atf4. *Neuron* **2019**, *104*, 724–735.e6. [CrossRef] [PubMed]
113. Ratan, R.R. The chemical biology of ferroptosis in the central nervous system. *Cell Chem. Biol.* **2020**, *27*, 479–498. [CrossRef] [PubMed]
114. Hiramatsu, N.; Messah, C.; Han, J.; LaVail, M.M.; Kaufman, R.J.; Lin, J.H. Translational and posttranslational regulation of XIAP by eIF2alpha and ATF4 promotes ER stress-induced cell death during the unfolded protein response. *Mol. Biol. Cell* **2014**, *25*, 1411–1420. [CrossRef] [PubMed]
115. Han, J.; Back, S.H.; Hur, J.; Lin, Y.H.; Gildersleeve, R.; Shan, J.; Yuan, C.L.; Krokowski, D.; Wang, S.; Hatzoglou, M.; et al. ER-stress-induced transcriptional regulation increases protein synthesis leading to cell death. *Nat. Cell Biol.* **2013**, *15*, 481–490. [CrossRef] [PubMed]
116. Donati, G.; Imbriano, C.; Mantovani, R. Dynamic recruitment of transcription factors and epigenetic changes on the ER stress response gene promoters. *Nucleic Acids Res.* **2006**, *34*, 3116–3127. [CrossRef] [PubMed]
117. Yamaguchi, H.; Wang, H.G. CHOP is involved in endoplasmic reticulum stress-induced apoptosis by enhancing DR5 expression in human carcinoma cells. *J. Biol. Chem.* **2004**, *279*, 45495–45502. [CrossRef]
118. Shiraishi, T.; Yoshida, T.; Nakata, S.; Horinaka, M.; Wakada, M.; Mizutani, Y.; Miki, T.; Sakai, T. Tunicamycin enhances tumor necrosis factor-related apoptosis-inducing ligand-induced apoptosis in human prostate cancer cells. *Cancer Res.* **2005**, *65*, 6364–6370. [CrossRef]
119. Hai, T.; Wolford, C.C.; Chang, Y.S. ATF3, a Hub of the cellular adaptive-response network, in the pathogenesis of diseases: Is modulation of inflammation a unifying component? *Gene Expr.* **2010**, *15*, 1–11. [CrossRef]
120. Edagawa, M.; Kawauchi, J.; Hirata, M.; Goshima, H.; Inoue, M.; Okamoto, T.; Murakami, A.; Maehara, Y.; Kitajima, S. Role of activating transcription factor 3 (ATF3) in endoplasmic reticulum (ER) Stress-induced sensitization of p53-deficient human colon cancer cells to tumor necrosis factor (TNF)-related apoptosis-inducing ligand (TRAIL)-mediated apoptosis through Up-regulation of death receptor 5 (DR5) by zerumbone and celecoxib. *J. Biol. Chem.* **2014**, *289*, 21544–21561. [CrossRef]
121. Li, T.; Su, L.; Lei, Y.; Liu, X.; Zhang, Y.; Liu, X. DDIT3 and KAT2A regulate TNFRSF10A and TNFRSF10B expression in endoplasmic reticulum stress-mediated apoptosis in human lung cancer cells. *J. Biol. Chem.* **2015**, *290*, 11108–11118. [CrossRef] [PubMed]
122. Iurlaro, R.; Püschel, F.; León-Annicchiarico, C.L.; O'Connor, H.; Martin, S.J.; Palou-Gramón, D.; Lucendo, E.; Muñoz-Pinedo, C. Glucose deprivation induces ATF4-mediated apoptosis through TRAIL death receptors. *Mol. Cell. Biol.* **2017**, *37*, e00479-16. [CrossRef] [PubMed]
123. Teske, B.F.; Fusakio, M.E.; Zhou, D.; Shan, J.; McClintick, J.N.; Kilberg, M.S.; Wek, R.C. CHOP induces activating transcription factor 5 (ATF5) to trigger apoptosis in response to perturbations in protein homeostasis. *Mol. Biol. Cell* **2013**, *24*, 2477–2490. [CrossRef] [PubMed]
124. Sharma, K.; Vu, T.T.; Cook, W.; Naseri, M.; Zhan, K.; Nakajima, W.; Harada, H. p53-independent Noxa induction by cisplatin is regulated by ATF3/ATF4 in head and neck squamous cell carcinoma cells. *Mol. Oncol.* **2018**, *12*, 788–798. [CrossRef] [PubMed]
125. Morsi, R.Z.; Hage-Sleiman, R.; Kobeissy, H.; Dbaibo, G. Noxa: Role in cancer pathogenesis and treatment. *Curr. Cancer Drug Targets* **2018**, *18*, 914–928. [CrossRef] [PubMed]
126. Oda, E.; Ohki, R.; Murasawa, H.; Nemoto, J.; Shibue, T.; Yamashita, T.; Tokino, T.; Taniguchi, T.; Tanaka, N. Noxa, a BH3-only member of the Bcl-2 family and candidate mediator of p53-induced apoptosis. *Science* **2000**, *288*, 1053–1058. [CrossRef] [PubMed]
127. Kim, J.Y.; Ahn, H.J.; Ryu, J.H.; Suk, K.; Park, J.H. BH3-only protein Noxa is a mediator of hypoxic cell death induced by Hypoxia-Inducible Factor 1alpha. *J. Exp. Med.* **2004**, *199*, 113–124. [CrossRef]
128. Hershko, T.; Ginsberg, D. Up-regulation of Bcl-2 Homology 3 (BH3)-only proteins by E2F1 mediates apoptosis. *J. Biol. Chem.* **2004**, *279*, 8627–8634. [CrossRef]

129. Qin, J.Z.; Ziffra, J.; Stennett, L.; Bodner, B.; Bonish, B.K.; Chaturvedi, V.; Bennett, F.; Pollock, P.M.; Trent, J.M.; Hendrix, M.J.C.; et al. Proteasome inhibitors trigger NOXA-mediated apoptosis in melanoma and myeloma cells. *Cancer Res.* **2005**, *65*, 6282–6293. [CrossRef]
130. Fernandez, Y.; Verhaegen, M.; Miller, T.P.; Rush, J.L.; Steiner, P.; Opipari, A.W.J.; Lowe, S.W.; Soengas, M.S. Differential regulation of Noxa in normal melanocytes and melanoma cells by proteasome inhibition: Therapeutic implications. *Cancer Res.* **2005**, *65*, 6294–6304. [CrossRef]
131. Du, H.; Wolf, J.; Schafer, B.; Moldoveanu, T.; Chipuk, J.E.; Kuwana, T. BH3 domains other than Bim and Bid can directly activate Bax/Bak. *J. Biol. Chem.* **2011**, *286*, 491–501. [CrossRef] [PubMed]
132. Vela, L.; Gonzalo, O.; Naval, J.; Marzo, I. Direct interaction of Bax and Bak proteins with Bcl-2 Homology Domain 3 (BH3)-only proteins in living cells revealed by fluorescence complementation. *J. Biol. Chem.* **2013**, *288*, 4935–4946. [CrossRef] [PubMed]
133. Dai, H.; Smith, A.; Meng, X.W.; Schneider, P.A.; Pang, Y.P.; Kaufmann, S.H. Transient binding of an activator BH3 domain to the Bak BH3-binding groove initiates Bak oligomerization. *J. Cell Biol.* **2011**, *194*, 39–48. [CrossRef]
134. Chen, H.C.; Kanai, M.; Inoue-Yamauchi, A.; Tu, H.C.; Huang, Y.; Ren, D.; Kim, H.; Takeda, S.; Reyna, D.E.; Chan, P.M.; et al. An interconnected hierarchical model of cell death regulation by the BCL-2 family. *Nat. Cell Biol.* **2015**, *17*, 1270–1281. [CrossRef] [PubMed]
135. Puthalakath, H.; O'Reilly, L.A.; Gunn, P.; Lee, L.; Kelly, P.N.; Huntington, N.D.; Hughes, P.D.; Michalak, E.M.; McKimm-Breschkin, J.; Motoyama, N.; et al. ER stress triggers apoptosis by activating BH3-only protein Bim. *Cell* **2007**, *129*, 1337–1349. [CrossRef]
136. Reimertz, C.; Kogel, D.; Rami, A.; Chittenden, T.; Prehn, J.H. Gene expression during ER stress-induced apoptosis in neurons: Induction of the BH3-onlyprotein Bbc3/PUMA and activation of the mitochondrial apoptosis pathway. *J. Cell Biol.* **2003**, *162*, 587–597. [CrossRef]
137. Li, J.; Lee, B.; Lee, A.S. Endoplasmic reticulum stress-induced apoptosis: Multiple pathways and activation of p53-up-regulated modulator of apoptosis (PUMA) and Noxa by p53. *J. Biol. Chem.* **2006**, *281*, 7260–7270. [CrossRef]
138. McCullough, K.D.; Martindale, J.L.; Klotz, L.O.; Aw, T.Y.; Holbrook, N.J. Gadd153 sensitizes cells to endoplasmic reticulum stress by down-regulating Bcl2and perturbing the cellular redox state. *Mol. Cell. Biol.* **2001**, *21*, 1249–1259. [CrossRef]
139. Yamamoto, K.; Ichijo, H.; Korsmeyer, S.J. BCL-2 is phosphorylated and inactivated by an ASK1/Jun N-terminal protein kinase pathway normally activated at G(2)/M. *Mol. Cell. Biol.* **1999**, *19*, 8469–8478. [CrossRef]
140. Fan, M.; Goodwin, M.; Vu, T.; Brantley-Finley, C.; Gaarde, W.A.; Chambers, T.C. Vinblastine-induced phosphorylation of Bcl-2 and Bcl-XL is mediated by JNK and occurs in parallel with inactivation of the Raf-1/MEK/ERK cascade. *J. Biol. Chem.* **2001**, *275*, 29980–29985. [CrossRef]
141. Llambi, F.; Wang, Y.M.; Victor, B.; Yang, M.; Schneider, D.M.; Gingras, S.; Parsons, M.J.; Zheng, J.H.; Brown, S.A.; Pelletier, S.; et al. BOK is a non-canonical BCL-2 family effector of apoptosis regulated by ER-associated degradation. *Cell* **2016**, *165*, 421–433. [CrossRef] [PubMed]
142. Sopha, P.; Ren, H.Y.; Grove, D.E.; Cyr, D.M. Endoplasmic Reticulum stress-induced degradation of DNAJB12 stimulates BOK accumulation and primes cancer cells for apoptosis. *J. Biol. Chem.* **2017**, *292*, 11792–11803. [CrossRef] [PubMed]
143. Lopes, U.G.; Erhardt, P.; Yao, R.; Cooper, G.M. p53-dependent induction of apoptosis by proteasome inhibitors. *J. Biol. Chem.* **1997**, *272*, 12893–12896. [CrossRef] [PubMed]
144. Rastogi, N.; Duggal, S.; Singh, S.K.; Porwal, K.; Srivastava, V.K.; Maurya, R.; Bhatt, M.L.; Mishra, D.P. Proteasome inhibition mediates p53 reactivation and anti-cancer activity of 6-gingerol in cervical cancer cells. *Oncotarget* **2015**, *6*, 43310–43325. [CrossRef] [PubMed]
145. Brancolini, C. Inhibitors of the Ubiquitin-Proteasome System and the cell death machinery: How many pathways are activated? *Curr. Mol. Pharmacol.* **2008**, *1*, 24–37. [CrossRef] [PubMed]
146. Qiao, S.; Lamore, S.D.; Cabello, C.M.; Lesson, J.L.; Muñoz-Rodriguez, J.L.; Wondrak, G.T. Thiostrepton is an inducer of oxidative and proteotoxic stress that impairs viability of human melanoma cells but not primary melanocytes. *Biochem. Pharmacol.* **2012**, *83*, 1229–1240. [CrossRef]
147. Arai, S.; Varkaris, A.; Nouri, M.; Chen, S.; Xie, L.; Balk, S.P. MARCH5 mediates NOXA-dependent MCL1 degradation driven by kinase inhibitors and integrated stress response activation. *Elife* **2020**, *9*, e54954. [CrossRef]

148. Djajawi, T.M.; Liu, L.; Gong, J.N.; Huang, A.S.; Luo, M.J.; Xu, Z.; Okamoto, T.; Call, M.J.; Huang, D.C.S.; van Delft, M.F. MARCH5 requires MTCH2 to coordinate proteasomal turnover of the MCL1:NOXA complex. *Cell Death Differ.* **2020**. [CrossRef]
149. Vaux, D.L.; Silke, J. IAPs, RINGs and ubiquitylation. *Nat. Rev. Mol. Cell Biol.* **2005**, *6*, 287–297. [CrossRef]
150. Scomazzon, S.P.; Riccio, A.; Santopolo, S.; Lanzilli, G.; Coccia, M.; Rossi, A.; Santoro, M.G. The zinc-finger AN1-type domain 2a gene acts as a regulator of cell survival in human melanoma: Role of E3-ligase cIAP2. *Mol. Cancer Res.* **2019**, *17*, 2444–2456. [CrossRef]
151. Pei, X.Y.; Dai, Y.; Grant, S. Synergistic induction of oxidative injury and apoptosis in human multiple myeloma cells by the proteasome inhibitor bortezomib and histone deacetylase inhibitors. *Clin. Cancer Res.* **2004**, *10*, 3839–3852. [CrossRef] [PubMed]
152. Ciotti, S.; Iuliano, L.; Cefalù, S.; Comelli, M.; Mavelli, I.; Di Giorgio, E.; Brancolini, C. GSK3β is a key regulator of the ROS-dependent necrotic death induced by the quinone DMNQ. *Cell Death Dis.* **2020**, *11*, 2. [CrossRef] [PubMed]
153. Vanlangenakker, N.; Vanden Berghe, T.; Krysko, D.M.; Festjens, N.; Vandenabeele, P. Molecular mechanisms and pathophysiology of necrotic cell death. *Curr. Mol. Med.* **2008**, *8*, 207–220. [CrossRef] [PubMed]
154. Del Re, D.P.; Amgalan, D.; Linkermann, A.; Liu, Q.; Kitsis, R.N. Fundamental mechanisms of regulated cell death and implications for heart disease. *Physiol. Rev.* **2019**, *99*, 1765–1817. [CrossRef]
155. Fontanini, A.; Foti, C.; Potu, H.; Crivellato, E.; Maestro, R.; Bernardi, P.; Demarchi, F.; Brancolini, C. The isopeptidase inhibitor G5 triggers a caspase-independent necrotic death in cells resistant to apoptosis: A comparative study with the proteasome inhibitor bortezomib. *J. Biol. Chem.* **2009**, *284*, 8369–8381. [CrossRef]
156. Tomasella, A.; Blangy, A.; Brancolini, C. A receptor-interacting protein 1 (RIP1)-independent necrotic death under the control of protein phosphatase PP2A that involves the reorganization of Actin cytoskeleton and the action of Cofilin-1. *J. Biol. Chem.* **2014**, *289*, 25699–25710. [CrossRef]
157. Darling, N.J.; Balmanno, K.; Cook, S.J. ERK1/2 signalling protects against apoptosis following Endoplasmic Reticulum stress but cannot provide long-term protection against BAX/BAK-independent cell death. *PLoS ONE* **2017**, *12*, e0184907. [CrossRef]
158. Ramdzan, Y.M.; Trubetskov, M.M.; Ormsby, A.R.; Newcombe, E.A.; Sui, X.; Tobin, M.J.; Bongiovanni, M.N.; Gras, S.L.; Dewson, G.; Miller, J.M.L.; et al. Huntingtin inclusions trigger cellular quiescence, deactivate apoptosis, and lead to delayed necrosis. *Cell Rep.* **2017**, *19*, 919–927. [CrossRef]
159. Wang, W.; Li, S.; Wang, H.; Li, B.; Shao, L.; Lai, Y.; Horvath, G.; Wang, Q.; Yamamoto, M.; Janicki, J.S.; et al. Nrf2 enhances myocardial clearance of toxic ubiquitinated proteins. *J. Mol. Cell. Cardiol.* **2014**, *72*, 305–315. [CrossRef]
160. Han, J.H.; Park, J.; Myung, S.H.; Lee, S.H.; Kim, H.Y.; Kim, K.S.; Seo, Y.W.; Kim, T.H. Noxa mitochondrial targeting domain induces necrosis via VDAC2 and mitochondrial catastrophe. *Cell Death Dis.* **2019**, *10*, 519. [CrossRef]
161. Schwarzer, R.; Laurien, L.; Pasparakis, M. New insights into the regulation of apoptosis, necroptosis, and pyroptosis by Receptor Interacting Protein Kinase 1 and caspase-8. *Curr. Opin. Cell Biol.* **2020**, *63*, 186–193. [CrossRef] [PubMed]
162. Coustry, F.; Posey, K.L.; Liu, P.; Alcorn, J.L.; Hecht, J.T. D469del-COMP retention in chondrocytes stimulates caspase-independent necroptosis. *Am. J. Pathol.* **2012**, *180*, 738–748. [CrossRef] [PubMed]
163. Rizzi, F.; Naponelli, V.; Silva, A.; Modernelli, A.; Ramazzina, I.; Bonacini, M.; Tardito, S.; Gatti, R.; Uggeri, J.; Bettuzzi, S. Polyphenon E(R), a standardized green tea extract, induces endoplasmic reticulum stress, leading to death of immortalized PNT1a cells by anoikis and tumorigenic PC3 by necroptosis. *Carcinogenesis* **2014**, *35*, 828–839. [CrossRef] [PubMed]
164. Rojas-Rivera, D.; Delvaeye, T.; Roelandt, R.; Nerinckx, W.; Augustyns, K.; Vandenabeele, P.; Bertrand, M.J.M. When PERK inhibitors turn out to be new potent RIPK1 inhibitors: Critical issues on the specificity and use of GSK2606414 and GSK2656157. *Cell Death Differ.* **2017**, *24*, 1100–1110. [CrossRef] [PubMed]
165. Luan, Q.; Jin, L.; Jiang, C.C.; Tay, K.H.; Lai, F.; Liu, X.Y.; Liu, Y.L.; Guo, S.T.; Li, C.Y.; Yan, X.G.; et al. RIPK1 regulates survival of human melanoma cells upon endoplasmic reticulum stress through autophagy. *Autophagy* **2015**, *11*, 975–994. [CrossRef]

166. Cheng, S.B.; Nakashima, A.; Huber, W.J.; Davis, S.; Banerjee, S.; Huang, Z.; Saito, S.; Sadovsky, Y.; Sharma, S. Pyroptosis is a critical inflammatory pathway in the placenta from early onset preeclampsia and in human trophoblasts exposed to hypoxia and endoplasmic reticulum stressors. *Cell Death Dis.* **2019**, *10*, 927. [CrossRef]
167. Li, J.; Cao, F.; Yin, H.L.; Huang, Z.J.; Lin, Z.T.; Mao, N.; Sun, B.; Wang, G. Ferroptosis: Past, present and future. *Cell Death Dis.* **2020**, *11*, 88. [CrossRef]
168. Bebber, C.M.; Müller, F.; Clemente, L.P.; Weber, J.; von Karstedt, S. Ferroptosis in cancer cell biology. *Cancers* **2020**, *12*, 164. [CrossRef]
169. Lee, Y.S.; Lee, D.H.; Choudry, H.A.; Bartlett, D.L.; Lee, Y.J. Ferroptosis-induced endoplasmic reticulum stress: Cross-talk between ferroptosis and apoptosis. *Mol. Cancer Res.* **2018**, *16*, 1073–1076. [CrossRef]
170. Rahmani, M.; Davis, E.M.; Crabtree, T.R.; Habibi, J.R.; Nguyen, T.K.; Dent, P.; Grant, S. The kinase inhibitor sorafenib induces cell death through a process involving induction of endoplasmic reticulum stress. *Mol. Cell. Biol.* **2007**, *27*, 5499–5513. [CrossRef]
171. Dixon, S.J.; Patel, D.N.; Welsch, M.; Skouta, R.; Lee, E.D.; Hayano, M.; Thomas, A.G.; Gleason, C.E.; Tatonetti, N.P.; Slusher, B.S.; et al. Pharmacological inhibition of cystine-glutamate exchange induces endoplasmic reticulum stress and ferroptosis. *Elife* **2014**, *3*, e02523. [CrossRef] [PubMed]
172. Chen, Y.; Mi, Y.; Zhang, X.; Ma, Q.; Song, Y.; Zhang, L.; Wang, D.; Xing, J.; Hou, B.; Li, H.; et al. Dihydroartemisinin-induced unfolded protein response feedback attenuates ferroptosis via PERK/ATF4/HSPA5 pathway in glioma cells. *J. Exp. Clin. Cancer Res.* **2019**, *38*, 402. [CrossRef] [PubMed]
173. Brigelius-Flohé, R.; Flohé, L. Regulatory phenomena in the glutathione peroxidase superfamily. *Antioxid. Redox Signal.* **2019**. [CrossRef] [PubMed]
174. Vitale, M.; Bakunts, A.; Orsi, A.; Lari, F.; Tadè, L.; Danieli, A.; Rato, C.; Valetti, C.; Sitia, R.; Raimondi, A.; et al. Inadequate BiP availability defines endoplasmic reticulum stress. *Elife* **2019**, *8*, e41168. [CrossRef]
175. Li, J.; Labbadia, J.; Morimoto, R.I. Rethinking HSF1 in stress, development, and organismal health. *Trends Cell Biol.* **2017**, *27*, 895–905. [CrossRef]
176. Gaglia, G.; Rashid, R.; Yapp, C.; Joshi, G.N.; Li, C.G.; Lindquist, S.L.; Sarosiek, K.A.; Whitesell, L.; Sorger, P.K.; Santagata, S. HSF1 phase transition mediates stress adaptation and cell fate decisions. *Nat. Cell Biol.* **2020**, *22*, 151–158. [CrossRef]
177. Schubert, U.; Anton, L.C.; Gibbs, J.; Norbury, C.C.; Yewdell, J.W.; Bennink, J.R. Rapid degradation of a large fraction of newly synthesized proteins by proteasomes. *Nature* **2000**, *404*, 770–774. [CrossRef]
178. Cenci, S.; Sitia, R. Managing and exploiting stress in the antibody factory. *FEBS Lett.* **2007**, *581*, 3652–3657. [CrossRef]
179. Ruggero, D. Translational control in cancer etiology. *Cold Spring Harb. Perspect. Biol.* **2013**, *5*, a012336. [CrossRef]
180. Yun, Y.S.; Kim, K.H.; Tschida, B.; Sachs, Z.; Noble-Orcutt, K.E.; Moriarity, B.S.; Ai, T.; Ding, R.; Williams, J.; Chen, L.; et al. mTORC1 coordinates protein synthesis and immunoproteasome formation via PRAS40 to prevent accumulation of protein stress. *Mol. Cell* **2016**, *61*, 625–639. [CrossRef]
181. Saxton, R.A.; Sabatini, D.M. mTOR signaling in growth, metabolism, and disease. *Cell* **2017**, *168*, 960–976. [CrossRef] [PubMed]
182. Hyer, M.L.; Milhollen, M.A.; Ciavarri, J.; Fleming, P.; Traore, T.; Sappal, D.; Huck, J.; Shi, J.; Gavin, J.; Brownell, J.; et al. A small-molecule inhibitor of the ubiquitin activating enzyme for cancer treatment. *Nat. Med.* **2018**, *24*, 186–193. [CrossRef] [PubMed]
183. Chui, M.H.; Doodnauth, S.A.; Erdmann, N.; Tiedemann, R.E.; Sircoulomb, F.; Drapkin, R.; Shaw, P.; Rottapel, R. Chromosomal instability and mTORC1 activation through PTEN loss contribute to proteotoxic stress in ovarian carcinoma. *Cancer Res.* **2019**, *79*, 5536–5549. [CrossRef]
184. Seo, J.H.; Rivadeneira, D.B.; Caino, M.C.; Chae, Y.C.; Speicher, D.W.; Tang, H.Y.; Vaira, V.; Bosari, S.; Palleschi, A.; Rampini, P.; et al. The mitochondrial unfoldase-peptidase complex ClpXP controls bioenergetics stress and metastasis. *PLoS Biol.* **2016**, *14*, e1002507. [CrossRef] [PubMed]
185. Llinàs-Arias, P.; Rosselló-Tortella, M.; López-Serra, P.; Pérez-Salvia, M.; Setién, F.; Marin, S.; Muñoz, J.P.; Junza, A.; Capellades, J.; Calleja-Cervantes, M.E.; et al. Epigenetic loss of the endoplasmic reticulum-associated degradation inhibitor SVIP induces cancer cell metabolic reprogramming. *JCI Insight* **2019**, *5*, e125888. [CrossRef] [PubMed]

186. Tsvetkov, P.; Detappe, A.; Cai, K.; Keys, H.R.; Brune, Z.; Ying, W.; Thiru, P.; Reidy, M.; Kugener, G.; Rossen, J.; et al. Mitochondrial metabolism promotes adaptation to proteotoxic stress. *Nat. Chem. Biol.* **2019**, *15*, 681–689. [CrossRef]
187. Torres, E.M.; Sokolsky, T.; Tucker, C.M.; Chan, L.Y.; Boselli, M.; Dunham, M.J.; Amon, A. Effects of aneuploidy on cellular physiology and cell division in haploid yeast. *Science* **2007**, *317*, 916–924. [CrossRef]
188. Ohashi, A.; Ohori, M.; Iwai, K.; Nakayama, Y.; Nambu, T.; Morishita, D.; Kawamoto, T.; Miyamoto, M.; Hirayama, T.; Okaniwa, M.; et al. Aneuploidy generates proteotoxic stress and DNA damage concurrently with p53-mediated post-mitotic apoptosis in SAC-impaired cells. *Nat. Commun.* **2015**, *6*, 7668. [CrossRef]
189. Vermulst, M.; Denney, A.S.; Lang, M.J.; Hung, C.W.; Moore, S.; Moseley, M.A.; Thompson, J.W.; Madden, V.; Gauer, J.; Wolfe, K.J.; et al. Transcription errors induce proteotoxic stress and shorten cellular lifespan. *Nat. Commun.* **2015**, *6*, 8065. [CrossRef]
190. Bastola, P.; Oien, D.B.; Cooley, M.; Chien, J. Emerging cancer therapeutic targets in protein homeostasis. *AAPS J.* **2018**, *20*, 94. [CrossRef]
191. Xie, J.L.; Jarosz, D.F. Mutations, protein homeostasis, and epigenetic control of genome integrity. *DNA Repair* **2018**, *71*, 23–32. [CrossRef] [PubMed]
192. Pfau, S.J.; Amon, A. Chromosomal instability and aneuploidy in cancer: From yeast to man. *EMBO Rep.* **2012**, *13*, 515–527. [CrossRef] [PubMed]
193. Brennan, C.M.; Vaites, L.P.; Wells, J.N.; Santaguida, S.; Paulo, J.A.; Storchova, Z.; Harper, J.W.; Marsh, J.A.; Amon, A. Protein aggregation mediates stoichiometry of protein complexes in aneuploid cells. *Genes Dev.* **2019**, *33*, 1031–1047. [CrossRef] [PubMed]
194. Donnelly, N.; Passerini, V.; Durrbaum, M.; Stingele, S.; Storchova, Z. HSF1 deficiency and impaired HSP90-dependent protein folding are hallmarks of aneuploid human cells. *EMBO J.* **2014**, *33*, 2374–2387. [CrossRef] [PubMed]
195. Zhu, J.; Tsai, H.J.; Gordon, M.R.; Li, R. Cellular stress associated with aneuploidy. *Dev. Cell* **2018**, *44*, 420–431. [CrossRef]
196. Mukhopadhyay, C.; Triplett, A.; Bargar, T.; Heckman, C.; Wagner, K.U.; Naramura, M. Casitas B-cell lymphoma (Cbl) proteins protect mammary epithelial cells from proteotoxicity of active c-Src accumulation. *Proc. Natl. Acad. Sci. USA* **2016**, *113*, E8228–E8237. [CrossRef]
197. Dodgson, S.E.; Santaguida, S.; Kim, S.; Sheltzer, J.; Amon, A. The pleiotropic deubiquitinase Ubp3 confers aneuploidy tolerance. *Genes Dev.* **2016**, *30*, 2259–2271. [CrossRef]
198. Sannino, S.; Guerriero, C.J.; Sabnis, A.J.; Stolz, D.B.; Wallace, C.T.; Wipf, P.; Watkins, S.C.; Bivona, T.G.; Brodsky, J.L. Compensatory increases of select proteostasis networks after Hsp70 inhibition in cancer cells. *J. Cell Sci.* **2018**, *131*, jcs217760. [CrossRef]
199. Chen, L.; Yang, X. TRIM11 cooperates with HSF1 to suppress the anti-tumor effect of proteotoxic stress drugs. *Cell Cycle* **2019**, *18*, 60–68. [CrossRef]
200. Jena, K.K.; Mehto, S.; Kolapalli, S.P.; Nath, P.; Sahu, R.; Chauhan, N.R.; Sahoo, P.K.; Dhar, K.; Das, S.K.; Chauhan, S.; et al. TRIM16 governs the biogenesis and disposal of stress-induced protein aggregates to evade cytotoxicity: Implication for neurodegeneration and cancer. *Autophagy* **2019**, *15*, 924–926. [CrossRef]
201. Harris, I.S.; Endress, J.E.; Coloff, J.L.; Selfors, L.M.; McBrayer, S.K.; Rosenbluth, J.M.; Takahashi, N.; Dhakal, S.; Koduri, V.; Oser, M.G.; et al. Deubiquitinases maintain protein homeostasis and survival of cancer cells upon glutathione depletion. *Cell Metab.* **2019**, *29*, 1166–1181.e6. [CrossRef] [PubMed]
202. Carugo, A.; Minelli, R.; Sapio, L.; Soeung, M.; Carbone, F.; Robinson, F.S.; Tepper, J.; Chen, Z.; Lovisa, S.; Svelto, M.; et al. p53 is a master regulator of proteostasis in SMARCB1-deficient malignant rhabdoid tumors. *Cancer Cell* **2019**, *35*, 204–220.e9. [CrossRef] [PubMed]
203. Mantovani, F.; Collavin, L.; Del Sal, G. Mutant p53 as a guardian of the cancer cell. *Cell Death Differ.* **2019**, *26*, 199–212. [CrossRef]
204. Sicari, D.; Fantuz, M.; Bellazzo, A.; Valentino, E.; Apollonio, M.; Pontisso, I.; Di Cristino, F.; Dal Ferro, M.; Bicciato, S.; Del Sal, G.; et al. Mutant p53 improves cancer cells' resistance to endoplasmic reticulum stress by sustaining activation of the UPR regulator ATF6. *Oncogene* **2019**, *38*, 6184–6195. [CrossRef]
205. Chatterjee, S.; Burns, T.F. Targeting Heat Shock Proteins in cancer: A promising therapeutic approach. *Int. J. Mol. Sci.* **2017**, *18*, 1978. [CrossRef]

206. Leu, J.I.J.; Barnoud, T.; Zhang, G.; Tian, T.; Wei, Z.; Herlyn, M.; Murphy, M.E.; George, D.L. Inhibition of stress-inducible HSP70 impairs mitochondrial proteostasis and function. *Oncotarget* **2017**, *8*, 45656–45669. [CrossRef]
207. Calderwood, S.K.; Gong, J. Heat Shock Proteins promote cancer: It's a protection racket. *Trends Biochem. Sci.* **2016**, *41*, 311–323. [CrossRef]
208. Gomez-Pastor, R.; Burchfiel, E.T.; Thiele, D.J. Regulation of heat shock transcription factors and their roles in physiology and disease. *Nat. Rev. Mol. Cell Biol.* **2018**, *19*, 4–19. [CrossRef]
209. Vangala, J.R.; Radhakrishnan, S.K. Nrf1-mediated transcriptional regulation of the proteasome requires a functional TIP60 complex. *J. Biol. Chem.* **2019**, *294*, 2036–2045. [CrossRef]
210. Dias, M.H.; Fonseca, C.S.; Zeidler, J.D.; Albuquerque, L.L.; da Silva, M.S.; Cararo-Lopes, E.; Reis, M.S.; Noël, V.; Dos Santos, E.O.; Prior, I.A.; et al. Fibroblast growth factor 2 lethally sensitizes cancer cells to stress-targeted therapeutic inhibitors. *Mol. Oncol.* **2019**, *13*, 290–306. [CrossRef]
211. Anderson, D.J.; Le Moigne, R.; Djakovic, S.; Kumar, B.; Rice, J.; Wong, S.; Wang, J.; Yao, B.; Valle, E.; von Soly, S.K.; et al. Targeting the AAA ATPase p97 as an approach to treat cancer through disruption of protein homeostasis. *Cancer Cell* **2015**, *28*, 653–665. [CrossRef] [PubMed]
212. Wilhelm, T.; Bick, F.; Peters, K.; Mohta, V.; Tirosh, B.; Patterson, J.B.; Kharabi-Masouleh, B.; Huber, M. Infliction of proteotoxic stresses by impairment of the unfolded protein response or proteasomal inhibition as a therapeutic strategy for mast cell leukemia. *Oncotarget* **2017**, *9*, 2984–3000. [CrossRef] [PubMed]
213. Mazurkiewicz, M.; Hillert, E.K.; Wang, X.; Pellegrini, P.; Olofsson, M.H.; Selvaraju, K.; D'Arcy, P.; Linder, S. Acute lymphoblastic leukemia cells are sensitive to disturbances in protein homeostasis induced by proteasome deubiquitinase inhibition. *Oncotarget* **2017**, *8*, 21115–21127. [CrossRef] [PubMed]
214. Pastorek, M.; Muller, P.; Coates, P.J.; Vojtesek, B. Intrinsic proteotoxic stress levels vary and act as a predictive marker for sensitivity of cancer cells to Hsp90 inhibition. *PLoS ONE* **2018**, *13*, e0202758. [CrossRef]
215. Xu, D.; Liang, S.Q.; Yang, H.; Lüthi, U.; Riether, C.; Berezowska, S.; Marti, T.M.; Hall, S.R.R.; Bruggmann, R.; Kocher, G.J.; et al. Increased sensitivity to apoptosis upon endoplasmic reticulum stress-induced activation of the unfolded protein response in chemotherapy-resistant malignant pleural mesothelioma. *Br. J. Cancer* **2018**, *119*, 65–75. [CrossRef]
216. Kijima, T.; Prince, T.L.; Tigue, M.L.; Yim, K.H.; Schwartz, H.; Beebe, K.; Lee, S.; Budzynski, M.A.; Williams, H.; Trepel, J.B.; et al. HSP90 inhibitors disrupt a transient HSP90-HSF1 interaction and identify a noncanonical model of HSP90-mediated HSF1 regulation. *Sci. Rep.* **2018**, *8*, 6976. [CrossRef]
217. Tomasella, A.; Picco, R.; Ciotti, S.; Sgorbissa, A.; Bianchi, E.; Manfredini, R.; Benedetti, F.; Trimarco, V.; Frezzato, F.; Trentin, L.; et al. The isopeptidase inhibitor 2cPE triggers proteotoxic stress and ATM activation in chronic lymphocytic leukemia cells. *Oncotarget* **2016**, *19*, 45429–45443. [CrossRef]
218. Majera, D.; Skrott, Z.; Bouchal, J.; Bartkova, J.; Simkova, D.; Gachechiladze, M.; Steigerova, J.; Kurfurstova, D.; Gursky, J.; Korinkova, G.; et al. Targeting genotoxic and proteotoxic stress-response pathways in human prostate cancer by clinically available PARP inhibitors, vorinostat and disulfiram. *Prostate* **2019**, *79*, 352–362. [CrossRef]
219. Yallowitz, A.; Ghaleb, A.; Garcia, L.; Alexandrova, E.M.; Marchenko, N. Heat Shock Factor 1 confers resistance to lapatinib in ERBB2-positive breast cancer cells. *Cell Death Dis.* **2018**, *9*, 621. [CrossRef]
220. Kültz, D. Evolution of cellular stress response mechanisms. *J. Exp. Zool A Ecol. Integr. Physiol.* **2020**, *333*, 359–378. [CrossRef]
221. Boos, F.; Labbadia, J.; Herrmann, J.M. How the mitoprotein-induced stress response safeguards the cytosol: A unified view. *Trends Cell Biol.* **2020**, *30*, 241–254. [CrossRef] [PubMed]
222. Jones, C.L.; Tepe, J.J. Proteasome activation to combat proteotoxicity. *Molecules* **2019**, *24*, 2841. [CrossRef] [PubMed]

MOLECULAR CANCER THERAPEUTICS | SMALL MOLECULE THERAPEUTICS

Enhancing Proteotoxic Stress in Leiomyosarcoma Cells Triggers Mitochondrial Dysfunctions, Cell Death, and Antitumor Activity *in vivo*

Luca Iuliano[1], Sara Drioli[2], Ymera Pignochino[3,4], Claudia Maria Cafiero[2], Martina Minisini[1], Francesca D'Este[1], Raffaella Picco[1], Emiliano Dalla[1], Giorgia Giordano[4,5], Giovanni Grignani[4], Eros Di Giorgio[1], Fabio Benedetti[2], Fulvia Felluga[2], and Claudio Brancolini[1]

ABSTRACT

Leiomyosarcomas are rare and aggressive tumors characterized by a complex karyotype. Surgical resection with or without radiotherapy and chemotherapy is the standard curative treatment. Unfortunately, a high percentage of leiomyosarcomas recurs and metastasizes. In these cases, doxorubicin and ifosfamide represent the standard treatment but with low response rates. Here, we evaluated the induction of proteotoxic stress as a possible strategy to kill leiomyosarcoma cells in a therapeutic perspective. We show that aggressive leiomyosarcomas coexist with high levels of proteotoxic stress. As a consequence, we hypothesized that leiomyosarcoma cells are vulnerable to further increases of proteotoxic stress. The small compound 2c is a strong inducer of proteotoxic stress. In leiomyosarcoma cells, it triggers cell death coupled to a profound reorganization of the mitochondrial network. By using stimulated emission depletion microscopy, we have unveiled the existence of DIABLO/SMAC clusters that are modulated by 2c. Finally, we have engineered a new version of 2c linked to polyethylene glycol though a short peptide, named 2cPP. This new prodrug is specifically activated by proteases present in the tumor microenvironment. 2cPP shows a strong antitumor activity *in vivo* against leiomyosarcomas and no toxicity against normal cells.

Introduction

Leiomyosarcomas (LMS) are rare and aggressive tumors that show some smooth-muscle features and represent approximately 10% of soft-tissue sarcomas (STS) of adults. Leiomyosarcomas are characterized by high mutational burden and a complex karyotype (1, 2). Recent progresses in genomic studies have provided a better classification of STS, including leiomyosarcomas and outlined the complex pattern of mutations (3–5).

The therapeutic perspectives for advanced leiomyosarcomas have not improved during the last decades. Available treatments are surgery and radiotherapy. Unfortunately, local recurrence and metastasis occur in approximately 40% of patients (2). Since the 1970s, doxorubicin is the first-line treatment with few additional options (6). Recently, some hopes have been raised by olaratumab, a human mAb that inhibits the PDGF receptor-α. Disappointingly, a phase III clinical trial in patients with advanced STS, including several leiomyosarcomas, did not evidence significant differences in overall survival after treatment with doxorubicin plus olaratumab versus doxorubicin plus placebo (7). Hence, new therapeutic approaches are urgently needed.

An unbalanced proteostasis triggers proteotoxic stress and, if unresolved, leads to cell death (8). In general, cancer cells present higher levels of proteotoxic stress. The increased metabolic and proliferative rates require elevated levels of protein synthesis, a process prone to errors (9). They are also more exposed to reactive oxygen species (ROS) and starvation, which can cause protein misfolding (8, 10). Aneuploidy, copy-number alterations, and the accumulation of point mutations in coding sequences are additional sources of proteotoxic stress (10–12). Cancer cells coexist with an increased level of proteotoxic stress by upregulating mechanisms counteracting protein misfolding including chaperones, the ubiquitin-proteasome system, and macroautophagy. As a consequence, cancer cells show an enhanced vulnerability to a further increase of proteotoxic stress and are more prone to die (10). Therefore, a new therapeutic option could be the exploitation of small molecules capable of triggering proteotoxic stress (13–15). In this article, we augmented the proteotoxic stress in leiomyosarcoma cells to elicit cell death. We used the small molecule 2c, a diaryldienone derivative, which is a well-known inducer of proteotoxic stress. These compounds make covalent adducts with free thiols by Michael addition (16, 17). In a therapeutic perspective, we have also engineered a new prodrug version of 2c that is activated in the tumor microenvironment after proteolytic cleavage.

Materials and Methods

Cell culture conditions, drug treatments, and propidium iodide staining

Leiomyosarcoma cell lines (SK-UT-1, SK-LMS-1, and DMR) were validated by RNA profiling and grown as described previously (18). The primary human uterine smooth-muscle cells (HUtSMCs) were obtained from ATCC and used within eight passages. All cell lines were weekly tested to be free from *Mycoplasma* contamination using

[1]Department of Medicine, Università degli Studi di Udine, Udine, Italy. [2]Dipartimento di Scienze Chimiche e Farmaceutiche, Università degli Studi di Trieste, Trieste, Italy. [3]Department of Clinical and Biological Sciences, University of Torino, c/o San Luigi Gonzaga Hospital, Orbassano, Torino, Italy. [4]Sarcoma Unit, Division of Medical Oncology, Candiolo Cancer Institute, FPO-IRCCS, Candiolo, Torino, Italy. [5]Department of Oncology, University of Torino, Torino, Italy.

Note: Supplementary data for this article are available at Molecular Cancer Therapeutics Online (http://mct.aacrjournals.org/).

Corresponding Author: Claudio Brancolini, Department of Medicine, Università di Udine, P. le Kolbe 4, Udine 33100, Italy. Phone: 39 043 249 4381; E-mail: claudio.brancolini@uniud.it

Mol Cancer Ther 2021;XX:XX–XX

doi: 10.1158/1535-7163.MCT-20-0521

Hoechst 33258 (Sigma) staining and microscopic inspection. For propidium iodide (PI) staining, cells were collected and resuspended in 0.1 mL of PBS and incubated with 10 μg/mL of PI (Merck), for 5 minutes at room temperature. PI fluorescence positivity was determined with Countess II FL automated cell counter (Invitrogen).

Mutation rate and genomic alteration analysis

The Cancer Genome Atlas (TCGA) tumor mutation counts based on exome-sequencing data, as well as information on the fraction of genome altered (FGA) defined by SNP arrays, were downloaded from cBioPortal (19). We analyzed the whole Sarcoma dataset (TCGA, PanCancer Atlas; $n = 255$) and within this dataset the patients with leiomyosarcoma ($n = 100$; ref. 20). From the same repository, we also retrieved the most recently updated matched Cancer Cell Line Encyclopedia (CCLE) samples (21) focusing on leiomyosarcoma cell lines.

Survival analysis

The R/Bioconductor package *cgdsr* was used to retrieve gene expression (RSEM) and clinical data from patients with leiomyosarcoma. The Kaplan–Meier survival analysis was performed considering the median expression value of each gene signature using the R/Bioconductor *survival* package as described previously (22). We used the "optimal" cut-off point to dichotomize the patients. To select the best cutoff, the R/Bioconductor *SurvMisc* package was used (23).

Chemicals, antibodies, and immunoblotting

The following chemicals were used: PI, Ferrostatin-1, Erastin, Thapsigargin, and DMSO (Merck); Bortezomib (LC Laboratories); TNF-related apoptosis-inducing ligand (TRAIL; ref. 24); Boc-D-fmk (Abcam); Necrostatin-1 (Enzo Life Sciences); 17-(Allylamino)-17-demethoxygeldanamycin (17-AAG; Cayman Chemicals). Immunoblotting was performed as described previously (25). After blocking for 1 hour at room temperature, membranes were incubated with the primary antibodies. The primary antibodies used were anti-Actin and NOXA/PMAIP1 (Merck), DIABLO/SMAC (26), HDAC4 (27), Ubiquitin (Covance), eIF2α, and p-eIF2α (Ser51; Cell Signaling Technology). Next, membranes were incubated with the proper horseradish peroxidase–conjugated secondary antibody for 1 hour at room temperature (Merck). Blots were developed using Super Signal West Dura (Pierce Waltham).

RNA extraction and qRT-PCR

Cells were lysed using Tri-Reagent (Molecular Research Center). A total of 1.0 μg of total RNA was retrotranscribed by using 100 units of M-MLV Reverse transcriptase (Life Technologies). qRT-PCRs were performed using SYBR green technology (KAPA Biosystems). Data were analyzed by comparative threshold cycle using *HPRT* and *GAPDH* as normalizer.

Synthesis of 2cPP and other 2c derivatives

Inhibitors 2c and 2cPE were prepared as reported previously (28). DU-DC2 was obtained in a 51% total yield by conversion of 2c into the O-succinimidoyl ester 2c-OSu (28) followed by reaction of the resulting activated ester with b-alanine. DU-MS1 was obtained in three steps and 56% total yield from 2c-OSu: the spacer was introduced first by reaction of the activated ester with 1,3-diaminopropane and the resulting amine was reacted with N-Boc-(L)-leucine under standard peptide coupling conditions (EDC, HOBt). Finally, the Boc protection was removed with trifluoroacetic acid. 2cPP was synthesized in 77% yield with a convergent approach: monomethoxy polyethylene glycol (PEG; 5,000 kDa) was converted into the corresponding succinimidoyl ester and this compound was reacted with b-alanine giving the PEG-5000-spacer fragment. The Gly-Gly portion was assembled sequentially by reaction of this fragment with glycine benzyl ester, followed by deprotection. The coupling (EDC, HOBt)—deprotection (H2, Pd/C) cycle was repeated twice to introduce the two Gly residues. The PEG-Spacer-Gly-Gly building block thus obtained was finally coupled to DU-MS1 (EDC-HOBt) giving 2cPP. All new compounds had spectral (1H NMR, ESI-MS) data in agreement with the structure. Full details of the syntheses will be reported elsewhere.

Proteases analysis

The list of peptidases was obtained from MEROPS, the peptidase database (https://www.ebi.ac.uk/merops). mRNA expression levels (RSEM data) of the selected peptidases in patients with leiomyosarcomas ($n = 99$) were derived from the Sarcoma dataset [TCGA, PanCancer Atlas; $n = 255$ (20)]. The mRNA expression levels of the selected peptidases in the leiomyosarcoma cell lines were retrieved from the CCLE database (29).

Immunofluorescence confocal and stimulated emission depletion microscopy

For immunostaining, cells grown on No. 1.5 coverslips were fixed with 3% paraformaldehyde (Merck) for 20 minutes at room temperature, quenched with 100 mmol/L glycine for 5 minutes, and permeabilized with 0.5% Triton X-100 for 5 minutes. Nonspecific binding was blocked with 1% BSA (Merck) in PBS for 1 hour at room temperature. Primary and secondary antibody incubations were carried out at 37°C in PBS supplemented with 1% BSA and 0.5% Triton X-100, for 45 and 30 minutes, respectively. The following primary antibodies were used: anti-DIABLO/SMAC [(26), 1:100 dilution]; anti-ATP Synthase β (Thermo Fisher Scientific, catalog No. MA1-930, 1:200 dilution); anti-Cytochrome c (CytC; Thermo Fisher Scientific, catalog No. 33-8200, 1:100 dilution). Secondaries included Alexa Fluor 532–conjugated anti-mouse (catalog No. A11002) and anti-rabbit (catalog No. A11009) antibodies, and Alexa Fluor 568–conjugated anti-mouse (catalog No. A11019) and anti-rabbit (catalog No. A21069) F(ab')2 fragments (Thermo Fisher Scientific, 1:100 dilution). Coverslips were mounted in Mowiol (Merck) supplemented with 2.5% DABCO (Merck).

Comparative confocal and stimulated emission depletion (STED) images were acquired on a Leica TCS SP8 STED confocal microscope (Leica Microsystems) equipped with a pulsed white-light excitation laser, a 660-nm STED depletion laser, HC PL APO CS2 100×/1.40 oil objective and time-gated hybrid detectors. Excitation was carried out at 514-nm for Alexa Fluor 532 and at 580 nm for Alexa Fluor 568. Signal was detected at 520 to 565 and 590 to 650 nm, respectively. Both fluorophores were depleted using the 660-nm laser. Images from single optical sections were acquired in sequential scanning mode using Leica Application Suite X (LAS X) 3.5.5 software. Contrast was linearly adjusted on the whole image using Adobe Photoshop. Averaged intensity profiles were measured along a 60-nm-wide line using LAS X. Each profile was normalized to its respective peak intensity.

Leiomyosarcoma xenograft tumors in mice

Six-week-old female athymic nude-foxn1nu mice (Envigo Italy) were utilized for SK-UT-1 xenograft experiments. Animal studies were carried out according to the guidelines enforced in Italy (DDL 116 of

Feb 21, 1992 and subsequent addenda) and in compliance with the Guide for the Care and Use of Laboratory Animals, Department of Health and Human Services Publication No. 86-23. *In vivo* xenografts were established from initial subcutaneous injection of SK-UT-1 cells in 12 mice. For DMR xenografts, 2×10^6 DMR cells were embedded in ice-cold 50% growth factor–reduced BD Matrigel TM (BD Biosciences): PBS and subcutaneously injected into the right flank of 6-week-old female NSG mice (Charles River Laboratory). When tumor size was approximately 0.1 cm^3, mice were treated intravenously every 4 days, for three times with 170 mg/kg of 2cPP dissolved in PBS. Before treatment, mice were randomly assigned to experimental groups ($n = 2$ with 6 mice/group). All animals were checked daily, and eventual behavioral changes, ill health, or mortality was recorded for each animal. At the end of the experiments, mice were sacrificed and autopsy was performed on all mice: thoracic and abdominal cavity was open, and all major organs were macroscopically examined. Livers from all animals were collected and weighted.

Statistical analysis

For experimental data, Student *t* test was employed. For comparisons between samples >2, ANOVA test was applied coupled to Kruskal–Wallis and Dunn multiple comparison test. We marked with *, $P < 0.05$; **, $P < 0.01$; ***, $P < 0.001$. Unless otherwise indicated, all the data in the figures were represented as arithmetic means ± the SDs from at least three independent experiments.

Results

Genomic alterations and proteotoxic stress in leiomyosarcomas

Induction of proteotoxic stress can be observed in relation to genomic alterations (10, 11, 12). The overexpression of genes, as well as the accumulation of mutations in coding regions, can alter the normal proteostasis (12, 30). These mutations would produce protein variants that are prone to misfolding, degradation, and aggregation.

To unveil the origin and the extent of proteotoxic stress, we evaluated the FGA in leiomyosarcomas and in STS. FGA is the percentage of genome that has been affected by copy-number gains or losses (31). More than 50% of patients with leiomyosarcomas show a very high percentages of genetic alterations (FGA > 50%). STS groups are a heterogeneous family of tumors that also comprise synovial sarcomas, marked by few genomic alterations. Not surprisingly, FGA is heterogeneous also in STS (**Fig. 1A**). Next, we compared the mutations burden [(mutation counts (MC)] in relation to FGA in leiomyosarcomas and STS (**Fig. 1B** and **C**). The mutations burden is also heterogeneous in leiomyosarcomas, with few cases presenting high MC (>100). Similar heterogeneity is observed in STS where leiomyosarcomas and myxofibrosarcoma comprise cases with the highest MC, whereas synovial sarcomas and dedifferentiated liposarcomas are characterized by lower MC (Supplementary Fig. S1).

Afterward, we evaluated FGA and MC in three leiomyosarcoma cell lines (RKN, SK-LMS-1, SK-UT-1). For comparison, we used fibroblasts as a reference of a normal genome. Interestingly, SK-LMS-1 cells resemble leiomyosarcomas with high FGA and relative low MC. In contrast, SK-UT-1 cells represent leiomyosarcomas, characterized by relative low FGA but high MC (**Fig. 1D**). As reported previously, more mutations are present in the cell lines compared with tissues (31). For the subsequent studies, we selected SK-LMS-1 and SK-UT-1 cells, as models of two different landscapes of genetic alterations observed in leiomyosarcomas.

The small molecule 2c makes covalent adducts with free thiols of cysteines and triggers proteotoxic stress and cell death (16, 17). Gene profile studies performed in B-cell chronic lymphocytic leukemia (B-CLL) have identified, among the early response genes to 2c, several components of the proteotoxic response, including: chaperons, proteasomal subunits, and antioxidants (16). We selected a signature of 38 genes upregulated in B-CLL cells in response to 2c (Supplementary Table S1) to evaluate its dysregulation in leiomyosarcomas. **Figure 1E** shows that this general signature is highly expressed in the subgroup of patients that shows a worse prognosis. We extracted from this general signature a specific signature of 18 genes that collects elements of the proteotoxic response, as defined by the Gene Ontology or by literature (Supplementary Table S1 or Supplementary Table S2). Not surprisingly, the proteotoxic signature comprises several chaperones. Interestingly, patients with reduced survival are characterized by high levels of expression of the 2c proteotoxic stress signature (**Fig. 1F**). Moreover, there is a good correlation between patients with leiomyosarcomas with high MC (>46 $n = 39$) and the expression of the 2c proteotoxic signature ($r = 0.46$; $P = 0.00325$).

2c triggers proteotoxic stress, mitochondrial dysfunctions, and cell death in leiomyosarcoma cells

The previous analysis suggests that aggressive leiomyosarcomas are characterized by high levels of proteotoxic stress. In these tumors, a further increase of protein misfolding could be deleterious for the survival of the neoplastic cells. To investigate this hypothesis, we evaluated the ability of 2c to trigger proteotoxic stress in SK-UT-1 and SK-LMS-1 cells. As a measure of proteotoxic stress induction, the mRNA levels of three chaperones: *HSPA1A*, *HSPA6*, and *DNAJB6* were analyzed.

The expression levels of *HSPA1A* and *HSPA6* are dramatically upregulated in the two leiomyosarcoma cells in response to 2c. In contrast, *DNAJB6* remains unaffected or slightly decreases (**Fig. 2A**). The induction of 2c-dependent proteotoxic stress is coupled with the appearance of cell death in both cell lines (**Fig. 2B**). This cell death is partially dependent on caspases, as proved by the incomplete effect of the caspase inhibitor (**Fig. 2B**). The combination TRAIL/bortezomib was used as a reference for the caspase-dependent cell death. 2c-induced cell death is unrelated to ferroptosis and only marginally entails necroptosis (Supplementary Fig. S2A). Erastin proved the efficiency of the ferroptosis inhibitor ferrostatin-1 (Supplementary Fig. S2B). To further confirm the induction of proteotoxic stress, cells were cotreated with 2c and the HSP90 inhibitor 17-AAG. The two compounds show an additive pro-death effect, particularly when used at low doses (Supplementary Fig. S2C). The pleiotropic nature of the cell death response elicited by 2c was also observed in previous studies (16, 17, 25, 26).

EC_{50} values for 2c are 4.47 + 1.04 μmol/L in SK-UT-1 and 15.60 + 2.81 μmol/L in SK-LMS-1 cells (Supplementary Fig S2D). The differential sensitivity to proteotoxic stress of the two leiomyosarcoma cells is confirmed by other inducers of proteotoxic stress: the proteasome inhibitor bortezomib and thapsigargin, an inhibitor of the SERCA transport ATPase (10). Both stressors are less potent in SK-LMS-1 cells with EC_{50} values of 32.79 + 0.67 μmol/L (bortezomib) and 33.64 + 0.54 μmol/L (thapsigargin) compared with 23.13 + 0.75 μmol/L and 28.92 + 0.57 μmol/L, respectively, in SK-UT-1 cells. In summary, leiomyosarcoma cells with higher MC are more sensitive to proteotoxic stress.

Cell death in leiomyosarcoma cells is characterized by the upregulation of the BH3-only protein NOXA/PMAIP1 (**Fig. 2C**), a component of the apoptotic pathway elicited by endoplasmic reticulum stress (12). The induction of caspase activity by 2c is verified by the proteolytic processing of death substrate HDAC4 (27). As expected, 2c triggers the

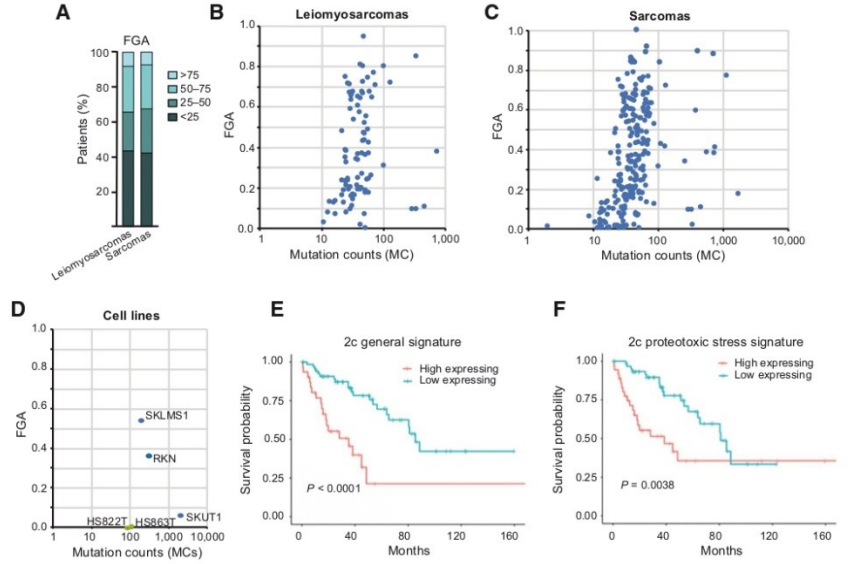

Figure 1.

Analysis of the mutational burden in patients with sarcoma and leiomyosarcoma. **A,** FGA in patients with sarcoma and leiomyosarcoma. Percent stacked bar charts illustrating the distribution of patients with sarcoma ($n = 255$) and leiomyosarcoma ($n = 100$) considering the FGA parameter (patients were divided into four groups based on this value). Data taken from the TCGA-PanCancerAtlas. **B,** Scatter plot showing the FGA and the distribution of MC in patients with leiomyosarcoma ($n = 100$). Data taken from TCGA-PanCancerAtlas. **C,** Scatter plot showing the FGA and the distribution of MC in patients with sarcoma ($n = 255$). Data taken from TCGA-PanCancerAtlas. **D,** Scatter plot of FGA and MC distribution in human fibroblasts and leiomyosarcoma cell lines. Data taken from the Broad Institute CCLE (2019) section of cBioPortal. **E,** Survival probability of patients having high and low median expression of the "2c general" gene signature ($n = 38$), as represented by Kaplan–Meier plot. Patients with sarcoma were stratified on the basis of the optimal cut-off point. **F,** Survival probability of patients having high and low median expression of the "2c proteotoxic stress" gene signature ($n = 18$), as represented by Kaplan–Meier plot. Patients with sarcoma were stratified on the basis of the optimal cut-off point.

rapid accumulation of polyubiquitylated proteins (16, 28) and the appearance of endoplasmic reticulum stress, as evidenced by eIF2α phosphorylation (**Fig. 2C**). The proteolytic processing of eIF2α later on further confirms the activation of caspases in 2c-treated cells (32). Dose-dependent studies confirmed the induction of proteotoxic stress by 2c, as testified by the accumulation of polyubiquitylated proteins and of NOXA/PMAIP1 (Supplementary Fig. S3).

Interestingly, after 2c treatment, the apoptotic protein DIABLO/SMAC accumulates as a higher molecular weight form. DIABLO/SMAC is a mitochondrial protein released into the cytoplasm during apoptosis. When imported into the mitochondria, it is processed by the inner membrane peptidase complex to generate the mature form (33). Hence, the accumulation of the DIABLO/SMAC precursor in cells treated with 2c is indicative of defects in the import machinery, possibly because of an early induction of the mitochondrial unfolded protein response (34). In fact, the analysis of the mitochondria network, using anti-DIABLO/SMAC and anti-ATP synthase (β subunit) antibodies, evidenced an early and dramatic fragmentation of mitochondria in response to 2c (**Fig. 2D**). *In vivo* time-lapse confocal microscopy confirmed the rapid (within 1 hour) induction of mitochondrial fission by 2c (Supplementary videos S1 and S2).

Sub-mitochondrial clusters of DIABLO/SMAC are perturbed by 2c treatment

To gain insight into the structural changes of the mitochondrial network in response to 2c, we used STED superresolution microscopy, which provides an optical resolution below the diffraction limit (35). The β subunit of the ATP synthase, a subunit of the multiprotein complex localized in the mitochondrial inner membrane, including the cristae, was selected to visualize mitochondria (36). We also analyzed DIABLO/SMAC localization, which maturation is under 2c influence. Confocal and STED images are shown for comparison. Both leiomyosarcoma cell lines are characterized by elongated tubular mitochondria. The ATP synthase shows a relative homogeneous distribution, as described previously (35, 36). STED microscopy unveiled that DIABLO/SMAC localizes as small clusters, well separated and usually peripheral with respect to the ATP synthase (**Fig. 3**). Normalized fluorescence intensity profiles confirmed this distribution

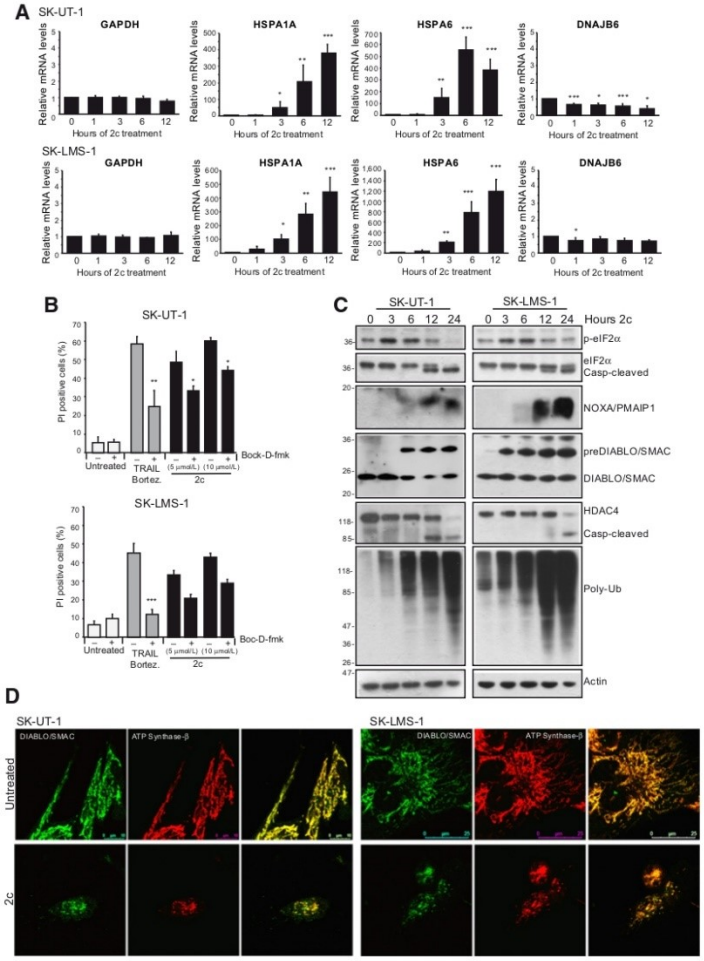

Figure 2.

2c triggers proteotoxic stress and cell death in leiomyosarcoma cells. **A,** qRT-PCR analysis of the mRNA levels of the indicated genes in SK-UT-1 or SK-LMS-1 cells treated with 10 μmol/L of 2c for the indicated times. **B,** SK-UT-1 and SK-LMS-1 cells were treated for 24 hours with the indicated concentrations of 2c or with a combination of TRAIL (2.5 ng/mL) and bortezomib (0.1 μmol/L). The broad caspase inhibitor Boc-D-fmk was used (50 μmol/L). Cell death was calculated as percentage of cells positive to PI staining. **C,** SK-UT-1 and SK-LMS-1 cells were treated with 2c (10 μmol/L) for the indicated times. Cellular lysates were generated and immunoblots were performed with the indicated antibodies. Actin was used as loading control. **D,** SK-UT-1 and SK-LMS-1 cells were treated or not with 10 μmol/L 2c for 4 hours. Immunofluorescence analysis was performed to visualize mitochondria morphology, using antibodies to visualize DIABLO/SMAC (green) and ATP synthase-β subunit (red). Confocal images are shown in pseudocolors and were acquired with a Leica SP8 LSM.

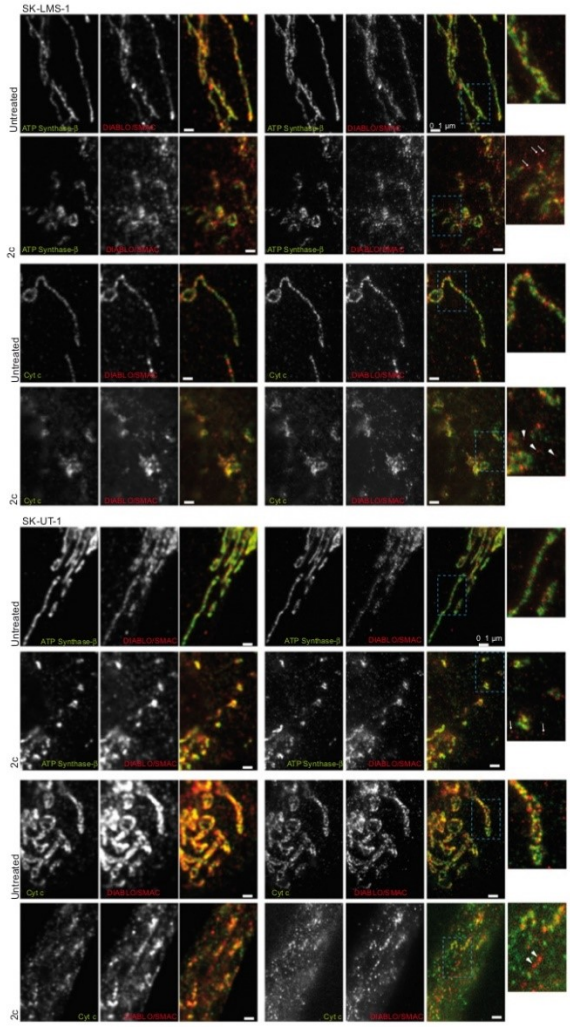

Figure 3.
STED superresolution microscopy of mitochondria under 2c-induced proteotoxic stress. Dual-color confocal and STED images of SK-UT-1 and SK-LMS-1 cells decorated with antibodies against ATP-synthase-β subunit (green)/DIABLO/SMAC (red) or with CytC (green)/DIABLO/SMAC (red). Cells were untreated or treated with 5 μmol/L of 2c for 4 hours. A single optical section is shown. Magnification was applied to the boxed areas. Bar = 1 μm.

(Supplementary Fig. S4). The peripheral localization of DIABLO/SMAC with respect to the ATP synthase-β is expected, because of the different compartmentalization of the two proteins. Overall, the described patterns of mitochondrial localization are similar in the two leiomyosarcoma cell lines.

2c induces a dramatic mitochondrial fragmentation. The 2D STED analysis in 2c-treated cells evidences that some DIABLO/SMAC clusters appear very distant from the ATP synthase domains (**Fig. 3** arrows). This observation is confirmed by the analysis of the fluorescence intensity profiles (Supplementary Fig. S4). The origin of these

distal DIABLO/SMAC clusters is unclear. They could represent the accumulation of the cytosolic precursor form of DIABLO/SMAC. To further understand the mitochondrial alterations triggered by 2c, we performed the STED colocalization analysis of CytC and DIABLO/SMAC, two proteins released into the cytoplasm from the intermembrane space during apoptosis. In untreated cells, separated clusters as well as partially colocalized clusters of CytC and DIABLO/SMAC can be observed (**Fig. 3**). In response to 2c, some partially colocalized clusters of CytC and DIABLO/SMAC persist. In parallel, DIABLO/SMAC clusters at a certain distance from small CytC spots appear (**Fig. 3** arrowheads in the magnification). A similar behavior is observed in the two leiomyosarcoma cells. Normalized fluorescence intensity profiles confirmed these different distributions (Supplementary Fig. S4). All the results were verified by reverting the secondary antibodies labeling (Supplementary Fig. S5 and S6).

In summary, this analysis demonstrates the existence of specific mitochondrial clusters of DIABLO/SMAC and that 2c triggers a profound reorganization of the mitochondrial network and of these clusters.

Optimization of 2c prodrug delivery in leiomyosarcoma cells

2c is poorly soluble in aqueous solutions, a limitation for its use *in vivo*. Recently, we have developed a prodrug version of 2c (2cPE), by using the PEG as a carrier. PEG promotes its solubility and improves the delivery (**Fig. 4A**). An ester linkage allows the release of active 2c from 2cPE, as operated by the secreted esterase PLA2G7 (28). To test the antitumoral potency of 2cPE *in vivo* against leiomyosarcomas, we first evaluated its ability to trigger cell death in leiomyosarcoma cells. Surprisingly, 2cPE is unable to trigger cell death in SK-UT-1 and SK-LMS-1 cells. The failure of 2cPE was further confirmed in DMR cells, another leiomyosarcoma cell line (**Fig. 4B**).

Peptide sequences cleaved by proteases have been utilized as bioactive linkers for the targeted delivery of specific drugs (37). The tumor microenvironment is characterized by increased levels of proteolytic activities, which promote tumor growth and invasion. Prodrug maturation, by tumor microenvironment proteases, could reduce off-target effects of a compound. Hence, we decided to adopt a new strategy to develop a new prodrug version of 2c. To increase its solubility and to specifically generate the active 2c at the tumor site, the compound was conjugated to PEG through a peptide linker. We selected a simple peptide linker constituted by the 3 aa Leu-Gly-Gly (LGG), a sequence that can be cleaved by different proteases secreted in the tumor microenvironment. **Figure 4C** illustrates the different proteases capable of processing the selected sequence and underlines the different sites. As expected, several cathepsins but also metalloproteinases are predicted to cleave the designed sequence. Several of the LGG proteases, particularly the matrix metalloproteinase *ADAM10* and *ADAMTS5*, are highly expressed in leiomyosarcomas (**Fig. 4D**). Curiously, leiomyosarcomas heterogeneously express *PLA2G7*. It is highly plausible that the group of leiomyosarcomas characterized by elevated levels of *PLA2G7* are those characterized by immune/inflammatory cells infiltrates (22). In fact, it is well known that inflammatory cells, including macrophages, express high levels of *PLA2G7* (38). Next, we investigated the expression levels of the putative LGG proteases in the two leiomyosarcoma cell lines. *CTSZ, CTSB, CTSL, CTSA, CTSD*, and *MMP2* are the most expressed proteases in SK-LMS-1 cells. The same group of cathepsins are also highly expressed in SK-UT-1 cells. In these cells the matrix metalloproteinase more abundantly expressed is *ADAM10*, which is also highly expressed in tumors (**Fig. 4E**). An important difference between tumors and cell lines regards the matrix metalloproteinases. In general, they are more abundantly expressed in tumors. It is possible that this difference stems from the presence of an activated stroma (39). The absence of *PLA2G7* expression in both cell lines explains the unresponsiveness to 2cPE treatment.

Generation of the protease-activated prodrug 2cPP

The main goal of this study is to test a new therapeutic strategy against leiomyosarcomas. Having confirmed that leiomyosarcomas express a repertoire of extracellular proteases capable of processing the sequence LGG, we decided to insert this sequence between the 2c and the PEG carrier.

The cleavage of the peptide sequence, connecting 2c to PEG can expose a negatively charged carboxy-terminus or a positively charged amino-terminus, depending on the orientation of the peptide sequence. To evaluate the effect of the negative and of the positive charges linked to 2c, we synthetized two variants of 2c: DU-DC2 with the exposed COO^- and DU-MS1 with a terminal NH_3^+ (**Fig. 5A**). When the ability to trigger cell death of the two compounds was compared respect to 2c, DU-DC2 resulted slightly less potent (**Fig. 5B**). It is possible that the introduced negative charge interferes with the cellular uptake of the 2c derivative and particularly with the interaction with the membrane. Although further studies are necessary to prove this hypothesis, we decided to introduce the LGG sequence with the orientation that will generate, after the proteolytic cleavage, the exposition of the NH_3^+ group. The new prodrug version was synthetized and named 2cPP (2c-protease–activated PEG-conjugated) and the structure is shown is **Fig. 5C**. The new molecule contains a diaminopropane linker that joins 2c to the LGG sequence and a D-alanine linker for the connection to the PEG moiety.

When leiomyosarcoma cell lines were treated with 2cPP, they all underwent cell death (**Fig. 5D**). The percentage of cell death is comparable with 2c treatment, with a slightly reduced potency of 2cPP. It is unclear whether this reduced *in vitro* potency is caused by a delay in the generation of the active drug, because of the protease-mediated processing. Similarly to 2c, 2cPP triggered cell death is partially dependent on caspase activation (**Fig. 5E**).

Induction of proteotoxic stress reduces tumor formation *in vivo*

To prove the antitumor efficiency of the new prodrug 2cPP *in vivo* against leiomyosarcomas, we selected SK-UT-1 cells that are able to efficiently process the prodrug in culture and show an aggressive growth *in vivo*. To exclude general toxicity, we initially evaluated the 2c and 2cPP against HUtSMCs, which represent the normal counterpart of SK-UT-1 cells. Cells were treated with the compounds and after 24 hours cell death was scored. 2c induces cell death with much lower efficiency in HUtSMC cells compared with SK-UT-1 (**Fig. 6A**). Most importantly, 2cPP was totally ineffective. Next, we compared the induction of proteotoxic stress by analyzing eIF2α phosphorylation and NOXA/PMAIP1 upregulation (**Fig. 6B**). HUtSMC show a lower level of basal eIF2α phosphorylation compared with SK-UT-1 cells. Hence, a higher proteotoxic stress seems to characterize cancer cells, as confirmed by the increased expression of *HSF1* in the two leiomyosarcoma cell lines compared with normal cells (Supplementary Fig. S7). Nevertheless, HUtSMC cells promptly augment eIF2α phosphorylation in response to 2c. In contrast, NOXA/PMAIP1 is upregulated only in SK-UT-1 cells. Therefore, normal cells seem to be protected from the vicious cycle of the proteotoxic stress–induced

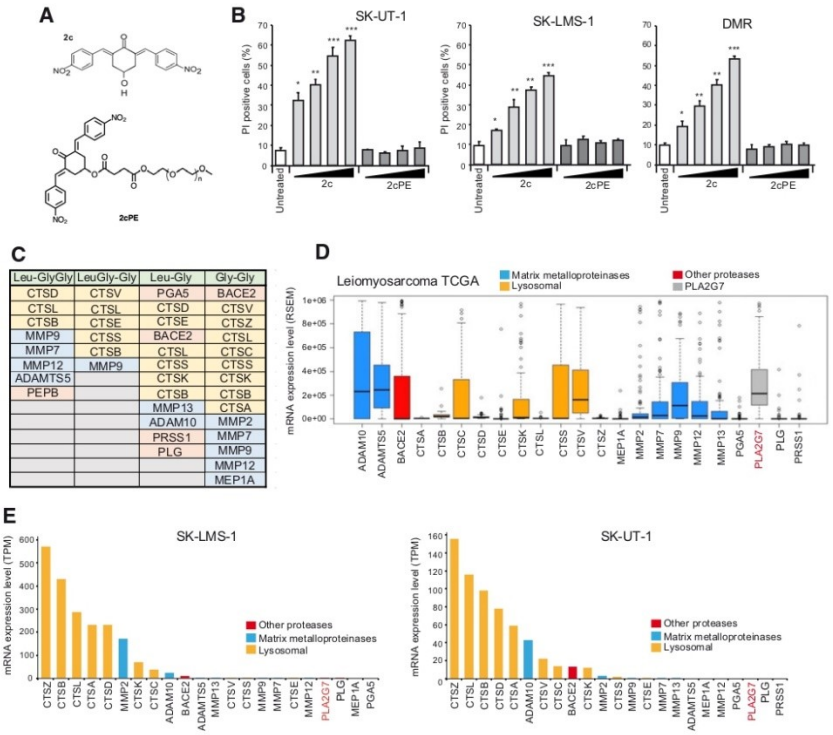

Figure 4.

Generation of a new prodrug version of 2c. **A,** Molecular structure of 2c and of its prodrug version 2cPE. **B,** The three leiomyosarcoma cell lines were treated for 24 hours with the increased concentrations of 2c or 2cPE (1/2.5/5/10 μmol/L). Cell death was calculated as percentage of cells positive to PI staining. **C,** List of the different proteases capable of cleaving the LGG sequence at the indicated sites as downloaded from MEROPS, the peptidase database (https://www.ebi.ac.uk/merops). Lysosomal proteases are in orange, metalloproteinases in light blue, other proteases in pink. **D,** Box plot representing mRNA expression levels (RSEM data) of LGG peptidases identified through MEROPS in patients with leiomyosarcomas ($n = 99$). Data were obtained from the whole Sarcoma dataset (TCGA, PanCancer Atlas; $n = 255$). Lysosomal proteases are in orange, metalloproteinases in light blue, other proteases in pink and PLA2G7 is identified in gray. **E,** mRNA expression levels (TPMs) of LGG peptidases identified through MEROPS in SK-UT-1 and SK-LMS-1 cell lines. Data were obtained from the database of the CCLE. Lysosomal proteases are in orange, metalloproteinases in light blue, other proteases in pink, and *PLA2G7* is identified in gray.

apoptosis. In HUtSMC, 2cPP is unable to trigger eIF2α phosphorylation, thus confirming its inactivity. This result suggests that normal cells are unable to efficiently generate the active drug by proteolytic processing.

Next, SK-UT-1 xenografts were generated in immunocompromised mice, and when the tumors reached the size of 0.1 cm^3, 2cPP (170 mg/kg) was administered intravenously, three times with 4-day intervals. This dose, considering the *in vitro* data, should correspond to approximately 11 mg/kg of the active compound. Alternatively, mice were treated with vehicle alone. 2cPP significantly inhibits tumor growth compared with control (**Fig. 6C**). The percentage of tumor growth inhibition (TGI) is 97.6% after 2 days from the first injection and the final TGI is 80.4%, compared with vehicle-treated animals. As expected from this analysis, tumors from 2cPP-treated mice weigh much less compared with those from vehicle-treated mice (**Fig. 6D**). No gross toxicity was observed and 2cPP does not induce any behavioral change or grossly visible pathologic changes. In the treated group, two mice show slight body weight loss (2.5%) and only a mouse evidenced a loss > 5% during the first week. This animal promptly recover weight during

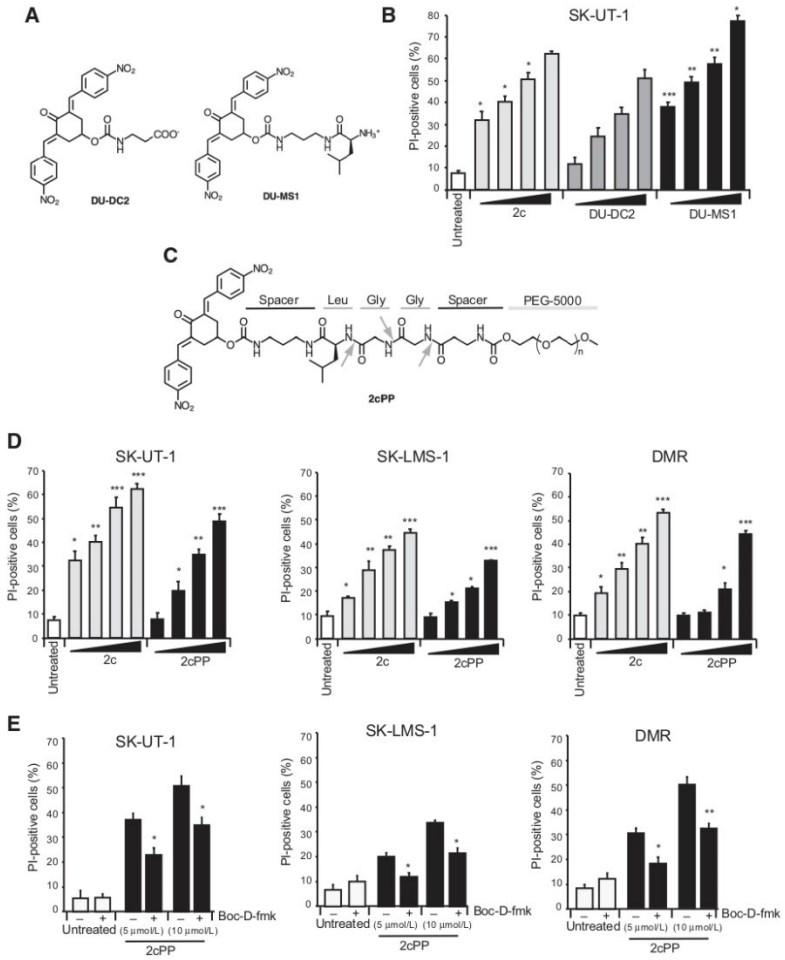

Figure 5.

Generation of the protease-activated prodrug 2cPP. **A,** Molecular structure of the new derivates of 2c with negative (DU-DC2) and positive (DU-MS1) charge. **B,** SK-UT-1 cells were treated for 24 hours with the increased concentrations of 2c, DU-DC2, or DU-MS1 (1/2.5/5/10 μmol/L). Cell death was calculated as percentage of cells positive to PI staining. **C,** Molecular structure of the new prodrug version of 2c (2cPP). Arrows indicate the possible sites of cleavage. Spacers and PEG are also indicated. **D,** The three leiomyosarcoma cell lines were treated for 24 hours with the increased concentrations of 2c or 2cPP (1/2.5/5/10 μmol/L). Cell death was calculated as percentage of cells positive to PI staining. **E,** The three leiomyosarcoma cell lines were treated for 24 hours with the indicated concentrations of 2cPP. The broad caspase inhibitor Boc-D-fmk was used (50 μmol/L). Cell death was calculated as percentage of cells positive to PI staining.

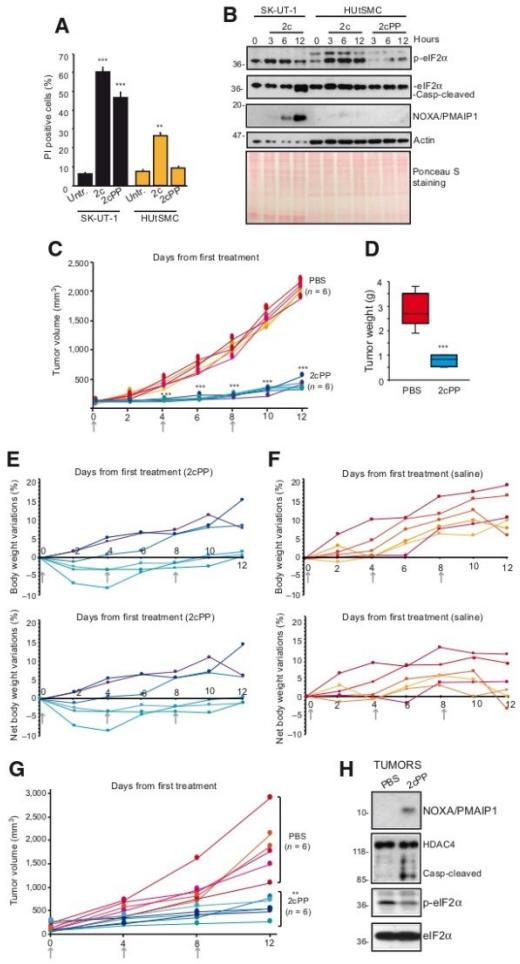

Figure 6.

Antitumor activity of 2cPP *in vivo*. **A,** HUtSMC and SK-UT-1 cells were treated for 24 hours with (10 μmol/L) of 2c or 2cPP. Cell death was calculated as percentage of cells positive to PI staining. **B,** HUtSMC and SK-UT-1 cells were treated with 2c (10 μmol/L) for the indicated times. Cellular lysates were generated and immunoblots were performed with the indicated antibodies. Ponceau S staining was included as loading control. **C,** Variations of SK-UT-1 leiomyosarcoma xenografts volume in mice following intravenous treatments with 2cPP (170 mg/kg) or a saline solution. Arrows indicate the injections. **D,** At day 12, tumors were dissected and final tumor weights measured. Mean tumor weights ± SD. **E,** Total body weights or net body weights (obtained by subtracting tumors) of mice treated with 2cPP, during xenograft studies with SK-UT-1 cells. Data are show as variations (%) relative to time 0. Arrows indicate the injections. **F,** Total body weights or net body weights (obtained by subtracting tumors) of mice treated with saline, during xenograft studies with SK-UT-1 cells. Data are show as variations (%) relative to time 0. Arrows indicate the injections. **G,** Variations of DMR leiomyosarcoma xenografts volume in mice following intravenous treatments with 2cPP (170 mg/kg) or a saline solution. Arrows indicate the injections. **H,** Immunoblot analysis using the indicated antibodies in xenografted tumors treated or not with 2cPP. Twenty-four hours after the last injection with 2cPP (170 mg/kg) or PBS alone, mice were sacrificed for the generation of tumor extracts.

the second week (**Fig. 6E**). Because of the strong TGI exhibited by 2cPP, tumors do not influence body weight of treated mice (compare body weight and net body weight variations). In contrast, in control mice tumor growth profoundly influences body weight (**Fig. 6F**). Next, we validated the potent antitumor activity of 2cPP in a second xenograft model of leiomyosarcomas using DMR cells. 2cPP was again efficient in blocking tumor growth (**Fig. 6H**). Immunoblot analysis confirmed the upregulation of NOXA/PMAIP1 and the induction of apoptosis, testified by HDAC4 cleavage, detectable only in tumors from 2cPP-treated mice (**Fig. 6G**). As observed above *in vitro* for SK-UT-1 (**Fig. 2**), after 24 hours from 2cPP injection eIF2α phosphorylation is exhausted.

In conclusion, augmenting proteotoxic stress in leiomyosarcoma cells exerts a strong antitumor activity *in vivo*.

Discussion

In this article, we have proved that raising proteotoxic stress can trigger cell death in leiomyosarcoma cells and reduce tumor growth *in vivo*. We have shown that aggressive leiomyosarcomas have an intrinsic higher level of proteotoxic stress, a condition that could render these tumors uncapable of managing further increases of proteotoxic stress.

Induction of proteotoxic stress is emerging as a new therapeutic option and compounds capable of enhancing proteotoxic stress are under investigation (8–10, 40–42). The main targets of these small molecules are the chaperone system and the ubiquitin-proteasome system (UPS; ref. 10). 2c belongs to the family of diaryldienone derivatives, small molecules able to alkylate various cellular nucleophiles and cysteines in particular (13, 16, 42). 2c is a nonselective inhibitor of the UPS because it reacts with the catalytic cysteines of deubiquitylases (16, 28). Further studies have shown that 2c can react also with cysteines exposed at the surface of several proteins (17). Hence, these compounds can elicit proteotoxic stress directly, through the alteration of protein folding and indirectly, by blocking the UPS (17, 43, 44). Diaryldienone derivatives can also affect the transport of misfolded proteins and aggresome formation, (45) and can reduce glutathione levels (46), thus inducing oxidative stress (43, 44). Mitochondrial functions are strongly affected by these compounds (25, 44). From all these dysfunctions, proteotoxic stress become unmanageable and ultimately cell death occurs.

DIABLO/SMAC is a mitochondrial proapoptotic protein, whose maturation is influenced by 2c-induced proteotoxic stress. DIABLO/SMAC is released into the cytosol and promotes caspase activities by inhibiting the inhibitors of apoptosis (IAP). DIABLO/SMAC maturation, as operated by the mitochondrial rhomboid protease PARLn, generates the amino-terminal IAP-binding motif (33). Few data are available on DIABLO/SMAC mitochondrial localization. By using two-color STED microscopy, we have defined that DIABLO/SMAC exists in the intermembrane mitochondrial space as demarcated clusters, partially colocalizing with CytC and distinct from ATP synthase-β. The organization in clusters was observed also for other mitochondrial proteins (36). In its mature form, DIABLO/SMAC acts as a tetramer to bind IAPs (47). Its status when sequestered into the mitochondria is unclear. Our data suggest that specific sub-mitochondrial domains enriched for DIABLO/SMAC exist. Interestingly, CytC can partially colocalize with DIABLO/SMAC clusters and CytC can localize also in the cristae (48). Whether these colocalizing clusters represent mitochondrial cristae deserves further studies. Importantly, in 2c-treated cells, a dramatic mitochondrial fragmentation occurs and small spots of DIABLO/SMAC appear. Because they appear very early and much earlier than caspase activation, it is improbable that these spots represent the mature form of DIABLO/SMAC released from the mitochondria. Instead, because dysfunctions in the import of mitochondrial proteins occur early in response to proteotoxic stress, (34) they could represent the cytosolic DIABLO/SMAC precursor.

To potentiate the antineoplastic activity of 2c, we have generated 2cPP, a prodrug version that should be activated in the tumor microenvironment. 2cPP is inactive in its native state and gain high potency immediately after proteases release the active 2c. The designed sequence LGG can be cleaved by different peptidases, including lysosomal cathepsins and certain metalloproteases, two families of proteases abundantly secreted in the tumor microenvironment (39, 49). By linking 2c to PEG through a peptide, we have resolved the poor solubility of the compound, increased the specificity of action and reduced the general toxicity. As final cleaved product 2c, through the diaminopropane linker maintains a Lys. This additional structure only partially influences the pro-death activity of 2c *in vitro*. Different approaches to generate amino acid or peptide-conjugated drugs have been exploited (37). Interestingly, pioneering studies demonstrated that a Leu–doxorubicin prodrug shows higher antitumor efficiency *in vivo* when compared with the parental drug (50).

Overinduction of proteotoxic stress can be deleterious also for normal cells. In uterine smooth-muscle cells, high doses of 2c can trigger cell death, although at much reduced extent compared with leiomyosarcoma cells. Importantly, the insertion of the protease sensitive linker further reduces the toxic effect of 2c against normal cells. Uterine smooth muscle cells are not influenced by 2cPP and mice treated with 2cPP do not evidence signs of toxicity. The strong antitumor activity of 2cPP against leiomyosarcoma cells *in vivo* demonstrates that the induction of proteotoxic stress can be a valid option to treat these malignant tumors.

Although we have focused the study on leiomyosarcomas, our discoveries can also be applied to other tumors where proteotoxic stress is elevated. Moreover, because we have selected a simple aa sequence for prodrug delivery, it is highly plausible that a set of proteases capable of activating 2cPP is present in the microenvironment of different tumors.

Authors' Disclosures

G. Grignani reports other support from Eisai, Lilly, Bayer, Novartis, Merck, and Glaxo Smith Kline outside the submitted work. F. Benedetti reports grants from POR-FESR Regione Friuli-Venezia Giulia, project ATeNA, during the conduct of the study. C. Brancolini reports grants from Sarcoma Foundation of America, POR-FESR Regione Friuli-Venezia Giulia project ATeNA, FPRC 5 × 1000 Ministero della Salute 2015 ImGen, and AIRC IG 23104 during the conduct of the study. No disclosures were reported by the other authors.

Authors' Contributions

L. Iuliano: Data curation, validation, investigation. **S. Drioli:** Resources, validation, methodology. **Y. Pignochino:** Data curation, investigation. **C.M. Cafiero:** Resources, investigation. **M. Minisini:** Investigation. **F. D'Este:** Resources, data curation, methodology. **R. Picco:** Data curation, formal analysis. **E. Dalla:** Data curation, formal analysis. **G. Giordano:** Validation. **G. Grignani:** Supervision. **E. Di Giorgio:** Methodology. **F. Benedetti:** Conceptualization, supervision, funding acquisition. **F. Felluga:** Resources, investigation, methodology, writing–original draft. **C. Brancolini:** Conceptualization, resources, data curation, supervision, funding acquisition, visualization, writing–original draft.

Acknowledgements

This study was supported by POR-FESR Regione Friuli-Venezia Giulia project ATeNA, to F. Benedetti and C. Brancolini, FPRC 5 × 1000 Ministero della Salute 2015 ImGen and AIRC IG 23104 to G. Grignani; and by the Sarcoma Foundation of America, to C. Brancolini.

We thank Andrea Rasola for kindly providing Radicicol.

The costs of publication of this article were defrayed in part by the payment of page charges. This article must therefore be hereby marked *advertisement* in accordance with 18 U.S.C. Section 1734 solely to indicate this fact.

Received June 22, 2020; revised November 27, 2020; accepted March 9, 2021; published first March 30, 2021.

References

1. Duffaud F, Ray-Coquard I, Salas S, Pautier P. Recent advances in understanding and managing leiomyosarcomas. F1000Prime Rep 2015;7:55.
2. Gladdy RA, Qin L, Moraco N, Agaram NP, Brennan MF, Singer S. Predictors of survival and recurrence in primary leiomyosarcoma. Ann Surg Oncol 2013;20: 1851–57.
3. Chibon F, Darbo E, Pérot G. Leiomyosarcomas: whole genome sequencing for a whole biology characterization. Curr Opin Oncol 2019; 31:317–21.
4. Mäkinen N, Aavikko M, Heikkinen T, Taipale M, Taipale J, Koivisto-Korander R, et al. Exome sequencing of uterine leiomyosarcomas identifies frequent mutations in TP53, ATRX, and MED12. PLoS Genet 2016;12:e1005850.
5. Abeshouse A, Adebamowo C, Adebamowo SN, Akbani R, Akeredolu T, Ally A, et al. Comprehensive and integrated genomic characterization of adult soft tissue sarcomas. Cell 2017;171:950–65.
6. Seddon B, Strauss SJ, Whelan J, Leahy M, Woll PJ, Cowie F, et al. Gemcitabine and docetaxel versus doxorubicin as first-line treatment in previously untreated advanced unresectable or metastatic soft-tissue sarcomas (GeDDiS): a randomised controlled phase 3 trial. Lancet Oncol 2017;18:1397–410.
7. Tap WD, Wagner AJ, Schöffski P, Martin-Broto J, Krarup-Hansen A, Ganjoo KN, et al. Effect of doxorubicin plus olaratumab vs doxorubicin plus placebo on survival in patients with advanced soft tissue sarcomas: the ANNOUNCE randomized clinical trial. JAMA 2020;323:1266–76.
8. McConkey DJ. The integrated stress response and proteotoxicity in cancer therapy. Biochem Biophys Res Commun 2017;482:450–3.
9. Chui MH, Doodnauth SA, Erdmann N, Tiedemann RE, Sircoulomb F, Drapkin R, et al. Chromosomal instability and mTORC1 activation through PTEN loss contribute to proteotoxic stress in ovarian carcinoma. Cancer Res 2019;79:5536–49.
10. Guang MHZ, Kavanagh EL, Dunne LP, Dowling P, Zhang L, Lindsay S, et al. Targeting proteotoxic stress in cancer: a review of the role that protein quality control pathways play in oncogenesis. Cancers 2019;11:66.
11. Ohashi A, Ohori M, Iwai K, Nakayama Y, Nambu T, Morishita D, et al. Aneuploidy generates proteotoxic stress and DNA damage concurrently with p53-mediated post-mitotic apoptosis in SAC-impaired cells. Nat Commun 2015; 6:7668.
12. Brancolini C, Iuliano L. Proteotoxic stress and cell death in cancer cells. Cancers 2020;12:2385.
13. Coughlin K, Anchoori R, Iizuka Y, Meints J, MacNeill L, Voge RI, et al. Small-molecule RA-9 inhibits proteasome-associated DUBs and ovarian cancer in vitro and in vivo via exacerbating unfolded protein responses. Clin Cancer Res 2014; 20:3174–86.
14. Le Moigne R, Aftab BT, Djakovic S, Dhimolea E, Valle E, Murnane M, et al. The p97 inhibitor CB-5083 is a unique disrupter of protein homeostasis in models of multiple myeloma. Mol Cancer Ther 2017;16:2375–86.
15. Yu Y, Zhao Y, Fan Y, Chen Z, Li H, Lu J, et al. Inhibition of ubiquitin-specific protease 14 suppresses cell proliferation and synergizes with chemotherapeutic agents in neuroblastoma. Mol Cancer Ther 2019;18:1045–56.
16. Tomasella A, Picco R, Ciotti S, Sgorbissa A, Bianchi E, Manfredini R, et al. The isopeptidase inhibitor 2cPE triggers proteotoxic stress and ATM activation in chronic lymphocytic leukemia cells. Oncotarget 2016;7:45429–43.
17. Ciotti S, Sgarra R, Sgorbissa A, Penzo C, Tomasella A, Casarsa F, et al. The binding landscape of a partially-selective isopeptidase inhibitor with potent pro-death activity, based on the bis(arylidene)cyclohexanone scaffold. Cell Death Dis 2018;9:184.
18. Di Giorgio E, Clocchiatti A, Piccinin S, Sgorbissa A, Viviani G, Peruzzo P, et al. MEF2 is a converging hub for histone deacetylase 4 and phosphatidylinositol 3-kinase/Akt-induced transformation. Mol Cell Biol 2013;33: 4473–91.
19. Cerami E, Gao J, Dogrusoz U, Gross BE, Sumer SO, Aksoy BA, et al. The cBio cancer genomics portal: an open platform for exploring multidimensional cancer genomics data. Cancer Discov 2012;2:401–4.
20. Cancer Genome Atlas Research Network; Weinstein JN, Collisson EA, Mills GB, Shaw KRM, Ozenberger BA, et al. The cancer genome atlas pan-cancer analysis project. Nat Genet 2013;45:1113–20.
21. Ghandi M, Huang FW, Jané-Valbuena J, Kryukov GV, Lo CC, McDonald ER 3rd, et al. Next-generation characterization of the Cancer Cell Line Encyclopedia. Nature 2019;569:503–8.
22. Di Giorgio E, Paluvai H, Picco R, Brancolini C. Genetic programs driving oncogenic transformation: lessons from *in vitro* models. Int J Mol Sci 2019; 20:6283.
23. Dardis C. survMisc: Miscellaneous Functions for Survival Data, R Package Version: 0.5.5; 2018. Available from: https://CRAN.R-project.org/package=survMisc.
24. Sgorbissa A, Tomasella A, Potu H, Manini I, Brancolini C. Type I IFNs signaling and apoptosis resistance in glioblastoma cells. Apoptosis 2011;16: 1229–44.
25. Fontanini A, Foti C, Potu H, Crivellato E, Maestro R, Bernardi P, et al. The isopeptidase inhibitor G5 triggers a caspase-independent necrotic death in cells resistant to apoptosis: a comparative study with the proteasome inhibitor bortezomib. J Biol Chem 2009;284:8369–81.
26. Tomasella A, Blangy A, Brancolini C. A receptor-interacting protein 1 (RIP1)-independent necrotic death under the control of protein phosphatase PP2A that involves the reorganization of actin cytoskeleton and the action of cofilin-1. J Biol Chem 2014;289:25699–710.
27. Paroni G, Mizzau M, Henderson C, Del Sal G, Schneider C, Brancolini C. Caspase-dependent regulation of Histone Deacetylase 4 nuclear-cytoplasmic shuttling promotes apoptosis. Mol Biol Cell 2004;15:2804–18.
28. Cersosimo U, Sgorbissa A, Foti C, Drioli S, Angelica R, Tomasella A, et al. Synthesis, characterization, and optimization for *in vivo* delivery of a nonselective isopeptidase inhibitor as new antineoplastic agent. J Med Chem 2015;58: 1691–704.
29. Barretina J, Caponigro G, Stransky N, Venkatesan K, Margolin AA, Kim S, et al. The cancer cell line encyclopedia enables predictive modelling of anticancer drug sensitivity. Nature 2012;483:603–7.
30. Zhu J, Tsai HJ, Gordon MR, Li R. Cellular stress associated with aneuploidy. Dev Cell 2018;44:420–31.
31. Domcke S, Sinha R, Levine DA, Sander C, Schultz N. Evaluating cell lines as tumour models by comparison of genomic profiles. Nat Commun 2013;4: 2126.
32. Satoh S, Hijikata M, Handa H, Shimotohno K. Caspase-mediated cleavage of eukaryotic translation initiation factor subunit 2alpha. Biochem J 1999;342: 65–70.
33. Saita S, Nolte H, Fiedler KU, Kashkar H, Venne AS, Zahedi RP, et al. PARL mediates Smac proteolytic maturation in mitochondria to promote apoptosis. Nat Cell Biol 2017;19:318–28.
34. Andréasson C, Ott M, Büttner S. Mitochondria orchestrate proteostatic and metabolic stress responses. EMBO Rep 2019;20:e47865.
35. Donnert G, Keller J, Wurm CA, Rizzoli SO, Westphal V, Schönle A, et al. Two-color far-field fluorescence nanoscopy. Biophys J 2007;92:L67–9.
36. Jans DC, Wurm CA, Riedel D, Wenzel D, Stagge F, Deckers M, et al. STED super-resolution microscopy reveals an array of MINOS clusters along human mitochondria. Proc Natl Acad Sci U S A 2013;110:8936–41.
37. Poreba M. Protease-activated prodrugs: strategies, challenges, and future directions. FEBS J 2020;287:1936–69.
38. Low HB, Png CW, Li C, Wang DY, Wong SBJ, Zhang Y. Monocyte-derived factors including PLA2G7 induced by macrophage-nasopharyngeal carcinoma cell interaction promote tumor cell invasiveness. Oncotarget 2016;7: 55473–90.
39. Gonzalez-Avila G, Sommer B, García-Hernández AA, Ramos C. Matrix metalloproteinases' role in tumor microenvironment. Adv Exp Med Biol 2020;1245: 97–131.
40. Harris IS, Endress JE, Coloff JL, Selfors LM, McBrayer SK, Rosenbluth JM, et al. Deubiquitinases maintain protein homeostasis and survival of cancer cells upon glutathione depletion. Cell Metab 2019;29:1166–81.
41. Dias MH, Fonseca CS, Zeidler JD, Albuquerque LL, da Silva MS, Cararo-Lopes E, et al. Fibroblast growth factor 2 lethally sensitizes cancer cells to stress-targeted therapeutic inhibitors. Mol Oncol 2019;13:290–306.
42. Karki SS, Das U, Umemura N, Sakagami H, Iwamoto S, Kawase M, et al. 3,5-bis(3-alkylaminomethyl-4-hydroxybenzylidene)-4-piperidones: a novel class of potent tumor-selective cytotoxins. J Med Chem 2016;59: 763–9.
43. Ciotti S, Iuliano L, Cefalù S, Comelli M, Mavelli I, Di Giorgio E, et al. GSK3β is a key regulator of the ROS-dependent necrotic death induced by the quinone DMNQ. Cell Death Dis 2020;11:2.
44. Zhang X, Pellegrini P, Saei AA, Hillert EK, Mazurkiewicz M, Olofsson MH, et al. The deubiquitinase inhibitor b-AP15 induces strong proteotoxic stress and mitochondrial damage. Biochem Pharmacol 2018;156:291–301.
45. Hillert EK, Brnjic S, Zhang X, Mazurkiewicz M, Saei AA, Mofers A, et al. Proteasome inhibitor b-AP15 induces enhanced proteotoxicity by inhibiting cytoprotective aggresome formation. Cancer Lett 2019;448:70–83.

46. Foti C, Florean C, Pezzutto A, Roncaglia P, Tomasella A, Gustincich S, et al. Characterization of caspase-dependent and caspase-independent deaths in glioblastoma cells treated with inhibitors of the ubiquitin-proteasome system. Mol Cancer Ther 2009; 8:3140–50.
47. Mastrangelo E, Vachette P, Cossu F, Malvezzi F, Bolognesi M, Milani M. The activator of apoptosis Smac-DIABLO acts as a tetramer in solution. Biophys J 2015;108:714–23.
48. Scorrano L, Ashiya M, Buttle K, Weiler S, Oakes SA, Mannella CA, et al. A distinct pathway remodels mitochondrial cristae and mobilizes Cytochrome C during apoptosis. Dev Cell 2002;2:55–67.
49. Vidak E, Javoršek U, Vizovišek M, Turk B. Cysteine cathepsins and their extracellular roles: shaping the microenvironment. Cells 2019;8:264.
50. Breistol K, Hendriks HR, Fodstad O. Superior therapeutic efficacy of N-L-leucyl-doxorubicin versus doxorubicin in human melanoma xenografts correlates with higher tumour concentrations of free drug. Eur J Cancer 1999;35:1143–49.